Photoplethysmography for the Evaluation of Diabetic Autonomic Neuropathy

Devi Ravindranathan

Cardiff University

Ph.D. Thesis

2009

ProQuest LLC
789 East Eisenhower Parkway
P.O. Box 1346
Ann Arbor, MI 48106-1346

Declaration and Statements

DECLARATION

This work has not previously been accepted in substance for any degree and is not concurrently submitted in candidature for any degree.

Signed ..Devi Ravendranathan.... (candidate)

Date ..26-07-2010.....

STATEMENT 2

This thesis is the result of my own investigation, except where otherwise stated. Other sources are acknowledged by explicit references. A bibliography is appended

Signed ..Devi Ravendranathan.... (candidate)

Date ..26-07-2010.....

STATEMENT 3

I hereby give consent for my thesis, if accepted, to be available for photocopying and for inter-library loan, and for the title and summary to be made available to outside organisations.

Signed ..Devi Ravendranathan..... (candidate)

Date...26-07-2010.....

Acknowledgment

Praise the bridge that carried you over.

- George Colman ("The Younger')

It has been a long road to completing this study and there are numerous people that I would like to thank for their help and support through out this journey.

I would like to express my sincere gratitude to,

My supervisor Professor JP Woodcock for believing in me and my work and giving me this brilliant opportunity to be a part of a great team and for his continuous encouragement and guidance when I needed them most

Dr Rhys Morris for his invaluable support and patience that he has shown me through out this study

Dr Nigel Gough for all his suggestions and guidance that he has provided through out this research work and for always willing to listen and help

To Huntleigh Diagnostics PLC for funding this research work and making this study possible

Professor David Owens and the Diabetes Research Unit at Llandough hospital for allowing me to carry out part of my research work in their premises

To all the staff at the Vascular Unit in the Department of Medical Physics and Bioengineering for keeping me sane when things did not look very promising and for the brilliant three years spent in the department

And lastly to my wonderful parents and my very patient husband for the support, love, and their faith in me without which this work would not be possible

List of Abbreviations

AC	Alternating Current
AV	Arteriovenous
bpm	Beats per minute
CAN	Cardiovascular Autonomic Neuropathy
CDM	Complex Demodulation
cpm	Cycles per minute\
DAN	Diabetic Autonomic Neuropathy
DC	Direct current
DFT	Discrete Fourier Transform
DM	Diabetes Mellitus
DPPG	Digital Photoplethysmography
ECG	Electro Cardiogram
FFT	Fast Fourier Transform
GI	Gastro-Intestinal
GU	Genito-Urinary
HF	High Frequency
HR	Heart Rate
Hz	Hertz
IDDM	Insulin Dependant Diabetes Mellitus (Type 1)
IIDM	Insulin Independent Diabetes Mellitus (Type 2)
IR	Infra red
LF	Low Frequency
NADP	Nicotinamide Adenine dinucleotide phosphate
NADPH	Reduced form of NADP
NO	Nitric Oxide
POAD	Peripheral Occlusive Arterial Disease
PPG	Photoplethysmography
Redox	Reduction-Oxidation process
ROS	Reactive oxidative species
VPT	Vibration Perception Threshold

Abstract

The aim of this study was to determine if photoplethysmography (PPG) could be used to analyse the foot microvascular changes caused by diabetic autonomic neuropathy. The digital PPG signals were collected from 37 healthy volunteers (Group I), 35 diabetic patients (Group II), and 38 diabetic patients with sensory neuropathy (Group III) and analysed using MATLAB. Prominent spectral peaks with sidebands were obtained at both the high frequency (HF) and the low frequency (LF) end of the Fourier spectrum of these PPG signals. Previous studies of microcirculation have shown that both are sympathetically and parasympathetically mediated and hence are a good measure of the autonomic activity.

In the HF analysis, the heart rate (HR) response from 13 participants in Group III was severely reduced and significantly different from the responses obtained from the other two groups. However the responses from remaining 25 participants had similar characteristics to those of Group II. Hence the HF analyses failed to both statistically and objectively differentiate between the diabetics with and without neuropathy.

The spectral density for the frequency bandwidth of 3-20 cpm was significantly reduced in the neuropathic group, compared to the other two groups. A Statistically significant difference was observed in the spectral densities calculated from Group II and III, though no difference could be established between Groups I and III. The LF analysis of this bandwidth differentiated between Groups II and III with a sensitivity of 84% and specificity of 61%.

Activities at the LF end of the spectrum mostly represent the sympathetic control as opposed to the HR variability that is mostly a measure of the parasympathetic control. These results suggest that sympathetic dysfunction possibly precedes parasympathetic dysfunction and that PPG can assess the changes in the skin microcirculation due to sympathetic damage with moderate success.

Table of Contents

Research Summary

Ulceration below the knee is a common complication of diabetes with a lifetime risk of its occurrence among diabetics estimated at 15% (Kenneth 2005). If left untreated the ulcerations could become infected and gangrenous and finally lead to amputations. In the UK 5000 diabetics are estimated to have amputations every year. Foot ulcers precede more than 80% of non-traumatic lower limb amputations (Boulton et al 2000). Diabetes can also damage the peripheral nerves resulting in neuropathy.

The sensory, motor and autonomic neuropathies are often the major components in the critical pathway for the development of diabetic foot ulcers. While motor neuropathy disrupts the biomechanics of the foot causing deformities and increased stress, the sensory neuropathy is responsible for the unawareness to any trauma that may have caused leading to the neglect of the wound from the patient's side. Autonomic denervation on the other hand can not only cause dry, callus skin prone to cracks and fissures, there by exposing the foot to a greater risk of developing ulcers, but they also disrupt the autoregulatory effect of the skin microcirculation causing reduced nutritive flow to the wound site and hence delay the healing time. Diabetic ulcers if not treated can become infected and ultimately lead to amputation. Thus it is imperative that the diabetic patients must be regularly screened for any early signs of warning of the disease process in order to reduce the incidence of ulceration.

In the UK diabetic patients generally undergo annual examination which includes the detailed examination of the foot to assess the sensory function, to check for any neglected wound and to assess the need for special foot wear to maintain the biomechanics of the foot. Apart from the annual check up, the patients are also advised to book themselves into a podiatry clinic for regular foot examination. Currently the autonomic function of the body is assessed using the cardiovascular autonomic function tests. Both the sympathetic and the parasympathetic branches of the autonomic system are assessed by these tests. Although studies indicate autonomic disruption in the early stages of diabetes, the protocol generally does not involve tests for the detailed assessment of the autonomic function in these patients due to the complex and demanding nature of these tests.

Early screening for signs of autonomic dysfunction amongst diabetic patients could prevent serious complications of the disease and improve the prognosis of the diabetic foot, as it is one of the major components in the ulceration pathway. The disruption in the vasomotor responses (sympathetic dysfunction) can be found as early as in the pre diabetic stages sometimes even before the manifestation of the parasympathetic dysfunction, detected by the CAN assessment tests (Meyer et al. 2003). Understanding of the foot blood flow at the microvascular level is imperative for the better understanding of the diabetic foot ulcers. This study looks at methods to device a simple, low cost screening tool to detect the autonomic dysfunction in the early stages of diabetes by analysing the foot blood flow. Ideally, the measurement technique being developed to study the skin microcirculation has to be relatively simple

to perform, reproducible, reliable and cheap to be able to be used as a screening tool.

In this study attempts have been made to use PPG to measure the changes in the skin microcirculation by analysing the PPG signals obtained from the soles of the feet. Signals were collected from three groups viz, healthy participants, diabetic patients with no neuropathy and diabetic patients with sensory neuropathy. Appropriate signal processing tools were applied using computing software, MATLAB to separate and analyse the various frequencies obtained from this complex signal and to identify any changes in the responses between healthy individuals and the diabetics. Further analyses were also performed to identify if any changes in the skin circulation between diabetics with and without neuropathy could be observed. If changes could be identified between the two groups, further analysis was done to see if these changes could be successfully used as predictive markers for subsequent ulceration of the foot amongst the diabetics without neuropathy as this could enable steps to be taken to prevent diabetic foot ulceration in these individuals.

Chapter I

Background

1.1 Introduction

Diabetes Mellitus has been recognised as a syndrome i.e. a collection of disorders resulting from impaired carbohydrate, protein and fat metabolism; caused either by a complete lack of insulin or by decreased sensitivity of the tissues to insulin or by a combination of both these factors (DeFronzo et al 2004). This syndrome is accompanied by several complications brought about mainly by the pathological and functional changes to the vasculature, right from the beginning of its onset. Autonomic neuropathy is one such complication of diabetes brought about by changes to the microvasculature of the body. In this chapter all the background information relevant to this project have been discussed in considerable detail.

1.2 Diabetic Complications

Diabetes is a multifactorial disease with chronic complications that manifests itself as a burden for both the patient and the health care system (Spijkerman et al 2003). This disease is characterised by an abnormal carbohydrate metabolism leading to an imbalance in the plasma glucose concentration in blood. Diabetes can mainly be classified into two types, namely the Type 1 or Insulin Dependent Diabetes Mellitus (IDDM) and the Type 2 or the Insulin

Independent Diabetes Mellitus (IIDM). Both genetic as well as environmental factors were found to play a key role in the susceptibility of both type of diabetes.

The primary pathology of diabetes was found to be an interaction of the metabolic and vascular dysfunction. The early effects of hyperglycaemia were mostly metabolic changes while the late effects were in the form of electrophysiological and morphological changes (Bhadada et al 2001). Diabetes Mellitus is usually characterised by an asymptomatic phase of about 4-7 years before the actual onset of the disease and its clinical manifestation. Persistent hyperglycaemia is one of the principle underlying causes for the development of diabetes related complications (Duby et al 2004). The chronic complications of diabetes manifest themselves in the form of both microvascular and macrovascular diseases as shown in the figure 1.1.

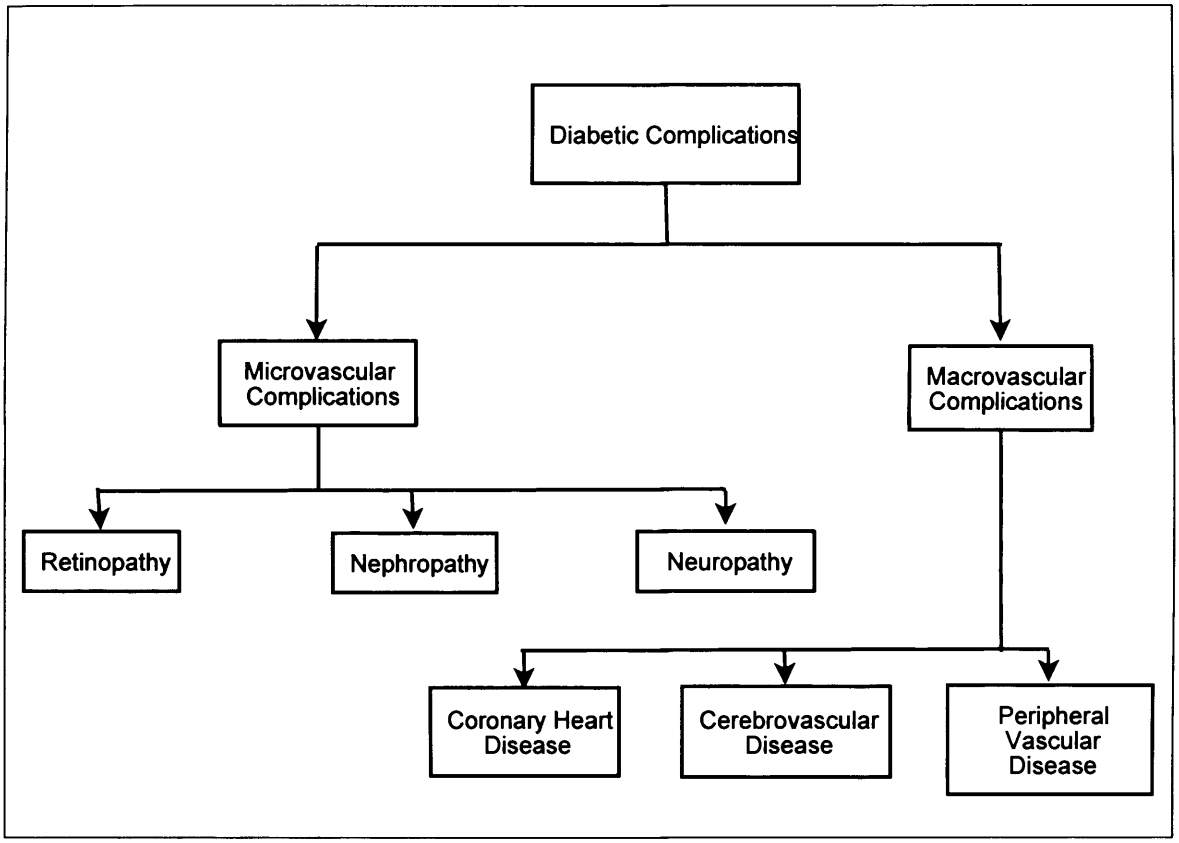

Figure 1.1: Flow chart illustrating the different type of complications due to diabetes

The macrovascular complications account for nearly 50% of deaths among Type 1 and 2 diabetics (LeRoith et al 2004). The primary pathology of the macrovascular complications is atherosclerosis. It is a condition referring to the thickening of the vessel wall with subsequent reduction in the lumen size of the large arteries. Though the exact process or cause of atherosclerosis is unknown, it has been proposed that diabetes could trigger endothelial dysfunction and the build up of plaque within the large vessels. The subsequent reduction in the lumen size also causes a decrease in the blood flow through these vessels. The three main types of macrovascular complications among diabetics are the Coronary heart disease, the cerebrovascular disease and the peripheral vascular disease, which often leads to myocardial infarction, strokes and amputations respectively. In most

cases all the three sites of circulation are affected and treatment of one can often aggravate the other.

Diabetes can also cause pathological and functional changes to the microvasculature of various tissues of the body, mainly affecting the eyes, kidneys and the nervous system. The pathogenesis of microvasculopathy is a complex process governed by several factors like the type of organ bed involved and the type and severity of diabetes. Though the manifestation of microvasculopathy occurs during the late stages of diabetes, studies have revealed that the structural and functional damage of the microvasculature begins from the very onset of raised glucose levels (Wiernsperger 2001). Therefore the microvascular complications of diabetes can be studied under an initial functional stage and then a structural stage. The initial functional stage is a reversible stage that can be achieved through controlled glucose level, while the latter involves structural remodelling of the microvasculature that ultimately leads to the microvascular failure (Tooke 1995). Retinopathy, nephropathy and neuropathy are the three main microvascular complications of diabetes affecting the eyes, the kidney and the nervous system respectively. Diabetes can also cause damage to the skin microcirculation.

1.2.1 Diabetic Neuropathy

The damage to the peripheral, the autonomic and the cranial nerves due to diabetes mellitus is termed diabetic neuropathy. It is a common but serious complication of diabetes, affecting almost every type of nerve fibre in the body

(Duby et al 2004). Long standing hyperglycaemia can cause certain pathological alterations in the nerve fibres, parent nerve cell bodies, neural vasculature and the supporting connective tissues resulting in nerve damage. Of the several models of classifications proposed over the years, a simple classification based on anatomical characteristics given by Thomas was widely accepted (Bhadada et al 2001). Under this classification diabetic neuropathy was broadly classified into **diffuse** and **focal** neuropathy as shown in the figure 1.2.

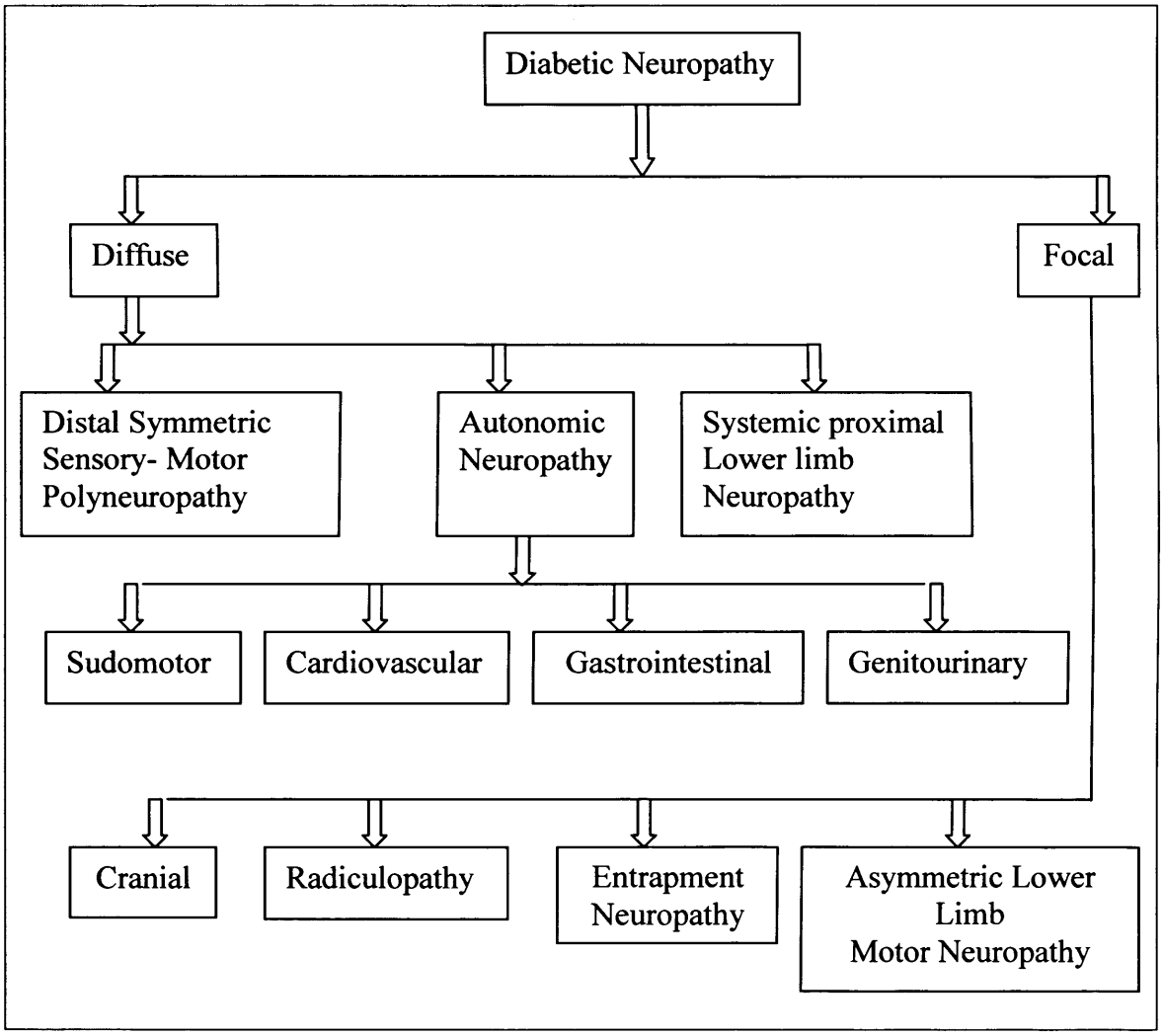

Figure 1.2: Classification of Diabetic Neuropathy

The distal symmetric sensory-motor polyneuropathy is by far the most common type of diabetic neuropathy, involving both large and small fibres (Bhadada et al 2001). As the name suggests, this type of neuropathy has a distal symmetrical form of disorder predominantly affecting the large nerve fibres and following a distal-proximal pathway also called the "stocking distribution" pattern. Progression of this disease occurs in several stages with varying degrees of severity in the symptoms (Bhadada et al 2001).

The proximal motor neuropathy primarily involves the motor neurons and is accompanied by wasting and weakening of muscles causing muscle atrophy. The weakening of muscles is accompanied by muscle imbalance and foot deformities, which cause abnormal concentrations of forces and stress in the soles of the feet thereby increasing the risk of trauma. This type of neuropathy may be symmetrical or asymmetrical, may or may not involve the loss of sensory nerve fibres and is also labelled diabetic amyotrophy. This disorder mostly tends to occur in the background of sensory polyneuropathy. Unlike the distal symmetrical sensory motor polyneuropathy, the motor neuropathy has a better prognosis and is a reversible condition (Bhadada et al 2001).

Both focal and multifocal neuropathies occur rarely among the diabetics, have an asymmetrical form of distribution and manifest themselves as isolated or multiple lesions of cranial, limb and truncal nerves. This is also a reversible condition where the patient recovers within three to four months (Bhadada et al 2001). Diabetic autonomic neuropathy is another important type of

symmetrical neuropathy that will be dealt in detail in the next section of this chapter.

1.3 Diabetic Autonomic Neuropathy or DAN

DAN is a complex heterogeneous disorder affecting the autonomic neurons of the peripheral nervous system (Vinik 2002). Most organ systems of the body are dually innervated with both sympathetic and parasympathetic divisions of the autonomic nervous system. Thus damage to these nerve fibres can cause widespread dysfunction of most organ systems of the body (Vinik and Erbas 2001).

Although the subclinical autonomic dysfunction can occur within a year or two of the diagnosis of diabetes mellitus, the clinical symptoms of this disorder remains asymptomatic until long after the onset of the diabetes (Vinik and Erbas 2001). Poor glycaemic control, age, duration of diabetes, female sex and obesity are some of the major risk factors in the development and progression of this disease (Vinik 2002). DAN was found to increase patient morbidity and mortality and to have a profound negative impact on the quality of life. Like all other neuropathies the early detection and treatment of this disease was observed to be vital for its delayed progression and improved quality of patient life.

1.3.1 Manifestation of DAN

Both the sympathetic and parasympathetic nerve fibres dually innervate most organ systems of the body; therefore the effects of DAN are varied and serious (Vinik 2002). Depending on the organ system that is damaged, DAN can be classified into four major divisions as shown in the figure 1.2.

Damage to the autonomic neurons that innervate the cardiac smooth muscles causes **Cardiovascular Autonomic Neuropathy** or CAN. The cardiac denervation involves both parasympathetic and sympathetic fibres. Abnormalities in the HR control and the vascular dynamics were observed in individuals with CAN (Vinik et al 2003). Decrease in the HR variability was considered to be one of the earliest indicators of symptomatic CAN. Individuals suffering from CAN were observed to have impaired exercise intolerance and were also associated with higher risk of suffering from silent myocardial infraction. The CAN could also cause orthostatic hypotension, which is the fall in blood pressure of more than 30 mmHg on standing. The symptoms include dizziness, weakness, fatigue and even occasional visual blurriness. Although DAN can remain asymptomatic for long period of time, the CAN dysfunctions occur in the early stages of diabetes. The tests to assess the cardiac autonomic function are sensitive, objective and reproducible. Thus they form the standard tests for the diagnosis of DAN (Vinik et al 2003).

The denervation of the autonomic neurons supplying the gastro-intestinal tract causes **gastro-intestinal (GI) autonomic neuropathy**. The resulting GI

disorders were varied and complex with symptoms that were common and not unique to this disease. These symptoms included diarrhoea, faecal incontinence, heartburn, constipation, bloating and nausea. Faecal incontinence due to impaired sphincter tone was also common among diabetics with this form of autonomic dysfunction (Vinik et al 2003).

Damage to the afferent nerve fibres supplying the genito-urinary system of the body due to autonomic neuropathy can cause both bladder dysfunction and sexual dysfunction. Autonomic neuropathy can also impair the respiratory reflexes, the bronchomotor tone and cause damage to the skin and eyes.

1.3.2 Current Diagnostic Approach for DAN

Historically research for the development of methods for the objective assessment of autonomic dysfunction has lagged behind those for the assessment of the more common sensory-motor neuropathies due to its largely asymptomatic nature (Vinik et al 2003). It was a common belief that autonomic neuropathy was a rare complication that affected only certain individuals. However in reality, though symptomatic autonomic neuropathy is rare, autonomic dysfunction has been observed to occur within the first couple of years of diagnosis of diabetes. Since DAN manifests itself as dysfunctions of several organ systems with symptoms being varied and common, objective diagnosis of the same is not always straightforward. Unlike the sensory-motor nervous system in which individual nerves can be tested, the study of the autonomic system is usually achieved by assessing the end organ function.

The symptoms of GI and GU autonomic dysfunctions are mostly subtle and non-specific. Therefore, traditionally the diagnosis of DAN has been through the assessment of the cardiovascular reflexes. These tests are both sensitive and reliable. They provide a direct and an objective assessment of the extent of the autonomic dysfunction (Vinik and Erbas 2001). A summary of the different diagnostic tests currently in use has been tabulated in figure 1.3.

Assessment of Cardiovascular Autonomic Function

Cardiovascular autonomic dysfunction is studied by assessing the performance of the heart. Both the sympathetic and parasympathetic fibres dually innervate the heart and work in opposition to each other. Thus one has to take into account the complexities of the autonomic innervations of the heart when interpreting the cardiovascular assessment test results. The tests currently in use include the measurement of the HR variability (HRV), measurement of the HR response during the Valsalva manoeuvre test or under deep breathing, HR response to standing up, pressure response to postural change and the pressure response to sustained hand grip. Of these tests, the resting HR and the HR response to deep breathing and standing are early indicators of the parasympathetic dysfunction, while the blood pressure response to standing, deep breathing and sustained handgrip is a measure of the sympathetic activity (Vinik et al 2003).

An increased resting HR of greater than 100 bmp and the measurement of the loss of normal HRV due to cardiac denervation is probably the best and the simplest test of the autonomic function (Mackay et al 1980). The ***HR***

response to deep breathing measures the beat-by-beat variation in the HR with breathing. The parasympathetic branch of the autonomic nervous system mainly influences the extent of the HR response to deep breathing. This test has a universal protocol and is considered to be extremely reliable. HR variations of less than 10 bmp and the expiration to inspiration ratio of greater than 1.17 are considered abnormal (Vinik and Erbas 2001).

Type of DAN	Current Diagnostic Tests
Cardiovascular Autonomic Neuropathy	1. HRresponse to deep breathing and standing 2. Valsalva manoeuvre 3. Diastolic pressure response to sustained hand grip 4. Spectral analysis of the HR
Gastro-Intestinal Autonomic neuropathy	1. Scintigraphic imaging of gastric emptying 2. Endoscopic examination 3. Manometric Tests 4. Detailed patient history
Genito-Urinary Autonomic Dysfunction	1. Ultrasound Imaging of bladder 2. Cystometrogram 3. Nocturnal penile tumescence 4. Penile –brachial pressure index measurement using Ultrasound 5. Detailed patient history
Sudomotor Autonomic neuropathy	1. Sudomotor axon reflex test 2. Sympathetic sweat response 3. Thermoregulatory sweat test

Figure 1.3: The current diagnostic tests for DAN

The ***HR response to standing*** measures the cardiovascular response brought about by the change from horizontal to vertical position. Parasympathetic innervations play a vital role in the regulation of the HR due to short-term postural change. Healthy individuals exhibit well-regulated variations in the heart rate. However among diabetics with autonomic dysfunction, this regulatory mechanism is disrupted. The ratio of the maximum HR at the 15^{th} beat to the minimum HR at the 30^{th} beat on standing is calculated and a ratio of less than 1.03 is classed abnormal (Vinik and Erbas 2001).

The **Valsalva Manoeuvre** represents a more complex reflex arc involving the sympathetic and parasympathetic pathways to the heart, the sympathetic pathways to the vascular tree and the baroreceptors in the chest and the lungs (Maser 1998). During the test the individual is asked to blow forcefully into a mouthpiece of an open manometer at a specific resistance of 40mmHg for around 15 seconds while the HR is continuously recorded and monitored using an Electrocardiogram from one minute before the manoeuvre till a minute after (Vinik et al 2003). Throughout the straining, release and recovery segments of the manoeuvre the HR is reported to exhibit well defined changes in healthy individuals (Kalbfleisch and Smith 1978). Since this exercise has both sympathetic and parasympathetic involvement, the Valsalva ratio is a good indicator of the progression of DAN in diabetics.

Sympathetic dysfunction leads to altered pressure response to postural changes and sustained handgrip. The extent of this response is used as a

measure to determine the extent of sympathetic damage due to autonomic neuropathy. A fall in diastolic pressure by more than 10mmHg or a drop in systolic blood pressure of more than 20mmHg within two minutes of standing is considered abnormal. The ***Diastolic pressure response to sustained handgrip*** is also a good indicator of sympathetic dysfunction. The muscle contraction is measured using a dynamometer. The dynamometer is first squeezed to maximum then held at 30% of the maximum strength for next 5 minutes. The muscle contraction causes a rise in systolic and diastolic pressure as well as a rise in the heart rate. An increase in diastolic pressure of less than 10mmHg is considered abnormal. With rapid advancement in technology most of these tests are performed using computerised system and are also simple to use (Vinik et al 2003).

Assessment of GU and GI autonomic dysfunction

Although the symptoms of both the GU and GI autonomic dysfunction are not any major cause of morbidity, they can be debilitating and reduce the quality of life. Tests like endoscopy, scintigraphic imaging and various manometric tests are performed at different levels of the digestive tract to diagnose and analyse GI autonomic dysfunction. Ano-rectal manometry is also performed to evaluate the internal and external anal sphincter tone and the rectal-anal inhibitory reflex that can be damaged due the autonomic dysfunction. Cystometrogram, renal function and urine culture tests are some of the diagnostic tests used to diagnose bladder dysfunction in the event of GU autonomic dysfunction (Vinik et al 2003). The measurement of nocturnal

penile tumescence and vaginal plethysmography are used to diagnose sexual dysfunction in both male and female (Vinik and Erbas 2001).

Though specific tests were available for the assessment of different types of autonomic dysfunctions, they were not considered to be sufficiently well standardised for routine clinical use (Vinik et al 2003). On the other hand CAN diagnostic tests were non-invasive, validated, sensitive and reproducible and therefore formed the core diagnosis of autonomic neuropathy Confirmed diagnosis of autonomic dysfunction was only provided in the event of one or more abnormal CAN tests. The CAN assessment tests, due to its reliability and precision were recommended as the gold standard test for diagnosing autonomic neuropathy (Vinik et al 2003).

Although CAN tests remain the gold standard for diagnosing autonomic neuropathy, they are only reliable once the clinical manifestation of the disease sets in. It is also known that DAN remains asymptomatic until long after the onset of diabetes. Early diagnosis of the autonomic damage is crucial for the delayed progression of the disease and for a better prognosis. Besides these tests are complex and require specialist's skill and equipment to perform. Therefore there is a need for a simple, non-invasive test that can be easily performed in GP surgeries and detect any early microvascular changes due to the autonomic dysfunction.

1.4 Cutaneous Microcirculation

The skin is a highly vascularised organ and its structural and functional complexities indicate its role in several important homeostatic mechanisms. The skin vasculature in general consists of an extensive arteriolar-capillary-venular network, which contains the slow flowing superficial vascular plexus and the deep vascular plexus. The middle layer of the skin known as the dermis consists of an extensive network of arteries, arterioles, capillaries and venules. The capillaries reach close to the skin surface and help in the exchange of nutrients, wound healing and fight infection. Besides this general structure, the cutaneous circulation of the palm, soles of the feet and on the face especially the extremities also consists of special capillary bypasses termed arteriovenous (AV) anastomoses. The cutaneous microcirculation of the soles of the feet was the primary site of interest in this study.

These AV anastomoses are coiled channels with a highly muscular wall and a lumen that connects the arterioles to the venules at the level or slightly superficial to the sweat glands (Frewin 1969). They are a specialised type of vessel that helps blood to bypass the capillary circulation by directly entering the venules from the small arteries and the arterioles. Each shunt consists of an arteriolar portion and a funnel shaped venous portion that terminate in the veins. They possess a small lumen but thick muscular wall. Vascular smooth muscles are attached to the tunica media of the arterioles, the venules and the AV nodes (Levick 2000). The capillaries arising from the small arteries and arterioles do not have any smooth muscles but the pre-capillary

sphincters attached to their point of origin and the venules control the capillary blood flow.

1.4.1 Regulation of Cutaneous Microcirculation

The main aim of peripheral circulation is to regulate the arterial blood pressure and maintain adequate metabolism, temperature and capillary filtration. The terminal arteries, arterioles and the venules are the principle resistance vessels of the body. The regulations of the blood flow though the skin is complex with autonomic fibres controlling both the vascular tone and the local reflexes within the skin. Several factors affect the cutaneous circulation, making it difficult to compute. Temperature regulation is an important function of the cutaneous microcirculation and the short muscular AV shunts play a vital role in the same.

The sympathetic vasoconstrictor nerve fibres innervate the AV anastomoses and these shunts provide a low resistance pathway by which the blood flow can be diverted from the arterioles to the venules, bypassing the capillary network. These shunts are usually maintained in a constricted state by a high sympathetic tone to ensure capillary flow to the skin tissue. But in the wake of any thermoregulatory disturbances this sympathetic tone is lost and the blood is diverted away from the skin.

From the above discussion it can be said that the skin microcirculation has two pathways viz, the capillary bed and the AV shunts (Fagrell and Intaglietta 1997). The capillaries exhibit a higher basal tone and are generally mediated

by local factors. On the other hand the AV shunts are highly innervated entities with little local mediation as they are found to dilate maximally when the nerves are cut off (Rushmer 1976). Both intrinsic and extrinsic factors regulate the cutaneous circulation

The intrinsic factors are those present within the end organ itself. The myogenic response, temperature, metabolites such as nitric oxide (NO) and chemicals generated locally are some of the main intrinsic factors. They mainly help in the local control and in autoregulation. The intrinsic control forms the primary level of control that looks after the needs of the individual organ (Levick 2000). The extrinsic factors control the basal tone from outside the end organ, serve the more general needs of the body and are more central in origin. Neural and hormonal factors belong to this category. While the local factors maintain the local needs of the organ system, the extrinsic factors represent a higher level of control that can modulate or override the local factors for the overall benefit of the individual.

In spite of the presence of several levels of control of the peripheral circulation, there always exists a balance between the intrinsic (myogenic, etc) and the extrinsic (neuro-hormonal) factors (Peter 1978). These controls tend to exhibit a random time dependant behaviour which produces an optimal steady state when averaged over time and space and can be termed as a chaotic process (Intaglietta 1990). This is representative of a healthy system and therefore any abnormal changes in microcirculation could potentially be linked to pathological conditions like diabetes.

Diabetic patients with neuropathic foot are observed to have distended foot veins, raised skin temperatures and increased skin blood flow, both in ulcerated and non-ulcerated foot (DeFronzo 2004). Studies have shown a possible relation between the increased skin blood flow and AV shunting. It is hypothesised that sympathetic denervation could lead to the loss of neural control on the AV shunts, thus opening up the low resistance pathway causing excessive shunting of blood into the venules, bypassing the capillary bed. The skin blood flow represents both the capillary and the AV flow (Shapiro et al 1998).

From the above discussion it can be rightly said that the skin blood flow can be used as a good indicator of the sympathetic activity of the peripheral nervous system. The ability to quantify the extent of sympathetic damage in the cutaneous circulation can provide valuable information in developing new treatment methods, for prevention and better prognosis of diabetic foot disease.

1.4.2 Cutaneous Flow Measurement Techniques

The skin blood flow is a complex entity comprising of both nutritional and non-nutritional flow. Though the skin is the largest and the most assessable organ for the study of microcirculation in the human body, it possesses some inherent limitations. The dual function of nutrition and thermoregulation and the highly unstable character of the skin blood flow make its measurement a challenging task. Both invasive and non-invasive methods have been developed to measure different aspects of the circulation. Doppler ultrasound

and Laser Doppler flowmetry are currently the most popular methods for blood flow measurement (Chittenden 1993).

The ultrasound blood flow meter used to measure the blood flow velocity is based on the Doppler principle. The pulsed wave in combination with colour duplex provides a measure of the mean velocity of the blood within a vessel. The Duplex scan is effectively being utilised to evaluate the blood flow in most parts of the body specially the arms, legs, heart and the neck. This method is currently the forerunner in blood flow measurement techniques and is the closest gold standard test available for blood flow measurement. However this technique has fallen short in measuring skin blood flow, as it involves very small Doppler shift due to the slow moving blood cells within the skin capillary bed.

One of the biggest disadvantages of the duplex ultrasound technique was that it could not be successfully applied to measure the blood flow in the microcirculation. The velocities of the blood cells within the capillaries were significantly lower, in the order of about 1 – 2 $mm.s^{-1}$. Thus the very low Doppler shift frequencies of the order of only a few Hz were extremely difficult to extract resulting in a poor signal to noise ratio. This disadvantage was overcome using light instead of sound waves where the high frequencies of the visible and infrared light were utilised to measure the tissue perfusion using the Doppler principle (Chittenden 1993). Laser Doppler flowmetry had the dual advantages of non-invasiveness and the real time monitoring of the tissue perfusion. However this technique also had several disadvantages.

Motion artefacts, multiple Doppler shifting, biological variations, expensive technology, dependency on the thickness and optical properties of individual skin type and the lack of a universal calibration unit due to the large inter and intra variations in the microvascular physiology were some of the disadvantages of this technique (Chittenden 1993)

The unpredictable nature of the microvascular architecture and physiology had rendered it impossible to compare any two techniques of the skin blood flow measurements at a given time. In spite of the presence of a wide array of techniques, there exists no 'gold standard' method for measuring skin blood flow. Each method investigates a different aspect of the skin microcirculation and has its own advantages and disadvantages. Thus it is vital to pre determine the exact nature of information that is to be extracted for any study before selecting a suitable method. This research project aims to diagnose neuropathy in its early stage by analysing and comparing the vasomotor changes in the microcirculation of the diabetics and the healthy individuals. Continuous research with improved electronics and computing has led to the development of several new measuring techniques. Amongst these the PPG has gained considerable importance for its operational simplicity, ruggedness, simple electronics and low cost. PPG is a non-invasive optical technique for measuring tissue perfusion. This study aims to investigate the cutaneous circulation using PPG and hence it has been dealt in great detail in the next few sections of this chapter.

1.5 Photoplethysmography (PPG)

Plethysmography is defined as a technique that measures any change in volume. It is derived from the Greek word *plethysmos*, which means to enlarge (Creager et al 1992). The history of PPG goes back to over 70 years. In 1938 Hertzman first discovered the relation between the intensity of the reflected light and the skin blood volume (Neumann and Maessen-Visch 1999). His device consisted of a light source, detector and an analyser and was used to record the arterial pulsations in the skin. In 1970's PPG was first used in the examination of the peripheral venous circulation (Blazek et al 1996). With increased application several potential sources of errors were reported such as the errors due to the incorrect positioning, skin contact, skin movement or the type of light source used (Allen 2007). The technical difficulties in calibrating and in the quantitative analysis of the measured data further limited its applications (Blazek et al 1996) . It was however the advancement in semiconductor technology, computing power and clinical instrumentation that led to the re establishment of PPG (Allen 2007). Blazek's and Schultz – Ehrenburg's group devised a self-calibrating system using the modern computing technology that lead to PPG's widespread application as a vascular diagnostic tool (Blazek et al 1996).

1.5.1 Working Principle

PPG is an optical technique that consists of a light source and a photosensor. Modern PPG sensors use low cost light emitting diodes (LED) and appropriate photodetectors working at the red or the near infra-red (IR)

wavelengths (Allen 2007). The LED and the photodetectors can be placed either on the same side of the skin surface under investigation or opposite to each other. Depending on the position of the source and the detector PPG probes can be classified into two functional modes. When the tissue under investigation is placed between the light source and the detector as shown in figure 1.5, it is known as the transmission mode and is widely used to investigate certain areas of the body with limited width e.g. fingers, ear lobe, etc. In this arrangement the detector receives the light after being transmitted through the tissue of interest. However, this kind of arrangement has its own limitation and cannot be used to measure skin blood volume for most parts of the body. When both the emitter and the detector are placed on the same side of the skin being measured it is known as the reflection mode. This arrangement is illustrated in figure 1.4. In this mode the incident light undergoes attenuation within the different tissue layers before being reflected back on to the detector. The intensity of this reflected and back scattered light is measured and the variation in the photo-detector current thereby produced is assumed to be related to the blood perfusion changes under the probe (Oberg and Lindberg 1991).

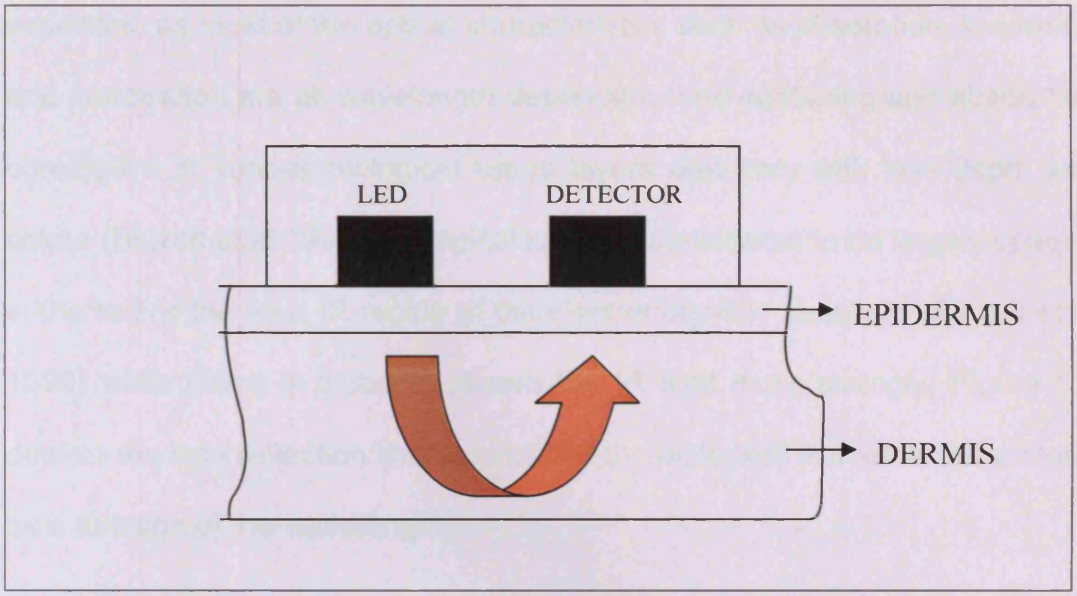

Figure 1.4: Reflection mode PPG

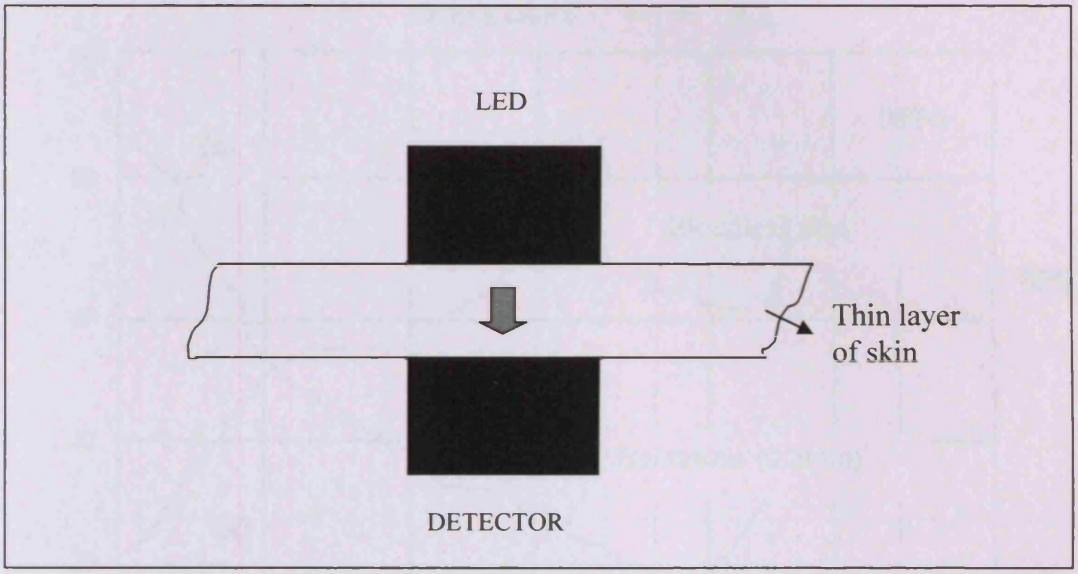

Figure 1.5: transmission mode PPG

The working principle of PPG is based on the optical properties of the skin. The light photons incident on the skin undergoes reflection, absorption, scattering, transmission and collision as they pass through the various layers of the tissue (Allen 2007). The choice of an appropriate wavelength is very

important, as most of the optical characteristics such as absorption, scattering and penetration are all wavelength dependant. The scattering and absorption co-efficient of various biological tissue layers also vary with skin depth and colour (Blazek et al 1996). Biological tissue is considered to be largely opaque in the red or the near IR region of the electromagnetic spectrum (Blazek et al 1996) while blood is found to absorb the IR light more strongly. Figure 1.6 depicts the light reflection characteristic of the biological tissues and the blood as a function of the wavelength.

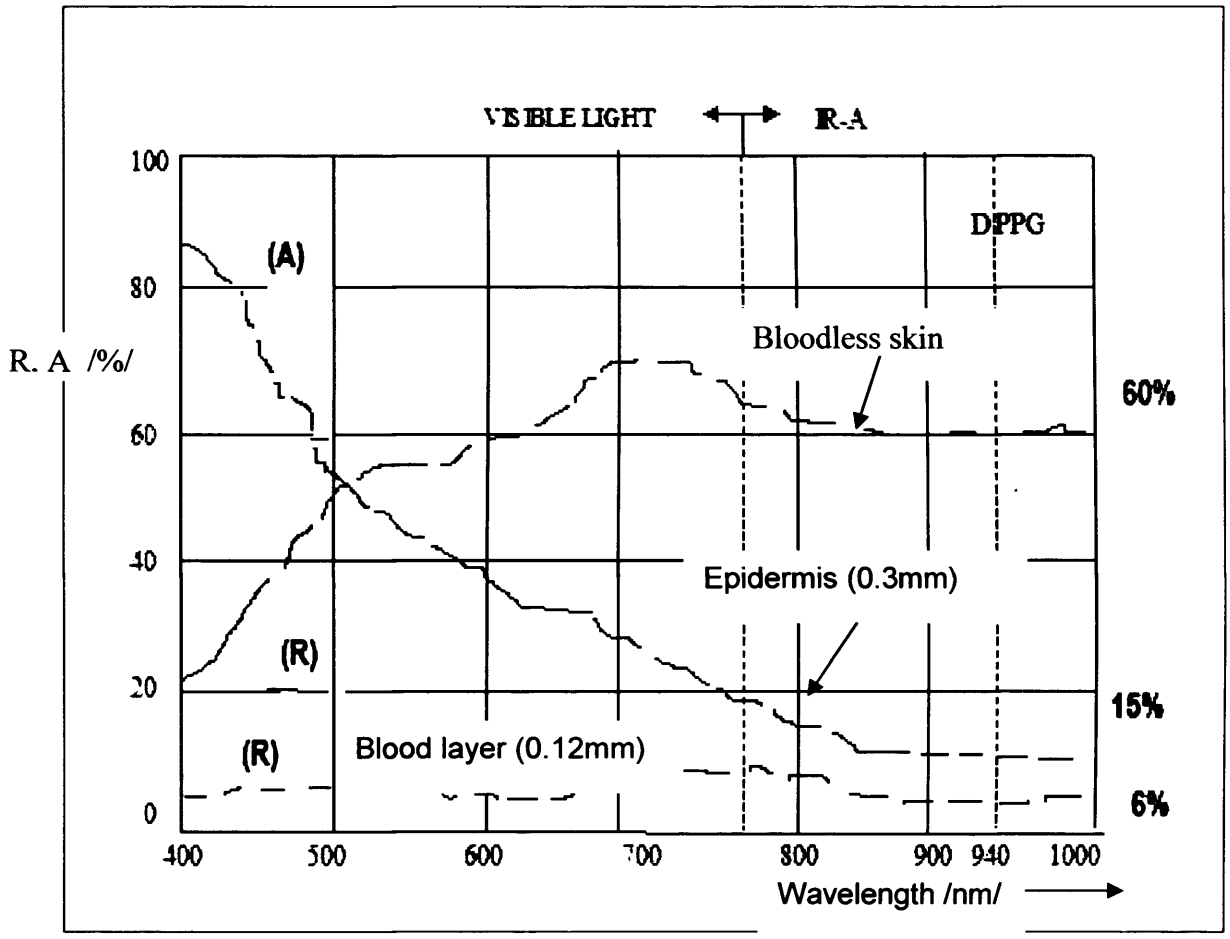

Figure 1.6: Light reflection (R) characteristics of the blood and the bloodless skin and light absorption (A) characteristic of the epidermis. Note that the light at the optimum wavelength 940nm is reflected from the bloodless skin 10 times more than the blood (Blazek et al 1996).

From the figure it can be rightly inferred that biological tissue without any blood reflects light many times greater than the blood. However between 780 nm and 940 nm this difference is found to be maximal and is also known as the favourable measurement window for optical sensing (Blazek et al 1996). Higher wavelength also has greater penetration into the tissue layers. The oxygenated and deoxygenated blood have different absorption coefficient for wavelengths less than 805nm (Allen 2007). Thus most modern sensors use LED of around 900 nm wavelength to achieve the maximal difference in the absorption characteristics of tissue and blood, the minimal difference in the absorption characteristics of oxygenated and de- oxygenated blood, and for the optimum skin penetration.

The PPG probe senses the blood volume change by measuring the amount of light reflected back onto the detector. An increase in the blood volume due to dilatation of the blood vessels results in increased absorption of light. The amount of light received by the detector decreases and hence a decrease in the PPG signal is registered. The reverse holds true during a decrease in the blood volume due to constriction of the blood vessels. Modern PPG sensors have a penetration depth of up to 4mm. This not only helps to detect the nutritional capillary flow but also provide valuable information on the deep vascular plexus containing the AV shunts, an area responsible for peripheral haemodynamic (Blazek et al 1996). Both the light source and the detector used in modern PPG probes are compact, low cost, mechanically robust, and reliable and have a fast response time (Allen 2007).

In a typical PPG measurement, of the total amount of light received by the detector, about 90% is estimated to be directly reflected back from the skin surface and the static biological tissues, 10% from the venous blood volume and only 0.1% from the oxygenated arterial blood volume. Thus a typical raw PPG signal consist of a large permanent offset from the static bloodless tissue layers, a slow moving DC (direct current) component and a pulsatile AC (alternating current) component (Blazek et al 1996). The pulsatile AC component is found to be superimposed on the slow moving DC component and the latter usually has amplitude of 1-2% of the former (Oberg and Lindberg 1991). The slow moving DC component provides information regarding the total blood volume change within the skin microcirculation and represents the total amount of blood pooling or blood flow under the detector. The AC component represents the blood volume change for every pulse due to the pumping action of the heart. Much of the skin has poor pulsatility but the pre capillary activity is present throughout. Both the gross volume change and the pulsatile change are closely related to the autonomic activity of the body and the combined information from the AC and the DC components provide a clearer understanding of the vascular changes in the skin microcirculation (Kamal et al 1989). Being a relatively inexpensive, non invasive and non traumatic technique, makes PPG a popular vascular diagnostic tool (Kamal et al 1989)

1.5.2 Limitations of PPG

The signal detected by the PPG is dependent on several factors such as the location of measurement, skin properties of the individual being measured,

environmental factors, movement artefacts, oxygen saturation of the blood, blood flow rate, and the initial blood volume under the probe. The reproducibility of such a measurement technique was also affected by factors such as method of probe attachment, movement artefacts, posture, relaxation, room temperature, breathing, wakefulness and acclimatisation. There are no international standards set for a photoplethysmographic measurement thereby limiting the replication of the study between research centres (Allen 2007). These limitations hindered the use of PPG as a diagnostic tool for many years. A study conducted by Jago and Murray (1988), stressed on the importance of taking bilateral measurements as they tend to be more repeatable than an individual site measurement (Allen 2007).

1.5.3 Quantitative Photoplethysmography

Of the various factors, the dependency of the PPG signal on the skin characteristics of an individual being measured was its greatest limitation. The optical properties of the skin were observed to depend on factors such as degree of pigmentation and its thickness. Besides, the amount of light received by the photo detector was also dependent on the degree of initial skin perfusion at the site of measurement. Thus a same amount of blood volume change could produce different PPG signals in different individuals due to the variation in their skin characteristics making it practically impossible to produce a quantitative measure of the blood volume change that was comparable with measurements from different individuals.

This further limited its use as a popular diagnostic tool for several years till the introduction of the quantitative PPG by Blazek and Schultz – Ehrenburg. This

involved an automated electronic calibrating system that used an optical closed loop measuring principle controlled by a microprocessor. This enabled the calibration of the signal before every measurement. Thus instead of using a uniform amount of optical radiation for all skin types, the amount of optical light incident was altered using the optical loop principle till a desired baseline of the PPG signal was obtained before every measurement. This ensured a constant starting value for every measurement that was both reliable and reproducible for every skin type. The quantitative PPG revolutionised its use as a diagnostic tool. The automated calibration helped to achieve a uniform initial reflection value irrespective of the individual skin characteristics and made intra individual comparisons of the PPG signals possible. Greater control on the measurements with signal storage possibilities along with quantitative and precise analysis of the measured data was made possible with the introduction of the quantitative PPG (Blazek et al 1996) .

1.5.4 Application of Photoplethysmography

PPG has been widely used in clinical physiological monitoring and various vascular assessments. The blood oxygen saturation measurement is regarded as one of the most significant contributions of PPG. Other physiological parameters that are monitored using PPG include beat-by-beat heart rate, pressure and respiration. The pulsatile AC component of a PPG signal represents the heartbeat. Complex computer algorithms have been developed to use this information to detect the beat-by-beat HR of an individual and have found its use in hospital based and ambulatory patient monitoring systems. The skin vascular changes influenced by the breathing

cycle can be monitored using PPG (Allen 2007). It has also been successfully used to measure both the arterial and venous circulation. The slow moving DC component of the PPG signal represents the total amount of blood pooling under the probe and this provides vital information of the venous circulation.

Studies have also been conducted to look into the feasibility of using the photoplethysmographic technique in the autonomic function assessments. In this project we aim to use PPG to study the vasomotor responses obtained from the soles of the feet of both healthy and diabetic patients with and without any known neuropathy.

1.6 Diabetic Foot Disease

Ulceration below the knee is a common complication of diabetes with a lifetime risk of its occurrence among diabetics estimated at 15% (Kenneth and Cummings 2005). Diabetic foot disease not only complicates and reduces the quality of life for the patients but also has a huge economic impact on the health care system. If left untreated the ulcerations could become infected and gangrenous and finally lead to amputations. In the UK 5000 diabetics are estimated to have amputations every year. Foot ulcers precede more than 80% of non-traumatic lower limb amputations (Boulton et al 2000).

The international consensus on diabetic foot defines a diabetic foot ulcer as a full thickness wound below the ankle in a patient with diabetes, irrespective of duration (Boulton et al 2000). There is no one universal method of classifying ulcers and all diabetic ulcers are commonly known as diabetic foot disease.

However the most widely used system grades ulcers on the extent of damage. The lowest being grade 0, which indicates pre ulcerative lesion. Untreated grade 0 ulcers could spread the infection from the outer skin, through the various tissue layers into the bone resulting in osteomyelitis. At this stage the ulcer becomes necrotic causing gangrene, a grade 4 ulcer. The final stage or grade 5 is when the whole foot becomes gangrenous and has to be amputated (Boulton et al 2000).

Diabetic ulcers have a very poor prognosis and the recurrence rate is very high. The principal risk factors for developing diabetic foot ulcers are duration of diabetes, presence of neuropathy and peripheral vascular disease, prior ulcers and prior amputations. The preoperative mortality rate of amputation within the UK was estimated to be around 10% to 15% with the median survival duration being 2 to 5 years. The recurrence rates of foot ulcers were reported to be around 35% to 40% in the first 3 years and as high as 70% over 5 years (Boulton et al 2000).

1.6.1 Pathogenesis of ulceration

Pathogenesis of diabetic foot disease is a complex interaction of various risk factors and environmental hazards around the patient that can potentially lead to lower limb amputations as shown in figure 1.6. Diabetic ulcers have an insidious onset and the progression from a minor trauma to gangrenous foot occurs in several stages. It has been observed that the primary risk factors for ulcerations like peripheral vascular disease and diabetic neuropathy very rarely can cause ulceration individually; rather it is a combination of these risk

factors and some minor trauma that leads to the breakdown of the diabetic foot (Boulton et al 2000).

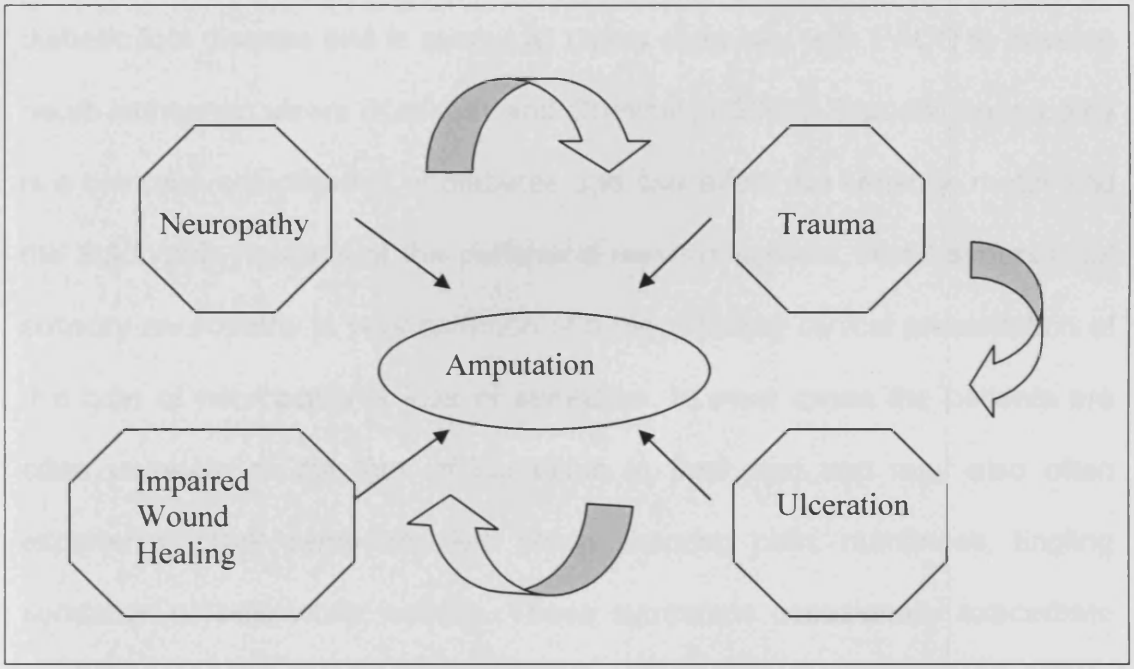

Figure 1.6: Pathway to the lower limb amputation in diabetics

The risk of developing peripheral occlusive arterial disease (POAD) is two to three folds amongst diabetics as compared to the non-diabetics (Hittel and Donelly 2002). POAD occurs in the early stages of diabetes and affects the peripheral blood vessels. It is a macrovascular complication of diabetes where the distal vessels become artherosclerotic causing narrowing of the large distal vessels and thereby heavily compromising the blood supply to the extremities. A minor trauma followed by infection in the feet, considerably increases the demand for blood supply. In the event of blocked peripheral arteries this excess demand cannot be met and hence the process of wound

healing is delayed. This condition is followed by ischaemic ulceration and if left untreated ultimately leads to amputation.

Diabetic neuropathy is another major risk factor for the development of diabetic foot disease and in almost all cases combines with PAOD to develop neuro-ischaemic ulcers (Kenneth and Cummings 2005). Diabetic neuropathy is a common complication of diabetes and can affect the sensory, motor and the autonomic neurons of the peripheral nervous system. Distal symmetrical sensory neuropathy is very common and the principal clinical presentation of this type of neuropathy is loss of sensation. In most cases the patients are often unaware of the loss of sensation in their feet and may also often experience other symptoms like sharp shooting pain, numbness, tingling sensation or pain while walking. These symptoms occasionally exacerbate during the night.

Due to the loss of sensation of the feet, the patient may suffer from trauma and be completely unaware of it. Little or no pain or sensation can lead to the neglect of the wound and in some cases the patient may suffer from multiple traumas. The increased duration of wound healing among diabetics coupled with neglect can cause infection that often leads to ulceration of the foot. The damage to the motor neurons causes extensive muscle wastage and foot deformities. This could alter the pressure distributions and cause abnormal pressure loading at the metatarsal heads. Pressure ulcers tend to occur mainly at the metatarsal heads due to repetitive pressure application while walking (Levin and Bowker 1993). Presence of peripheral sympathetic

autonomic neuropathy can further aggravate the risk of ulceration. The skin under the foot becomes very dry and thick and callus tissues develop as a consequence of sympathetic neuropathy, thus putting the diabetic foot at a greater risk of ulceration.

Microvascular dysfunction among diabetics may not directly cause ulceration but there is sufficient evidence to link this to delayed wound healing among diabetics. Sympathetic dysfunction in the skin causes increased shunting of blood through the AV shunts. This leads to decreased capillary flow and hence to a decreased tissue nutritive flow. This is one of the few possible explanations for delayed wound healing among diabetics. Some of the other risk factors include age, duration and severity of diabetes and prior foot ulceration. The risk of ulceration and amputation is found to increase two to fourfold with both age and duration of diabetes (Levin and Bowker 1993). Studies have revealed that the rate of the re-occurrences of diabetic foot ulcers is often very high amongst diabetics and is one of the risk factors for its development (DeFronzo et al 2004).

Sympathetic dysfunction is one of the major components in the pathway to diabetic ulcerations. Sympathetic dysfunction is also known to cause alterations at the microvascular level. Several studies have been conducted to study the microvascular changes under pathological conditions like diabetes. In the next chapter I have reviewed some of the studies relevant to this project.

Chapter II

Literature Review

2.1 Introduction

DAN is a complex disorder with multiple causative mechanisms that cause wide spread damage to the whole of the autonomic nervous system. A combination of metabolic and microvascular dysfunction causes damage to the nerve fibres. The complete understanding of the pathogenesis of DAN and its affects on skin microvasculature was vital for the development a screening tool. Besides, several studies have been conducted over the years looking at the various methods of analysing the skin microcirculation under pathological conditions. A detailed literature review on the pathogenesis of this diabetic complication along with previous work done in analysing skin microcirculation for the diagnosis of DAN has been discussed in this chapter.

2.2 Pathogenesis of DAN

In spite of several studies conducted worldwide, the exact pathogenesis of DAN still remains unclear (Tooke 1995). It is suggested to be a multifactorial disease where several factors combine to damage the autonomic nervous system. Progression of this disease can be explained in three stages. The initial stage is that of functional neuropathy where biochemical alterations in

the nerve function occurs with no visible pathology. This is a reversible condition, which is followed by structural neuropathy. Here the structural loss of nerve fibres is observed and this stage is also found to be reversible. The final irreversible stage is that of nerve death, where a critical decrease in the nerve fibre density is observed leading to neuronal death (Vinik 2002). Poor glycaemic control, prolonged duration of diabetes, increasing age, and a higher BMI was found to have a profound negative impact on the progression of DAN.

Similar to other microvascular complications of diabetes, hyperglycaemia can cause structural and functional alterations to the nerve cells and the adjoining neurovasculature (DeFronzo et al 2004). The autonomic nervous system and the microcirculation have strong physiological co dependence. The microcirculation relies on the autonomic branch for its normal functioning while the autonomic nervous system relies on the microcirculation for the nutritive flow. It has been suggested that both microvascular dysfunction and neuropathy occur early in diabetics and forms a potential pathogenic vicious cycle where damage to the peripheral nerves disrupts the auto regulatory function of the microcirculation and damage to the latter cause's neural hypoxia leading to further nerve degeneration (Kilo et al. 2000).

Several hypotheses regarding the pathogenesis of DAN have been put forward based on studies carried out in this field. The aetiological factors suggested by these hypotheses include hyperglycaemic activation of the polyol pathway, advanced glycosylation, generation of free radicals and

oxidative stress, neurovascular insufficiency, autoimmune damage and neurohormonal growth factor deficiency. Almost all these complex process occurs at a cellular level. In healthy tissues at cellular level the redox (reduction – oxidation) homeostasis is always maintained and hence the accumulation of **r**eactive **o**xidative **s**pecies (ROS) like O_2^- and H_2O_2 is prevented. But under pathological conditions like diabetes, this homeostasis is lost and hence an increased accumulation of ROS will lead to an increase in the **oxidative stress**. This rise in oxidative stress causes endothelial damage of the microvessels and structural damage to the neurons (DeFronzo e al 2004).

Another popular hypothesis suggests the activation of the **polyol pathway** at the cellular level when exposed to long-term hyperglycaemia (DeFronzo et al 2004). In this pathway the first half of the reaction converts the excessive cellular glucose to sorbitol and the second half converts this sorbitol to fructose. At each half of the reaction, nicotinamide adenine dinucleotide phosphate (NADP) was generated from its reduced form, NADPH. The increased activation of the pathway under hyperglycaemia caused excessive accumulation of sorbitol and fructose within the cell, as these substances were found to be relatively impermeable through the cell membrane. Besides, a reduction in the NADPH to NADP ratio was also observed during the first half of the pathway. A decrease in the NADPH concentration within the cell interrupts the NO synthesis causing excessive concentration of the oxygen free radicals. These toxic substances cause damage to the endothelial lining of the vessel wall. The second half of the pathway causes the acceleration of

advanced glycosylation due to increased fructose production. The accumulation of the end products of the advanced glycosylation reaction also causes damage at the cellular level. Thus we can see how a combination of these factors can cause widespread structural damage to the neuro-microvasculature especially in the form of endothelial dysfunction among diabetics.

As mentioned earlier the pathogenesis of DAN involves damage to both the nerve cells and the neurovasculature. Besides, damage to the autonomic system also causes wide spread damage to the microcirculation. The study of the evolution of diabetic microangiopathy is a complex process as the progression of the disease varies with the type of organ bed involved and also with the type and severity of diabetes. However it can be studied under an initial functional stage and then a structural stage. The initial functional stage is a reversible stage with controlled glucose level, while the latter involves structural remodelling of the microvasculature ultimately leading to microvascular failure.

The **"haemodynamic" hypothesis** is another well-known hypothesis that could provide a possible insight to the mechanisms of diabetic microangiopathy (Tooke 1995). The semi rhythmic contraction/dilatation of the arterioles helps to produce an economic flow through the capillary units at a controlled rate thereby increasing the efficiency of the capillary bed. Reserve channels are present for use when needed. Early measurements of the blood flow in the vascular beds reveal an increased perfusion, which forms the basis

of the haemodynamic hypothesis. According to this hypothesis, early diabetes is characterised by increased microvascular flow. This increased perfusion can cause shear stress and tangential pressure on the vascular endothelium leading to tissue injury. As a response to tissue injury accumulation of extracellular matrix occurs resulting in endothelial basement thickening. This causes a decreased vasodialatory capacity of the blood vessel in times of increased flow demands and also may interfere with the flow autoregulation. The vasodialatory capacity was found to decrease with the increased severity and duration of diabetes. The pathogenic mechanism of diabetic microangiopathy was found to vary with the type of diabetes. Unlike Type 1 diabetes where the haemodynamic hypothesis holds well, Type 2 early diabetes is characterised by a normal flow. Here the occurrence of arterial hypertension profoundly decreases the vasodialatory reserve (Fagrell and Intaglietta 1997).

As per the various hypotheses proposed, changes in the microvascular flow occur with autonomic dysfunction. Increased shunting of blood flow through the AV shunts bypassing the capillaries due to sympathetic denervation was observed in diabetics. These specialised vessels called the AV shunts that are completely innervated by the sympathetic branch of the autonomic nervous system are found in abundance in the skin microcirculation. Thus of all the microvasculature, the skin microcirculation should mainly respond to any autonomic dysfunction that occurs within the body.

2.3 Vasomotion

Vasomotion is another physiologically important characteristic of the microcirculation. Microvasculature is markedly different from the large vessels of the body as it has specific roles like pressure regulation and delivery of nutrients to the organ bed. While the second and third order arterioles of the microvasculature respond to changes in the local pressure under myogenic control, the lowest order of arterioles and capillaries ensures autoregulation of the flow under sympathetic control. As mentioned earlier the vascular bed is a highly innervated entity and is under sympathetic control. They play a vital role in regulating blood flow by opening and closing of the AV anastomoses and capillary arterioles (Lefrandt et al 2003). Hence damage to these nerves in pathological conditions like diabetic neuropathy, can cause disruptions to the regulated blood flow. The flow through the microcirculation has been observed to be chaotic with only a fraction of the capillary units being perfused at a time under resting conditions (Wiernsperger 2001). Generally the capillaries are arranged into units being fed by a single arteriole. The sympathetic nerves control the anastomoses of these arterioles in a semi rhythmic manner and the phenomenon is called ***vasomotion*** (Stansberry et al 1996).

Vasomotion can be defined as oscillations of vascular tone generated from within the vascular wall (Nilsson and Aalkjaer 2003). In spite of several years of study the exact mechanism of the generation of these oscillations still remain unclear. Vasomotion is the spontaneous semi rhythmic oscillations of the diameter in the arterioles and venules. These semi periodic changes in

the diameter of the blood vessels enable the supply of nutritive blood to the tissues in an economic fashion. As per the Poiseuille's law, the resistance of the vessel whose diameter changes in a sinusoidal manner is less than that of a vessel of fixed diameter (Shapiro et al 1998).

Thus vasomotion helps to decrease the total vessel resistance, there by increasing local flow and proper perfusion of the tissues. Vasomotion has been a difficult entity to measure due to its unpredictable nature. Besides it has been non repeatable and difficult to replicate under in-vitro conditions. While some debate the occurrence of vasomotion only under pathological conditions, other studies have revealed the presence of vasomotion under normal conditions. Several factors contribute to the exact occurrence of this phenomenon. However current studies have revealed the presence of vasomotion at all times with a decreased activity under pathological conditions (Wiernsperger 2001).

Vasomotion is a local activity, with unsynchronised signals contributing to its chaotic appearance. Some of the factors that influence this phenomenon include neural, chemical or transmural pressure. The sympathetic control of vasomotion could be either through periodic nerve discharges or through facilitations of an endogenous vascular pacemaker. The neural influence on vasomotion can be reinstated as this phenomenon is completely eliminated under anaesthesia (Bernardi et al. 1997).

Whatever may be the exact mechanism of its occurrence, vasomotion was found to be of profound functional importance. Its functions include delivery of blood to the tissues in an economic fashion, to ensure a local pressure for blood flow, the transmural exchange of fluids and cyclic contraction of the lymphatics. The decreased effective vessel resistance due to vasomotion was found to increase the blood flow thereby providing proper tissue perfusion and oxygenation (Nilsson and Aalkjaer 2003).

2.3.1 Pathophysiological Role of Vasomotion

There is sufficient evidence that the phenomenon of vasomotion is disrupted under pathological conditions, particularly in diabetics with autonomic neuropathy (Wiernsperger 2001). Tests conducted revealed a significantly reduced vasomotion in both Type1 and Type 2 diabetics at rest. These abnormalities were found to be present as early as in pre diabetic stages. Stansberry et al observed a marked decrease in the amplitude of vasomotion in the finger to about 20% among both types of diabetics and thereby concluded that vasomotion was impaired in 75% of diabetics (Nilsson and Aalkjaer 2003).

Diabetic microangiopathy was reported to affect most capillary beds in a similar pattern (Rendell et al 1989). As mentioned earlier the skin microvascular bed was found to be most accessible, hence was extensively studied using several techniques, which included video microscopy, venous occlusion plethysmography and Laser Doppler flowmetry. The extremities were considered as desirable sites for the study due to its easy accessibility

for the placement of probes and also as they tend to have a higher density of AV anastomoses under sympathetic control. In one study the nail fold microcirculation was analysed by measuring the blood velocity using a dual window television automatic estimating system (Yuan et al 1999). Their results showed a marked decrease in the middle, high and ultra high-speed peaks in the blood flow indicating microcirculatory disturbances among diabetics.

Diabetic neuropathy resulting from the neurosensory loss may cause the Charcot Joint leading to deformity of the bones and loss of sensation. Shapiro, et al in their study examined the possible relationship between the Charcot Joint and vasomotion at the dorsum of the foot. Here the blood flow was measured using a Laser Doppler flowmetry with local skin warming. The signal obtained was subjected to Fast Fourier Transform (FFT) to obtain the vasomotion index. Both the vasomotion as well as the blood flow velocity was considerably increased in healthy individuals and patients with the Charcot foot under locally increased temperature. However both the pattern of vasomotion as well as the blood flow velocity was severely distorted among diabetics with neuropathy alone. It is still unclear as to why the Charcot foot despite being one of the manifestations of diabetic neuropathy shows healthy vascular responses. However the author is suggestive of the fact that his results might be an indication of vasomotion as an autonomic entity (Shapiro et al 1998).

In their study, Shapiro et al, 1998 did a three-way comparison of healthy controls, diabetics with neuropathy but no Charcot deformity and diabetics with both neuropathy and Charcot foot. Here the two groups of the diabetic patients were age matched but they were not age matched with the healthy controls. In this study I had also aimed to make a three-way comparison between healthy controls, diabetics with no neuropathy and diabetics with neuropathy. Also the two groups of the diabetic patients in my study were age matched, but the healthy controls had a much younger age range. The diabetic patients with and without Charcot arthropathy in this study were classed as moderately to severely neuropathic only after a detailed sensory and autonomic function testing using the standard tests available. The study was unable to explain the similarities in the result obtained from the normal and the patients with Charcot arthropathy, although they belonged to the two extremes of the disease spectrum. However their conclusion of vasomotion as an autonomic entity was highly relevant to my study

In another study the arteriolar vasoconstriction was observed to be defective in both the pre diabetic as well as in the advanced diabetic stages (Wiernsperger 2001). The microcirculation mostly was studied using the Laser Doppler flowmetry or the venous plethysmography (Eicke et al 2003). However Eicke et al used an alternative technique of continuous wave Doppler sonography to assess the vasomotor responses in the radial artery. They calculated a resistance index as an indicator to the vasomotion activity by measuring the mean blood flow velocities at the radial arteries of 25 diabetic patients with the diabetic foot syndrome. Their data suggested the

existence of decreased vessel elasticity among the diabetics with autonomic neuropathy, perhaps due to the presence of endothelial dysfunction of the autonomic vasomotor system as mentioned in the previous section (Eicke et al 2003). This study compared the Doppler results from the patient group with their nerve conduction velocities to evaluate potential correlation between the autonomic and the somatosensory system. Results indicated a decreased vasomotor response in most of their patient group although they were diagnosed with moderate to severe sensory neuropathic. This conclusion was relevant as in my study the patient group were selected mainly on the basis of their vibration perception threshold (VPT) scores.

Lefrandt et al in 2003 recorded the blood flow velocity oscillations using a laser Doppler flowmetry at the median ankle. They studied the sympathetically mediated vasomotion by determining the power spectrum of the recorded data. The LF components between 0.02-0.14 Hz were most affected by postural stimulation and anaesthetics thereby suggesting their representation of vasomotion. The total power of the LF components of the blood flow velocity spectrum i.e. the vasomotion amplitude was considerably reduced in diabetics with neuropathy as compared with that of healthy individuals. Their study once again demonstrated abnormalities in sympathetic modulation in diabetic patients with autonomic neuropathy (Lefrandt et al 2003).

The characterisation of the subjects recruited for this study was excellent. Lefrandt et al, 2003 in their study had three groups similar to my research project. They were the control group, diabetics with no neuropathy and

diabetics with peripheral sensory neuropathy. The groups were individually matched for age, sex and the BMI index. The diabetic groups were also matched for the type of diabetes. The protocol used for my study was largely based on the study protocol used by Lefrandt et al, 2003. However once again this group similar to the previously discussed study assessed their neuropathic subjects only for the peripheral somatosensory dysfunction and not their autonomic function. The results once again indicate that the sympathetically mediated vasomotion decreases with the sensory motor neuropathy.

A few years prior to Lefrandt et al, similar study was also conducted by Bernardi, et al (Bernardi et al. 1997). They suggested that the spectral analysis of the Doppler data would provide precise quantitative identification of the different sources of the fluctuations present within the signal. They observed the presence of at least two main sources of fluctuation within the power spectrum of the Doppler signal. The lower frequency components of the range 0.1Hz was found to be influenced by the sympathetic control and the higher frequency components between 0.18 Hz and 0.40 Hz linked to respiration, was found to be mostly independent of the sympathetic tone. Results from twenty-three controls and diabetics were compared and one of their principle exclusion criteria was the absence of any clinical manifestation of DAN. The microvascular fluctuations studied using the Doppler signal was also compared with the standard autonomic function test results obtained from the subjects. Some interesting and useful conclusions were drawn from this study. Firstly, reduced LF fluctuations were observed in diabetic patients.

This decreased response was not only obtained from patients with or more altered CAN tests, but also in those with normal cardiovascular reflexes and therefore extrapolated their results to conclude the possibility of impaired vasomotion as an early index of autonomic neuropathy among diabetics. Secondly this study also indicated a significant influence of age on the amplitude of both the LF and HF fluctuations.

A similar study was also conducted by Meyer et al, where they analysed the vasomotion by laser Doppler anemometry (Meyer et al. 2003). In this method a highly focused beam of about $10\,\mu m$ diameter was used to measure the blood cell velocity in single capillaries and hence unlike the laser Doppler flowmetry the rhythmic variation of the blood cell velocity caused due to vasomotion was visible directly without the spectral analysis of the signal obtained. The velocity of the blood cell was directly proportional to the Doppler frequency shift of the reflected Laser beam. The pulsatile component corresponding to the HR was removed from the Doppler signal using an appropriate filter. Along with the assessment of vasomotion the test subjects were also assessed for CAN using the standard tests that included the Valsalva manoeuvre, the HR response to deep breathing and the HR variability test. They were also assessed for sensory neuropathy, retinopathy and nephropathy. Impaired vasomotion was diagnosed if the amplitudes of the signal obtained were two standard deviation below the mean value obtained from normal individuals. Their study revealed the existence of impaired vasomotion in 90% of Type 1 diabetic patients with one or more altered CAN tests and in 40% of those with normal CAN assessment results.

The latter results help to justify the hypothesis that the disruption in the vasomotor responses in the microcirculatory flow of the skin may be an early disturbance in the natural history of the disease. Their data indicates that the impairment of the 0.1 Hz vasomotion which corresponds to sympathetic dysfunction precedes the parasympathetic dysfunction assessed by the various CAN tests and there by can be considered as an early index of peripheral sympathetic dysfunction amongst diabetics. Bernardi, et al 1997 and Meyer et al 2003 drew similar conclusions from their study but used different methods to study the skin microcirculation. They both concluded the impairment of the LF fluctuations in the diabetics with one or more altered CAN tests and also in some patients with normal CAN results. However this group could not establish any correlation between the impairment of sensory threshold and autonomic dysfunction.

Most studies reviewed so far have established vasomotor responses as an autonomic entity (Shapiro et al). Reduction in these responses was observed in diabetic patients with abnormal cardiovascular reflexes (Lefrandt et al) and sometimes also in diabetics with normal CAN test (Meyer et al, 2003) (Bernardi et al). Studies have also suggested the possibility of sympathetic dysfunction occurring together with sensory neuropathy. These results further strengthen the possibility of observing altered vasomotor responses from the neuropathic group recruited in this study in spite of recruiting them mainly on the basis of their VPT scores. Review of these studies has also provided vital information regarding the spectral make up of the various signals obtained

from the skin where the different frequency fluctuation peaks were matched with specific physiological process of the body.

2.4 PPG and Autonomic Function Tests

PPG is an optical technique that has been widely used in clinical physiological monitoring and various vascular assessments. Only limited studies have been conducted to look into the feasibility of using the photoplethysmographic technique in the autonomic function assessments. The skin microcirculation is a complex entity. The raw PPG signal contains both LF and HF information. While the LF information represents respiration, blood pressure regulation and thermoregulation, the HF components represent the cardiac activity of the individual (Kamal et al 1989). These physiological functions are indicative of the autonomic activity of the body and hence could potentially be used for autonomic function testing. The very small frequency components and the spontaneous fluctuations of the PPG signal represent the vasomotor activity of the microcirculation. These relate to the sympathetic activity of the body and this is further corroborated by the decrease of these components under anaesthesia (Buchs et al 2005).

In a study by Barron, et al work was done on comparing and analysing the DC component of the PPG signal obtained from the response of the finger vasculature to standard tests of vasomotor function. The main aim of this study was to detect the changes in the vasomotor responses in the skin vasculature using PPG and attempt to analyse the role of PPG in early diagnosis of the diabetic neuropathy. Conducting simultaneously standard tests for the assessment of diabetic neuropathy and comparing the two

achieved the latter part of the aim. Here due to the variability in the PPG signal amplitude even among the healthy individuals, the results were regarded as abnormal only under total absence of the signal. In this study, patients with abnormal PPG signals were found to have at least one abnormal cardiovascular assessment test. Since the DC component of the PPG signal represented the volume content, a sudden change in the blood volume caused due to a sudden inspiratory gasp, or ice water immersion, was clearly exhibited by the PPG signal. PPG was chosen for the study due to its operational simplicity and cost effectiveness (Barron et al. 1993). This study was of particular interest because of the similarities in the aim of this group and my research project. They conducted this study to assess the potential role of PPG in the evaluation of diabetic sympathetic neuropathy. They too tried to analyse the results by having a three-way comparison between healthy controls, diabetics with no neuropathy and diabetics with known autonomic dysfunction. The healthy controls and the diabetics with no autonomic dysfunction were assessed for both autonomic and somatosensory function. Barron et al, 1993 in their study however used a transmission PPG and the site of interest was the index finger. Besides, they only performed visual analyses of the signal looking into the amplitude variability as responses to several external stimuli. In my study the analysis of the PPG signal was to include both visual and spectral analysis and this is where the next study reviewed was hugely relevant.

This study by Bernardi, et al the autonomic control of the microcirculation was closely assessed using the power spectrum of the photoplethysmographic signals. Several factors of both local and central origin were found to control

the PPG signal from the skin microcirculation giving it a chaotic appearance. These frequency components were analysed using spectral analysis. An infrared photoplethysmographic probe was used for the purpose. Apart from the PPG signal, the ECG, respiration and the blood pressure were also recorded for a 4min period in supine and in active standing positions. Detailed analysis of the power spectrum of these signals revealed the LF components around 0.1 Hz to be common through out. Besides, the spectra of the blood pressure oscillations as well as the PPG signal were found to be similar in normal individuals with similar directional and proportional changes with sympathetic activation observed in both these signals. This suggested the possibility of further analyses of these frequency components for the study of autonomic regulation of skin microcirculation (Bernardi et al 1996). This group studied the PPG fluctuations obtained from multiple sites of the body from both healthy controls and patients admitted to the intensive care who required the monitoring of arterial blood pressure by the catheterisation of the radial artery. The aim and the study protocol in their study were very different from what I had set out to do. However the detailed discussion provided useful information regarding the spectral analysis of PPG signal, the wealth of information that can be obtained from them and stressed on the importance of assessing the reproducibility of PPG signals obtained from multiple sites. The latter was of particular importance as PPG signals from both the left and right feet were used in my study.

In another study conducted by Nitzan and his team, they looked into the possibility of using the variability of the PPG signal as a potential method for the evaluation of the autonomic function. Here for each PPG pulse three

components were identified namely a) the pulse baseline, b) its amplitude and c) Its period corresponding to one heart beat. The signal variability for each of these parameters were noted and was found to be adequately reduced for diabetic patients as compared to the healthy individuals and hence could be identified as an index of autonomic function among the individuals (Nitzan et al 1998). Nitzan et al, 1998 did not perform any spectral analysis on their PPG signals obtained from both healthy controls and diabetic patients, instead they performed a detail visual analysis of the signals from the two groups. Their analysis indicated certain features of the raw PPG signals that could be potential markers of autonomic activity and this information was useful during the visual analysis of the raw PPG signals obtained in my study.

Another paper that was repeatedly cited in this study is a review article by Kamal et al, 1989. This review article discussed a wide range of topics on PPG. The topics included discussion on the different skin blood flow measurement techniques available, introduction to skin PPG, basic construction of PPG, detailed discussion on the PPG signal and finally the up to date information on the applications of PPG. The spectral components of the PPG signal were explained in great detail and the different frequencies in the spectrum were matched with various physiological process of the body. This was important information for the better understanding of the PPG signals collected and analysed in this study. They suggested that the very LF components of the spectrum are a direct effect of the sympathetic control on the pre capillary sphincter itself. These very LF components represented physiological activities like breathing, blood pressure regulation also called the

Traub-Hering-Meyer wave (THM) and temperature regulation (Burton waves) and these could be represented as markers of the autonomic activity of the body(Kamal et al 1989) . Another more recent review article by (Allen 2007) on PPG was also reviewed for this study. Although both the review articles discussed similar topics, greater emphasis was given to the applications of PPG in this paper.

The literature review done so far provided vital information regarding the pathogenesis of DAN, vasomotion and its pathophysiological role and finally regarding studies that have used PPG to evaluate autonomic changes due to diabetes. In this project we aim to use PPG and study the signal responses obtained from the sole of the feet of both healthy and diabetic patients with and without any known neuropathy.

Chapter III

Signal Analysis Method

3.1 Introduction

The PPG signals collected from the participants of all three groups was post-processed using the mathematical and technical computing software, MATLAB®. FFT, Complex Demodulation (CDM), Digital Filtering along with various graphical techniques were used for the purpose. The results obtained were also statistically analysed. This chapter explains in detail the various methods used to process and analyse the raw PPG signal.

3.2 Fast Fourier Transform

The word transform in mathematics means a method to convert one form of data set to another form of data set (Smith 1997). The Fourier Transform is a mathematical technique based on the principle of decomposing a periodic signal into a number of sinusoidal components of suitable amplitude, frequency and phase (Lynn 1993). Here the input signal in its time domain is converted into amplitudes of the component sine and cosine waveforms also known as the frequency domain of the signal. Biological signals such as the raw PPG signals are mainly periodic in nature and are almost in all cases sampled at a fixed rate by the investigating device to produce a discrete data. The Fourier Transform of discrete periodic signals such as the PPG signals

obtained in this study is termed Discrete Fourier Transforms (DFT) (Smith 1997).

The FFT is a complex algorithm developed to calculate the DFT of a time domain signal efficiently and at least 100 times faster than by solving simultaneous equations or by correlation (Smith 1997). This algorithm was based on the principle of complex DFT where the time domain signal was also composed of two parts (N points each) viz the real part and the imaginary part. The actual data was however present only in the real part of the signal while the imaginary part was padded with zeros. FFT converted these two parts of the time domain signal into N point real and imaginary frequency domain signals. These N sinusoidal waves of unit amplitude of the DFT are termed the basis functions. Each of these basis functions are scaled according to its contribution in the input signal such that these can add up to form the original input signal. Though each part constituted of N points, only the first half of the data points (0 – N/2) for both the real and imaginary parts contained the relevant frequency domain information (Smith 1997).

The FFT algorithm, though very complex, could be broken down into three main stages. In the first stage the N point time domain signal was decomposed into N time domain signals each composed of a single point. This decomposition occurred in stages where at each instance the signal was separated into its even and odd numbered samples. The number of stages required to completely decompose a N point time domain signal into N time domain signals was given by $\log_2 N$, where N is the length of the raw data.

The second stage involved calculating the frequency spectra for each of the N time domain signals. Finally the N frequency domain spectra calculated were summarised by a complex process to obtain an N point frequency spectrum. This algorithm was also repeated for the imaginary part of the time domain signal. Though both parts were calculated simultaneously, for practical purposes only the real FFT was used to process the raw PPG signals in this study (Smith 1997).

3.2.1 MATLAB implementation of the FFT

In MATLAB the DFT of a time domain signal is calculated using the 'fft' function. The practical use of this function can be explained using a simple example that has been illustrated in figure 3.1. A random signal of 1000 samples with a sampling rate of 1 kHz was generated using MATLAB and this was mixed with two sinusoidal waves of 30 Hz and 100 Hz. As per the Nyquist–Shannon sampling theorem the maximum frequency that could possibly be detected using FFT on this signal was 500 Hz. The time domain signal generated was subjected to DFT using the fft function in MATLAB.

The time domain signal as shown in Figure 3.1a does not reveal any information regarding the two sine waves present within the raw signal. However the fft of the same produced amplitudes of the two component sine waves at 30 Hz and 100 Hz respectively within the random signal spectrum (Fig 3.1b) there by providing valuable frequency information of the raw signal which otherwise could not be obtained from the analysis of the signal in its time domain.

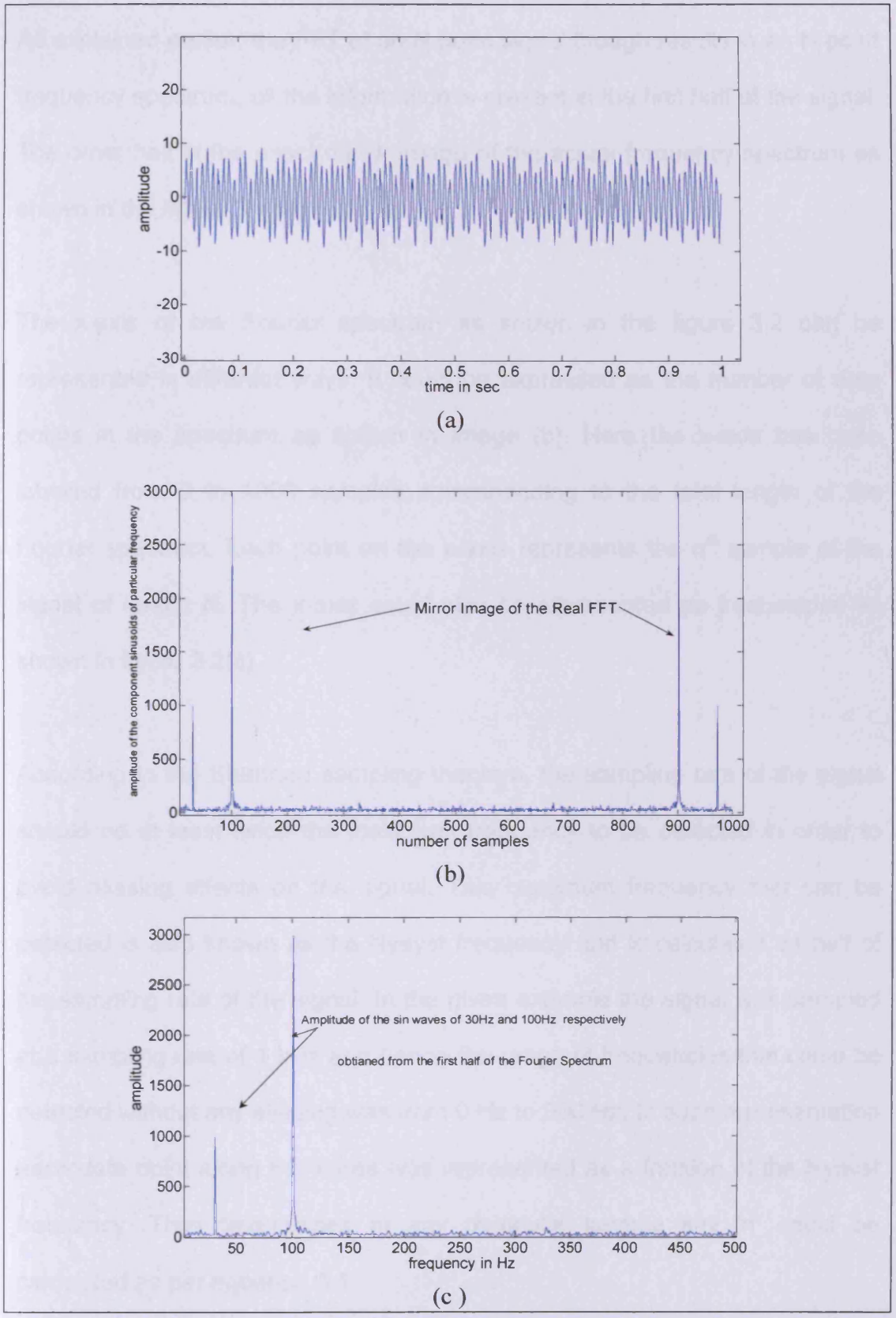

Figure 3.1: (a) random signal generated using MATLAB and mixed with two sinusoids of fixed frequency. (b) FFT of the random signal generated along with its mirror image. (c) Only the real FFT of the image

As explained earlier, the FFT of an N point signal though results in an N point frequency spectrum, all the information is present in the first half of the signal. The other half is the exact mirror image of the actual frequency spectrum as shown in the figure 3.1 (b).

The x-axis of the Fourier spectrum as shown in the figure 3.2 can be represented in different ways. It could be expressed as the number of data points in the spectrum as shown in image (b). Here the x-axis has been labelled from 0 to 1000 samples corresponding to the total length of the Fourier spectrum. Each point on the x-axis represents the n^{th} sample of the signal of length N. The x-axis could also be represented as frequencies as shown in figure 3.2(c).

According to the Shannon sampling theorem, the sampling rate of the signal should be at least twice the maximum frequency to be detected in order to avoid aliasing effects on the signal. This maximum frequency that can be detected is also known as the Nyqyst frequency and is calculated as half of the sampling rate of the signal. In the given example the signal was sampled at a sampling rate of 1 kHz and hence the range of frequencies that could be detected without any aliasing was from 0 Hz to 500 Hz. In such representation each data point along the x-axis was represented as a fraction of the Nyqyst frequency. Thus frequencies at any particular sample say 'n' could be calculated as per equation 3.1.

$f_n = (n/N) \times f_s$ Equation: 3.1

Where

f_n = Frequency at the n^{th} sample

N = Length of the Spectrum

f_s = Sampling rate of the raw signal

This kind of representation of the x-axis was more in real time and convenient to identify the frequency components present within the spectrum of the signal and therefore was used through out this study. The frequency unit used in this study was Hz. The y –axis represented the amplitude of the component sinusoids present within the spectrum and was expressed in absolute units.

A raw PPG signal is a typical example of a biomedical signal with a plethora of information contained in it. An example of a raw PPG signal collected for 10 minutes is illustrated in figure 3.2 (a). The segments of the raw PPG signal corresponding to the two stress tests of two minutes each have also been marked in the figure. Decreased amplitude of the PPG signal indicated increased blood flow under the probe and vice versa. In the example provided an increase in the blood flow (decreased amplitude) during the two stress tests was observed. However no information regarding the frequency characteristics of the signal could be obtained from the raw signal. An FFT on the signal however produced several frequency peaks in its spectrum. Spectral activity was observed at both the HF and the LF end of the spectrum. The three major frequency bands present in the spectrum have been illustrated in figure 3.2(b).

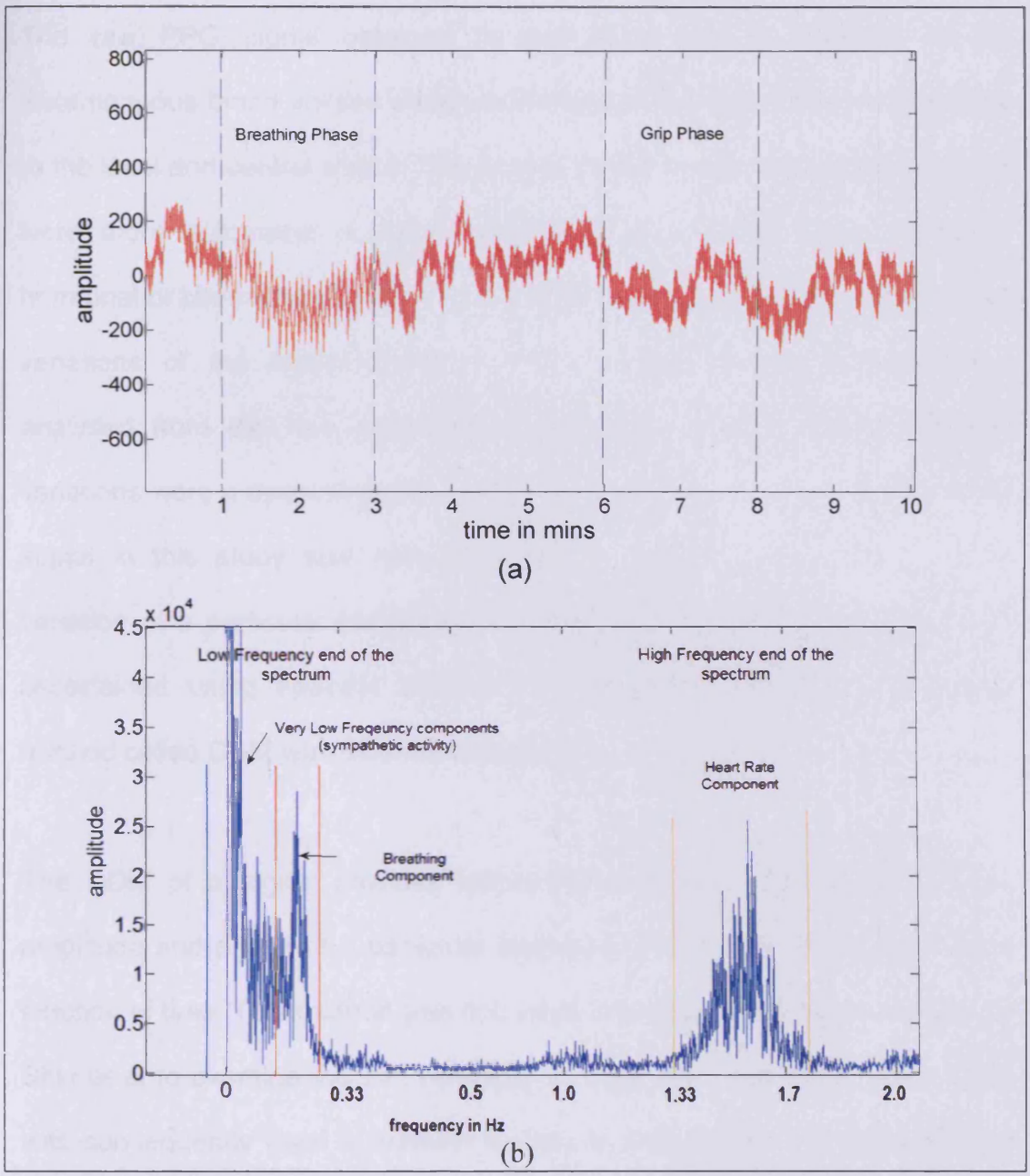

Figure 3.3: (a) Raw PPG signal collected from the right leg of the participants for 10mins. The protocol consisted of two stress tests viz; the breathing phase and the grip phase with intermediate resting phases. Decreased amplitude in the two test phases indicate an increase in blood flow
(b) FFT of the raw PPG signal consisting of the LF and the HF end of the spectrum. The heart rate, breathing and the very LF components of the signal were the prominent frequency bands identified using the frequency domain analysis.7

3.3 Complex demodulation

The raw PPG signal obtained in this study was a measure of the instantaneous blood volume changes in the skin microcirculation in response to the local and central stimuli. The central stimuli at the microcirculatory level were more autonomic in nature while the local stimuli were myogenic, hormonal or chemical in origin. These stimuli manifest themselves as rhythmic variations of the microcirculation. These variations were extracted and analysed from the raw signal through spectral analysis. These rhythmic variations were a dynamic entity, constantly changing with time. The raw PPG signal in this study was collected over ten minutes. Information on the variation of a particular frequency over the whole ten minutes could not be ascertained using spectral analysis; therefore another signal processing method called CDM was used for the purpose.

The CDM of a signal provides information regarding the changes in the amplitude and phase of a particular frequency component of the signal as a function of time. This method was first used in physiological signal analysis by Shin et al to examine the HR variability in dogs (Kim and Euler 1997). CDM was subsequently used in several studies to analyse the HR variability and the autonomic function in both animals and humans. CDM is a non-linear time domain analysis capable of providing information regarding the dynamic amplitude and phase changes of a particular frequency as function of time (Kim and Euler 1997).

3.3.1 Principle of CDM

CDM can be explained in three simple stages. Once the frequency of interest was established in a signal, the spectrum of the signal was shifted to the zero frequency end of the spectrum. This was achieved by multiplying the original signal with its complex sinusoid centred on the chosen frequency. In the next stage the resultant complex signal was low pass filtered to obtain only those frequency components centred on and around zero. Finally the real and the imaginary parts of the filtered complex signal was converted to the polar form to obtain the amplitude and phase information of the signal centred on the chosen frequency as a function of time. These steps can also be illustrated through the following set of equations.

Let us consider a time domain signal x_t of a particular frequency λ, amplitude A_t, phase φ_t and a constant DC component of z_t. Such a signal can be expressed as

$$x_t = A_t \cos(\lambda t + \varphi_t) + z_t \qquad \text{Equation: 3.2}$$

The aim of CDM was to obtain the changes of A_t and φ_t as a function of time. The complex equivalent of equation 3.3 can also be written as:

$$x_t = 1/2 A_t \{e^{(i[\lambda t + \varphi_t])} + e^{(-i[\lambda t + \varphi_t])}\} + z_t \qquad \text{Equation: 3.3}$$

The first step of CDM involved shifting the time domain signal of a particular frequency of interest to the zero frequency by multiplying the signal with its complex sinusoid centred on the chosen frequency. Let the new complex signal generated be y_t .

$$y_t = 2 \times x_t \times e^{(-i\lambda t)} \qquad \text{Equation: 3.4}$$

This can be further expanded as

$$y_t = 2 \times 1/2 A_t \{e^{(i[\lambda t + \varphi_t])} + e^{(-i[\lambda t + \varphi_t])}\} e^{-i\lambda t} + 2 \times z_t e^{-i\lambda t} \qquad \text{Equation: 3.5}$$

$$y_t = A_t \times e^{(i\lambda t + i\varphi_t)} \times e^{-i\lambda t} + A_t \times e^{(-i\lambda t - i\varphi_t)} \times e^{-i\lambda t} + 2 \times z_t \times e^{-i\lambda t}$$

Equation: 3.6

$$y_t = A_t e^{i\varphi_t} + A_t e^{(-2i\lambda t + i\varphi_t)} + 2 z_t e^{-i\lambda t} \qquad \text{Equation: 3.7}$$

The resultant complex signal that had all its frequencies shifted by $-\lambda$ contains three components. The first term does not contain any frequency component and is centred on the zero frequency. The second term oscillates at a frequency of 2λ while the third DC term was assumed not to have frequencies centred on the zero frequency. CDM not only shifts the region of interest but also all the other frequency components present within the signal by $-\lambda$. Thus all the frequency components with the original frequency above λ (the second term) do not reach the zero frequency and those below λ, such

as the DC component move to the negative part of the frequency axis. Thus the last two terms of the complex signal do not appear to oscillate with frequencies centred on zero frequency.

The second stage of CDM involved passing this complex signal through a low pass filter with a cut-off frequency around the zero frequency. Such a filter would only allow those frequency components with very low frequencies centred on zero frequency such as the first term of the complex signal to pass while eliminating the second and the third term of the complex signal. Let the filtered complex signal be y_t which can be expressed as equation 3.9.

$$y_t = A_t \times e^{(i\varphi_t)} \qquad \text{Equation: 3.8}$$

The last stage involves obtaining the amplitude and the phase information from equation 3.9 using equations 3.10 and 3.11.

$$A_t = |y_t| \qquad \text{Equation: 3.9}$$

$$\varphi_t = \tan^{-1}[imaginary(h)/real(h)]$$

Where $h = y_t / |y_t|$ Equation: 3.10

Thus by altering the desired frequency component of interest, most frequency components within the raw time domain signal were analysed. The cut-off frequency used for the low pass filter helped to identify the bandwidth of

frequencies that needed to be analysed and this could vary with every application and study requirements. The ability of the CDM to distinguish between adjacent frequencies depended on the performance of the low pass filter. Increasing the order of the filter at the cost of lost data points could enhance filter performance (Hayano et al 1993), (Hayano et al 1994).

3.3.2. Application of CDM in this study

The spectral analysis of the signal revealed several frequency bands of interest. Each of these frequency bands were analysed separately in this study. Further analysis of the very HF band of 1-2 Hz (60-120 cpm) required the extraction of the beat-by-beat HR of the individual. The HR extraction program was written using MATLAB and was made up of several stages. The spectral analysis of the raw PPG signal revealed the frequency location of the very HF bandwidth within its spectrum that was associated with the individual's heart rate. Once this band of frequencies were identified within the spectrum, it was essential to characterise its dynamic changes with time. This information was extracted using CDM. CDM was used to extract the amplitude and phase changes of the signal centred on the chosen frequency (between 1-2 Hz) calculated in the previous step. The complex demodulated signal was then subjected to a zero crossing detector to identify the time of the occurrence of the peaks and thereby help in the beat-by-beat extraction of the individual's heart rate.

CDM was performed using MATLAB. The central frequency of interest i.e. the mean HR of the individual was calculated from the previous step. The raw

PPG signal was multiplied by a complex sinusoid with a frequency centred on the mean heart rate. This complex signal was then subjected to a 5^{th} order Butterworth filter with a cut off frequency of 0.33 Hz (20 cpm) using a *'filtfilt'* function in MATLAB. Thus if the individuals mean HR was calculated to be 1.33 Hz (80 cpm), then the desired bandwidth of frequency ranged from 1 Hz (60 cpm) to 1.66 Hz (100 cpm).

The amplitude of the filtered signal was obtained by calculating the magnitude of the complex signal while the phase information was obtained using the MATLAB function called *angle*. This function returned the phase angles of every element of the complex signal in radians and had a value of $\pm\pi$. The complex demodulated signal X_t was then generated by combining the amplitude and phase information, just calculated using equation 3.11.

$$X_t = Amplitude \times \sin([centerfrequency \times time] + phase) \quad \text{Equation: 3.11}$$

The complex demodulated signal thus calculated gave insight into the dynamic changes of the amplitude and phase of the signal with a central frequency of the mean HR with time. A zero crossing detector principle was used to detect the number and location of the peaks of the complex demodulated signal as it occurred in the time domain. A zero crossing detector detected the transition of the signal from positive to negative value and each such transition points represented a peak in the complex demodulated signal as shown in figure 3.3. Each of these transition points along the time axis also represented the time of occurrence of a single heart

beat. Thus CDM was successfully used to extract the beat-by-beat HR trace of the individual from the raw PPG signal.

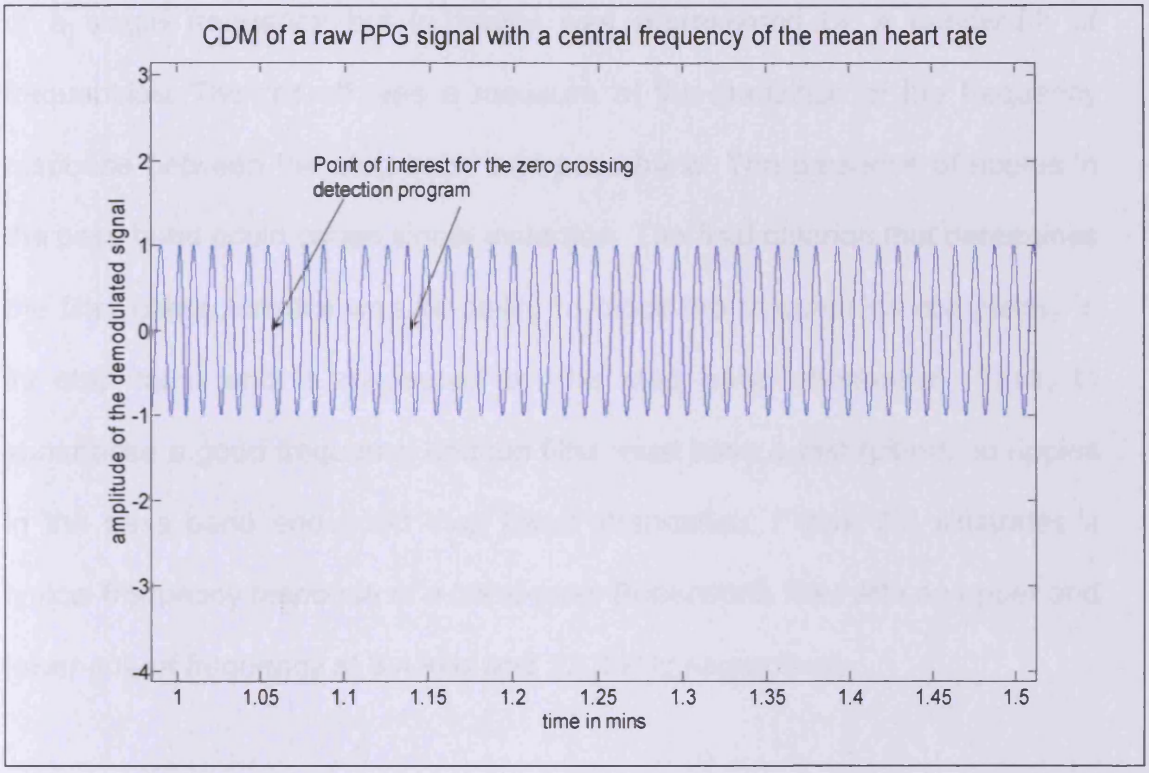

Figure 3.3: CDM of a high pass filtered raw PPG signal with a central frequency of 1.3 Hz (77 cpm).

3.4 Digital Filters

Filters are essential tools in signal processing used in either separating the signals or restoring them. Most of this study involved separating and analysing several frequency bands within the raw PPG signal. The frequency domain filters were used under such circumstances to separate the different frequency bands present within the signal (Smith 1997). The frequency response of such a filter consisted of a pass band region that allowed

frequencies to pass through it unaltered and a stop band region that stopped the frequencies from passing through itself.

Ideally the transition from the stop band to the pass band should only consist of a single frequency but in reality was represented by a bandwidth of frequencies. The roll off was a measure of this transition of the frequency response between the stop band and pass band. The presence of ripples in the pass band could cause signal distortion. The final criterion that determines the filter characteristics was its ability to block the frequencies completely in its stop band and is measured by the stop band attenuation. Thus, to summarise a good frequency domain filter must have a fast roll-off, no ripples in the pass band and good stop band attenuation. Figure 3.4 illustrates a typical frequency response of a band-pass Butterworth filter with an upper and lower cut-off frequency at 8.4 kHz and 13.2 kHz respectively.

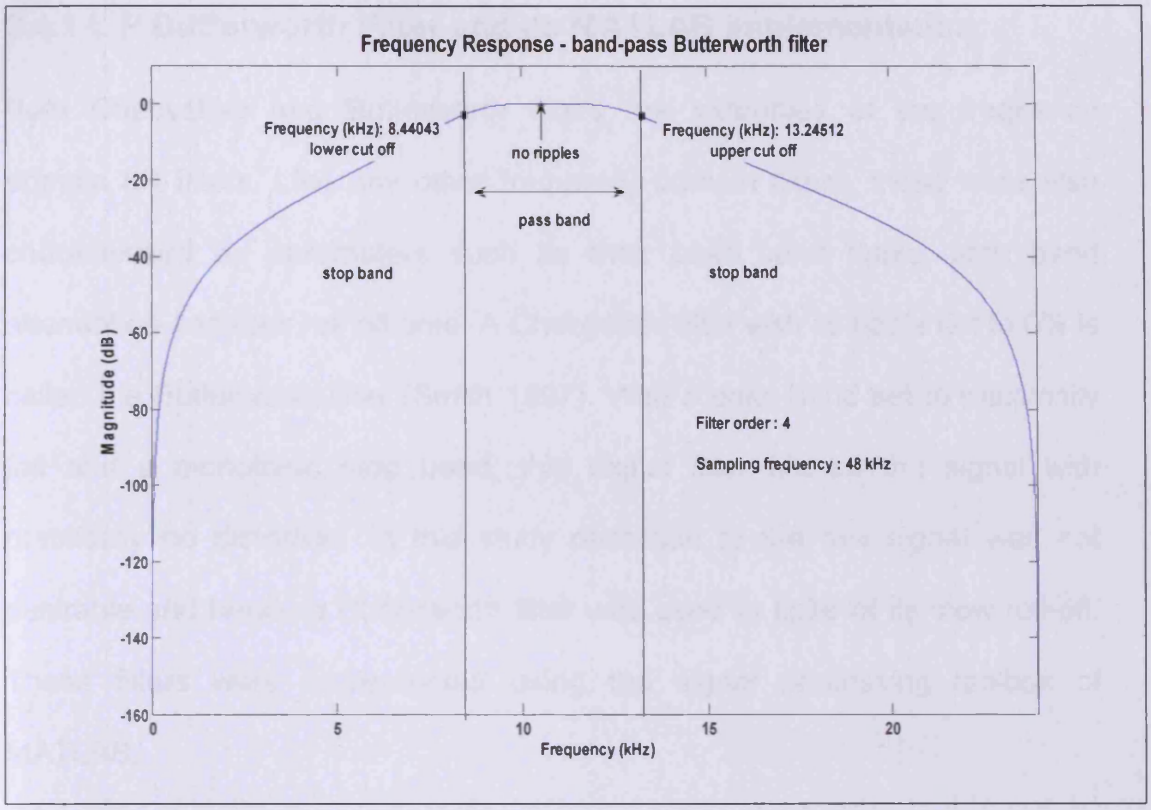

Figure 3.4: The frequency domain properties of a 4th order band-pass Butterworth filter with an upper and lower cut off frequencies at 8.4 kHz and 13.2 kHz respectively. The stop band region of the filter lies on either side of the cut-off frequencies.

The primary requirement of the study was a digital filter that was simple, fast with excellent frequency domain characteristics. Though a window sinc filter (FIR filter) had excellent frequency response, it could be implemented only in a large number of stages and hence was slow in its execution. Thus an IIR filter with moderate frequency domain characteristics but excellent execution speed was used. Throughout this study the frequency domain IIR filter used was called the Butterworth filter. The IIR filters can be a low pass, high pass, band pass or a band stop filter as per its function in the frequency domain analysis. All the other filter kernels can be mathematically derived from the low pass filter kernel that provides the base for digital filter design.

3.4.1 L P Butterworth Filter and its MATLAB implementation:

Both Chebyshev and Butterworth filters are examples of the frequency domain IIR filters. Like any other frequency domain filters, these were also characterised by parameters such as their pass band ripple, stop band attenuation and their roll off time. A Chebyshev filter with its ripple set to 0% is called the Butterworth filter (Smith 1997). With a pass band set to maximally flat and a monotonic stop band, this digital filter filtered the signal with practically no distortion. In this study distortion to the raw signal was not desirable and hence a Butterworth filter was used in spite of its slow roll-off. These filters were implemented using the signal processing toolbox of MATLAB.

In MATLAB the Butterworth filter was implemented using the 'butter' and 'filtfilt' functions. Most digital filters were generated from their analog counterpart and a suitable transformation algorithm was used to transform the analog filter output into its digital form (Lynn 1993). In MATLAB, three parameters were usually specified to design a filter viz, the desired cut-off ratio, the order of the filter and the type of filter (low, high, band pass or band stop filter) required. The cut-off frequency of the filter required was expressed as a fraction of the Nyquist frequency of the signal to be filtered. Thus if a low pass filter with a cut off frequency of 50Hz was designed to filter a signal being sampled at 1kHz then the cut-off frequency was specified as a ratio of 50/500 i.e. 0.1.

In MATLAB a five step algorithm called the called the bilinear transformation method was used to convert an nth order analog filter with n s-planes to a digital IIR filter with n z plane poles and n z plane zeros (© 1994-2005 The MathWorks, Inc). The order, the cut-off ratio and the type of the filter required were specified and this transformation was carried out using the 'butter' function. This step generated a set of recursion co-efficients for the specified filter design. The signal was then filtered using the 'filtfilt' function using these co-efficients. Figure 3.5 is an example of a 9^{th} order low pass Butterworth filter with a cut off frequency of 50 kHz and a sampling frequency of 48 kHz generated using MATLAB.

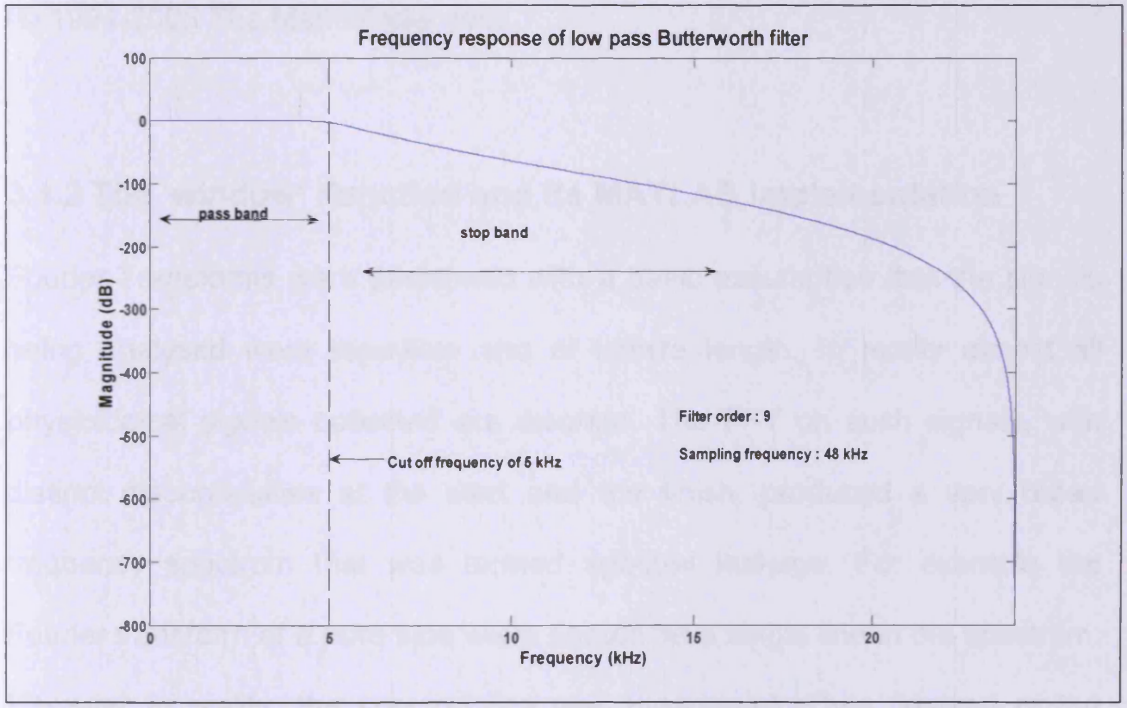

Figure 3.7: The frequency response of a low pass Butterworth filter with a cut-off frequency of 5 kHz and filter order of 9 generated using MATLAB

The phase response of an IIR filter was mostly non-linear. This was because in the design of IIR filters only the recursion co-efficients were specified and hence in almost all cases the impulse response thus produced were asymmetrical. In digital signal processing this short fall of the IIR filter was compensated by a method called bi-directional filtering. This process involved filtering the raw signal in one direction say from sample 0 to the end of the signal. Then this filtered signal was further subjected to the filter kernel in the opposite direction i.e. from the last sample to the first sample. In performing such bi-directional filtering all IIR filters were converted into a zero phase filter. In MATLAB such bi-directional filtering was achieved by simply using the *'filtfilt'* function instead of the *'filt'* function while implementing such IIR filters (© 1994-2005 The MathWorks, Inc).

3.4.2 The 'window' Function and its MATLAB implementation

Fourier Transforms were performed with a basic assumption that the signals being analysed were repetitive and of infinite length. In reality almost all physiological signals collected are discrete. The FFT on such signals, with distinct discontinuities at the start and the finish, produced a very broad frequency spectrum that was termed spectral leakage. For example the Fourier transform of a pure sine wave should be a single line in the spectrum. However in reality, the spectral line was broadened. Thus, instead of the signal energy to be concentrated only on one frequency it was spread out to the neighbouring frequencies as well. The spectral leakage resulted from the abrupt discontinuities of the signal ends. If these discontinuities were made to be gradual rather than abrupt, the spectral broadening could be significantly

reduced. Spectral leakage does not arise because of the finite length of the FFT; instead it arises due to the finite length of the measurement time (Lynn 1993; Smith 1997). The spectral leakage could mask frequencies of interest during signal analysis and hence was not a desirable parameter.

The raw PPG signal analysed in this study were also discontinuous signals of a finite length. These signals do not gradually become zero but come to an abrupt end after a finite length of time. The resulting spectral broadening was minimised using a window function. This was a special function that had a range of values within a certain period of time but was zero outside this period. Multiplying the raw signal with a suitable window in the time domain was equivalent to convolving the two in its frequency domain. Multiplying the signal with a suitable window that had gradual tapering ends ensured a smooth fall in value of the signal at its ends there by terminating the truncating problems of the signal (Lynn 1993). Gaussian, Blackman, Bartlett, Hamming, Hanning, etc are some of the popular window functions used in signal processing analysis and each of these windows can be represented using a set of equations. The window function used in this study was a Hanning window also known as a raised cosine bell function (Lynn 1993). Such a window can be defined using equation 3.12. Figure 3.6 is an example of a 100 point Hanning window generated using MATLAB function 'win'. The length and the name of the window required were specified when using this function.

$$w_n = 0.5 + 0.5\cos(n\pi / N), \quad \text{for} \quad -N < n < +N$$

$= 0$ elsewhere Equation: 3.12

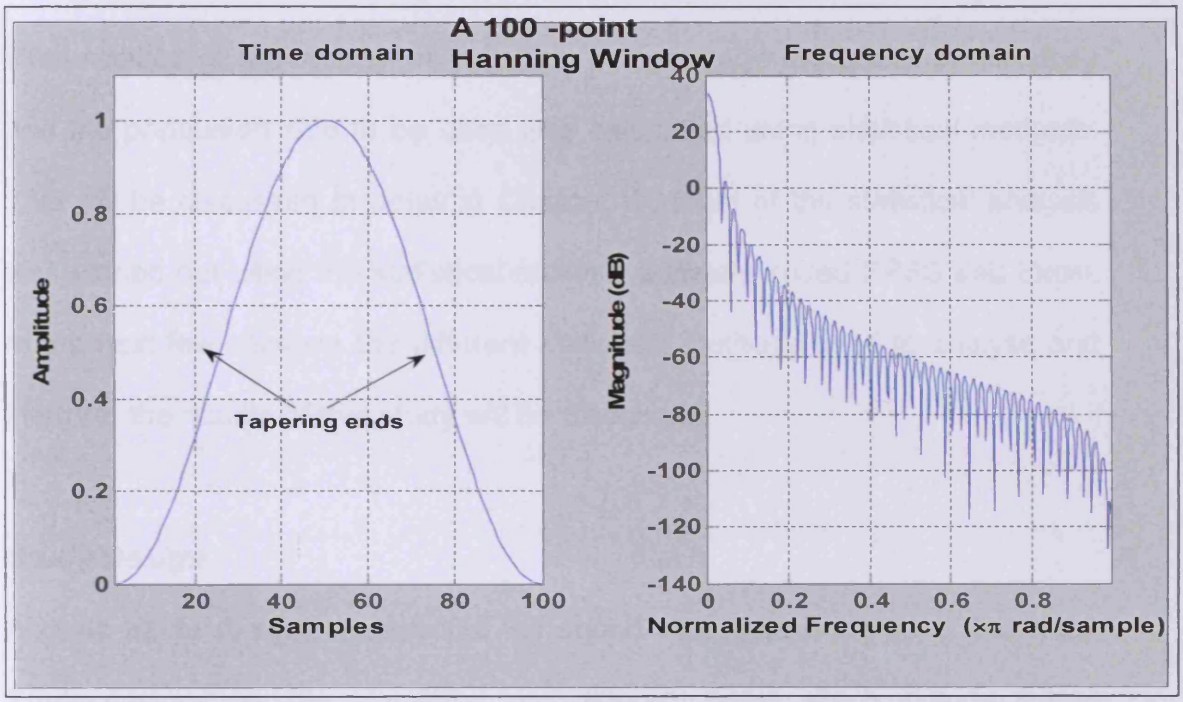

Figure 3.6: The time and frequency domain of a 100-point Hanning window. Note the bell shaped cure in the time domain with gradually tapering ends that are very useful in reducing the spectral leakage during signal processing.

3.5 Statistical Analysis

Statistics forms a vital research tool used to describe the data, design studies and test various relationships between variables. It also helps to extend the inferences from the results of smaller studies to the larger population. Statistics contribute to the various stages of the study from its design to the interpretation of the results. In the study design stage the power of the study and the population size to be used was calculated using statistical methods. This will be discussed in detail in Chapter IV. Most of the statistical analysis was carried out using the statistical analysis software called SPSS and Excel. In the next few sections the different statistical methods used to analyse and interpret the results of this study will be discussed.

Study Design

A good study design is essential for sound statistical analysis of the data. Study designs can be classified into different types which include cohort study, longitudinal study, case control study, etc. Though the data in this study was collected from participants of all the three groups, most significant comparisons were performed on variables of interest calculated from Group II and III. This study has been loosely based on the case control type of study design. The participants of Group II were diabetic patients with no known diagnosis of neuropathy. They therefore represented the 'control' group without the disease of interest, which was neuropathy while the participants of Group III were the 'cases' with known neuropathy. When comparisons were made between Groups I and II or between Groups I and III, participants from

Group I formed the control group while Groups II and III formed the 'cases' for the study.

Bland Altman Plot

Both tabulation and graphical representations were used to present the data analysed and observed in this study. The Bland Altman plot was one such graphical representation that was widely used. Two statisticians, J. M. Bland and D.G. Altman developed this plot to compare the same variable obtained from two different measurement techniques. In this study the Bland Altman was used to measure the degree of agreement between the left and the right beat-by-beat heart rate. The plot first calculated the mean difference in the two variables and its standard deviation. The mean ± 2 SD limits were also calculated. Then the differences in the beat-by-beat HR trace from both legs were plotted against the mean difference and the limits. In case of good agreement between the two variables, 95% of these differences should lie within the agreement limits calculated previously. Wider limits with a large spread in the difference values indicate poor agreement between the two variables (Bland and Altman 2003).

Parametric Test

The selection of a suitable statistical test for analysing a given set of data depends on several assumptions and the nature of the data set itself. Factors such as the type of the data, its distribution, the null hypothesis selected, etc were considered prior to selection of a suitable test. Both parametric and non-

parametric tests have been used in this study. These tests were used to compare the inter-group relation of the variables being analysed.

In this study the mean spectral density for a bandwidth of 0.33-0.13 Hz (2-8cpm) calculated for each participant across the three groups were compared using a parametric test. Parametric tests are based on three main assumptions i.e. the data set to be analysed must follow a normal distribution, secondly the groups to be compared must be independent of each other and lastly they should have equal variances. The one way ANOVA (analysis of variance) was a preferred statistical test when the means from more than two groups were compared using a parametric method. This test was also less stringent about the assumptions made on the data set prior to the analysis (Riffenburgh 2006).

One-way ANOVA is a two-part test. The test can be explained through the following steps

1. The first part of the test was to verify the null hypothesis
2. The difference of each observed value (k) from the overall group mean (m) was calculated, squared and the '***sum of squares within groups***' was calculated for each group as shown in equation 3.13

$$Sum\ of\ squares = \sum (k-m)^2 \qquad \text{Equation 3.13}$$

3. The '***sum of squares between groups***' was calculated using equation 3.14 where m was the individual group mean and m_1 was the overall mean for all three groups

$$Sum\ of\ squares\ between\ groups = \sum (m - m_1)^2 \qquad \text{Equation 3.14}$$

4. The sum of squares calculated for both within groups and between groups was converted to a known variance by dividing them by their respective degrees of freedom and this was called the ' ***mean squares***' value.
5. The ratio of the mean square value within groups and the mean square value between group was calculated and was called the F distribution

$$F = \frac{\text{mean square value between groups}}{\text{mean square value within groups}}$$

6. Ideally the value of F should be 1 and this value would be indicative of equal variance between the three groups being compared
7. The p value denotes the significance of the test. A value of less than 0.05 was said to be statistically significant
8. If the first result was found to be statistically significant, the null hypothesis was rejected
9. The second part of the ANOVA analysed these differences between the groups further
10. In this part multiple comparisons were made between the group means using two main tests viz; the Tukey HSD (honestly significant difference) and the Fisher LSD (least significant difference)
11. These two tests compared the mean values obtained from each group, a pair at a time
12. A very small p value in each case indicated unequal mean for the pair being compared

Thus the one way ANOVA not only gave us the overall relation between the mean spectral densities obtained from the three independent groups but also the relation of the variable of interest between the groups

Non – Parametric Test

The data set that does not follow any specific distribution cannot be compared using the parametric methods; rather they were compared using non-parametric tests. In this method parameters such as medians and ranks were used for the comparison (Altman 1992). Non parametric methods are free of assumptions and hence more appropriate for hypothesis testing rather than directly comparing the medians (Altman 1992).

Different tests were applied depending on the number of groups being compared. When two, independent, continuous data sets with a non – normal distribution were to be compared, the Mann-Whitney test was the preferred method of comparison. This is the non-parametric equivalent of a simple t-test (parametric method). The Mann – Whitney test ranks the observations from both groups in a particular order before analysing them. It involves the calculation of two test statistics viz the Wilcoxon T statistic and the Mann-Whitney U statistic. While the T statistic was the sum of the ranks obtained from the smaller of the two groups, the U statistic was calculated using equation 3.15, where n_1 and n_2 were the number of observation in both groups. The SPSS package calculated the probability value along with the U and Z statistics. A very low p value indicated a statistically significant result.

$$U = n_1 n_2 + 1/2 n_1 (n_1 + 1) - T$$ Equation 3.15

The Kruskal- Wallis test was used when three or more independent, continuous data sets that do not follow the basic assumptions of parametric testing were compared. They are the non-parametric equivalent of the one-way ANOVA method. Once again the test required all the observations across all three groups to be ranked. The SPSS package calculated the mean rank for each group, the χ^2 value, the degrees of freedom and the corresponding probability value for this test. A very low p only indicates that the median for the different groups being compared were significantly different. Further inter group relation could not be obtained using this test.

The raw PPG signals collected in this study were analysed using methods detailed in this chapter. The results of the study and the subsequent discussion are discussed in chapters V and VI.

Chapter IV

Materials and Methods

4.1 Introduction

As mentioned earlier in chapter 1, prevention remains the best method to avoid the debilitating effects of the diabetic foot ulcers. It has been estimated that up to 80% of the diabetic foot ulcers can be prevented with a proper screening programme involving regular visual and clinical examination of the foot and the neurological and vascular assessment of the 'at risk ' diabetic patients (DeFronzo et al 2004). Changes in the microvascular blood flow under pathological conditions are a well-recorded fact and could potentially be linked to conditions like diabetes.

Till date PPG has been successfully used in various vascular assessments under clinical settings. The primary objective of this research project was to identify if a simple optical device such as the digital PPG was able to detect the changes in the skin microcirculation in diabetics with sympathetic denervation. Secondary objective was to further investigate if these changes in the skin microcirculation could be detected in the early stages of diabetes before clinical diagnosis of diabetic neuropathy. The answers to these objectives could help to develop a simple, cost effective screening method to identify those diabetic patients at risk of developing diabetic foot ulcers of

neuro-ischaemic nature. In this chapter the study protocol, the equipments used and the preparatory work done have been discussed in detail.

4.2 The Vascular PPG Assist

The DPPG device used in this study was the Huntleigh Vascular Assist® as shown in figure 4.2. It is a simple portable device with a docking station. The docking station is used for recharging purposes and contains ports to connect to the computer and the printer. Huntleigh Vascular Assist comes with a dual PPG probe that can be used to measure the skin blood flow at any two places simultaneously. These circular probes have an IR emitter and a photodetector built in a reflection mode configuration. The probes are attached to the skin at the site of investigation with help of a double-sided adhesive tape as shown in figure 4.1.

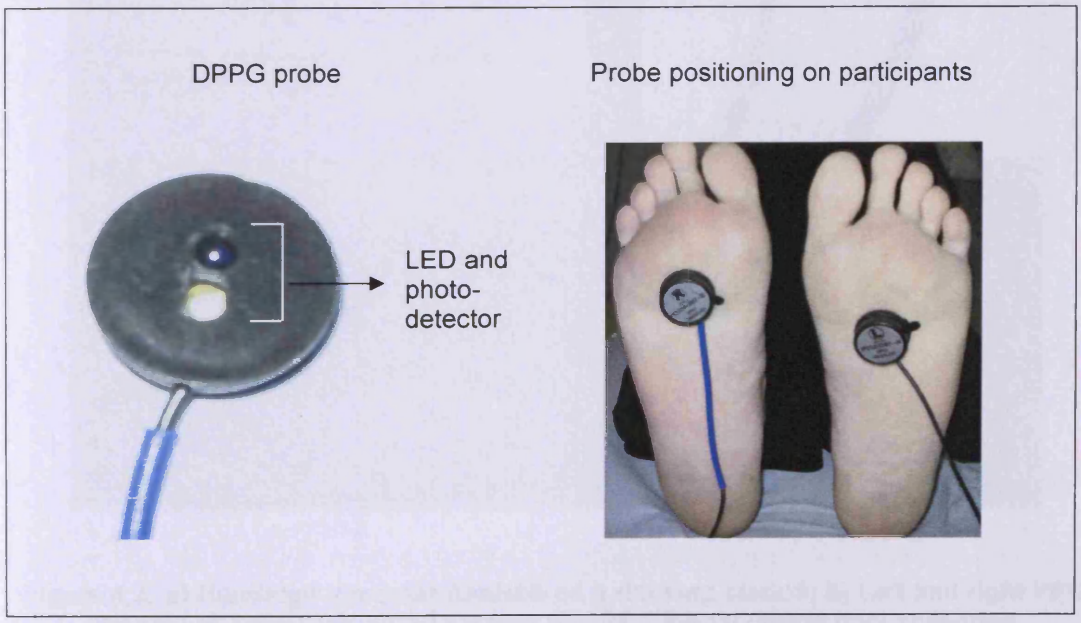

Figure 4.1: The DPPG probe from the Vascular Assist and it's positioning on the participants

The LED emits IR light of wavelength of 940 nm that undergoes absorption, refraction, attenuation and reflection as it passes through the various layers of the skin. The skin blood volume under the probe influences the amount of light received by the detector. The analog output generated by the photodetector is digitised by the analog to digital converter where the signal is sampled at 6.25 Hz. The digitised PPG signal is displayed on the screen in real time as shown in figure 4.2c. The digitised data can be stored on the hard drive inbuilt in the Assist. The system is also provided with a card reader to store the digital data on an external storage device such as a personal computer (PC) card. The data from the PC card can be transferred to other external sources like a computer for further analysis of the PPG signal.

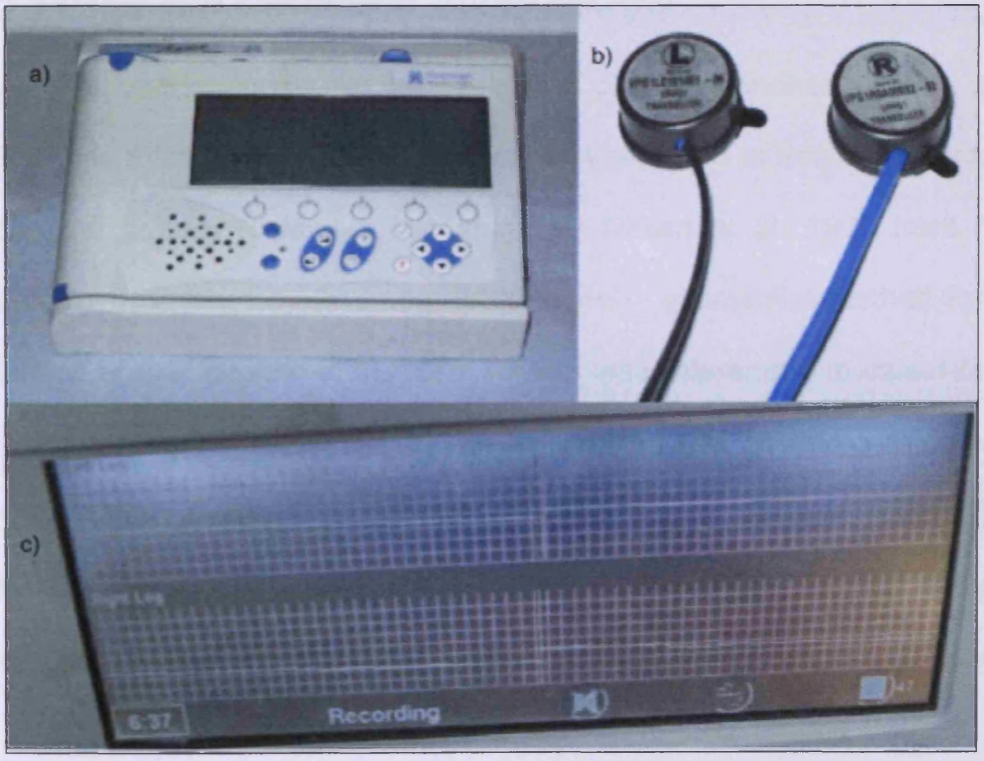

Figure 4.2: a) Huntleigh Vascular Assist® on a docking station; b) Left and right PPG probes; c) Assist recording screen- raw PPG signal during data collection

4.3 Experiment Design

The ethical approval of the study was obtained from the South East Wales Research Ethics Committee. As per the research ethics committee rules, a detailed study protocol along with the participant information sheet and the consent form to be used in the study was submitted with the application. The sample size required for the study was also calculated. The sample size is a measure of the number of measurements to be taken for obtaining statistically significant result. The factors effecting the sample size calculation include the effect size, the confidence level or the study error and the desired power for the study.

4.3.1 Sample size calculation

Only limited studies looked at the evaluation of the autonomic function using PPG. Those relevant to my project have been reviewed in detail in Chapter II. Among the papers reviewed, the study by Nitzan et al, 1998 titled "The variability of the photoplethysmographic signal - a potential method for the evaluation of the autonomic nervous system was referenced to calculate the sample size for this study. Visual analysis of the raw PPG signal obtained from the different groups was intended to be one of the main methods of analysis to be used in my study. The study by Nitzan et al 1998 also analysed certain physical parameters of the raw PPG signal while comparing between the groups and hence was chosen to be referenced for the sample size calculation. In their study, Nitzan et al 1998 analysed the variations in the baseline, amplitude and the period of the raw PPG signal. The intensity of the

spontaneous fluctuations for these parameters were assessed by the relative standard deviation i.e. the standard deviation of the parameter divided by its mean (Nitzan et al. 1998). The results indicated the relative standard deviation of the amplitude to be 11.26 in the non-diabetic group, and much lower at 7.12 in the diabetic group. These values provided the expected effect size required for the two groups for the sample size calculation. The power of the study was set to 80%, and the significance level of the study was also set to 5%. A mean standard deviation of the amplitude of the PPG signal of 11.26 % was set as the expected effect size for the normal population and 7.12% for the diabetic population. The sample size was calculated using a sample size calculator and the minimum sample size required for a statistically significant result was calculated to be 63. With the minimum sample size calculated as 63 for a two-group study, the number of recruits in each group would be an average of 32 participants. However in this study the PPG signals from three groups were to be analysed. In order to compensate for converting from a two-sample study to a three-sample study, the strength of the third group was made similar to the other two groups. Considering the potential for participant dropouts, difference in the two studies and three groups of participants to be recruited rather than two, a total sample size of 105 was decided for this study.

4.3.2 Participant Recruitment

As per the sample size calculation participants were recruited for three distinct groups viz, Group I with 35 healthy individuals with no evidence of diabetes or any familial history of the disease, Group II constituting of 35 diabetics with no

evidence of neuropathy and Group III of 35 diabetics with confirmed diagnosis of one or more types of neuropathy (primarily sensory neuropathy).

The participants for Group I were mainly recruited from amongst the staff members at the department of Medical Physics and Clinical Engineering, University Hospital Wales due to the likelihood of some level of flexibility to allow attendance to the hospital during normal working hours. An email was sent to all staff members in the department detailing the purpose and aims of the study and an appointment was then provisionally made with the interested candidates at least 7 days prior to the test date and was asked to confirm their participation nearer to their appointment date. They were also informed of the questionnaire regarding their general health that they would have to answer when they arrived for the experiment. The questionnaire was used to identify if any of the participants had a strong familial history of the disease or presented with undiagnosed diabetes and manifested some common symptoms of diabetes mellitus like; frequent thirst, frequent urination, tiredness, blurring of vision or sudden weight loss. Those with three or more of these symptoms were then excluded from the study. The participants that did not comply with the inclusion criteria set for the study were also excluded. In total 37 healthy individuals with no known diabetes were recruited and among them were 20 males and 17 females.

The participants for Group II were primarily recruited from the Diabetes Investigations Clinic at Llandough Hospital, Cardiff and they were diabetics with no known neuropathy. These patients were reviewed on a yearly basis by

the Consultant diabetologist Prof David Owens and his team. During this review appointment their fasting blood glucose level, eyesight, blood pressure and sensory functions were tested and the records were updated yearly. They were approached on a one to one basis during one of their review appointment and the information sheets and consent forms were made available to the interested candidates. In order to avoid patient inconvenience of returning to the clinic on another day just to partake in the study and also to prevent the disruption of the normal working procedures and clogging up of the patients list of the diabetes clinic the patient were asked to decide on the same day. A total of 35 diabetics, 1 Type I and 34 Type II were recruited. 25 of the participants were males and 10 were females.

The participants for group III were recruited from a list of diabetic patients who had previously participated in another study conducted by a diabetes specialist nurse based at Llandough Hospital, Cardiff three years prior to this project. Her study involved at identifying diabetics across Cardiff and Vale area that may be at risk of developing diabetic foot disease. The study involved looking at the general foot hygiene, general health of the patient and evaluating the sensory function of the foot using a biothesiometer. Those patients at risk of developing the foot disease were primarily identified using a biothesiometer reading of their vibration perception ability at the sole of their feet. Studies have indicated that patients with a VPT score of greater than 25 V were at a greater risk of developing foot ulceration (Young et al 1994; Lavery et al 1998).

Studies have also indicated the presence of sympathetic dysfunction along with sensory impairment (Eicke 2003; Lefrandt 2003). Due to funding difficulties and lack of resources the patients recruited for this group did not undergo the assessment of their autonomic function using the CAN tests. Neuropathy is an irreversible condition, where the structural and functional damage to the peripheral nerves cannot be reversed. Although the participants for Group III were selected from the patient population who were assessed for their sensory impairment three years prior to this study, it was assumed that the neuropathy would have only progressed or at the least be at the same level over the three year period. Therefore only those patients with a VPT score of around 25 V and greater were approached for this study by telephone. This way attempts were made to ensure that all participants of this group were patients with varying degree of sensory impairment. A brief overview of the aim and the purpose of the study were explained during the conversation. A detailed copy of the patient information sheet, a consent form, an appointment letter and a site map was posted to these interested candidates. For their convenience most of the participants were recruited from within a 5-mile radius of Llandough Hospital. Prior to the experiment, their height, weight, blood pressure and temperature of their feet were noted. They were also asked about their medications and their general heath. A brief history of their other cardiovascular problems was also noted. A total of 30 males and 8 females were recruited for this group. They all were diabetics (5 Type I and 33 Type II) with primarily sensory neuropathy indicated by their high VPT score. The VPT score in this group ranged from 25 V to a maximum score of 48 V.

4.3.3 Inclusion and Exclusion Criteria

The participants of the control group or Group I were healthy individuals within the age range of 24 to 61 years. The mean age ± SD for the control group was 40.75 ± 12.6 years. Smokers, individuals on drugs known to affect the blood flow like the anti coagulants, vasodilators, etc, participants with cardio-vascular diseases either arterial or venous, individuals suffering from any known neurological abnormalities or diseases affecting the microcirculation such as dermatitis, psoriasis, collagen vascular diseases and Reynaud's syndrome were excluded from the study.

The participants of Group II (diabetics) and Group III (neuropathic) belonged to an older population within the age range of 45 – 80 years. The mean age ± SD for Group II was 63 ± 7.0 years while the mean age ± SD for Group III was 70 ± 5.5 years. No attempts were made to age match the disease group (Groups II and III) with the control group. Studies have indicated age related changes in the vasomotor responses(Bernardi et al. 1997). The digital PPG device used in this study was never used before to assess the vasomotor responses. If the diseased and the control group were age matched, the signal from older healthy individuals could have age related changes. This would make differentiating an abnormal signal from a normal PPG signal very difficult. Therefore PPG signals from young healthy individuals were used for the analysis. The general exclusion criteria for Groups II and III were similar to Group I. Participants with any known symptoms of neuropathy were also excluded from Group II. Diabetes is also a major risk factor for cardiovascular complications and hence it was difficult to exclude participants suffering from

CVD while maintaining the number of participants required for the study. However only 6 diabetics (17%) of Group II out of a total of 35 suffered from some form of cardio vascular complications. However around 47% (18 out of 38) of the participants in Group III had at least some form of cardiovascular complication in the past. All participants were refrained taking any caffeinated drinks two hours prior to the study.

4.6.4 Stress Tests

The diagnosis of DAN is usually achieved by evaluating the cardiovascular autonomic function of the individual. The common tests for the evaluation of CAN include evaluation of the HR and the pressure responses to certain stimulus viz, breathing, grip or postural change. Thus a need arose while designing the study protocol to introduce some stress tests to evaluate the autonomic function of the body at both the relaxed and the excited condition. The PPG signal is very sensitive to movement artefacts, thus tests involving postural changes were avoided and the breathing and grip tests were adopted for the experiment protocol.

The Valsalva manoeuvre has been a popular test for evaluating the cardiac autonomic reflexes. Well defined changes were observed in the HR and the blood pressure of healthy individuals during this manoeuvre (Kalbfleisch and Smith 1978). The HR fluctuations with deep breathing are a result a vagal control of the sinus rhythm and hence this manoeuvre is a very good index of the parasympathetic activity of the individual (Kamal et al 1989). Though very useful, this test was difficult to perform specially for the older population. The

target population for this study who may be at risk of developing foot ulcers due to long-term diabetes tend to be over 60 years. As the main aim of the study was to devise a screening tool it was necessary to keep the protocol simple, with good patient compliance.

A simple breathing test mimicking the Valsalva Manoeuvre, but with reduced intensity was devised as a part of the experiment protocol. A special device called the PowerLung® was used to aid the participants during the breathing test. PowerLung® as shown in figure 4.3b is a commercial breathing device used to train and strengthen the respiratory muscles*. The model has separate inhalation and exhalation control with five different levels that can be altered independently. Using the PowerLung® the participants were in effect inhaling and exhaling at a particular set resistance which was normally set to its minimal level of 1. Set at its minimum resistance, it was expected to mimic the Valsalva Manoeuvre in evaluating the baroreflex integrity of the individual, however with better patient compliance than the manoeuvre itself.

Another popular diagnostic test for CAN is the blood pressure response to a sustained hand grip where the participant is made to grip a hand held device at their maximum capacity initially and then at 30% of his/her maximum grip strength for the next 5 minutes. During this exercise the sympathetic reflexes are triggered and as a result an increase in both the blood pressure and the HR is observed. This test was observed to be a good indicator of the sympathetic function of the body. Maintaining a 30% level of grip for 5 minutes could be a challenging task even for a healthy young individual, thus to make

* For more Technical Details visit: http://www.powerlung.com/us/en/

it more patient compliant it was decided to decrease the level to 10% of the individual's maximum grip strength and the time to 2 minutes. A commercial device called the Baseline® Hydraulic Hand Dynamometer as shown in figure 4.3c was used as the gripping device. It was robust and simple to use with the strength reading available in both pounds and kilogram. The device had a standard dial gauge with a mechanical reset that could measure grip strength of up to 90 kg. The handgrip also had a 5 level adjustment for better and stronger grip. By the introduction of these two stress tests, it was hoped to achieve a measure of both the sympathetic and the parasympathetic activity of the individuals using PPG.

Figure 4.3: a) Huntleigh Vascular Assist®; b) PowerLung ® BreatheAir® c) Baseline® Hydraulic Hand Dynamometer; d) IR temperature sensor and e) PPG probes

4.6.5 Experiment Protocol

The study protocol involved taking the photoplethysmographic blood flow signals from the sole of the participant's feet using two PPG probes of the ***Vascular PPG Assist*** ® of Huntleigh Diagnostics. The Assist was a simple device to operate and required very little operator skills. Before the beginning of the test the participant's height, weight, blood pressure and the temperature of their feet were noted. Participants of the control group (Group I) were also asked to complete a questionnaire regarding their general health and were checked of any familial history of diabetes. The participants were then asked to be in a supine position and had their legs covered with a blanket to prevent cold feet. The experiments were to be carried out in the same room under similar conditions each time to produce a uniform test environment through out the study. The participants were given time to relax for about 10 to 15 minutes before the beginning of the study as it was essential to achieve a baseline PPG recording before the stress tests. Before the beginning of the experiment the maximum grip strength of the participant was also determined using the dynamometer. The sequence of the different stages of the protocol is illustrated in figure 4.4. The signals were recorded for 1 minute under complete rest and then the participants were asked to breathe in and out of the Power Lung™ set at the minimal level for two minutes. After this exercise they were asked to relax for further three minutes. The PPG signals from the sole of the participant's foot were recorded continuously through out the procedure. After the three minutes of rest the subjects were once again asked to perform the second stress test of sustained handgrip using the dynamometer. The participants gripped the dynamometer at 10% of their

maximum grip strength (determined before the beginning of the procedure) for two minutes and then relaxed completely for the remaining two minutes. The PPG signals from the soles of the feet were recorded and stored automatically on to the memory card by the Assist™ for further analysis. The whole experiment did not take more than 25 minutes and once the procedure was complete the participant could leave immediately as there were no side effects to the procedure.

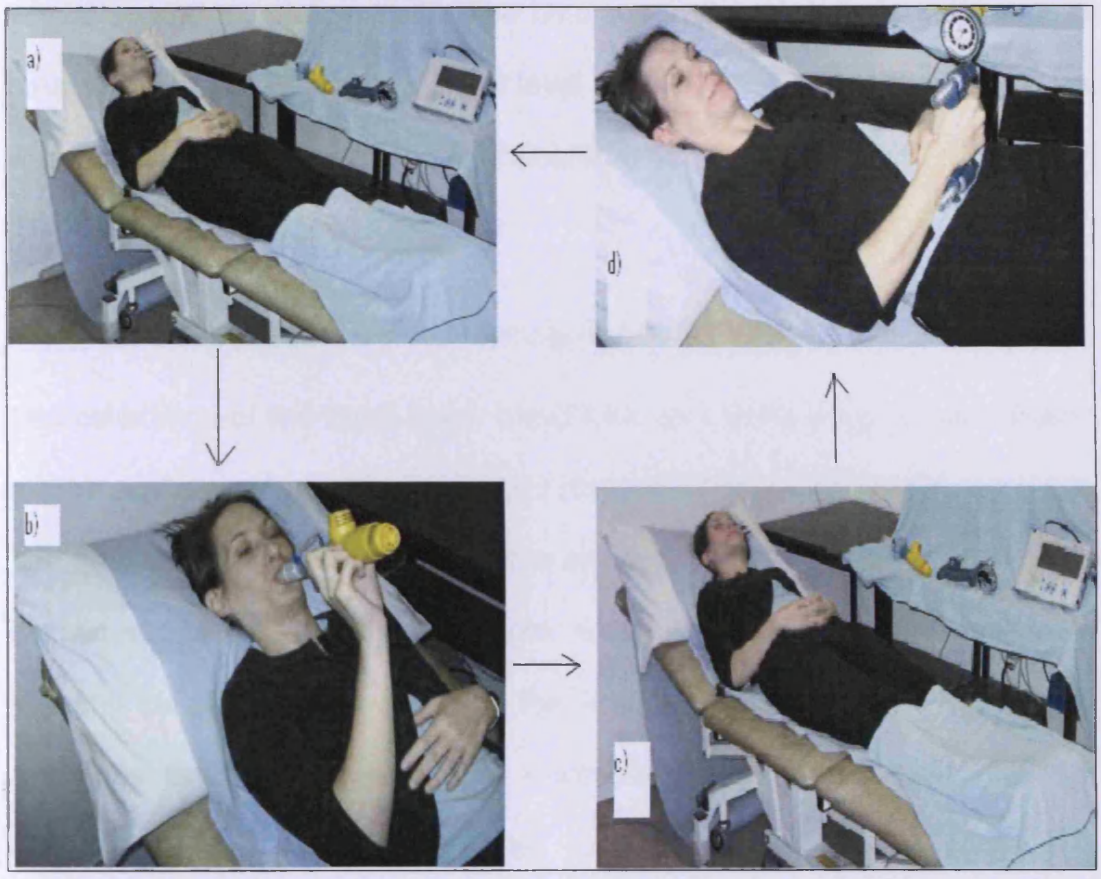

Figure 4.4: Different stages of the study protocol; a) initial resting phase of 2 minutes; b) 2 minutes breathing phase; c) intermediate resting phase of 3 minutes; d) 2 minutes grip phase and final 1 minute of resting

4.4 Preparatory Work

The Vascular PPG Assist ®, the Baseline® Hydraulic Hand Dynamometer and the PowerLung Breathe Air® were the three main pieces of equipments used in this study. Apart from these, an automatic Blood Pressure monitor and an infrared (IR) temperature sensor were also used. These were all commercial devices and were provided with their specifications. Though the inhalation and exhalation circuits of the PowerLung Breathe Air® could be controlled independently, their characteristics were not very clear. The device was calibrated using an old mechanical ventilator, which helped to mimic the inhalation and exhalation cycle. The changes in the peak flow and the peak pressure with the Resistance index level of the device during the two cycles were measured, calibrated and their characteristic graphs plotted.

4.4.1 Calibration of the PowerLung BreatheAir®

The calibration of the PowerLung BreatheAir was done using a Cape Waine mk3 anaesthetic mechanical ventilator and a PTS -2000-calibration analyser. The mechanical ventilator was used to simulate the inhalation and exhalation technique and the calibration analyser was used to measure the peak flow rate and the peak pressure through the breathing device during each cycle at a set resistance Index level. The Cape Waine is a mechanical ventilator manufactured by Cape Engineering Company Ltd. It could produce a maximum relief pressure of 7.0 kPa with the respiratory frequencies ranging from 10-50 cycles/min. The expiratory assistance had a maximum and minimum range while the volume could range from 300 ml to 1700 ml. The

ventilator had two independent circuits that were driven by bellows. While one mimicked the inhalation process and blew air into the patient at a +ve pressure, the other produced a –ve pressure and helped to suck air out of the patient's lungs.

Calibration of the inhalation circuit of the PowerLung®

The expiratory circuit of the ventilator was used to calibrate this part of the PowerLung®. The ventilator was connected to the High flow exhaust of the PTS 2000 calibration analyser and the PowerLung® was connected to the high flow inlet of the same in a straight line such that the negative pressure generated by the expiratory circuit of the ventilator could suck the air through the PowerLung® mimicking inhalation at various load. This set up is illustrated in figure 4.5. Both the peak pressure and the peak flow rate were noted for each cycle and five such readings were taken at each resistance index of the PowerLung® device. The characteristic graphs for both the peak pressure and the flow rate were also plotted using Microsoft Excel spreadsheet.

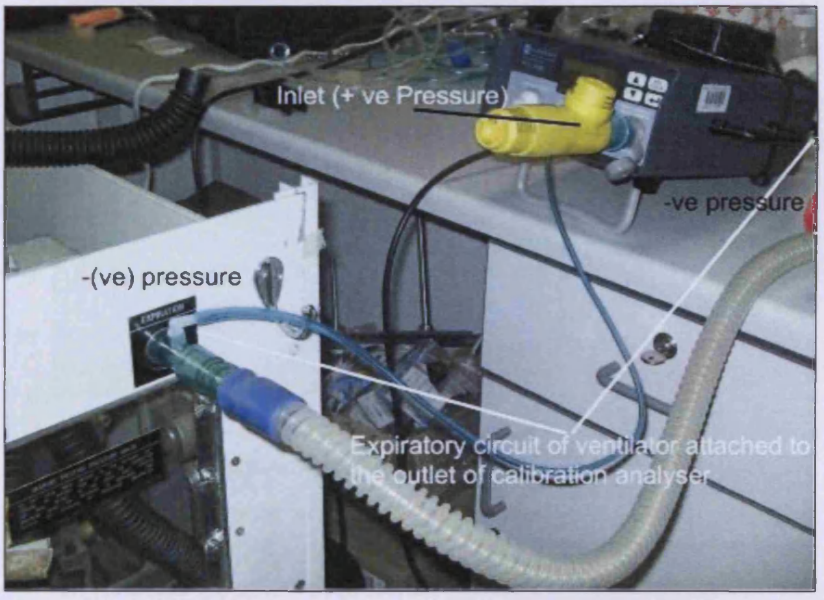

Figure 4.10: The experimental set up for the calibration of the inhalation circuit of the PowerLung®

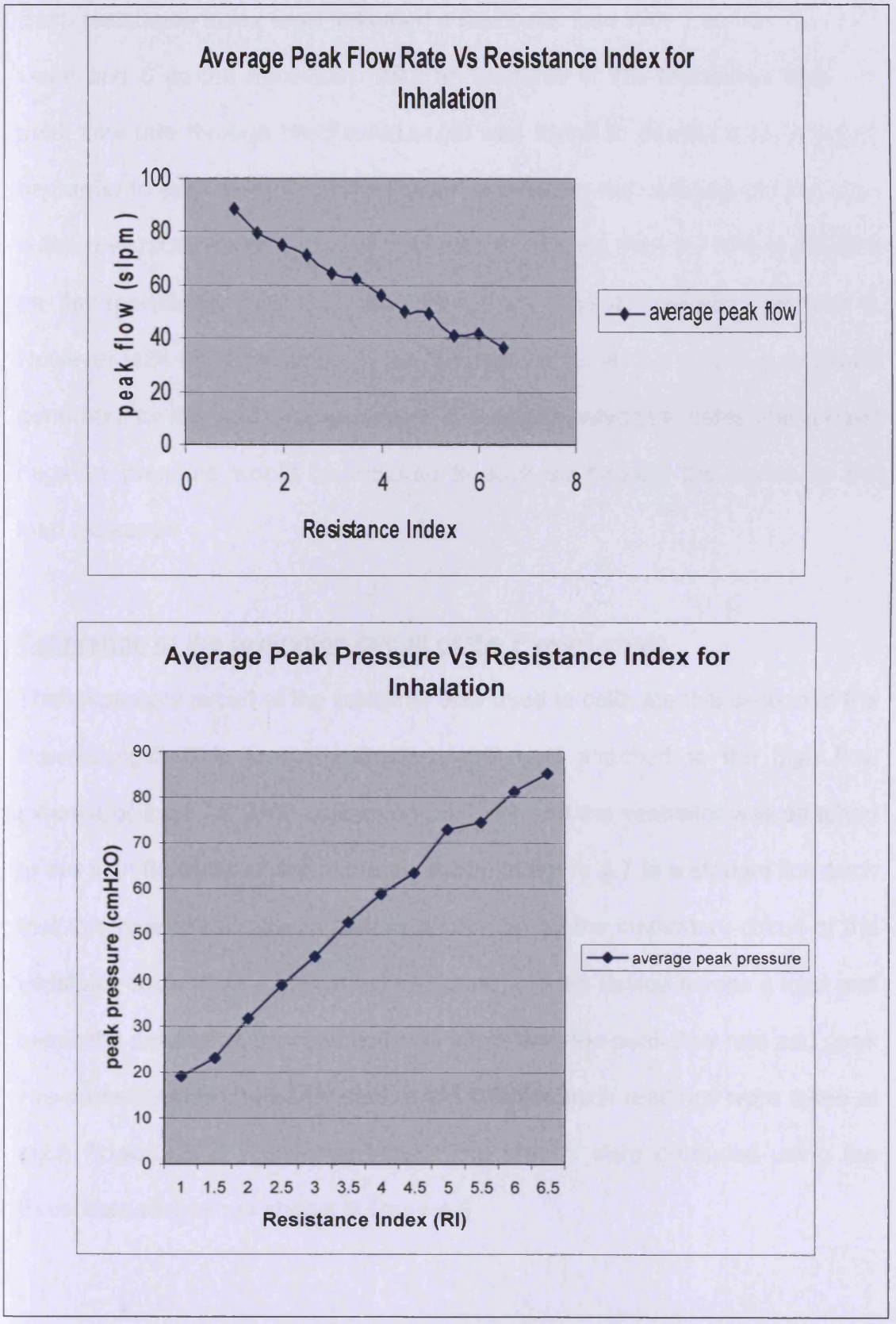

Figure 4.6: The Inhalation characteristic of the PowerLung BreatheAir®

Each resistance index level indicated a particular load with 1 as the minimum value and 6 as the maximum. With an increase in this resistance level the peak flow rate through the PowerLung® was found to decrease i.e. it would be harder to suck air through the PowerLung device with subsequent increase in the resistance level. The peak flow rate decreased from 8.7 kPa to 3.5 kPa as the resistance level was increased from 1 to a maximum level of 6. However with each increase in the Resistance Index the negative pressure generated by the ventilator was found to increase, which indicates that greater negative pressure would be required to suck air through the device as the load increases

Calibration of the expiration circuit of the PowerLung®

The inspiratory circuit of the ventilator was used to calibrate this section of the PowerLung®. This time the PowerLung® was attached to the high flow exhaust of the PTS 2000 calibration analyser and the ventilator was attached to the high flow inlet of the same as shown in figure 4.7 in a straight line such that this time the positive pressure generated by the inspiratory circuit of the ventilator could blow a known volume of air into the device across a load and mimic the exhalation procedure. Once again both the peak flow rate and peak +ve pressure were noted for each cycle and five such readings were taken at each PowerLung® resistance index. The graphs were produced using the Excel spreadsheet as shown in figure 4.8

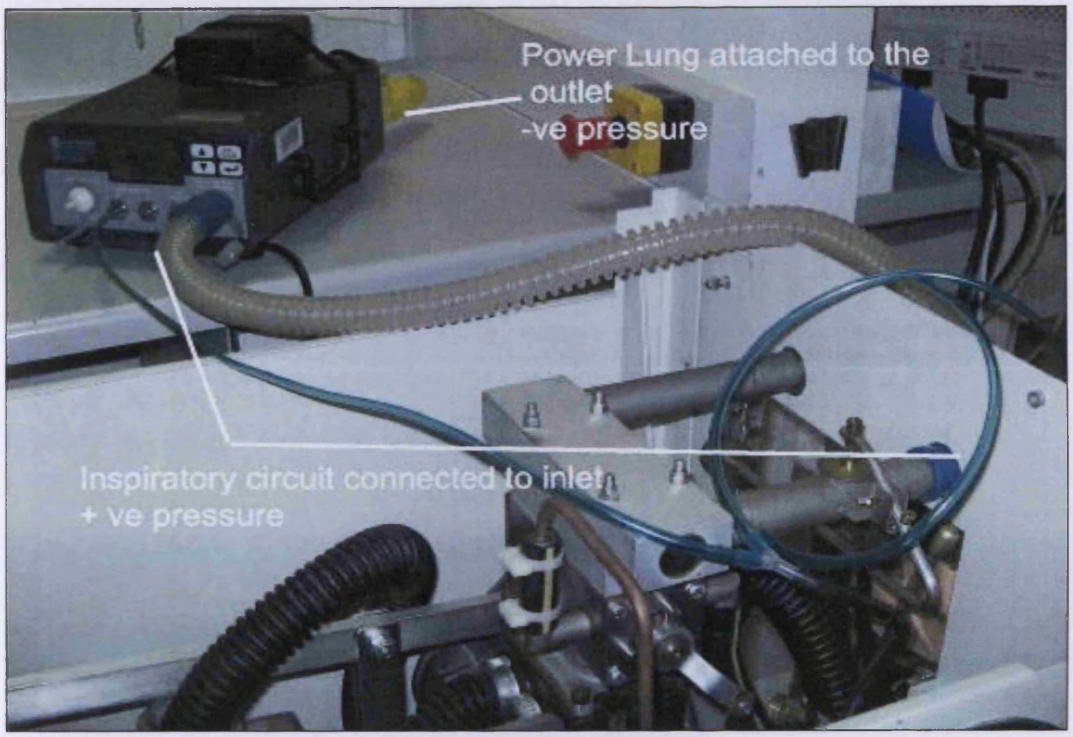

Figure 4.7: Calibration of the exhalation circuit of the PowerLung®

The exhalation circuit of the PowerLung device was provided with only 3 different resistance levels. Here the peak flow was also found to decrease with the increase in the load as in the previous case. However this decrease in the flow rate was found to be less than that of the inhalation process, thereby indicating a lower equivalent load on exhalation as compared with that of the inhalation circuit of the PowerLung® for each resistance index. The drop was from an average peak flow rate of 5.7 kPa to 4.4 kPa. The peak pressure increased with an increase in the resistance index. A maximum peak pressure of approximately 6.2 kPa was achieved at the highest resistance index.

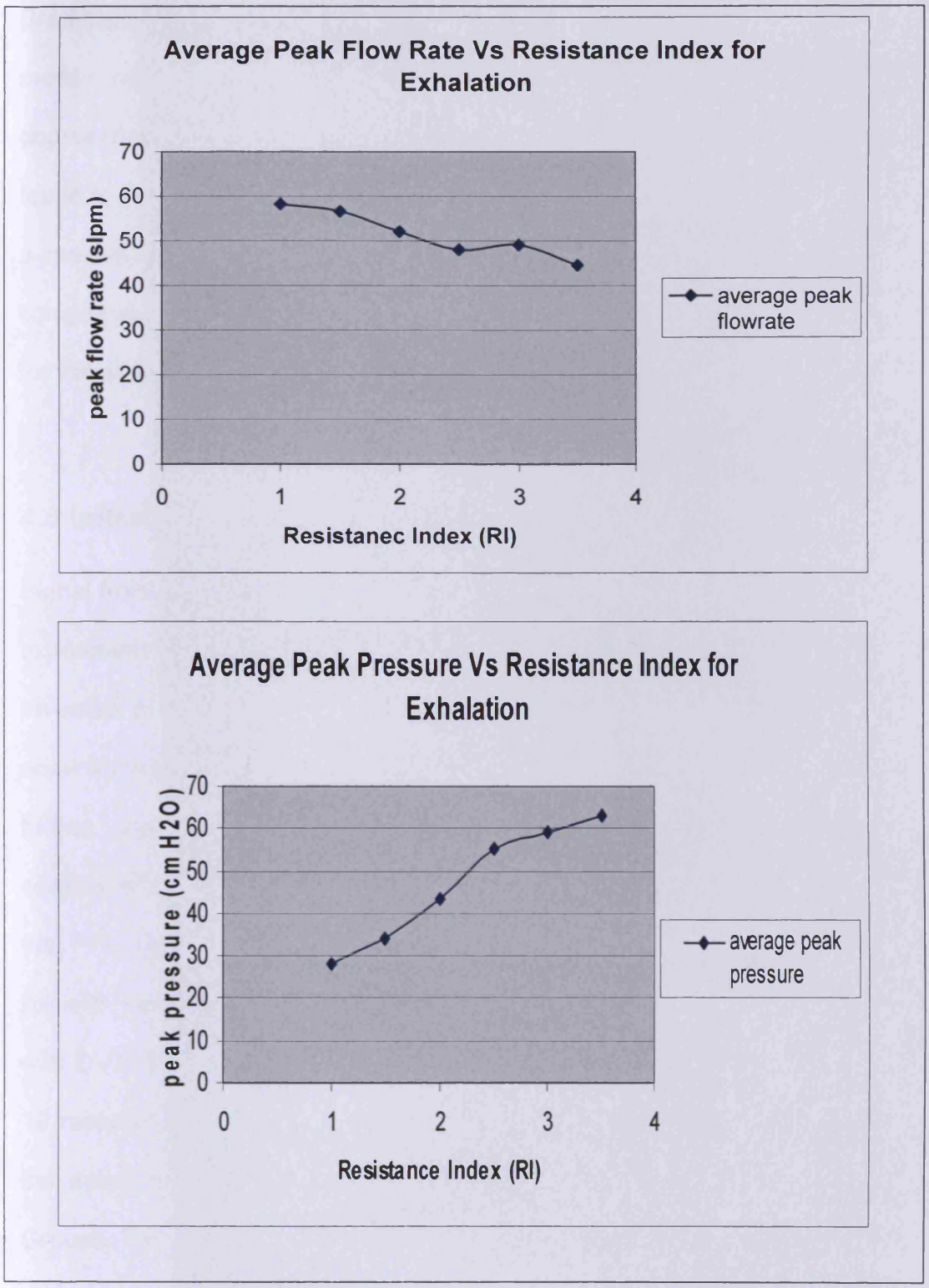

Figure 4.8: The Exhalation characteristic of the PowerLung BreatheAir®

BreatheAir™ and Trainer™ were similar products from PowerLung. The two models were calibrated in a similar manner in order to compare and select the appropriate device for this study. During the calibration the peak pressure was found to reach a staggering level of 11.7 kPa in the Trainer™ as compared to a maximum of 6.2 kPa in the BreatheAir™ model. Thus for better patient compliance the BreatheAir™ was selected to be used as the breathing device for this study.

4.5 Initial Study

Signal from 5 healthy individuals were taken using the PPG device as per the experiment protocol and these signals were visually analysed. The study revealed a decrease in the probe signal to noise ratio. Thus the signals obtained were slightly noisy. Besides in order to appreciate the HR and for further analysis of the same the sampling frequency of 6.25 Hz was considered insufficient. The length of the study was a total of 10 minutes and the PPG signal was to be collected throughout the experiment. The PPG Assist® was designed commercially for venous measurements in patients with DVT. Thus the program had to be modified by the Company to provide 10 minutes of continuous PPG signal. These modifications were made and the actual study was carried on all the participants recruited for the three Groups. The new sampling frequency of the PPG Assist® was 1 kHz and the data was directly stored onto a memory card. The data was then transferred at the researcher's convenience on to a P.C. for further analysis.

Chapter V – Results

Visual Analysis

5.1 Introduction

PPG signals were collected from the participants of all three groups as mentioned in chapter IV. These signals measured the instantaneous skin blood volume present under the probe. An increase in the instantaneous blood volume resulted in a decrease in the signal amplitude and vice versa as per the optical properties exhibited by the probe. The skin microcirculation is controlled by both intrinsic and extrinsic factors. While the intrinsic factors are more local in origin resulting in more spontaneous local vascular changes, the extrinsic factors are central in their origin and causes uniform rhythmic changes in the entire microcirculation. The raw PPG signal obtained from the participants were analysed using the signal processing toolbox of the mathematical software MATLAB. The results obtained in this study has been divided and discussed in three chapters viz; Visual Analysis (Chapter V), HF Analysis (Chapter VI) and the LF Analysis (Chapter VII). This chapter details the visual analysis of the raw PPG signal and its Fourier spectrum.

5.2 Visual Analysis of the raw PPG signal

The raw PPG signals obtained from all three groups were first visually analysed. The raw signals from each group did not have waveforms characteristic of their own group. However certain interesting features were observed for each of the three groups. The two stress tests used were a breathing exercise and a handgrip test. The former was conducted between the first and the third minute and the latter between the sixth and the eighth minute. Any change in the PPG baseline during these two, 2 minutes period was considered as a response to these stress tests. Figure 5.1, illustrates sample raw PPG signals obtained from each of the three groups.

In Group I (healthy participants), most waveforms had a very strong AC component superimposed on the slow moving DC component indicating a very strong pulse being detected by the PPG probe. Figure 5.1a is a good representative of the PPG signals obtained from this group. A sudden dip in the PPG baseline with a gradual recovery over the two-minute period was observed during the breathing test. Presence of a similar response in PPG signals obtained from both the left and the right foot indicate a more central response rather than a local reflex. This sudden dip in the baseline indicates an increase in the instantaneous total blood volume under the probe during the onset of the breathing exercise. A dip in the baseline of the signal was once again observed during the handgrip test. However the degree of dip in the baseline was considerably lower when compared to the breathing test. This pattern was observed in most participants from this group.

The AC component was superimposed on the slow moving DC component in the raw PPG signal obtained from participants in Group II (diabetic participants with no known neuropathy). However the strength of the pulses detected in these signals was weaker when compared to the signals from Group I. The amplitude changes observed in Group I during the two stress tests was considered as the bench mark for comparing the signals from the diseased groups. A dip in the signal baseline at the onset of the breathing phase but with a quick recovery of the signal was observed in this group as shown in figure 5.1b. The degree of the dip in the baseline observed in this group was reduced when compared with those of the healthy participants The response to the grip test was found to be similar in both Group I and II.

The raw PPG signals obtained from Group III (diabetic patients with known neuropathy) were influenced by several factors. Most patients in this group were old and frail and many were not able to perform the tests as well as the participants from other groups. Besides, the group also contained signals from diabetics with different degrees of neuropathy. All these factors in combination resulted in large variations between the signals within the group. Over all, once the large DC offset was removed, the amplitude variations in the signal were severely reduced compared to the other two groups and in some cases even absent (flat raw PPG signal) with little or no response to the two stress tests as shown in figure 5.1c.

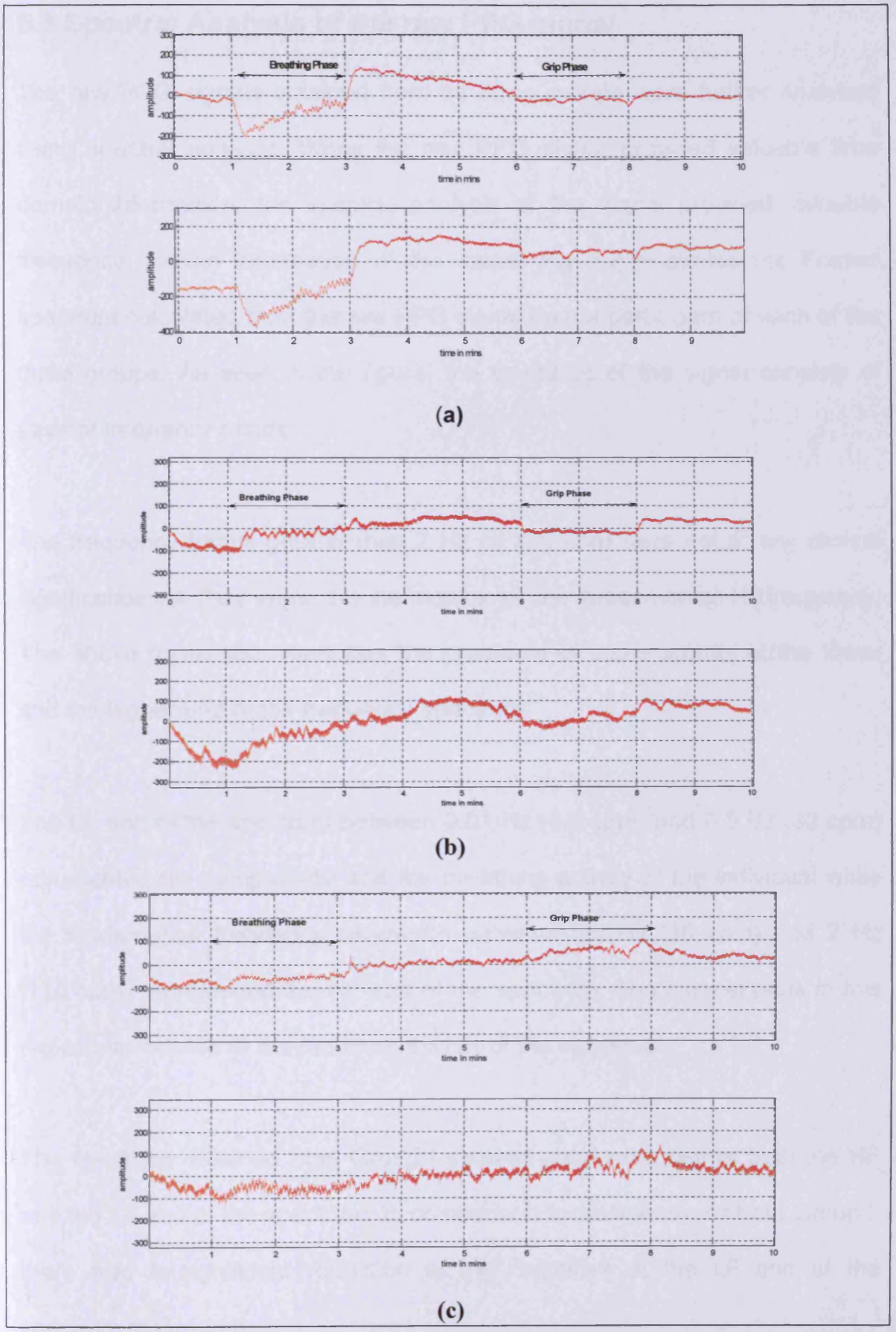

Fig 5.1: The Raw PPG signal from a normal (a), diabetic (b) and neuropathic (c) participant. Each signal is from both left (above) and right (below) leg

5.3 Spectral Analysis of the raw PPG signal

The raw PPG signals obtained from all three groups were further analysed using spectral analysis. While the raw PPG signal provided valuable time domain information, the spectral analysis of the signal provided valuable frequency domain information of the same. Fig 5.2 illustrates the Fourier spectrum calculated from the raw PPG signal from a participant of each of the three groups. As seen in the figure, the spectrum of the signal consists of several frequency bands.

The frequency bands greater than 2 Hz or 120 cpm were not of any clinical significance as they were the harmonics of the fundamental HRfrequency. The above figure also illustrates the presence of some activity at the lower and the higher end of the frequency spectrum.

The LF end of the spectrum between 0.01 Hz (0.6 cpm) and 0.5 Hz (30 cpm) represented the sympathetic and the breathing activity of the individual while the fundamental frequency bandwidth between 0.5 Hz (30 cpm) and 2 Hz (120 cpm) represented the HF end of the spectrum. The highest peak in this region was related to the fundamental HR of the individual.

The spectrum obtained from Group I showed good response at both the HF and the LF end of the spectrum. In comparison to the spectrums from Group I, there was a significant reduction in the response at the LF end of the spectrum in Group II.

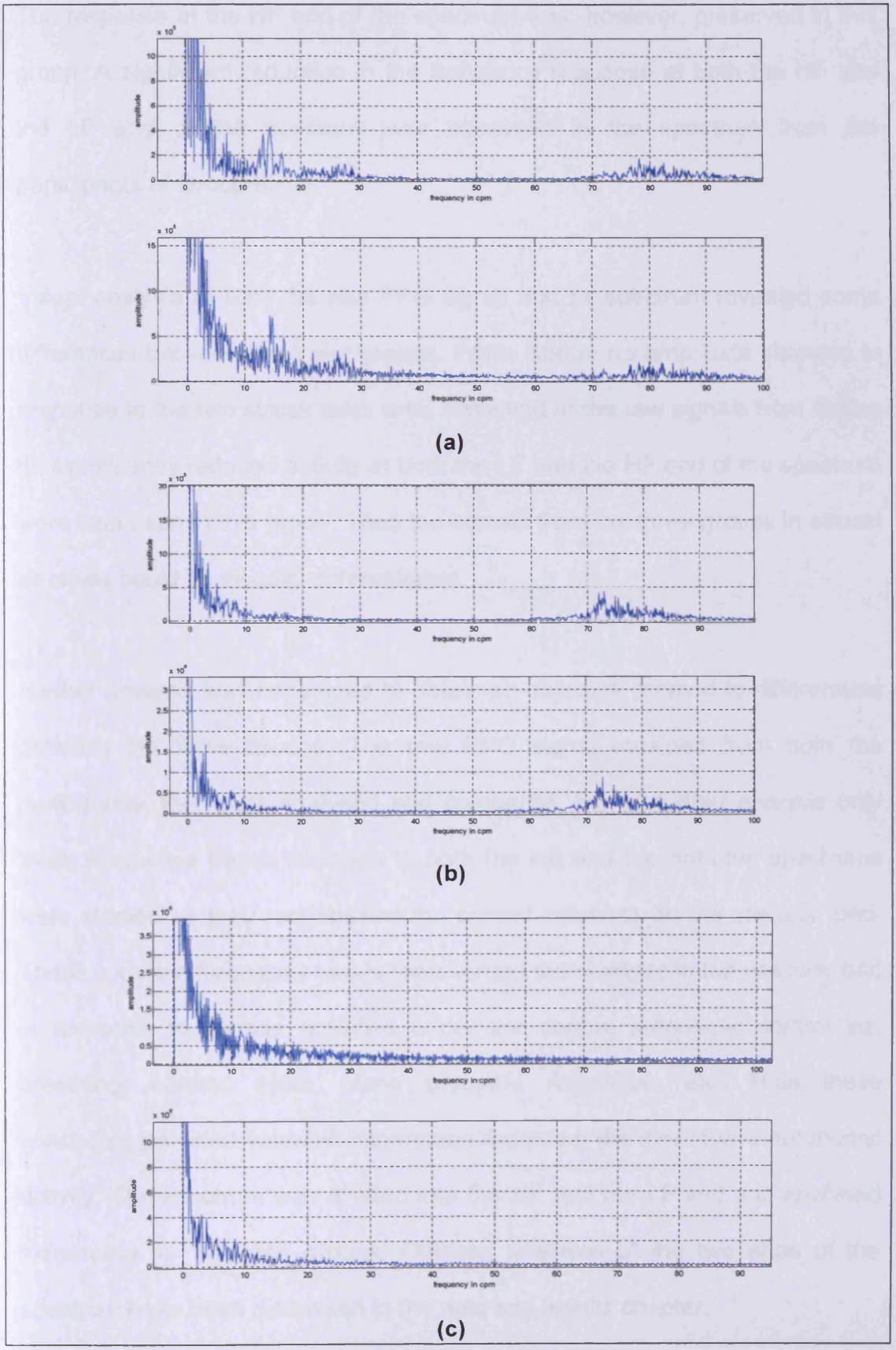

Figure 5.2: The Fourier spectrum of the raw PPG signal from a normal (a), diabetics (b) and neuropathic (c) participant. Each signal is from both left (above) and right (below) leg

The response at the HF end of the spectrum was, however, preserved in this group. A significant reduction in the frequency response at both the HF and the LF end of the spectrum was observed in the spectrum from the participants of Group III.

Visual analysis of both the raw PPG signal and its spectrum revealed some differences between the three groups. While little or no amplitude changes in response to the two stress tests were observed in the raw signals from Group III, significantly reduced activity at both the LF and the HF end of the spectrum were also seen in this group. Thus the signals from the three groups in almost all cases could be visually differentiated.

Further analysis was conducted to obtain an objective method to differentiate between the three groups. The raw PPG signal obtained from both the participants' feet were analysed and compared. For all further analysis only those frequency bands common to both the left and the right leg spectrums were studied as they represented the central influence on the vascular bed. These common frequency bands represented the changes in the vascular bed in response to various activities under the central autonomic control viz, breathing, cardiac cycle, blood pressure regulation, etc. Thus these spectrums provided valuable information regarding the individual's autonomic activity. The spectrum was divided into the HF and the LF end and analysed individually for all three groups. Detailed analyses of the two ends of the spectrum have been discussed in the next two results chapter.

Chapter VI – Results

High Frequency Analysis

6.1 Introduction

The response at the HF end of the spectrum represents changes in the skin microcirculation due to the individual's cardiac cycle. The HR of an individual is not represented by a single frequency but by a bandwidth of frequencies where the central prominent frequency represents the individual's fundamental heart rate. Damage to the autonomic fibres can result in abnormalities of the cardiac and the vascular dynamics. The HR of an individual varies with every beat and thus is represented in the HF end of the spectrum as a bandwidth rather than a single frequency. Both divisions of the autonomic nervous system viz, the sympathetic and parasympathetic branches work in finely balanced opposition to each other to control the HR and various other end organs of the body (Vinik and Erbas 2001). Several tests to objectively measure and diagnose the CAN are in routine clinical use. Almost all these tests use the HR trace obtained from the ECG. In this study, attempts were made to extract the HR information from the raw PPG signal and to try to use the information to differentiate between the three groups. A MATLAB program was written to extract the HR bandwidth from the HF end of the spectrum. This program was further improved to also extract the beat-by-beat HR trace from each of the spectrums. Both the bandwidth and the HR trace were then compared and analysed for all three groups.

6.2 Analysis of the HR bandwidth

In general the HR for most individuals lies between 60-100 beats per minute (bpm). While extracting the HR information from the spectrum, the highest peak between 0.8 Hz (48 cpm) and 2 Hz (120 cpm) was regarded as the fundamental HR of the individual. Any other peaks obtained beyond 2 Hz were considered to be the harmonics of the fundamental heart rate. A MATLAB program was written to detect the highest peak between 0.5 Hz and 2 Hz. Seventy percent of this maximum peak was then used as a threshold to obtain the lower and the upper limit to calculate the HR bandwidth from the spectrum as shown is figure 6.1. The size of the bandwidth represented the degree of variability present within the HR of the individual. Broader bandwidths obtained in Group I meant a greater number of frequencies within the bandwidth, and a higher HR variability. The reverse was true for sharp narrow bandwidths obtained from the participants of Group II.

The bandwidth of the HR and the fundamental HR frequency (the highest peak) were calculated for both legs from each participant of all the three groups. Three variables were calculated from these parameters viz; the mean bandwidth for both feet, the degree of agreement of the bandwidth calculated from both feet (left leg bandwidth – right leg bandwidth) and the degree of agreement in the fundamental HR obtained from both feet (Left leg fundamental HR – right leg fundamental HR) using Excel. The scatter plots of the latter two variables calculated from both feet were analysed. They however did not produce any significant results and hence were not analysed

any further. Only the mean bandwidth calculated for each of the participants across the three groups were compared and analysed.

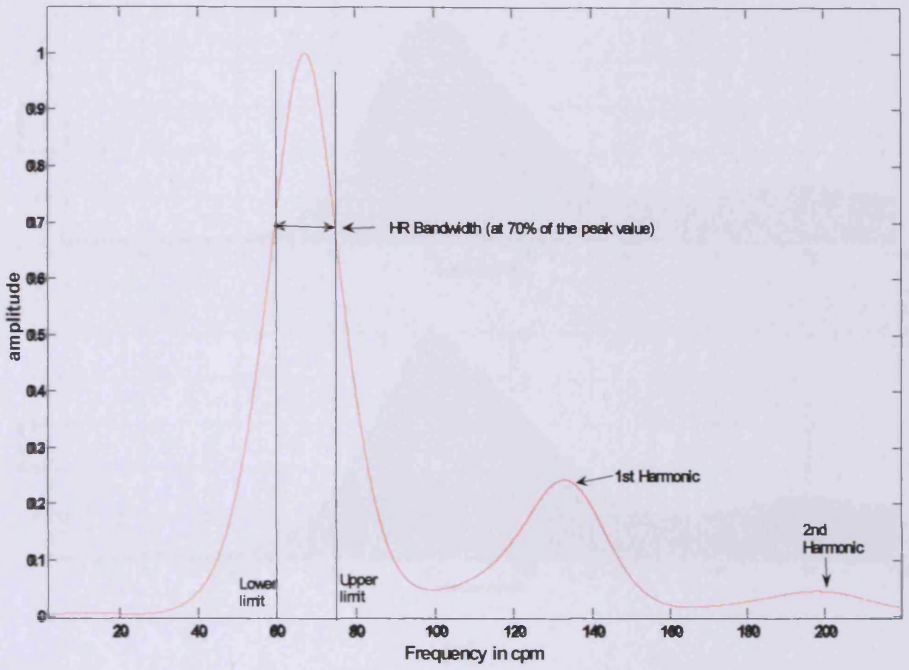

Fig 6.1: The HF end of the spectrum from a typical raw PPG signal with a fundamental HR bandwidth and the subsequent harmonics

6.2.1 HR bandwidth comparison by visual analysis

The HR bandwidths calculated from the spectrums from all three groups were visually analysed. The typical HR bandwidth obtained from the participants from Groups I and II have been illustrated in figure 6.2. In all these figures generated by MATLAB, signals from both the left (above) and right (below) foot are shown. The bandwidth obtained from Group II participants were found to be narrower when compared to the bandwidth calculated from the participants in Group I. Smaller bandwidths obtained from the diseased group

suggest decreased HR variability. Earlier studies have shown decreased HR variability to be one of the earliest signs of parasympathetic dysfunction.

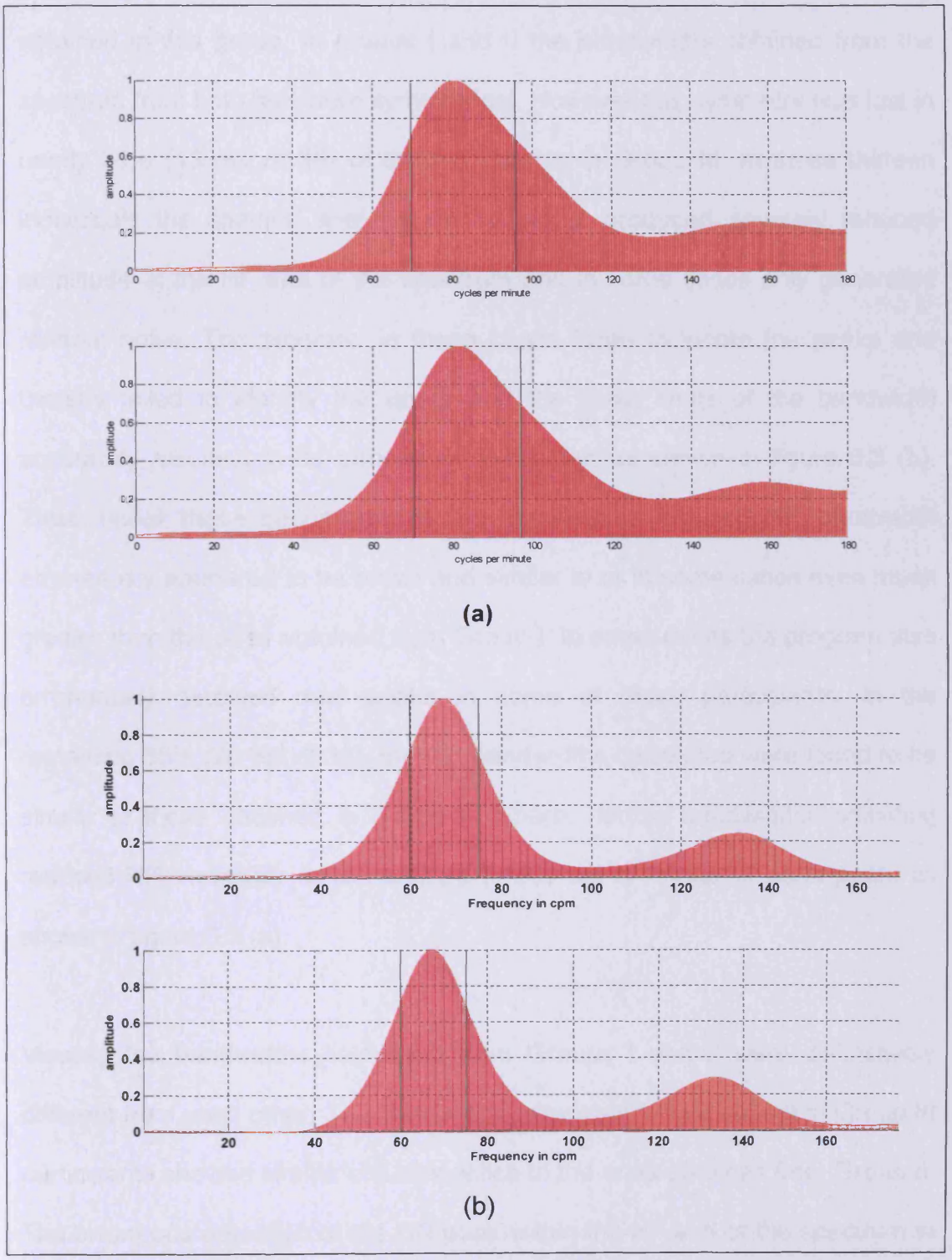

Fig 6.2: The HR bandwidth obtained from a Group I (a) and Group II (b) participant. Note the narrower bandwidth observed in a Group II participant as compared with the one from Group I.

Visual analysis of the bandwidth extracted from the participants in Group III produced some interesting observations. A variety of bandwidth sizes were obtained in this group. In groups I and II the bandwidths obtained from the spectrum from both feet were symmetrical. However this symmetry was lost in nearly 35% (13 out of 38) of the participants in Group III. In these thirteen individuals the spectral analysis of the signal produced severely reduced amplitude at the HF end of the spectrum and in some cases only generated random noise. The program, in these cases failed to locate the peaks and thereby failed to identify the upper and the lower limits of the bandwidth accurately resulting in its erroneous calculation as shown in figure 6.3 (b). Thus, under these circumstances the significantly reduced HR bandwidth erroneously appeared to be broad and similar to or in some cases even much greater than the ones obtained from Group I. In some cases the program also erroneously detected dual peaks in some of these participants. In the remaining 65% (25 out of 38), the HR bandwidths calculated were found to be similar to those obtained in Group II. Sharp, narrow bandwidths indicating reduced HR variability were obtained in this set of Group III participants as shown in figure 6.3 (a).

Visually the bandwidths calculated from Groups I and II were distinctively different from each other. The bandwidth calculated from a subset of Group III participants showed similar characteristics to the ones obtained from Group II. The erroneous detection of the HR peak within the HF end of the spectrum in the 13 individuals from Group III also resulted in the erroneous calculation of

their beat-by-beat HR trace. Thus a need arose to exclude the data from these 13 individuals within Group III from all future analysis using the HF end of the spectrum. Thus the new subset generated with only 25 group III participants was called Group IIIa. Statistical analyses were however performed using both, Group III as a whole and with the new subset Group IIIa, to understand the affect of the data from these 13 individuals on the results from the statistical analysis.

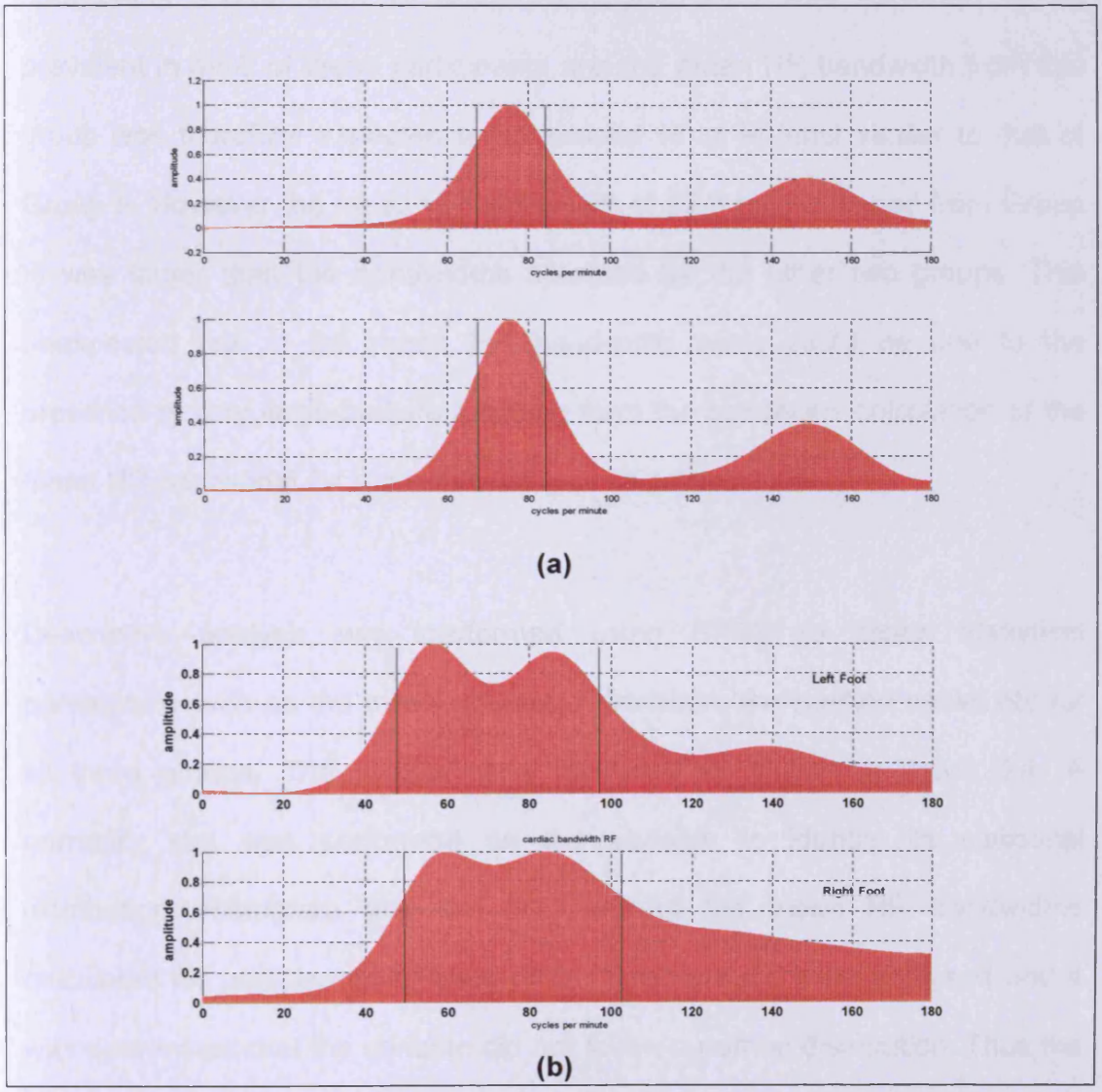

Fig 6.3: The variation in the HR bandwidth obtained from the participants in Group III. 65% of the participants produced the bandwidth shown in (a) while 35% produced bandwidth as shown in (b)

6.2.2 Statistical Analysis using data from participants in Group III

Statistical analyses were carried out to understand the distribution of the mean bandwidths calculated within each group and across the three groups. The mean HR bandwidth calculated for groups I, II and III were 27.6 bpm, 22.4 bpm and 32.6 bpm respectively. A reduction in the mean HR bandwidth for Group II was observed as compared to the value obtained from Group I. The participants of Group III were diabetic patients with varying degree of neuropathy. Some form of autonomic dysfunction was expected to be prevalent in most of these participants and the mean HR bandwidth from this group was therefore expected to be smaller to or at least similar to that of Group II. However the mean HR bandwidth of 32.6 bpm obtained from Group III was larger than the bandwidths obtained for the other two groups. This unexpected rise in the mean HR bandwidth value could be due to the presence of very large outliers resulting from the erroneous calculation of the mean HR bandwidth for more than 35% of its participants.

Descriptive analysis was performed using SPSS to obtain statistical parameters such as the mean, standard deviation, the median value, etc for all three groups. The results were tabulated as shown in figure 6.4. A normality test was performed on the variable to identify its statistical distribution. Histogram and the Q-Q plot of the mean HR bandwidths calculated for participants of each of the three groups were analysed and it was determined that the variable did not follow a normal distribution. Thus the distribution of the variable in each of the groups was better expressed using the median rather than the mean bandwidth value.

Group I		*Group II*		*Group III*	
Mean	26.9	Mean	24.2	Mean	30.3
Standard Error	1.53	Standard Error	1.73	Standard Error	1.77
Median	23.5	Median	20	Median	29
Standard Deviation	9.15	Standard Deviation	10.2	Standard Deviation	10.9
Sample Variance	83.8	Sample Variance	105	Sample Variance	119
Kurtosis	1.3	Kurtosis	2.38	Kurtosis	-1.26
Skewness	1.27	Skewness	1.82	Skewness	0.29
Range	38	Range	38	Range	37
Confidence Level (95.0%)	3.1	Confidence Level (95.0%)	3.52	Confidence Level (95.0%)	3.59

Fig 6.4: Comparison of the descriptive statistics of the mean HR bandwidth obtained from Groups I, II and III

Kruskal-Wallis Test

Ranks

	group	N	Mean Rank
mean bandwidth for each participant -Group I	group I	32	54.22
	group II	33	38.21
	group III	37	61.00
	Total	102	

Test Statistics(a,b)

	mean bandwidth for each participant - Group I
Chi-Square	10.740
df	2
Asymp. Sig.	.005

a Kruskal Wallis Test

b Grouping Variable: group

Figure 6.5: k^{th} sample non-parametric test to obtain the inter-group relation of the mean HR bandwidth calculated from the three groups

The inter-relation of the variable calculated from the three groups was also statistically analysed using the hypothesis-testing model. The null hypothesis for this analysis was set as there being no difference in the mean bandwidth obtained from all three groups at a statistically significant level. Since the mean HR bandwidth calculated for the three groups were continuous, independent and followed a non normal distribution, a non-parametric test was used. Since three groups were compared, a k^{th} sample non-parametric test also known as the Kruskal Wallis Test was chosen as a suitable test. The test was performed using the SPSS package. The first output table produced the mean ranks for each group and the second table produced the detailed test statistics as shown in figure 6.5. The Chi-square value of 10.740 with 2 degrees of freedom gave a p value of 0.005 indicating that the results were statistically significant and subsequently rejecting the null hypothesis. Thus it could be rightly concluded from the above test that the mean bandwidths of the three groups were different from each other. This test however did not provide any further information regarding the relationship of the variable between each pair of groups. In order to do so the two groups were taken at a time and the 2 sample non-parametric test i.e. the Mann – Whitney test was performed. The results of these tests indicated statistically significant difference in the mean HR bandwidth calculated from Groups I and II and between Groups II and III. However no significant difference could be established between the mean HR bandwidth from Groups I and III.

6.2.3 Statistical Analysis using the subset Group IIIa

The statistical analysis detailed in the previous section was repeated to compare the HR bandwidth obtained from Groups I and II to those obtained from the new subset created from Group III called Group IIIa. This subset excluded the data from the thirteen individuals whose HR information could not be accurately extracted from the raw PPG signal. By performing statistical analysis using both the whole group and its subset separately, the results thus obtained were expected to provide valuable information of the influence of the data from these 13 individuals on the entire group (Group III). The descriptive statistics for Group III and IIIa were obtained and compared using EXCEL spreadsheet. The results have been tabulated in figure 6.6.

Group III		***Group IIIa***	
Mean	30.3	Mean	24.2
Standard Error	1.77	Standard Error	1.47
Median	29	Median	21
Mode	17	Mode	17
Standard Deviation	10.9	Standard Deviation	7.37
Sample Variance	119	Sample Variance	54.3
Kurtosis	-1.26	Kurtosis	0.27
Skewness	0.29	Skewness	1.01
Range	37	Range	27
Largest(1)	53	Largest(1)	43
Smallest(1)	16	Smallest(1)	16
Confidence Level (95.0%)	3.59	Confidence Level (95.0%)	3.04

Figure 6.6: Comparison of the descriptive statistics of Groups III and its subset IIIa

From the above tabulation is can been seen that by excluding the data from the thirteen individuals, the mean HR bandwidth of the group decreased from 30.3 bpm to 24.2 bpm. The mean bandwidth obtained from the subset was

similar to bandwidth obtained from the participants of Group II. Visual analysis of the raw PPG signal and the HR bandwidth in the subset had revealed similar characteristics to Group II data. The participants of Group III were at varying stages of their neuropathy. All the 13 participants, whose data was excluded from the new subset, had a VPT score of greater than 30 mV in both legs, indicating sensory loss probably due to diabetic sensory neuropathy. Though we did not have any direct test to measure the autonomic function of the individuals in this group, the possibility of having both autonomic and sensory dysfunction due to diabetic neuropathy in these individuals is highly probable. The inability to extract reliable HR information from the HF end of the spectrum from these signals could be due to the early parasympathetic damage in these individuals due to autonomic dysfunction. The remaining 25 participants however had an intact HF end of the spectrum and hence the HR information could be reliably extracted from these raw PPG signals.

A Man-Whitney test was performed to obtain the statistical relationship between the groups using the new subset created. The results have been tabulated in figure 6.7. The mean bandwidth for Group I was higher than the other two groups, indicating greater HR variability within this group as expected. Although the mean bandwidth of Group IIIa was smaller than Group I, no statistical difference could be established between the two groups. This could be due to the difference in the group size as the non-parametric test involved ranking of each data and their summation. However statistical difference could be established between Groups I and II with a very small p value.

Analysis of the HR bandwidth highlighted the failure of the Vascular Assist in picking up reliable HF information from 13 participants of Group III. The PPG signals from these patients had a severely reduced or absent HR information. The HR bandwidth characteristics of the remaining 25 participants of this group were similar to those obtained from diabetics with no neuropathy. Statistical difference could be established only between the mean bandwidths of Groups I and II. On analysing the bandwidth information from Group III as a whole, the mean bandwidth for this group was similar to the value obtained from Group I. This was not an expected result as the two groups represented the extreme ends of the disease spectrum. The healthy participants of Group I were expected to have the highest HR variability, followed by Group II and the least variability was expected in participants of Group III. Statistical analysis of the new subgroup IIIa formed by excluding the signals from these 13 individuals also could not statistically differentiate between Groups I and IIIa. However the mean bandwidth of this group was similar to Group II and was more in line with the expected result. The next part of the HF analysis involved extracting the beat-by-beat HR trace from these PPG signals. The HR traces could not be extracted from 13 neuropathic participants and hence could not be assessed any further. Therefore from the signal analysis point of view it became necessary to exclude them from the group for the remaining HF analysis. Signals from all 38 participants of Group III were considered for the LF analysis discussed in the next chapter.

Ranks

	groups	N	Mean Rank	Sum of Ranks
bandwidth	normal	36	40.99	1475.50
	diabetic	35	30.87	1080.50
	Total	71		

Test Statistics(a)

	bandwidth
Mann-Whitney U	450.500
Wilcoxon W	1080.500
Z	-2.069
Asymp. Sig. (2-tailed)	.039

a Grouping Variable: groups

Ranks

	groups	N	Mean Rank	Sum of Ranks
bandwidth	diabetic	35	29.24	1023.50
	neuropathic	25	32.26	806.50
	Total	60		

Test Statistics(a)

	bandwidth
Mann-Whitney U	393.500
Wilcoxon W	1023.500
Z	-.662
Asymp. Sig. (2-tailed)	.508

a Grouping Variable: groups

Ranks

	groups	N	Mean Rank	Sum of Ranks
bandwidth	normal	36	33.44	1204.00
	neuropathic	25	27.48	687.00
	Total	61		

Test Statistics[a]

	bandwidth
Mann-Whitney U	362.000
Wilcoxon W	687.000
Z	-1.294
Asymp. Sig. (2-tailed)	.196

a. Grouping Variable: groups

Figure 6.7: Man-Whitney test to compare the intergroup relation. Statistical difference could be established between Groups I& II but statistical difference could not be established between Groups II & IIIa and I & IIIa

6.3 Analysis of the beat-by-beat HR trace

The analysis of the HR bandwidth was followed by the analysis of the beat-by-beat HR trace. The MATLAB program written to extract the HR bandwidth from the raw PPG signal was further modified to extract the beat-by-beat HR trace.

The upper and the lower limits of the HR bandwidth calculated using the previous program was used in the next stage. These values were used as cut off frequencies of the band pass filter used for filtering the original raw PPG signal. The filtered signal was then complex demodulated at the frequency of the mean fundamental HR (frequency with the largest amplitude) calculated from both feet. The complex demodulated signal was then passed through a peak detection program using the zero crossing detector principle to detect the peaks on the demodulated signal. The time of the occurrence of each of these peaks was calculated. Their difference provided the information of the time between two consecutive peaks otherwise known as the R-R interval. The inverse of the R-R interval calculated for every beat produced the HR for that beat. The beat-by-beat HR trace extracted contained spikes that were effectively removed using a spike filter. The final filtered HR trace was then plotted against the time vector as a new figure in MATLAB. The program generated the beat-by-beat HR trace from both legs for each participant. They were then visually analysed and compared using objective methods. The flow chart of the program steps for generating the HR trace is shown in figure 6.8.

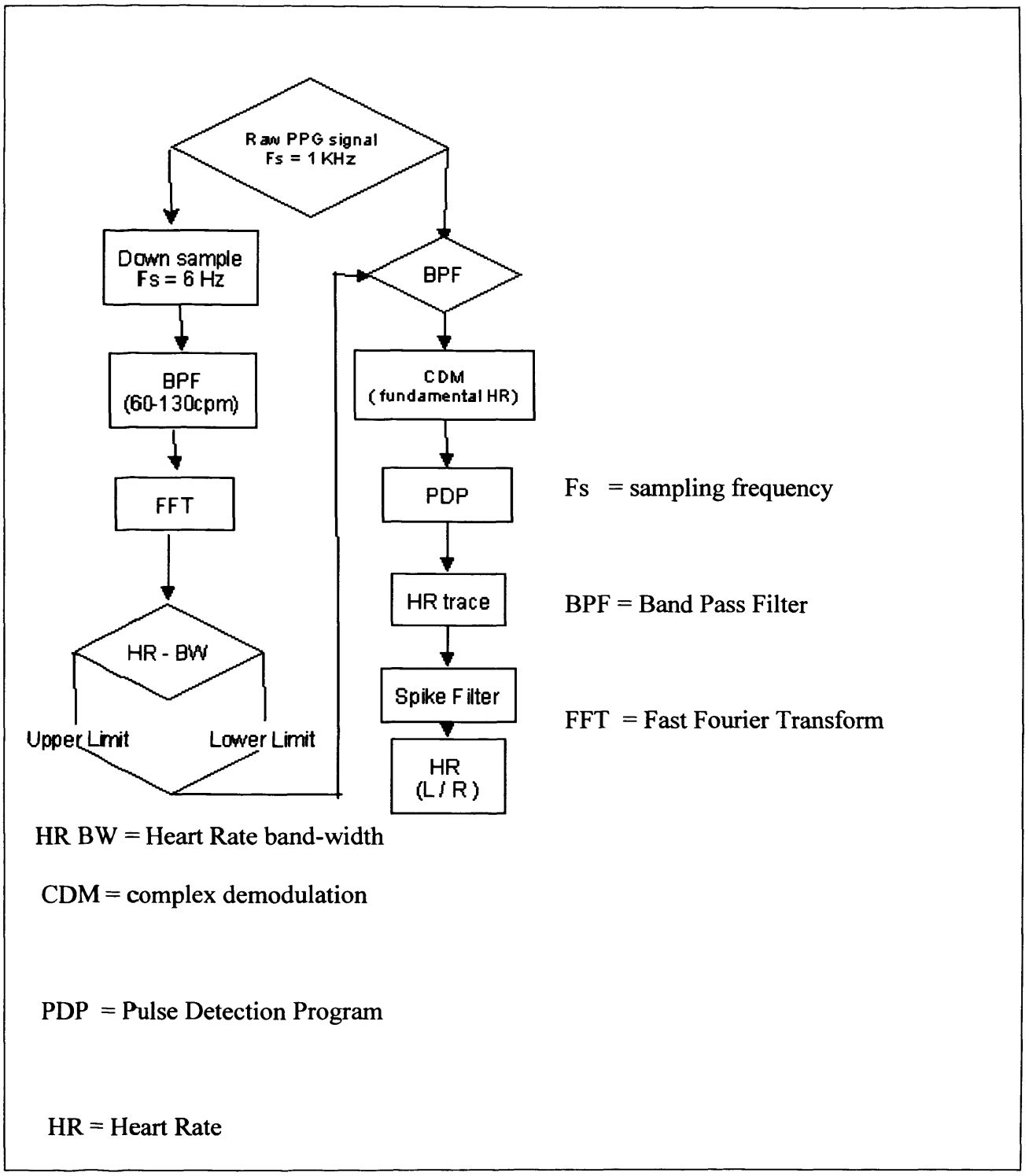

Figure 6.8: Flow Chart representing the heart rate extraction program

6.3.1 HR Agreement Analysis

Once the HR trace was extracted from the spectrum, the agreement between the traces obtained from both feet was studied. Ideally the traces extracted from both feet should be identical as they both represent the beat-by-beat HR of the individual. However inherent errors in programming and the data collection could result in some discrepancies in the two traces. The degree of discrepancies between the two traces was a measure of the success in extracting the HR from the spectrum. A Bland-Altman plot was used to measure the degree of agreement between the HR trace extracted from the left and the right foot signal.

A MATLAB program was written to produce this plot. The difference between the HR extracted from the left and the right foot for every beat and the mean of this difference were calculated for each participant. The standard deviation of the difference between the two traces was calculated and the upper (mean difference + standard deviation) and the lower (mean difference – standard deviation) limit were determined for each individual. The mean HR for every beat from the two traces for the whole 10 minutes of the signal was also calculated. The difference between the two traces was plotted against the mean HR along with the mean of the difference and the ±one standard deviation limit. The upper and the lower limit of the difference indicate the degree of agreement between the two HR trace. Tighter limits indicate better fit between the left and the right HR trace. However these limits were also influenced by the presence of very large outliers. Hence, in cases where the HR from both feet were in good agreement with each other for most part of

the signal but had spikes which produced huge differences in other instances, the limits were pushed further apart from each other giving a rather erroneous picture. Therefore, the mean of the difference between the two HR trace provided a better insight to the degree of agreement between the left and the right HR trace where a smaller mean difference indicated fewer discrepancies between the two traces and hence a better agreement. The degree of agreement between the left and the right HR trace were both visually and statistically analysed and the mean difference for each individual was noted.

6.3.1.1 Visual Analysis of Group I

The beat-by-beat HR trace for both feet was plotted using MATLAB along with the Bland-Altman plot. The trace obtained from each of the participants was visually analysed for all three groups. Certain observations were made after the visual analyses of the traces from Group I. An example of the HR trace and its Bland Altman agreement plot obtained from a participant in Group I is illustrated in figures 6.9 and 6.10.

As expected the HR for an individual was not constant for the whole ten minutes but varied with every heartbeat. This beat-by-beat variability was found to be very high in the participants of this group. Beat-by-beat variation of up to 30 bpm was observed in this group. The difference between the minimum and the maximum HR in most participants was greater than 20 bpm. A strong response of the HR to the two stress tests was also observed with a steady rise in the HR especially during the breathing test. Overall, the response to the grip test was not as effective as the breathing test. This could

be due to the fact that the individuals during the grip test were not exerted enough to produce any visible results.

The high beat-by-beat variability in the HR trace introduced some phase shift among the left and the right HR trace in 53% of the participants in this group. Further examination of these phase shifts did not produce any specific pattern. However of this 53%, 14% of the traces were found have phase shifts only in parts of the signal with perfect phase in the rest of the signal. Those participants with smaller beat-by-beat variability were found to have perfect phase matching.

Important information was also obtained from the Bland Altman plots. The beat-by-beat mean HR for this group varied from 65-105 bpm suggesting excellent variability. The mean difference in the two traces was found to be around 0 with a ±1 SD of less than 10bpm in most participants of this group.

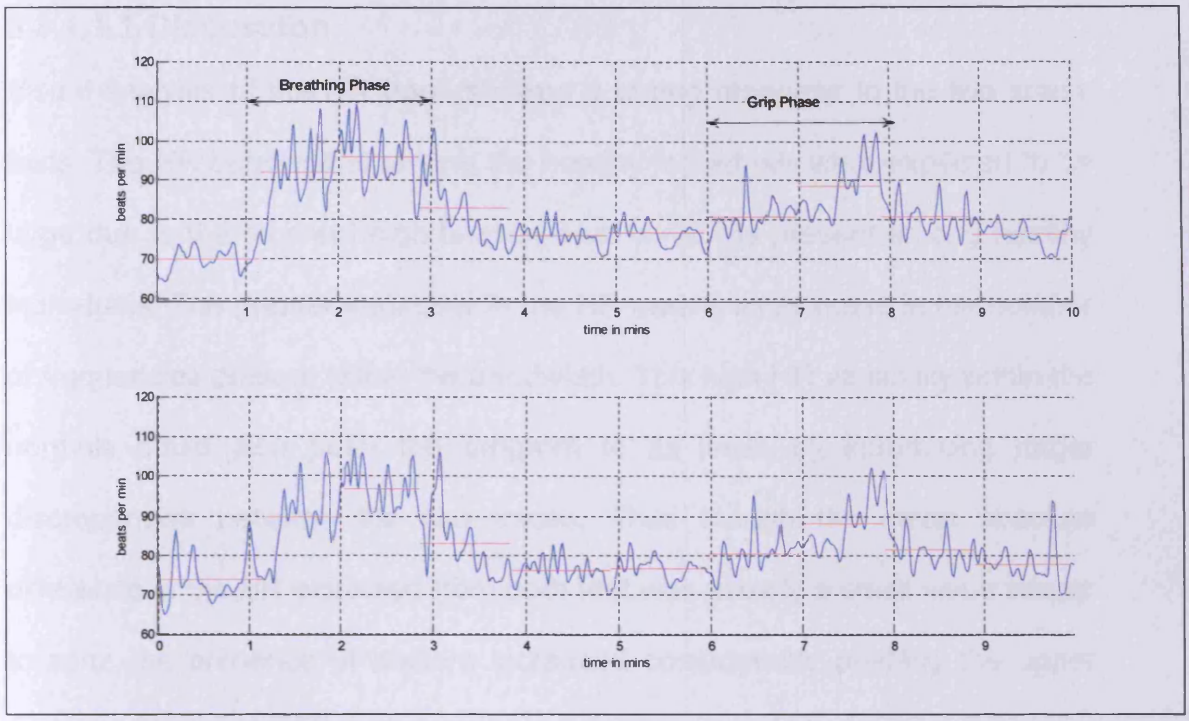

Figure 6.9: The HR trace extracted from left and right foot of a healthy individual

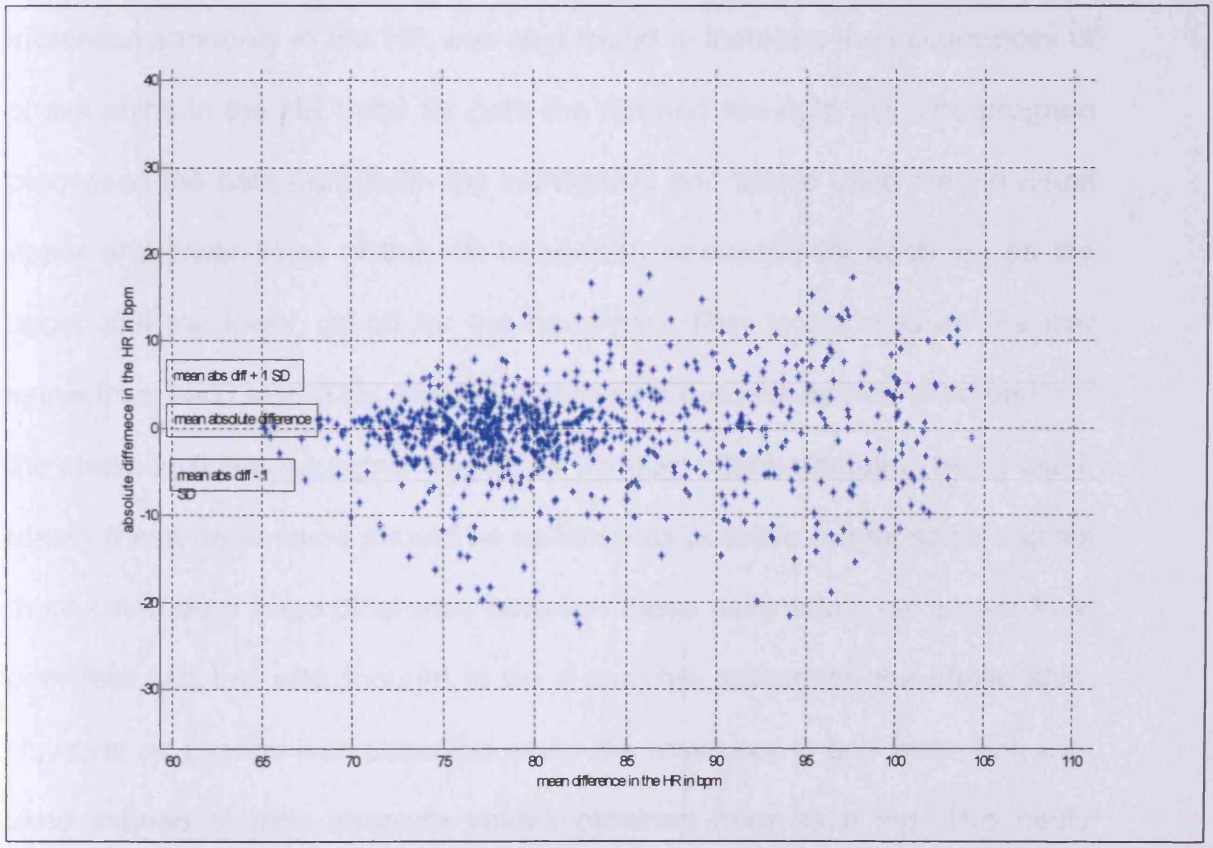

Figure 6.10: The Bland Altman plot of the HR shown in the previous figure with the ±1 SD limits of ±6bpm

6.3.1.1.1 Discussion

Visual analysis of the HR trace showed a strong response to the two stress tests. The HR bandwidths among the healthy individuals were expected to be large due to the inherent high beat-by-beat variability present among healthy individuals. The greater variability in the HR meant an increase in the number of frequencies present within the bandwidth. This high HR variability within the normals could also push the program to its limits by introducing larger discrepancies between the two traces. Thus though the mean absolute difference in the HR extracted from both feet was usually a small value nearer to zero, the presence of outliers increased considerably pushing the upper and lower limits of 1 SD further apart.

Increased variability in the HR was also found to increase the occurrences of phase shifts in the HR trace for both the left and the right leg. The program processed the data from each leg individually and hence used the individual upper and lower limits of the HR bandwidth calculated for each leg as the upper and the lower cut-off for the band-pass filter to be used on the raw signal from each side. This was thought to be a possible source of introducing the phase shift into the signal due to the different filter parameters being used. Ideally these parameters should be as close as possible but for some signals there could be a huge difference between these parameters calculated from both feet and this was thought to be a possible reason for the phase shift. However no change was observed when the mean upper and lower limit was used instead of their absolute values obtained from each leg. This could indicate the possibility of some physiological explanation for this apparent

phase shift in the HR trace obtained from both the legs, observed only within this group.

6.3.1.2 Visual Analysis in Group II

The visual analysis of the HR traces from Group II revealed certain features specific to this group. An example of a HR trace and its corresponding Bland Altman plot obtained from this group are illustrated in figure 6.11 and 6.12. The beat-by-beat variability in the HR was comparatively lower than that observed in Group I. The maximum variability in this group was less than 15 bpm. The low variability in the HR trace produced much better agreement between the left and the right leg traces. Even in the event of any discrepancy between the left and the right foot HR trace the absolute difference calculated was significantly smaller resulting in fewer outliers. Thus the resulting Bland Altman plot produced a smaller spread of the difference in the HR trace.

The low variability also produced good phase matching between the two traces keeping the mean absolute difference between the left and the right HR trace to very small values. In spite of reduced HR variability, strong responses to the two stress tests were observed in 13 participants (37%) of this group. The HR traces from 14 patients (40%) were found to have a moderate response to the tests as shown in figure 6, while the traces from 7 patients (20%) were absolutely flat with no response to the two tests. In the HR trace as shown in figure 6.11, a slight increase (approx of about 5 bpm) in the HR during the breathing test was observed but it was still less than the normals where the HR increased by about 15 bpm or more in most participants. The

program was unable to extract the HR from the signal of 1 patient (2%) resulting in a noisy HR trace.

The analysis of the Bland Altman plots reflected the results from the visual analysis of the HR traces from this group. The mean HR for every beat ranged between 70bpm and 90bpm. This was significantly lower than Group I. The mean absolute difference in the two traces was zero or near zero with tight ± 1 SD limits of less than ± 2 bpm with the presence of very few outliers.

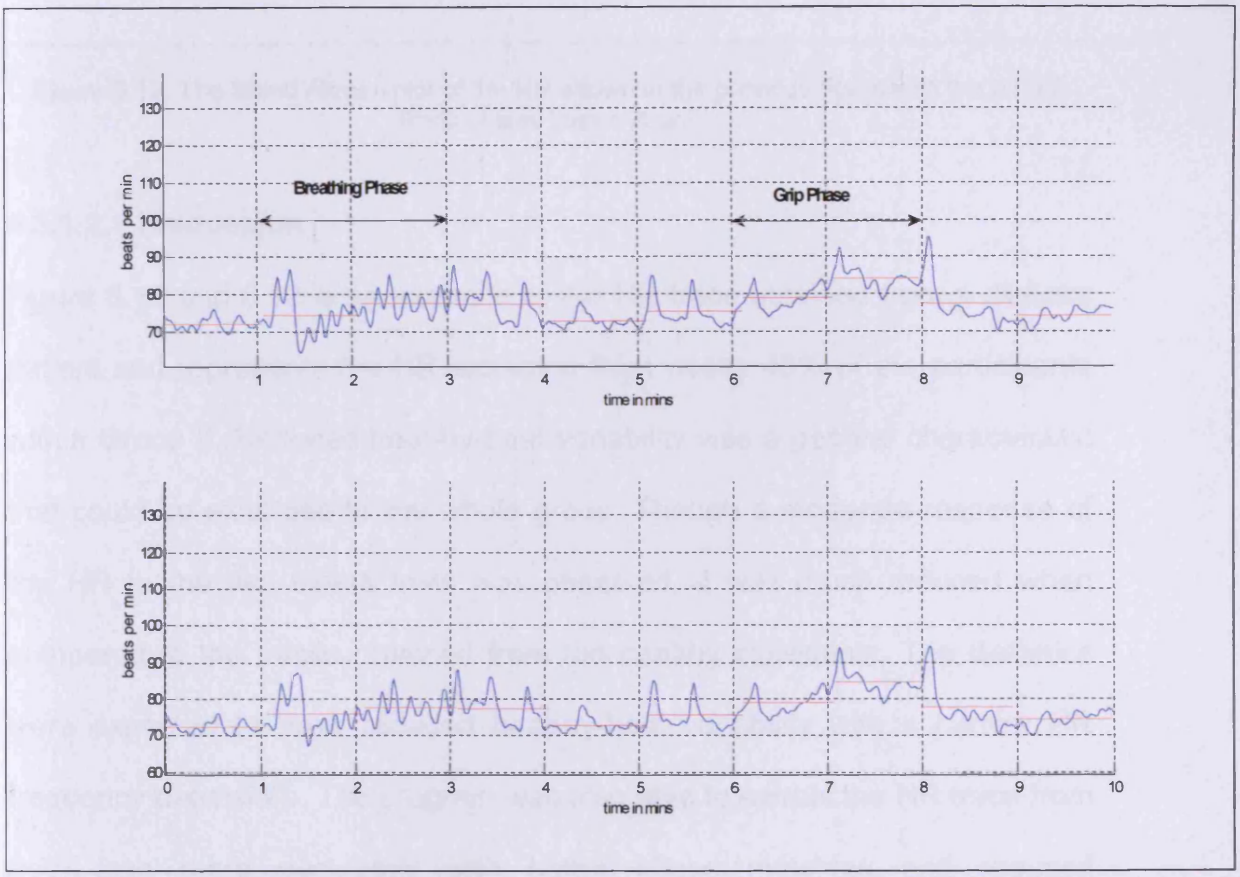

Figure 6.11: The HR trace extracted from left and right foot of a diabetic participant

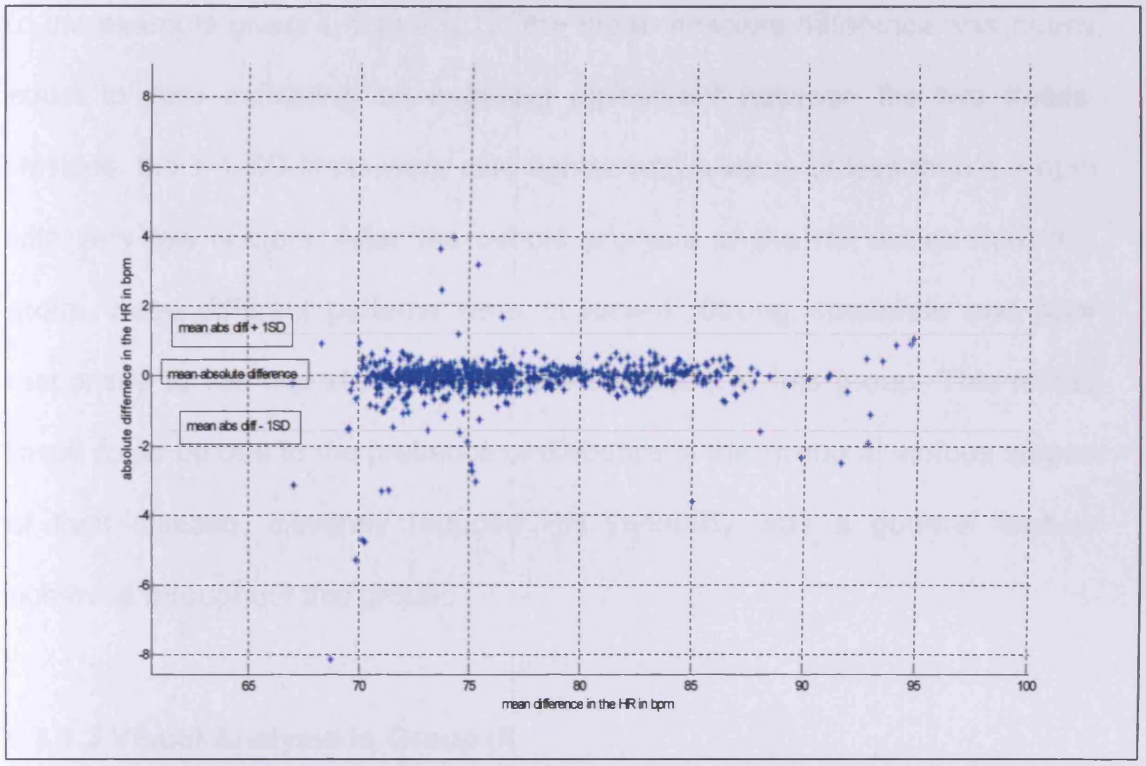

Figure 6.12: The Bland Altman plot of the HR shown in the previous figure with the ±1 SD limits of less than ± 2bpm

6.3.1.2.1 Discussion

Figure 6.11 and 6.12 is an example of the HR trace obtained from a diabetic patient and represents the HR extracted from nearly 40% of the participants within Group II. Reduced beat-by-beat variability was a general characteristic that could be extended to the whole group. Though a moderate response of the HR to the two stress tests was observed, it was much reduced when compared to the traces obtained from the healthy individuals. The diabetics were expected to have reduced beat-by-beat variability with a narrow HR frequency bandwidth. The program was also able to extract the HR trace from both legs more accurately with better phase matching and reduced discrepancies due to this decreased variability.

In the example given in figure 6.12, the mean absolute difference was nearly equal to zero indicating an excellent agreement between the two traces. Besides, the ± 1 SD limits were also tighter with a value of less than ± 2 bpm with very few outliers. After the overall analysis of the HR traces from this group, three different patterns were observed. Strong, moderate and poor responses to the two stress tests were observed in this group. This mixed result could be due to the presence of diabetics in this group at various stages of their disease. Severely reduced HR variability was a general feature observed throughout this group.

6.3.1.3 Visual Analysis in Group III

Visual analysis of the HR trace from all participants of this group did not reveal a common pattern. Variations in the HR trace were observed in the 38 neuropathic participants. Overall the HR variability was significantly reduced as compared to the other two groups. The HR trace from 9 participants (24%) had very little or no variability and also showed no response to any of the stress tests. These traces were similar to the ones obtained from 20% of the participants in Group II. The traces from 5 of the participants (13%) had a moderate response to the tests similar to the 40% of the participants in Group II. The HR trace from 4 participants of Group III (10%) had a good response to the two stress tests (especially the breathing test) similar to 37% of Group II. Finally a unique pattern of HR trace was obtained from 7 of the participants (18%) in this group. These traces had a very slow beat-by-beat variability with practically no response to the stress tests. Of these seven individuals three were associated with severe cardiovascular complications and neuropathic

symptoms and two were severely neuropathic with very high VPT score. The latter however did not have any known cardiovascular problems. The last two of these seven participants did not have any neuropathic or cardiovascular symptoms in spite of high VPT score. The program was unable to extract the HR accurately from 13 participants (35%) of this group due to severely reduced HF response in their spectrum.

The example illustrated in Figure 6.13 represents the HR trace obtained from around 25% of the participants in Group III. Decreased HR variability along with little or no response to the two stress tests was observed in this participant. The corresponding Bland Altman plot as shown in figure 6.14 also produces similar conclusions. The mean difference between the two traces was found to be zero with very tight ± 1 SD limit of less than ± 2bpm.

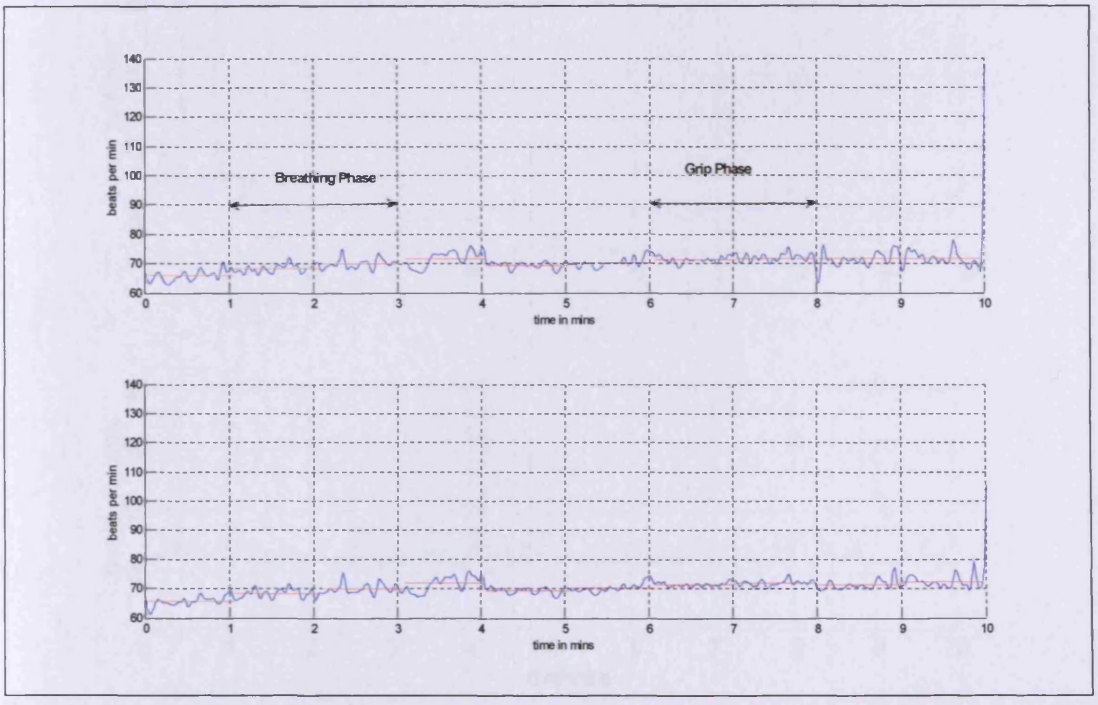

Figure 6.13: The HR trace extracted from left and right foot of a neuropathic participant

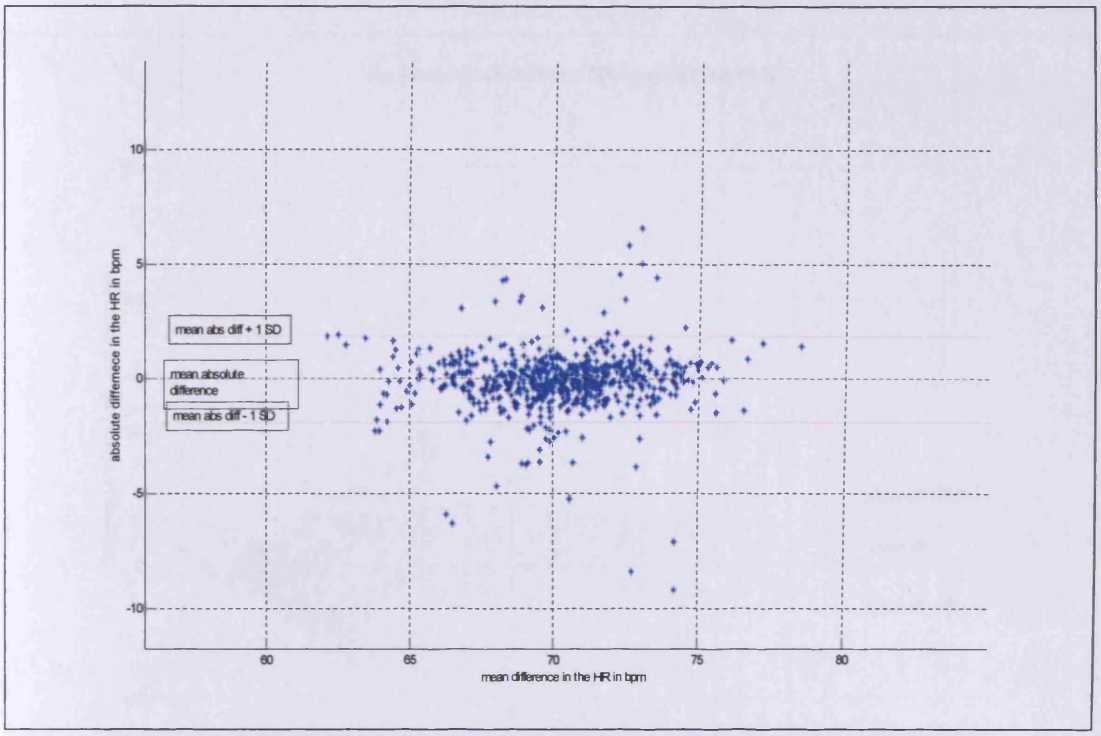

Figure 6.14: The Bland Altman plot of the HR shown in the previous figure with the ±1 SD limits of less than ± 2bpm

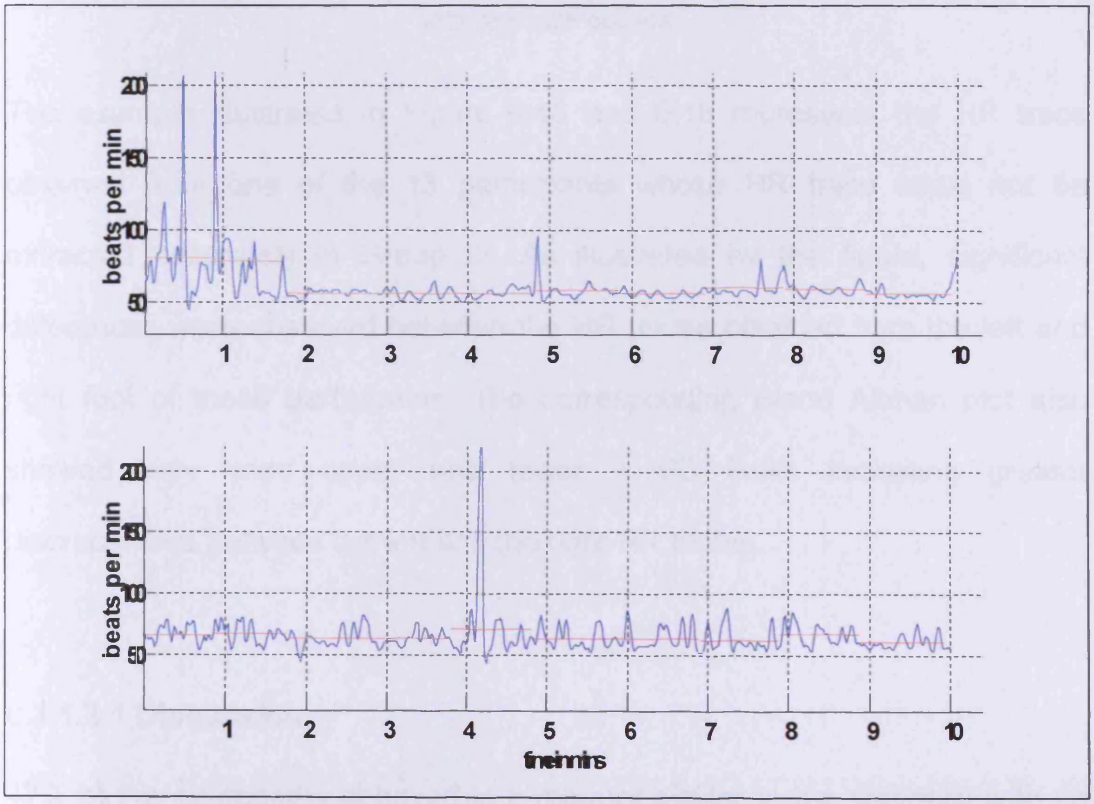

Figure 6.15: HR trace extracted from one of the 13 participants of the group with absent HF information. Note the difference in the traces obtained from the left and the right foot

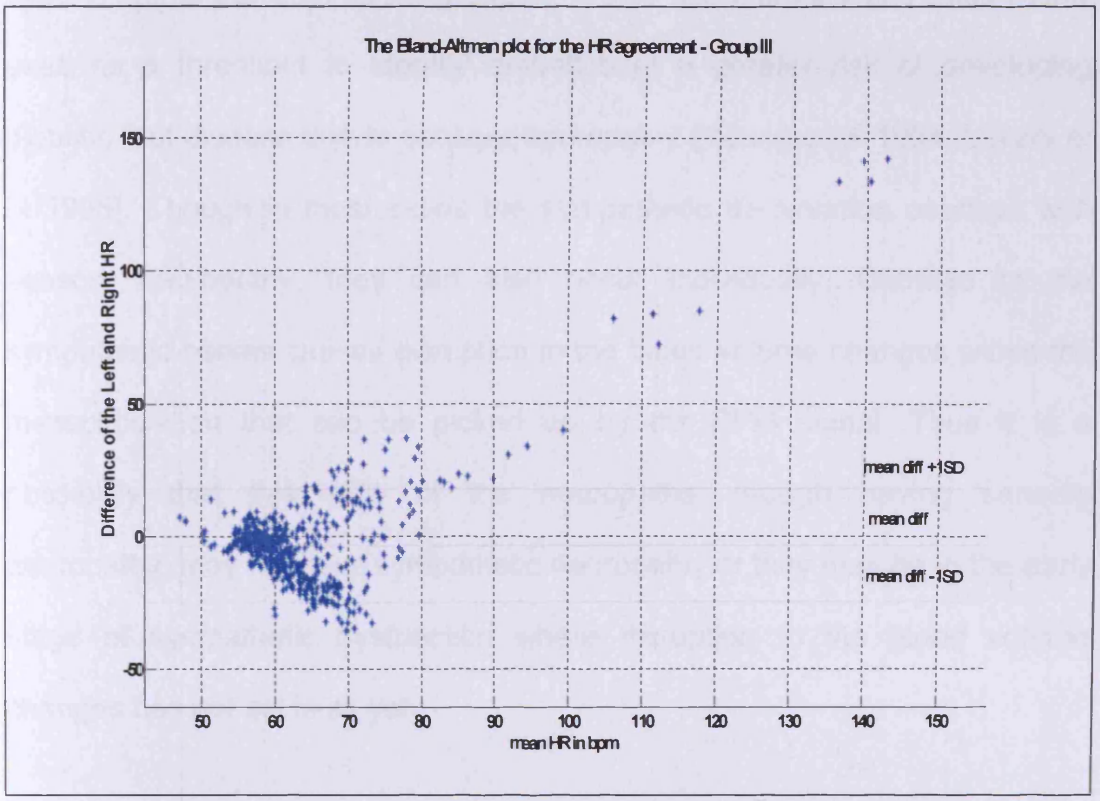

Figure 6.16: Bland Altman plot of the above HR traces with the 1 SD limits over 26pm and with very high outliers

The example illustrated in Figure 6.15 and 6.16 represents the HR trace obtained from one of the 13 participants whose HR trace could not be extracted accurately in Group III. As illustrated by the figure, significant differences were observed between the HR traces obtained from the left and right foot of these participants. The corresponding Bland Altman plot also showed very wide upper and lower 1 SD limits indicating greater discrepancies between the left and the right HR traces.

6.3.1.3.1 Discussion

47% of the neuropaths behaved in a manner similar to the diabetics with no neuropathy. The VPTscore of 25 V or greater, was the only inclusion criterion

used to recruit participants for Group III. A VPT score of 25 V is a value widely used as a threshold to identify diabetics at a greater risk of developing diabetic foot disease due to sensory neuropathy (Young et al 1994; Lavery et al 1998). Though in most cases the sympathetic denervation overlaps with sensory neuropathy, they can also occur individually. Damage to the sympathetic nerves causes disruption in the blood volume changes within the microcirculation that can be picked up by the PPG signal. Thus it is a possibility that this 47% of the neuropaths, though having sensory neuropathy, may not have sympathetic neuropathy or they may be in the early stage of sympathetic dysfunction where disruption to the blood volume changes has not set in as yet.

Eighteen percent of the neuropaths had a unique HR trace. The patient history suggests that 71% of these 7 neuropaths had a high VPT score and also complained of loss of sensation and tingling indicating severe sensory neuropathy. However some of them also had cardiovascular complications that can influence the peripheral blood flow. There is also a distinct possibility of these individuals suffering from sympathetic denervation as well. Figure 6.13 & 14 are the HR trace and its Bland Altman plot respectively obtained from a neuropathic patient of Group III. The HR trace in the given example shows little or no response to the two stress tests as compared to the traces obtained from the other two groups. The beat-by-beat variability was also reduced significantly with the difference in the maximum and minimum mean heartbeat being less than 10 bpm. This kind of trace was obtained from some diabetic patients with no known neuropathy as well. Decreased response of

the HR to the stress tests could indicate sympathetic dysfunction among the neuropathic patients. The diabetics with no known neuropathy in Group II could have non-symptomatic sympathetic dysfunction and this could be the possible explanation for obtaining similar trace from individuals within this group as well. Decreased variability similar to the diabetics once again produced a Bland Altman plot with tighter limits suggesting a better agreement of the HR trace extracted from both legs. In the given example, the ± 1 SD was also less than ± 2 bpm. It should however be noted that the given example only represents one type of the trace obtained from this group. The mean absolute difference in the HR trace extracted from both feet for each individual across the three groups was used for further objective analysis. Since different types of traces were obtained in this group, the value of this variable was spread out and hence appeared erroneously similar to data obtained from participants in Group I or the healthy individuals. However the HR traces from both these groups were visually very distinct from each other.

The inability to obtain a proper HR trace from 13 individuals could be due to several factors. Peripheral vascular disease is a common complication among diabetics resulting in decreased flow in the legs. Though these patients did not have a confirmed diagnosis of PVD, some of them did have a history of intermittent claudication, one of the many symptoms of PVD. This could be a probable explanation for the inability of the probes to pick up the pulses. However some of these individuals also had a very high VPT and had been diabetic for a long period of time indicating severe sensory loss that could be accompanied by sympathetic dysfunction. Autonomic or sympathetic

dysfunction among diabetics remains largely asymptomatic despite an early onset. In those individuals damage to the sympathetic nerves may cause the AV shunts to collapse and excessive blood to pass though them by passing the capillaries. Thus the foot feels warm but the skin does not receive any nutritive flow. These vessels under such circumstances act as a large capacitance with excessive pooling of blood but the pulsatile changes in the blood volume is heavily dampened. PPG was used in this study to detect the changes in the skin microcirculation observed mostly in the event of sympathetic dysfunction. Patients suffering from diabetes over a long period of time tend to develop very poor thick callus skin and also may suffer from water retention in the legs. Both these factors could greatly influence the PPG signals collected from these individuals.

Visual analysis of the HR traces and their corresponding Bland Altman plots produced certain interesting observations. Further objective analysis were carried out by studying the characteristics of the distribution of mean beat-by-beat HR for each of the participants across the three groups.

6.3.2 Analysis of the beat-by-beat HR distribution

Further detailed analysis of the Bland Altman plots also revealed some interesting facts about each individual's beat-by-beat HR distribution. The nature of the distribution of any variable can be studied by plotting its histogram. Fig 6.17 is a histogram of the beat-by-beat HR distribution

obtained from a healthy individual over ten minutes and is representative of the whole group.

In normal healthy individuals greater HR variability resulted in a wider spread of the mean beat-by-beat heart rate. On average a mean increase in the beat-by-beat HR of approximately 30 bpm was observed during the breathing and the handgrip phase of the study protocol for Group I. This was also reflected in the Bland Altman plot and in the histogram. Although most of the mean beat-by-beat heart rates were clustered around 70 bpm – 90 bpm, higher beat-by-beat heart rates of around 100-120 bpm were also observed. The presence of these higher HR values could be possibly explained as the systemic response to the two stress tests. Their presence was also observed to skew the individual's HR distribution.

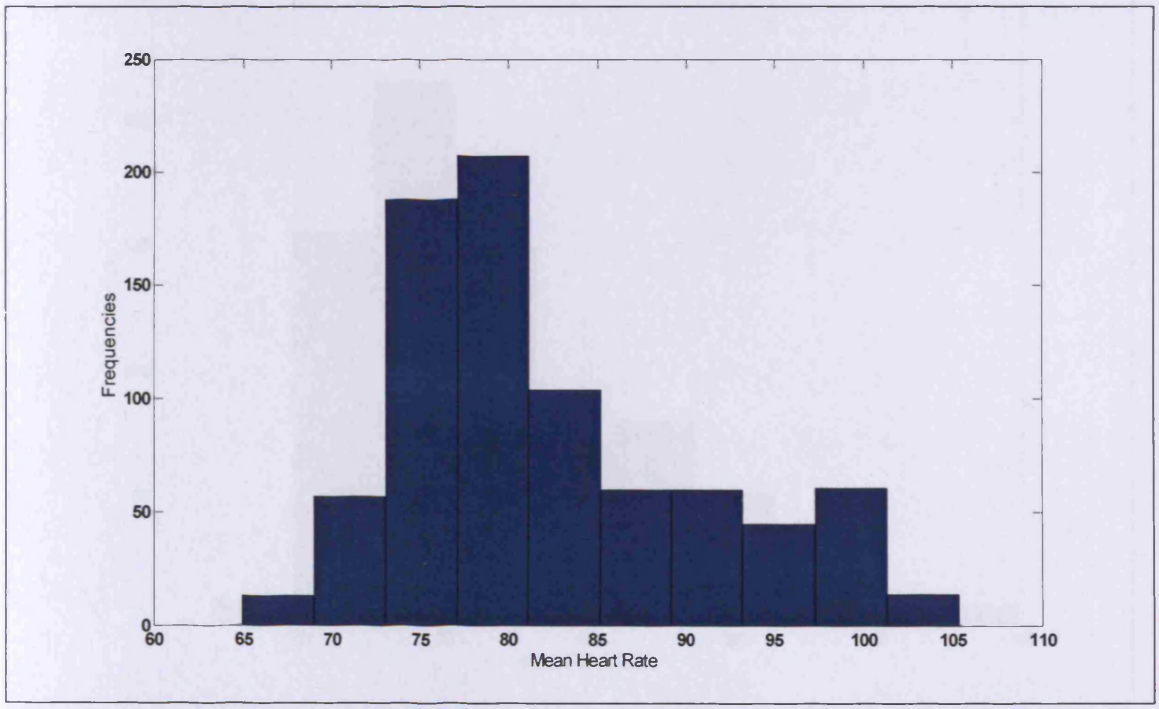

Figure 6.17: Histogram of the HR distribution of a participant from **Group I**

As explained in section 6.3.1, the beat-by-beat HR variability was observed to be comparatively lower in Group II than that obtained in Group I. The degree of rise in the HR in response to the two stress tests was also reduced to less than 20 bpm in this group. Once again most HR values were strongly clustered between 70 bpm – 90 bpm with very few high HR values of greater than 90 bpm. Fig 6.18 is a histogram of the HR values from a diabetic patient in Group II. This is a good representation of the whole group where most values lie within a tight limit with very few outliers. The distributions observed in this group were found to be closer to a normal distribution than the distributions observed in Group I and hence lower skewness value of the distribution was expected from this group when compared with normals in Group I.

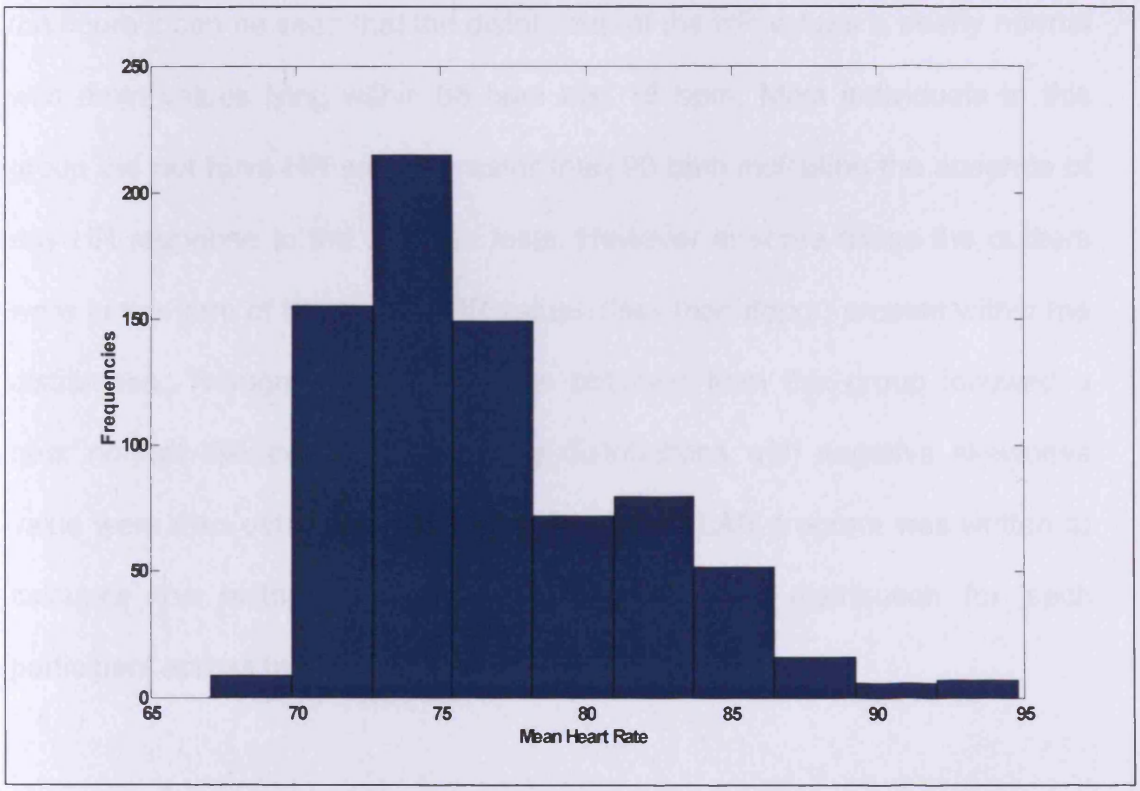

Figure 6.18: Histogram of the HR distribution of a participant from **Group II**

In Group III mixed results were obtained. The program was unable to accurately extract the HR trace from 13 individuals of this group as explained in the previous section. This analysis was performed using data from the remaining 25 individuals whose HR could be successfully extracted by the program. A spectrum of variations in the HR trace was observed in individuals from Group III. However in general there was little or no HR response to the two stress tests. Amongst those individuals who showed some response to these stresses, the increase in the HR was observed to be even less than 10bpm. In general the HR traces obtained from these 25 individuals were observed to be nearly flat. Figure 6.19 illustrates the histogram for the beat-by-beat HR values obtained from a participant in Group III. This histogram can be considered a good representative of the participants in Group IIIa. From the figure it can be seen that the distribution of the HR values is nearly normal with most values lying within 66 bpm and 76 bpm. Most individuals in this group did not have HR values greater than 90 bpm indicating the absence of any HR response to the 2 stress tests. However in some cases the outliers were in the form of the smaller HR values (less than 66pm) present within the distribution. Though most distributions obtained from this group followed a near normal distribution, occasionally distributions with negative skewness value were also obtained from this group. A MATLAB program was written to calculate the histogram and the skewness of the distribution for each participant across the three groups.

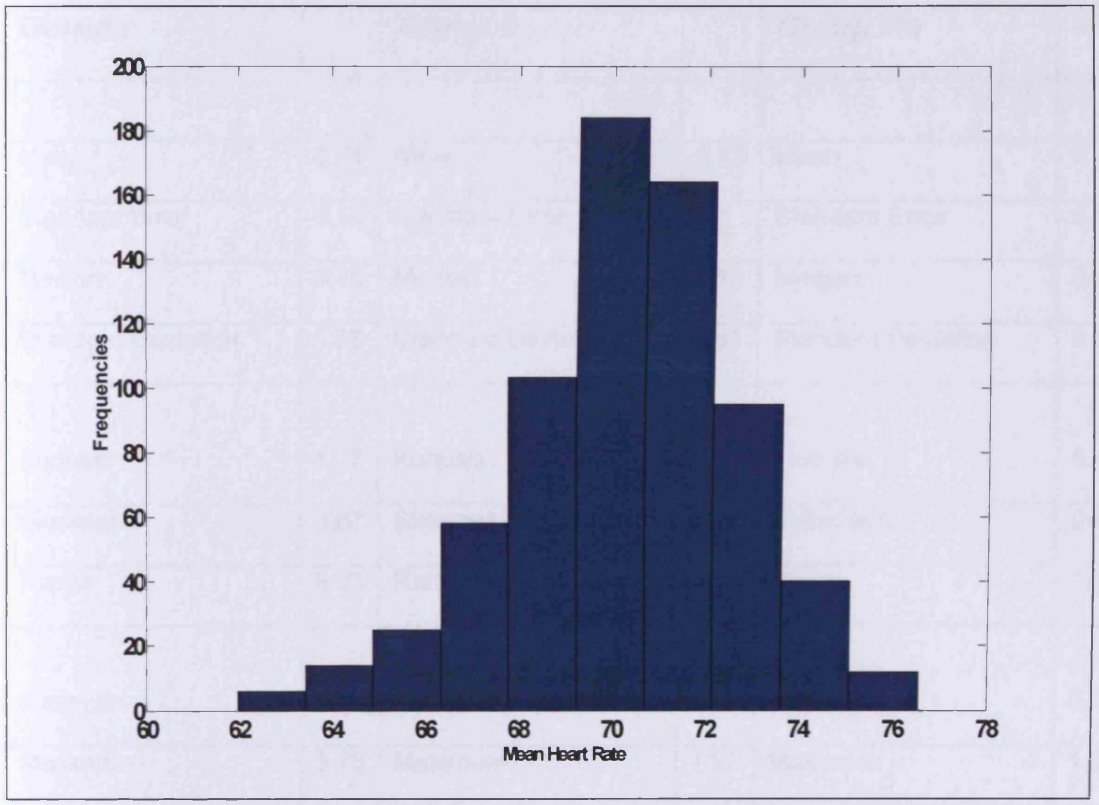

Figure 6.19: Histogram of the HR distribution of a participant from **Group IIIa** Note the presence of lower HR values producing a negative skewness in the distribution.

6.3.3 Statistical Analysis of the beat-by-beat heart rate

Most of the HF analysis so far involved the visual analysis of the HR trace extracted from the raw PPG signal, the degree of their agreement between the left and the right HR trace, and the histogram of the beat-by-beat HR values. These methods were however mainly subjective in nature. Further object analysis was performed on the HF end of the spectrum using statistical analysis. The skewness of the distribution calculated from participants from all three groups were further analysed in detail. The descriptive statistics were calculated using an Excel spread sheet and the result obtained is tabulated in figure 6.20.

Group I		***Group II***		***Group IIIa***	
Mean	0.64	Mean	0.17	Mean	0.14
Standard Error	0.18	Standard Error	0.1	Standard Error	0.1
Median	0.45	Median	0.13	Median	0.16
Standard Deviation	1.05	Standard Deviation	0.61	Standard Deviation	0.5
Kurtosis	17.5	Kurtosis	2.27	Kurtosis	-0.45
Skewness	3.67	Skewness	0.17	Skewness	0.47
Range	6.55	Range	3.24	Range	1.94
Minimum	-0.8	Minimum	-1.3	Minimum	-0.64
Maximum	5.78	Maximum	1.99	Maximum	1.3
Confidence Level (95.0%)	0.36	Confidence Level (95.0%)	0.21	Confidence Level (95.0%)	0.21

Figure 6.20: Descriptive Statistics for the skewness of the HR distribution

The mean skewness of the HR distribution in Group I was 0.64 and this value was found to be considerably larger than the mean values obtained in Group II (0.17) and Group III (0.14). These results therefore indicate the presence of increased HR variability in healthy individuals as compared to the diseased group. The mean skewness obtained from Groups II and IIIa were very similar indicating a similar HR distribution within the two groups. As explained earlier, around 47% of the Group III participants had HR trace similar to the ones obtained from Group II. Only 18% of them had a unique trace specific for the group. Thus in this analysis most of the participants in Group III had HR traces similar to those obtained from Group II and this could possibly explain the similarity in the mean values for these two groups.

The skewness of the HR distribution calculated from all the three groups was also plotted using a scatter plot, shown in figure 6.21. From the scatter graph it was not possible to completely distinguish between the three groups and the skewness of the HR distribution calculated were within similar ranges. A larger difference was observed between the skewness values calculated from Groups I and III. Hence a threshold of a skewness value of +0.31 was set and the sensitivity and specificity of the test was calculated. The participants with a skewness value of less than 0.31 was considered to be diseased while those with values greater was considered to be non diseased. The true positives and negatives and false positives and negatives were noted and the sensitivity and the specificity of the test were calculated. Using the skewness of the HR distribution as a variable to distinguish between the two groups, the test was found to have a sensitivity of 68% with a specificity of 72%.

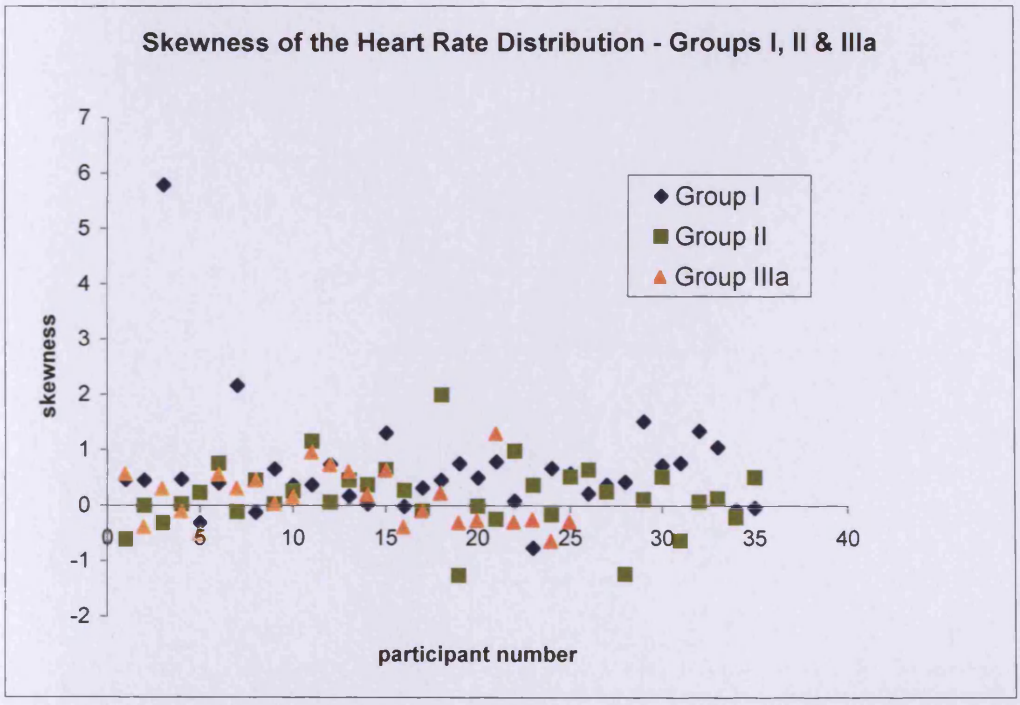

Figure 6.21: Scatter plot of the skewness of the beat by bear HR distribution calculated from each participant across the three groups

The observed differences between the three groups were further statistically analysed using non–parametric tests. The statistical package SPSS ® was used for the analysis. The three groups were analysed in pairs therefore a two-sample non–parametric test called the Man – Whitney test was used for the purpose. The results are tabulated in figure 6.22.

Ranks

	groups	N	Mean Rank	Sum of Ranks
skewness	1.00	35	41.57	1455.00
	2.00	35	29.43	1030.00
	Total	70		

Test Statistics(a) – Groups I & II

	skewness
Mann-Whitney U	400.000
Wilcoxon W	1030.000
Z	-2.496
Asymp. Sig. (2-tailed)	.013

a Grouping Variable: groups

Ranks

	groups	N	Mean Rank	Sum of Ranks
skewness	2.00	35	31.34	1097.00
	3.00	25	29.32	733.00
	Total	60		

Test Statistics(a)- Groups II & III

	skewness
Mann-Whitney U	408.000
Wilcoxon W	733.000
Z	-.442
Asymp. Sig. (2-tailed)	.658

a Grouping Variable: groups

Ranks

	groups	N	Mean Rank	Sum of Ranks
skewness	1.00	35	35.46	1241.00
	3.00	25	23.56	589.00
	Total	60		

Test Statistics(a)- Groups I & III

	skewness
Mann-Whitney U	264.000
Wilcoxon W	589.000
Z	-2.601
Asymp. Sig. (2-tailed)	.009

a Grouping Variable: groups

Figure 6.22: Non –parametric test results for the inter-group comparison of the skewness of the HR distribution. Values 1.00, 2.00 and 3.00 represent Groups I, II and III respectively.

The variable skewness calculated from the three groups were analysed in pairs. Both the Man-Whitney (U) and the Wilcoxon (W) parameter were calculated. The test statistics from the comparison of Groups I and II revealed a small p value of 0.013. A p value of less than 0.05 indicates that the observed difference in the mean skewness value between the two groups is at a 5% statistically significant level. A similar comparison between Groups II and III however resulted in a very high p value of 0.7. Such a high p value indicates that the difference in the mean skewness calculated from the diabetics (Group II) and diabetics with neuropathy (Group IIIa) are not statistically significant, i.e. no difference could be statistically established between Groups II and III. Comparison between the skewness calculated from the healthy normal individuals (Group I) and diabetics with neuropathy also resulted in a very small p value of 0.009. Thus the difference in the mean skewness calculated from the two groups was also statistically significant.

Comparing and statistically analysing the skewness of the HR distribution calculated from all three groups resulted in some interesting results. A statistical difference could be established between Groups I and II and between Groups I and III. However no statistical difference could be established between the diabetics with and without neuropathy (Groups II and IIIa). Although a very small p value of 0.009 was obtained indicating a very significant statistical difference between the skewness calculated from Group I and the Group IIIa, the test was only able to distinguish between the two groups with a sensitivity and specificity of 68% and 72% respectively.

Chapter VII - Results

Low Frequency Analysis

7.1 Introduction

The raw PPG signal contains valuable information regarding the autonomic control of the skin microcirculation. The simultaneous occurrences of the prominent frequency bands in the spectrum from both legs of the participants indicate the central origin of this control. The analysis of the HF end of the spectrum in the previous chapter produced some interesting results. In this chapter the results from the analysis of the LF end of the spectrum will be discussed.

The LF end of the spectrum was represented by frequency bands from 0.016 Hz (1cpm) to 0.42 Hz (25cpm). Several studies have been conducted to explore this LF end as they provide valuable information regarding the local and central activity of the skin microcirculation. For example the frequency band around 0.02 Hz (1.6 cpm) represented the thermoregulatory response of the body also called the Burton Waves while the frequencies around 0.1 Hz (6 cpm) represented the autonomic regulation of blood pressure (Kamal et al 1989). A MATLAB program was written to extract the LF information from the raw PPG signal. The program used a 2^{nd} order high pass Butterworth filter with a cut off frequency of 0.001 Hz (0.08 cpm) and a 3^{rd} order low pass Butterworth filter with a cut-off frequency of 0.42 Hz (25 cpm). The band pass

filter thus generated allowed all frequencies between 0.0001 Hz (0.08 cpm) and 0.42 Hz (25 cpm) of the signal to pass through unaltered while attenuating all other frequencies outside this range. The filtered raw PPG signal therefore contained only the LF information. The time domain signal was then converted to the frequency domain using the Fast Fourier Transform (FFT) to extract the frequency information present within the signal. The signal was windowed using a Hanning window prior to the FFT. The Fourier spectrum generated from all the participants across the three groups was both visually and objectively analysed.

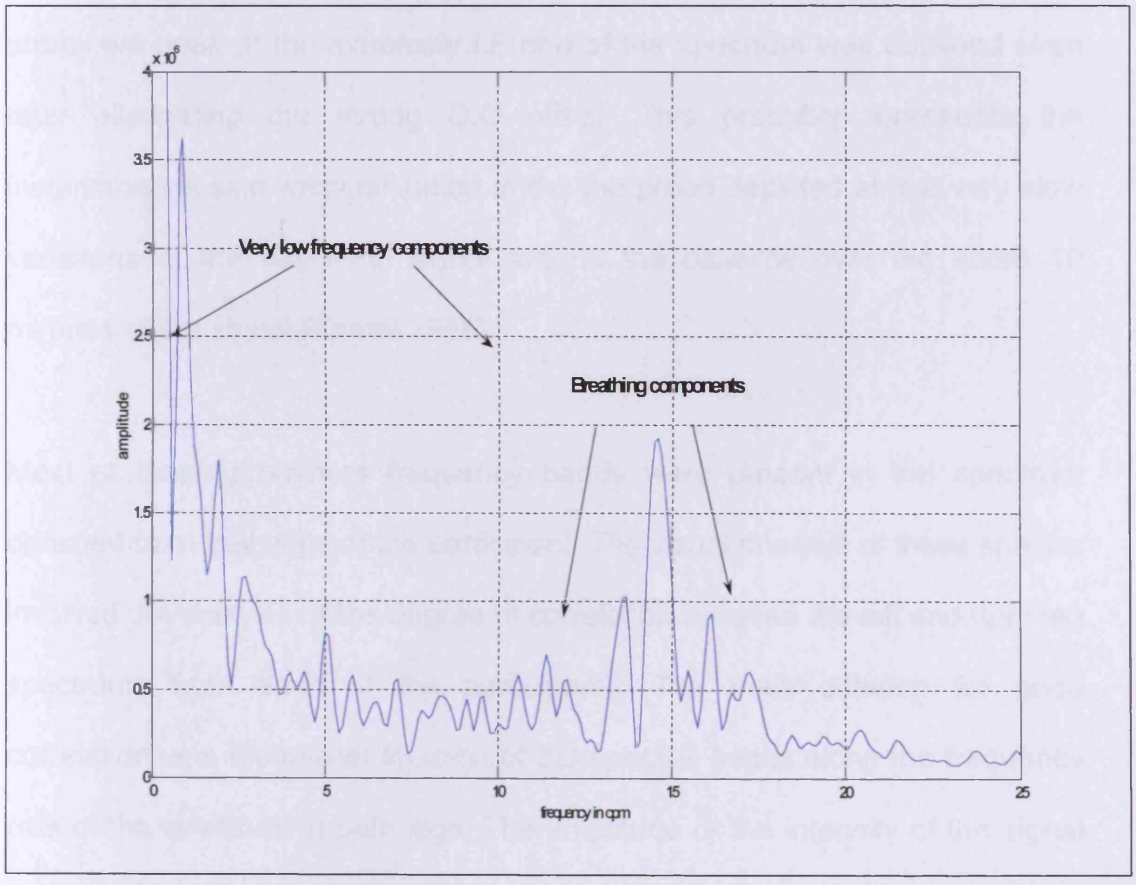

Figure 7.1: The spectrum of a raw PPG signal that was band pass filtered with cut off frequencies of 0.001Hz (0.08 cpm) and 0.42 Hz (25 cpm)

7.2 Visual analysis

An example of a typical LF spectrum generated using MATLAB is shown in figure 7.1. In the figure, several prominent frequency bands were observed between 0.016 Hz (1 cpm) and 25 cpm (0.42 Hz). The very LF (VLF) bands between 1cpm (0.016 Hz) and 10 cpm (0.17 Hz) represented the vascular changes under autonomic influence and the LF bands between 10cpm (0.17 Hz) and 20 cpm (0.33 Hz) represented the vascular changes influenced by the breathing cycle. Apart from these physiologically important frequency ranges within the LF end of the spectrum, a very strong, high amplitude peak was also observed between 0.2 cpm (0.003 Hz) and 0.5 cpm (0.008 Hz). This prominent peak at the extremely LF end of the spectrum was obtained even after eliminating the strong D.C offset. This probably represents the instantaneous skin vascularisation under the probe depicted as the very slow variations of the raw PPG signal around the baseline over the entire 10 minutes of the signal (Kamal 1989).

Most of these prominent frequency bands were present in the spectrum obtained from both legs of the participant. The visual analysis of these spectra involved the analysis of the degree of correlation between the left and right leg spectrums from each of the participants. The main criterion for good correlation was the similar location of the spectral peaks along the frequency axis of the spectrum in both legs. The amplitude or the intensity of the signal was not considered for this purpose. Both the filtered raw PPG signal and the LF spectrum were analysed across the three groups.

7.2.1 Visual Analysis in Group I

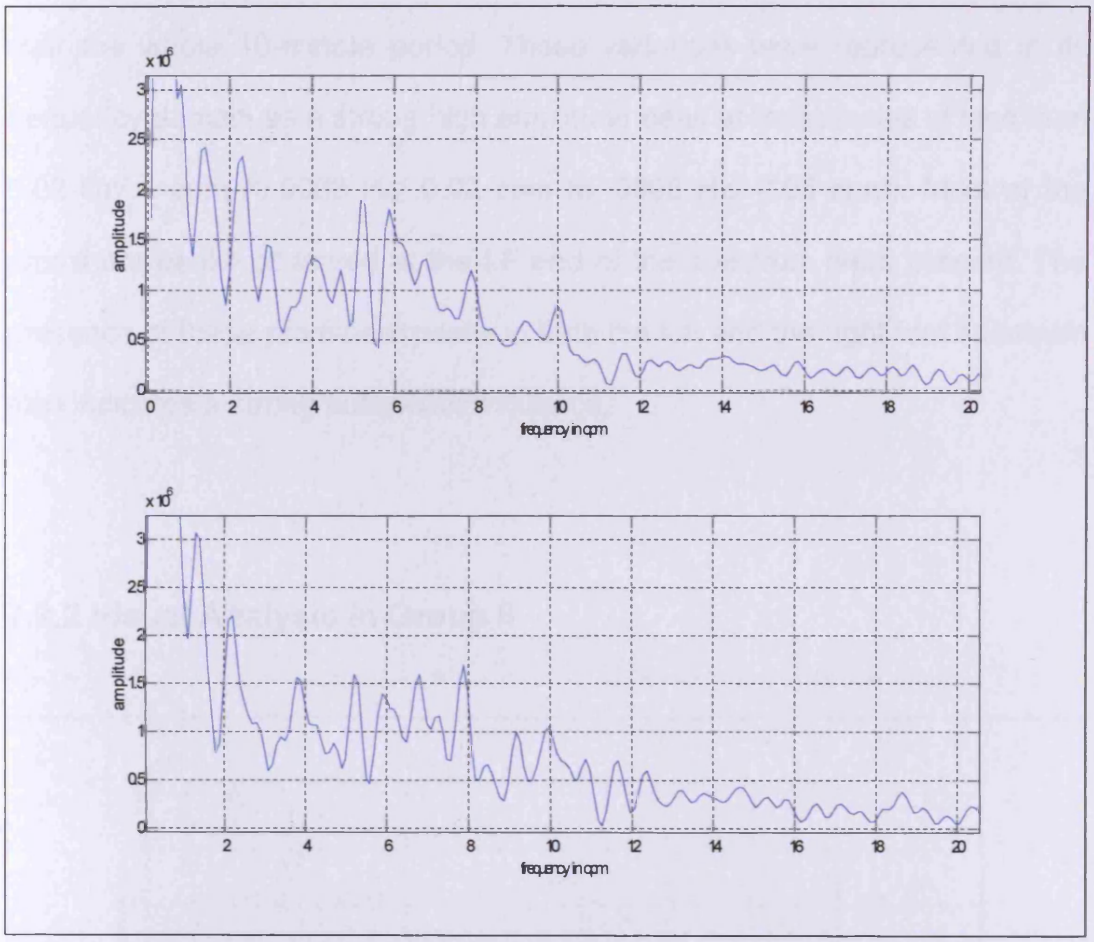

Figure 7.2: LF spectrum obtained from a healthy participant of Group I

Figure 7.2 illustrates a typical LF spectrum obtained from participants in Group I. Good correlation between the spectra from both legs were observed in 67.5% (25) of the participants in this group. The spectrums were considered to have poor correlation if more than two of the prominent frequency bands were absent or different in both the spectrums. Poor co-relation between the two spectrums from both legs was observed in 32.5% (12) of the participants.

Visual analysis of the filtered raw PPG signal in its time domain revealed significant slow moving amplitude variation around the zero baseline level over the whole 10-minute period. These variations were represented in its frequency domain as a strong high amplitude peak at frequencies of less than 0.02 Hz/ 1 cpm (0.0003 Hz/ 0.02 cpm to .0008 Hz/ 0.05 cpm). Most of the prominent peaks observed at the LF end of the spectrum were present. The presence of these prominent peaks in both the left and the right foot spectrum also indicates a strong autonomic influence.

7.2.2 Visual Analysis in Group II

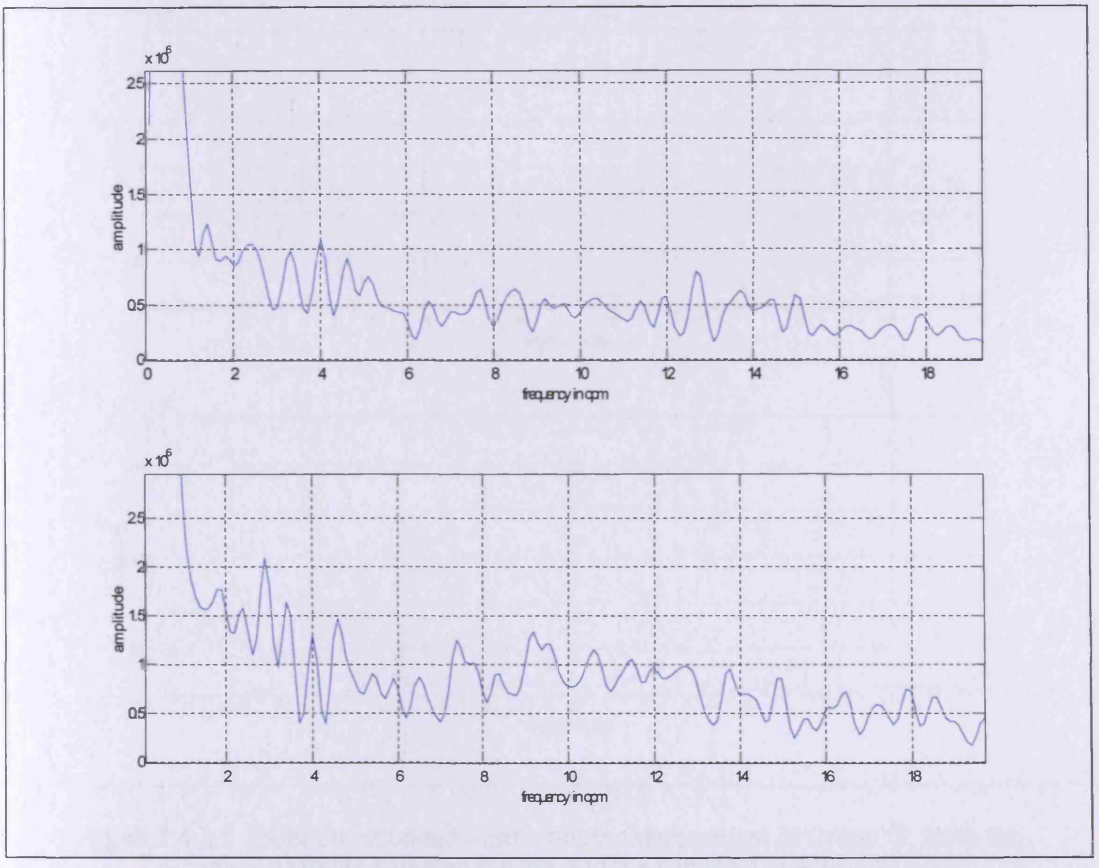

Figure 7.3: LF spectrum obtained from a diabetic patient with no known neuropathy of Group II

A typical LF spectrum obtained from participants in Group II is illustrated in figure 7.3. As in the figure, the number of prominent peaks at the LF end of the spectrum was fewer when compared to the spectrum from Group I. Good correlation between the left and the right LF spectrum was observed only in 47% (17) of the participants while 53% (18) had poor co-relation. The slow moving amplitude variations of the raw PPG signal over the ten-minute period was also significantly reduced in this group, with any variation in the signal amplitude mostly restricted to the two stress tests.

7.2.3 Visual Analysis in Group III

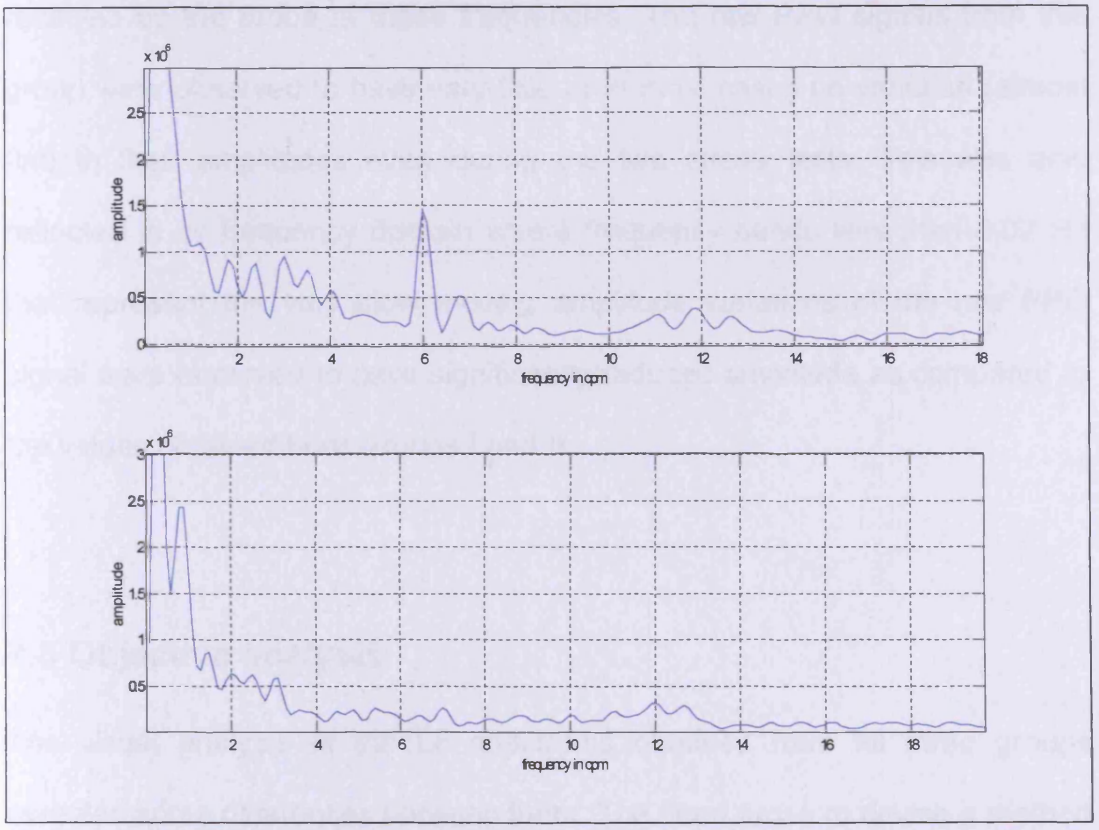

Figure 7.4: LF spectrum obtained from a neuropathic patient of Group III. Note the dissimilarities between the left and the right foot spectrums

Figure 7.4 illustrates a typical LF spectrum obtained from Group III. Participants in this group were diabetic patients with known neuropathy. The spectrums from both legs were observed to be dissimilar in most cases. Poor correlations between the left and right spectrums with at least two prominent frequency bands being absent or different were observed in 26.3% (10) of the participants in this group, while 73.7% (26) showed no correlation at all as illustrated in figure 7.4. The reduced or absent correlation between the left and the right foot LF spectrum indicate a probable loss of the various autonomic responses of the skin vascularisation. The amplitude of the peaks, if present within the spectrum, was significantly reduced when compared to the other two groups. This decrease in amplitude suggests reduced response received by the probe at these frequencies. The raw PPG signals from this group were observed to have very little or in most cases no variation (almost flat) in their amplitudes even during the two stress tests. This was also reflected in its frequency domain where frequency bands less than 0.02 Hz that represent the very slow moving amplitude variations of the raw PPG signal were observed to have significantly reduced amplitude as compared to the values obtained from Groups I and II.

7.3 Objective analysis

The visual analysis of the LF spectrums obtained from all three groups revealed some differences between them. The need arose to devise a method to quantify these differences in order to be able to objectively and statistically separate the spectrums into their respective groups. An average spectrum for

each group was generated using MATLAB. A program was written to obtain the LF spectrum for each leg and average the spectrums obtained from all participants for each of the three groups. The averaged left and the right spectrum of the three groups were visually analysed to identify the prominent frequency bands present within the spectrum. Frequency bands around 0.005 Hz (0.3 cpm), 0.033 Hz (0.2 cpm), 0.067 Hz (0.4 cpm), 0.08 Hz (0.5 cpm), 0.1 Hz (0.6 cpm) and 0.13 Hz (0.8 cpm) were identified as the prominent very LF bands. The frequency band representing the breathing cycle was obtained between 0.2 Hz (12 cpm) and 0.42 Hz (25 cm). The number of frequency bands present in the spectrum obtained from the neuropathic group was considerably reduced as compared to the other two groups. The signal was split into the various segments of the experiment protocol. Five segments viz, initial resting phase, breathing phase, intermediate resting phase, grip phase and the final resting phase were analysed in the similar manner but the averaged spectrum for each phase did not reveal any useful information. Further objective analysis were performed on the spectrums using these prominent frequency bands.

7.3.1 Analysis using 'Area under the Curve'

Visual analysis of the spectrum revealed a significant reduction in both the number of frequency bands present and in their amplitude in the spectrum from Group III as compared to the other two groups. Thus in order to objectively differentiate the three groups, the area under the curve over a specific range of bandwidth was thought to be a useful variable for further investigation. A program was written in MATLAB to calculate this variable. In

order to analyse the LF end of the spectrum, a maximum sampling frequency of 2 Hz (120 cpm) was sufficient. The sampling frequency of 1 kHz (60,000 cpm) used in this study far exceeded the requirement. Thus, in order to decrease the run time of the program, the signal was down sampled to 120 cpm or to 2 Hz. In this study the PPG signals were acquired at sampling rate of 1 kHz. Reducing the sampling rate of the raw signal by 500 times can result in aliasing due to under sampling of the data. Thus in order to prevent this, an anti aliasing filter was used. It was applied to the signal to attenuate the very HF components using a low pass Butterworth filter with a cut-off equal to a quarter of the proposed sampling frequency. This low pass filtered signal was down sampled to 2 Hz. The filtered down sampled raw PPG signal was then subjected to a band pass filter generated using a combination of a high pass and low pass Butterworth filters to attenuate all frequency components outside the range of 0.03 Hz – 0.25 Hz (2-15 cpm). Visual analysis revealed the most prominent frequency bands present at the lower end of the spectrum to be between 2 and 8 cpm and hence the area under the curve was calculated by summing all the data points of the spectrum between 0.03 Hz (2 cpm and 0.13 Hz (8 cpm). Finally the mean area of the left and the right leg spectrum was calculated for each participant. The mean area under the curve between 0.03 Hz – 0.13 Hz for each participant for each of the three groups was obtained and plotted as a scatter plot as shown in figure 7.5.

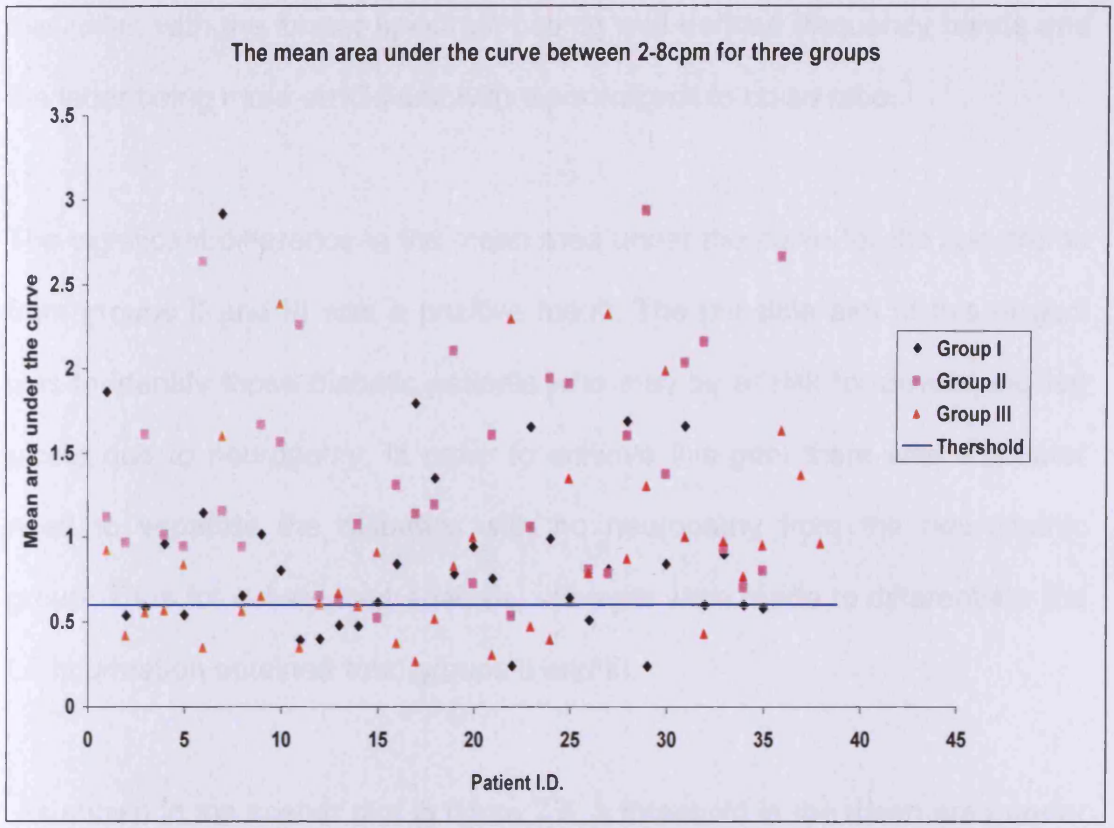

Figure 7.5: The scatter plot of the mean area under the curve between 2-8cpm for all three groups

Visual analysis of the scatter plot revealed a significant difference in the mean area between diabetics with no known neuropathy (Group II) and the neuropaths (Group III). However normals (group I) showed a reduced area under the curve similar to the neuropaths.

Closer analysis of the spectrum obtained from the three groups revealed the frequency bands present in the spectrum from Group II were well defined and with high amplitudes resulting in a larger area under the curve. The frequency bands in the spectrum from Group III however, were erratic resulting in a smaller area under the curve. Though the mean area under the curve for Group I and Group III were within a similar range, visually they were very

dissimilar, with the former spectrum having well defined frequency bands and the latter being more erratic and with a poor signal to noise ratio.

The significant difference in the mean area under the curve for the spectrums from groups II and III was a positive result. The principle aim of this project was to identify those diabetic patients who may be at risk for developing leg ulcers due to neuropathy. In order to achieve this goal there was a greater need to separate the diabetics with no neuropathy from the neuropathic group. Thus for subsequent analysis, attempts were made to differentiate the LF information obtained from groups II and III.

As shown in the scatter plot in figure 7.5, a threshold in the mean area under the curve of 0.6 was set, such that all participants with a mean area equal to or less than the threshold were considered to be neuropathic while those with an area greater than 0.6 were considered to be diabetics with no neuropathy. The number of true positives, true negatives, false positives and false negatives were calculated and the specificity and the sensitivity of the test were obtained. The sensitivity and specificity of a test is a measure of its diagnostic capability. The sensitivity of a test is the proportion of true positives correctly identified by it and the specificity is the proportion of the true negatives rightly ruled out by the test. These statistical variables have been discussed in detail in chapter 3. With a threshold of 0.6, 28 true positives and 23 true negatives were identified with a sensitivity and specificity value of 74% and 64% respectively for the test. This result indicates that using the area under the curve for 0.03 Hz –0.13 Hz, 74% of the neuropathic patient could be

identified while ruling out 64% of the diabetic participants. The purpose of good screening tool is to identify as many true positives as possible, even sometimes at the cost of including few false positives. This means that for a test to be classified as a good screening tool, it must aim for a high sensitivity. All LF analysis conducted from here on was aimed at identifying the best possible method to differentiate between Groups II and III with the highest possible sensitivity without drastically reducing the specificity.

7.3.2 Analysis using spectral density

Spectral density is a measure of the total power of a specific bandwidth of frequencies and its contribution to the Fourier spectrum. It was calculated by dividing the area under the curve by the bandwidth that defines the curve. The MATLAB program written to calculate the area under the curve was used to calculate the spectral density with some modifications. A frequency band between 2-8 cpm was selected as most of the physiologically important frequency bands were thought to be present within this range. The spectral density for this bandwidth was calculated for each of the participants for all three groups. The final output of the program was the mean of the spectral densities obtained from both the feet for each participant across the three groups. The variable was potted using a simple scatter plot in Excel as shown in figure 7.6

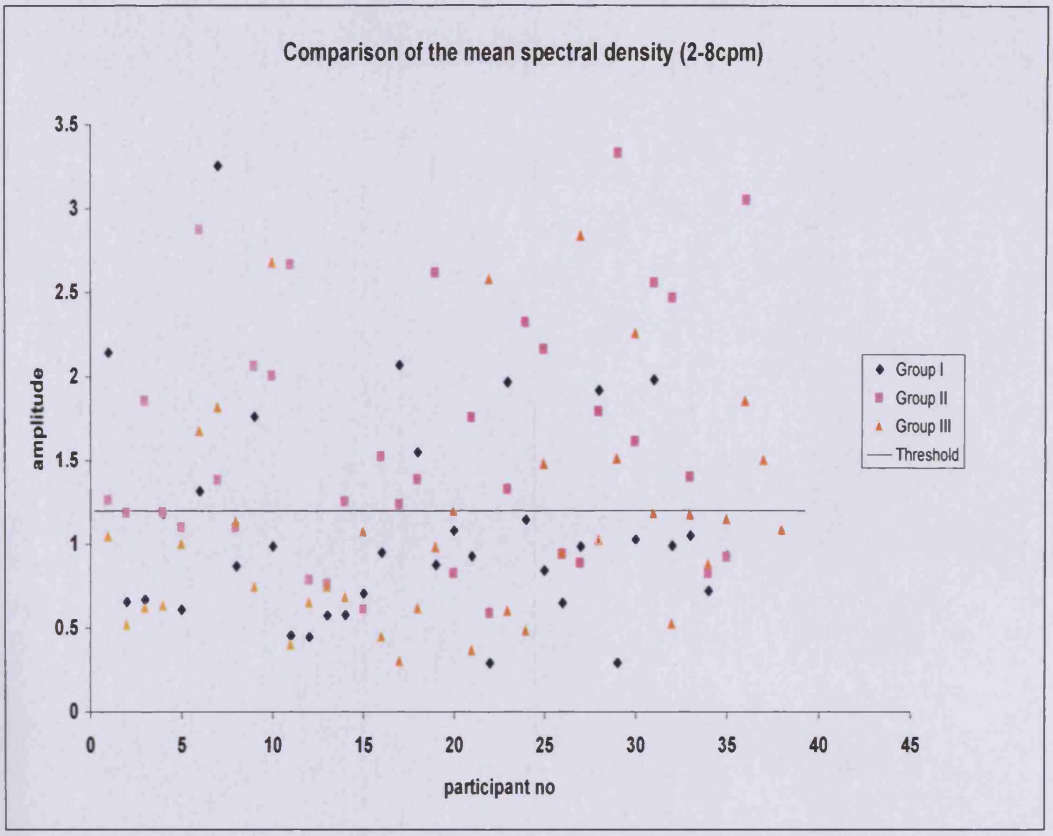

Figure 7.6: The scatter plot of the mean spectral density for the frequency bandwidth of 2-8cpm for the three groups

Visual analysis of the scatter plot revealed similar results as the previous analysis for the mean area under the curve. A significant difference in the mean area between groups II (diabetics) and III (neuropathic participants) was observed. However once again signals from group I (normal) showed reduced spectral densities similar to group III. Once again for reasons explained in the previous section, attempts were made to differentiate Groups II and III. This time the sensitivity and specificity of the test were calculated using two different thresholds values. As explained earlier the sensitivity and specificity of a test are a measure of its screening capability and is often a trade off between the two values. The aim of any good screening test is to have the maximum sensitivity while still maintaining a good specificity.

Two threshold values were used to identify the best possible value that would provide the optimum separation between groups II and III. First the sensitivity and specificity of this test were calculated by setting the mean spectral density of 1.20 as the threshold such that any participant with a value equal to or less than this threshold were considered to be neuropathic and those with value above 1.20 were considered to be non neuropathic. Using this threshold the test was able to identify 28 out of 38 as to be positively neuropathic and exclude 22 out of 34 diabetics with no known neuropathy as negatives. The sensitivity and specificity of the test were calculated to be 74% and 65% respectively. The threshold was then slightly raised to a mean spectral density value of 1.50. Using this new value the test was now able to rightly identify 31 out of 38 as to be positively neuropathic but managed to exclude only 15 out of 34 diabetics with no known neuropathy as negatives. By increasing the threshold of the study, the sensitivity of the test was raised to 82% but the specificity decreased to 44%.

Thus by altering the threshold values, the sensitivity and the specificity values of the test could be adjusted. A range of thresholds was considered for all subsequent analysis and the sensitivity and specificity for each of the thresholds were calculated and compared. The threshold that differentiated between the diseased and the non-diseased with the highest sensitivity and maintained the specificity of the test at above 60% was considered to be the best choice.

In the HF analysis as explained in Chapter 6, the HR could not be extracted from the raw PPG signal from 13 individuals in Group III due to the greatly reduced activity at the HF end of the spectrum It was essential to rule out similar possibility in the LF analysis as well. Hence the whole analysis was repeated using data from the subset Group IIIa.

The mean spectral densities calculated from the Groups I, II and IIIa were plotted using a scatter plot as shown in figure 7.7. Visual analysis of the scatter plot does not reveal any obvious difference between figure 7.6 (using Group III) and 7.7 (using Group IIIa). However a similar threshold of 1.2 was set to calculate the sensitivity and specificity of the test.

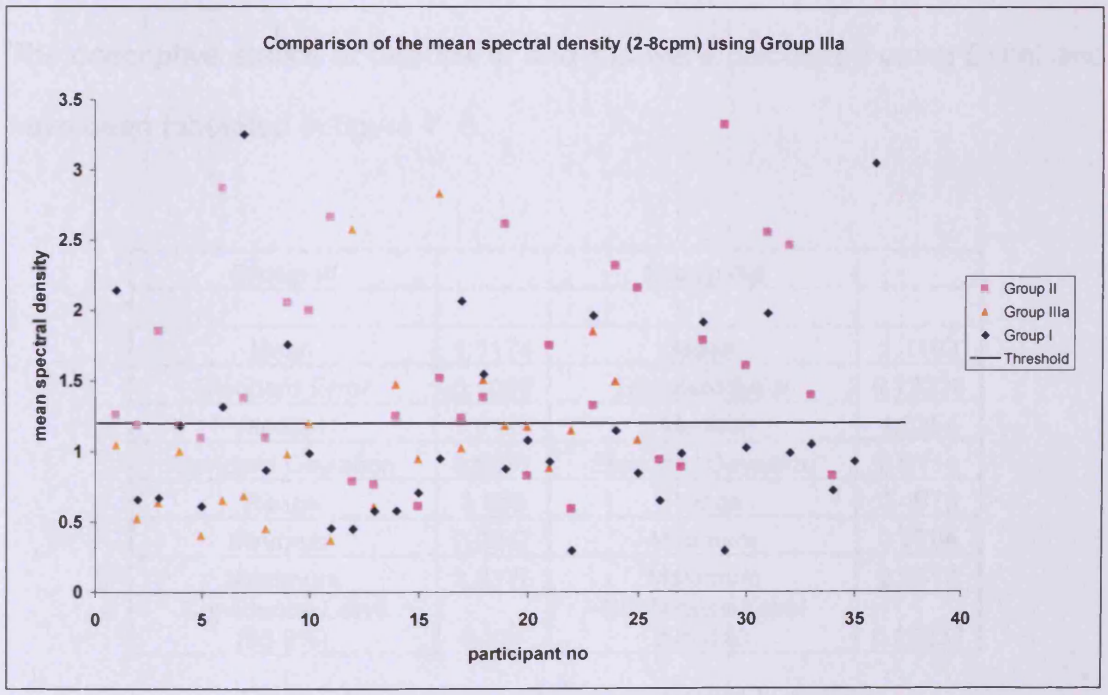

Figure 7.7: The scatter plot of the mean spectral density for the frequency bandwidth of 2-8 cpm for the Groups I, II and IIIa

Visual analysis of the scatter plot indicates reduced spectral density in participants from Group IIIa when compared to Group II. Thus participants with a mean spectral density value equal to or less than 1.2 were considered to be neuropathic and those with values greater than the threshold were considered to be diabetics with no neuropathy. By using data from Groups IIIa instead of the whole group, the test was able to distinguish between the diseased and the non –diseased with a sensitivity of 76% and specificity of 65%. The test using both Group III as a whole and the new subset Group IIIa produced similar sensitivity and specificity values.

Though the sensitivity and specificity of the test remained relatively unchanged with using the whole group or its subset, the descriptive statistics of the two were compared to identify any statistical differences between them. The descriptive statics of Groups III and IIIa were calculated using Excel and have been tabulated in figure 7. 8.

Group III		***Group IIIa***	
Mean	1.1174	Mean	1.1102
Standard Error	0.1056	Standard Error	0.12228
Median	1.0134	Median	1.0254
Standard Deviation	0.6511	Standard Deviation	0.6114
Range	2.533	Range	2.4673
Minimum	0.3047	Minimum	0.3704
Maximum	2.8377	Maximum	2.8377
Confidence Level (95.0%)	0.214	Confidence Level (95.0%)	0.25237

Figure 7.8: Descriptive statistics for Groups III and IIIa

The descriptive statistics for the whole group and the subset were almost identical suggesting no possible statistical difference between the two. These results indicate that the LF information can be extracted from all the participants in Group III and the data from the whole group can be used for all further LF analysis.

7.3.3 Statistical Analysis using spectral density

The scatter plot as shown in figure 7.6 and 7.7, revealed decreased spectral densities for group III as compared to the other groups. There was a need to identify if these differences between the groups picked up by visual analysis of the scatter plot were at a statistically significant level. The spectral densities of the three groups were statistically analysed using the hypothesis testing method. A null hypothesis that 'there is no difference in the mean spectral densities obtained from the three groups' was set for the purpose. Both the histogram and the Q-Q plot were generated to test if the variable had a normal distribution. Mean spectral densities from all three groups were found to follow a near-normal distribution.

A parametric test such as the one-way ANOVA was chosen as a suitable statistical test to compare the mean spectral densities of the three groups. Both Tukey HSD (Highly significant difference) and LSD (least significant difference) tests were chosen for the multiple comparisons using SPSS statistical package. In SPSS the one-way ANOVA generated two sets of result. This test has been explained in detail in chapter 3 section 3.4.2. The results from the test were tabulated in figure 7.9.

The F value of 5.4 indicates unequal variances both between groups and within the group. The p value of 0.006 obtained was also a statistically significant result Thus, the first part of the test established that the mean spectral densities obtained for the three groups were not equal.

The second part of the test further looked into the inter group variability in the mean spectral density values. Both the Tukey HSD and the LSD comparison methods indicate that the difference observed in the mean spectral densities of group II and III were at a statistically significant level with a p value of 0.008. The tests were however unable to establish any significant difference in the mean spectral densities calculated for groups I and III due to the very high p value of 0.974. These results were consistent with those obtained in the HF analysis and in the analysis using area under the curve.

ANOVA

Mean spectral density of the LF bandwidth between 2-8 cpm

	Sum of Squares	df	Mean Square	F	Sig.
Between Groups	5.319	2	2.659	5.438	.006
Within Groups	52.329	107	.489		
Total	57.647	109			

Multiple Comparisons

Dependent Variable: mean spectral density

	(I) group	(J) group	Mean Difference (I-J)	Std. Error	Sig.	95% Confidence Interval	
						Lower Bound	Upper Bound
Tukey HSD	group I	group II	-.44996111(*)	.16483199	.020	-.8417285	-.0581937
		group III	.03448363	.16264869	.976	-.3520946	.4210618
	group II	group I	.44996111(*)	.16483199	.020	.0581937	.8417285
		group III	.48444474(*)	.16264869	.010	.0978665	.8710229
	group III	group I	-.03448363	.16264869	.976	-.4210618	.3520946
		group II	-.48444474(*)	.16264869	.010	-.8710229	-.0978665
LSD	group I	group II	-.44996111(*)	.16483199	.007	-.7767213	-.1232009
		group III	.03448363	.16264869	.833	-.2879484	.3569157
	group II	group I	.44996111(*)	.16483199	.007	.1232009	.7767213
		group III	.48444474(*)	.16264869	.004	.1620127	.8068768
	group III	group I	-.03448363	.16264869	.833	-.3569157	.2879484
		group II	-.48444474(*)	.16264869	.004	-.8068768	-.1620127

* The mean difference is significant at the .05 level

Figure 7.9: Parametric test or one-way ANOVA to compare the mean spectral density of the three groups

7.3.3 Spectral density of various combination of bandwidths

The LF analysis performed so far only used the frequency bandwidth of 0.03-0.13 Hz. The visual analysis of the LF spectrum from healthy individuals revealed the presence of several prominent frequency bands between 0.03 Hz 0.42 Hz. Most of these frequency bands were also physiologically important. Using a single bandwidth of frequency (0.03-0.42 Hz) the test both visually and to some extent statically was able to separate the groups from each other. The mean spectral densities of different bandwidths were further analysed.

The analysis was not only performed on the spectrum obtained from the whole PPG signal, but also on the three main exercise segments viz, the breathing phase, the intermediate resting phase and the grip phase as well. The bandwidths chosen were 0.03-0.13 Hz (2-8 cpm), 0.08 -.13 Hz, (3-7 cpm), 0.06-0.12 Hz (5-7 cpm), 0.05- 0.33 Hz (3-20) cpm and 0.08- 0.33 Hz (5-20 cpm). The last two were chosen to include the breathing components as well. MATLAB was used to perform the analysis and was done in two steps. The first step involved generating a scatter plot for the mean spectral densities for the different bandwidths being analysed. After visual examination of the scatter plots a range of possible threshold values of the mean spectral density was selected for each bandwidth. The main aim of the study was to find a suitable method that could best distinguish between the three groups. As explained earlier efforts were made to establish the best possible method to separate groups II and III. The scatter plots generated for the mean spectral density values across the three groups did not have any clear

demarcation between them as the values were spread out with a wide range. Thus a range of threshold values was analysed to obtain the most optimum level of separation between the two groups.

The second step involved calculating the number of true positives and negatives that could be identified using a particular threshold value. The scatter plots revealed reduced spectral densities for participants in group III. Hence if the value of the spectral density for a participant was equal to or less than the threshold value, the participant was regarded as diseased (in this case neuropathic) or else regarded as non diseased (in this case diabetics with no neuropathy). The true positives and true negatives thus generated were used to calculate the sensitivity and specificity of the test for that particular threshold. This analysis was performed on the whole signal, the breathing phase, the intermediate resting phase and the grip phase individually.

The MATLAB Program

The above-mentioned analysis was performed using both MATLAB and Microsoft Excel. Three lists namely normal, patient and neuropathic list were created in MATLAB containing the data from groups I, II, and III respectively. Though the program was written to analyse all three groups, only the data from Groups II and III were used for calculating the sensitivity and specificity of each of the tests. The lists were loaded one at a time, analysed, and the final set of results were outputted after going through all three groups. In the

next few paragraphs the sequence of the program to analyse the data from a single participant would be explained.

The flow chart for the program is illustrated in figure 7.10. The sequence as shown in the figure was repeated for all participants in one list before moving on the next list where the whole sequence was once again repeated. This program was not only used to analyse the whole PPG signal but with slight modifications was also used to analyse the individual segments of the whole PPG signal.

Once loaded the huge DC offset was removed by subtracting the signal from its mean. The sampling rate of the Assist was very high at 1 KHz and it exceeded our sampling rate requirement while analysing the LF end of the spectrum. Thus in order to decrease the run time of the program, it was decided to resample the raw PPG signal at a much smaller sampling rate of 120 cpm or 2 Hz. In order to avoid any possible aliasing during the re-sampling of the PPG signal, an anti-aliasing filter was used. A second order low pass Butterworth filter with a cut-off frequency of 0.5 Hz cpm was used for the purpose. The filtered signal was then re-sampled at the new sampling rate and was band pass filtered between 2 cpm and 15 cpm. A Combination of 2^{nd} order high pass filter with a cut off of 0.03 Hz (2 cpm) and 3^{rd} order low pass filter with a cut off of 0.42 Hz (25 cpm) was used to band pass the signal such that all frequencies above and below the cut-off frequencies were attenuated producing a signal mainly containing the LF information. The spectral analysis was then carried out on the modified raw PPG signal. The signal was

windowed using a Hanning window before a full length FFT was performed. Once the spectrum was generated the mean spectral density of the bandwidth of interest was calculated from the left and the right spectrum.

A range of possible threshold values of the mean spectral density were analysed. For each threshold value the number of true positives and negatives were calculated. If the mean spectral density of a participant was equal to or less than the threshold value then they were considered positives, i.e. positively neuropathic and if their mean spectral density was above the threshold value they were considered negatives or only diabetic (with no neuropathy). The final output of the program generated the true positives and true negatives calculated for all three groups, however only the data from Groups II and III were used for the analysis.

The program generated two column vectors for each group, containing the number of positives and negatives calculated for each threshold selected within the group for a particular bandwidth of interest. The values calculated for Group II and III were noted and transferred to the Excel spread sheet. Using Excel the sensitivity, specificity, positive predictive value, negative predictive value and the accuracy of the test were calculated. This program was repeated for 6 different ranges of bandwidth and also for the different segments of the PPG signal. These values were carefully studied and the threshold that provided the best sensitivity and specificity for the test was selected for each bandwidth and these results were tabulated in figure 7.11.

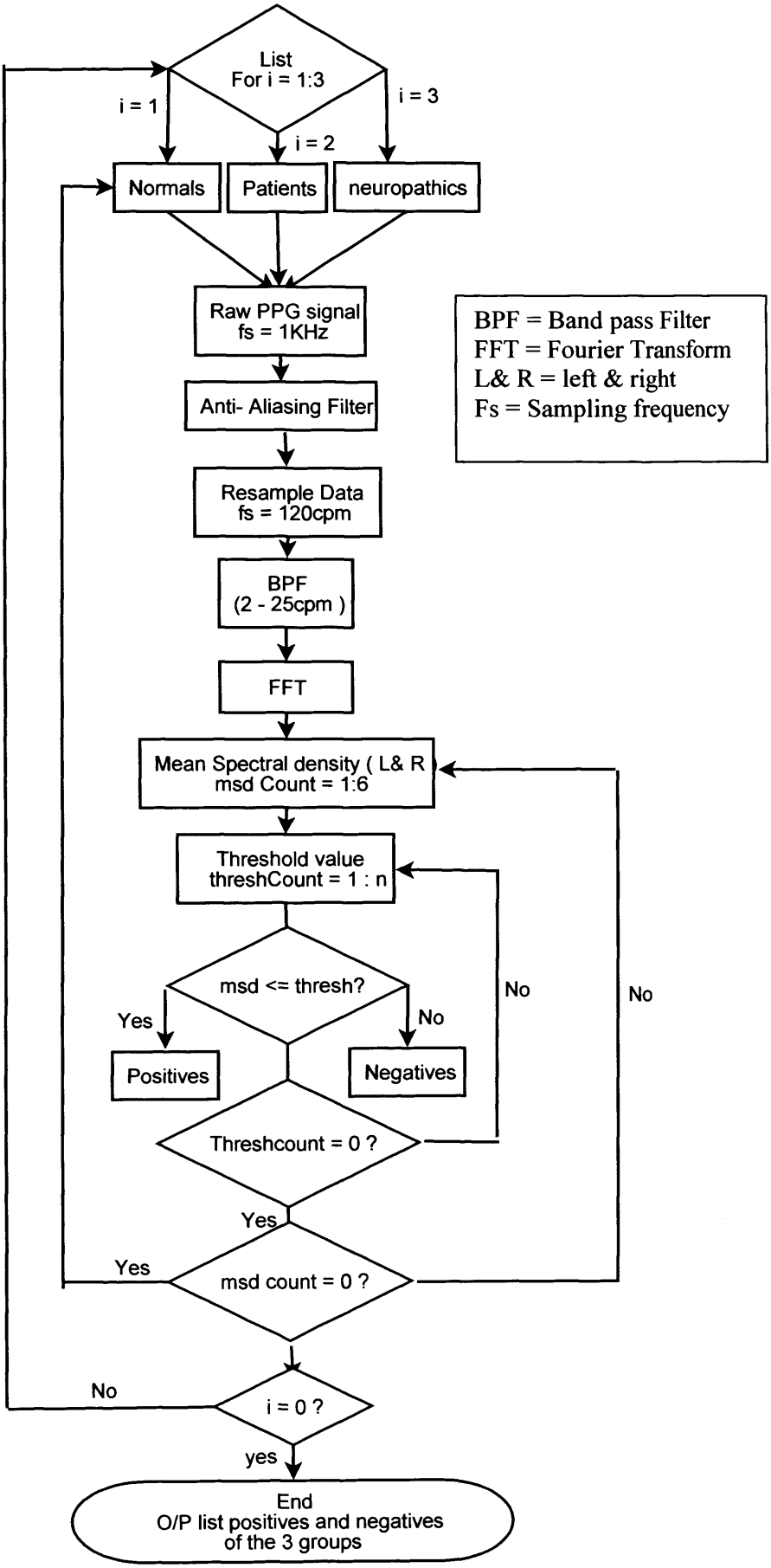

Figure 7.10: Flow Chart of the MATLAB program to calculate the sensitivity & specificity of test using mean spectral density

	Bandwidth (cpm)	Sensitivity (%)	Specificity (%)	PPV (%)	NPV (%)	Accuracy (%)
Whole Signal	2-8	73.7	63.88	68.29	69.69	68.91
	5-8	71.0	61.1	65.8	66.7	66.2
	3-7	71.0	61.1	65.8	66.7	66.2
	4-7	73.7	50	61	64.2	62.2
	3-20	76.3	53	63	68	65.0
	5-20	71.0	55.6	62.8	64.5	63.5
Breathing Phase	2-8	71.05	61.11	65.85	66.67	66.22
	5-8	76.32	58.33	65.91	70.00	67.57
	3-7	68.42	66.67	68.42	66.67	67.57
	4-7	73.68	61.11	66.67	68.75	67.57
	3-20	84.2	61.1	69.57	78.57	62.97
	5-20	84.21	58.33	68.08	77.78	71.62
Resting Phase	2-8	76.3	58.3	65.9	70.0	67.57
	5-8	78.9	50.0	62.5	69.23	64.86
	3-7	71.05	69.44	71.05	69.44	70.27
	4-7	68.4	64.0	66.7	65.71	66.21
	3-20	79.0	55.6	65.2	71.43	67.57
	5-20	79.0	55.6	65.22	71.4	67.60
Grip Phase	2-8	65.78	75.00	73.52	67.50	70.27
	5-8	76.31	47.22	60.41	65.39	62.16
	3-7	65.78	61.11	64.10	62.85	63.51
	4-7	65.78	61.11	64.10	62.85	63.51
	3-20	78.9	41.66	58.82	65.21	60.81
	5-20	73.68	41.67	57.14	60.00	58.10

Figure 7.11: The sensitivity and specificity of the test obtained for various bandwidth combinations on the whole and the individual test segments of the signal

The breathing, the intermediate resting and the grip phase represented the different stages of the experiment protocol. The breathing phase was a two minute segment during which the participant was asked to breathe in and out across some resistance using the Power Lung®, while the grip phase was another two minute segment during which the participant was asked to grip the dynamometer at 10% of their maximum grip strength. The resting phase represented the intermediate resting period of three minutes between the two stress tests and could be used as representative of a signal with no stress tests. However there is a strong possibility of observing some spill over effect of the breathing phase onto this phase. The aim of analysing the different segments of the PPG was to determine the extent of influence of these stress tests on the raw PPG signal and their importance is identifying the true positives (group III) and ruling out the true negatives (group II).

Visual analyses of the HF and LF end of the spectrum so far have revealed far greater response of the peripheral circulation to the breathing exercise as compared to the grip test. The blood pressure response to the grip test is a commonly used diagnostic test for autonomic neuropathy. The grip test used in this study was intended to replicate similar pressure changes which being a sympathetic response was thought to be reflected in the peripheral circulation. The reduced response may be influenced by the level of stress chosen for the study. Prior to the actual study, two different levels of grip test viz; 10% and 20% were tested on volunteers within the department and the 10% level was found to be more user friendly. As most patients requiring screening were the elderly it was essential for the tests chosen to be patient compliant. Hence the

stress level was kept to only 10% of the person's maximum grip strength. However later during the analysis of the data reduced response to the grip test was observed across the three groups, mainly Groups II and III. This could be perhaps due to the lower level of stress used for the study. Visual analysis of the signals have revealed a good response to the breathing test in both the normals and the diabetics with no neuropathy and this response was found to be severely reduced in neuropathic patients. The table in figure 7.11 illustrates the different sensitivity and specificity values calculated for different frequency bandwidths on the whole signal and the three segments of the raw PPG signal. The table depicts the different degrees of success achieved in separating groups II and III. Some interesting conclusions were drawn after a detailed analysis of the table.

Analysis on the grip phase of the segment resulted in the poorest sensitivity and specificity calculation for the test. The sensitivity and specificity calculation is often a trade off between the two. The best combination of the two was obtained when the mean spectral density for a bandwidth of 0.05-0.12 Hz (3-7 cpm) was calculated and compared between the diabetics and the neuropathics. A sensitivity of approx 66% and specificity of approx 61% was calculated. However, including the whole spectrum of the LF components including the breathing components (3-20 cpm) increased the sensitivity of the test to 79% but the specificity dropped to around 42%.

Analysis on the resting phase produced better results than the analysis on the whole signal and the grip phase. The best combination of specificity and

sensitivity were obtained while comparing the mean spectral density of bandwidth of 0.05-0.12 Hz (3-7 cpm). A sensitivity of 71% and specificity of 69% was achieved. Once again it was observed that the sensitivity of the study was higher while comparing the mean spectral density of the whole LF spectrum including the breathing components 0.05-0.33 Hz (3-20 cpm). The sensitivity rose to 79% but the specificity fell to 56%.

Similar conclusions can be extended to the results of analysing the whole PPG signal. Once again the best combination of optimum sensitivity and specificity of the test was obtained by comparing the mean spectral densities of 0.05- 0.12 Hz (3-7 cpm). A sensitivity of 71% and specificity of 61% was obtained using this method of analysis. Once again by including the breathing components 0.05- 0.33 Hz (3-20 cpm) as well the sensitivity of the study could be increased to 76% but at the cost of reduced specificity of 53%.

Amongst all the different signal segments, the analysis on the breathing phase produced a significantly better result. Analysis of the mean spectral density for 0.03- 0.12 Hz (3-7 cpm) produced a sensitivity of 68% with a specificity of 66%. However the analysis of the mean spectral density for 3-20 cpm achieved the best results with a sensitivity and specificity value of 84% and 61% respectively.

The above results indicate that the analysis on the breathing phase of the signal and calculating the spectral density for 0.05- 0.33 Hz (3-20 cpm) including the breathing components produced the best possible results. The

spectral density is a measure of the contribution of a frequency band in the spectrum. Of the various bandwidths analysed, the results improved significantly with the addition of the breathing components. There must be a significant difference in the spectral density of the breathing components between the two groups. The group mean value ± SD was obtained by evaluating the descriptive statistics of the mean spectral density values from all three groups. The mean spectral density for Groups I, II and III were 0.65 ± 0.47, 0.97 ± 0.83 and 0.48 ± 0.3 respectively. The mean spectral density values for Group III was lowest amongst the three groups and it was also found to be significantly lower than the mean value obtained for Group II. Previous analysis of both the raw signal and the spectrum revealed reduced response to the breathing test amongst group III participants as compared to the other two groups. The results from this analysis also indicate a reduced LF response in the neuropathic group as compared to the diabetics with no known neuropathy.

7.3.4 Analysis using the spectral density of very LF bandwidths

In all the analysis so far, the LF bandwidths (0.03 Hz– 0.13 Hz) and high LF bandwidth (0.16 Hz – 0.33 Hz) have been analysed. As mentioned previously, almost all the spectrums from across the three groups also presented with a high amplitude peak at the very LF end of the spectrum at frequencies below 1 cpm (0.2 cpm – 0.5 cpm). These very low frequencies represent the instantaneous skin vascularisation under the probe. Skin microcirculation is a dynamic environment where the blood flow changes with the local metabolic demand. The flow at the microcirculatory level is controlled by the AV shunts.

The selective opening and closing of these shunts causes this change in the capillary flow. The sympathetic branch of the autonomic nervous system, as mentioned in the first chapter, controls these AV shunts. In healthy individuals opening of these shunts are usually maintained at a higher resistance allowing most of the nutritive blood to flow through the capillaries as per the local metabolic demand while limiting the flow through these shunts into the venules. In the event of any autonomic dysfunction, this high resistance pathway is completely lost and almost all the blood is shunted into the venular circulation, bypassing the capillaries. In these individuals the PPG probably detects mainly the flow through the AV shunts and not the capillary flow. Also in such individuals, the microcirculation loses the capacity to alter capillary blood flow as per the local metabolic demand and therefore the very slow amplitude changes picked up by the probe may be absent in their raw PPG signal obtained over the whole 10-minute period.

During the visual analysis of the raw signal, the slow moving amplitude changes were found to be prominent in the healthy individuals with an exaggerated response during the two stress tests. On the contrary the signals from Group III were almost flat with very little or no amplitude variations over the whole 10 minutes of the signal. Thus it was essential to identify if the spectral densities of these very LF bands could distinguish Groups I, II and III. The program used in the previous sections with some minor modifications in the band pass filter specifications, was used to calculate the mean spectral density at these low frequencies. The cut off frequency of the band pass filter was altered to allow the very LF to pass through it.

The mean spectral density for bandwidths of 0.002 – 0.005 Hz (0.1-0.3 cpm) and 0.002 – 0.008 Hz (0.1-0.5 cpm) were calculated and compared for all three groups. The peak frequency for both bandwidths was at 0.003 Hz (0.2 cpm). Figure 7.12 and 7.13 are the scatter plots for the mean spectral densities calculated for both bandwidths. The mean spectral densities calculated were absolute values and hence had no units.

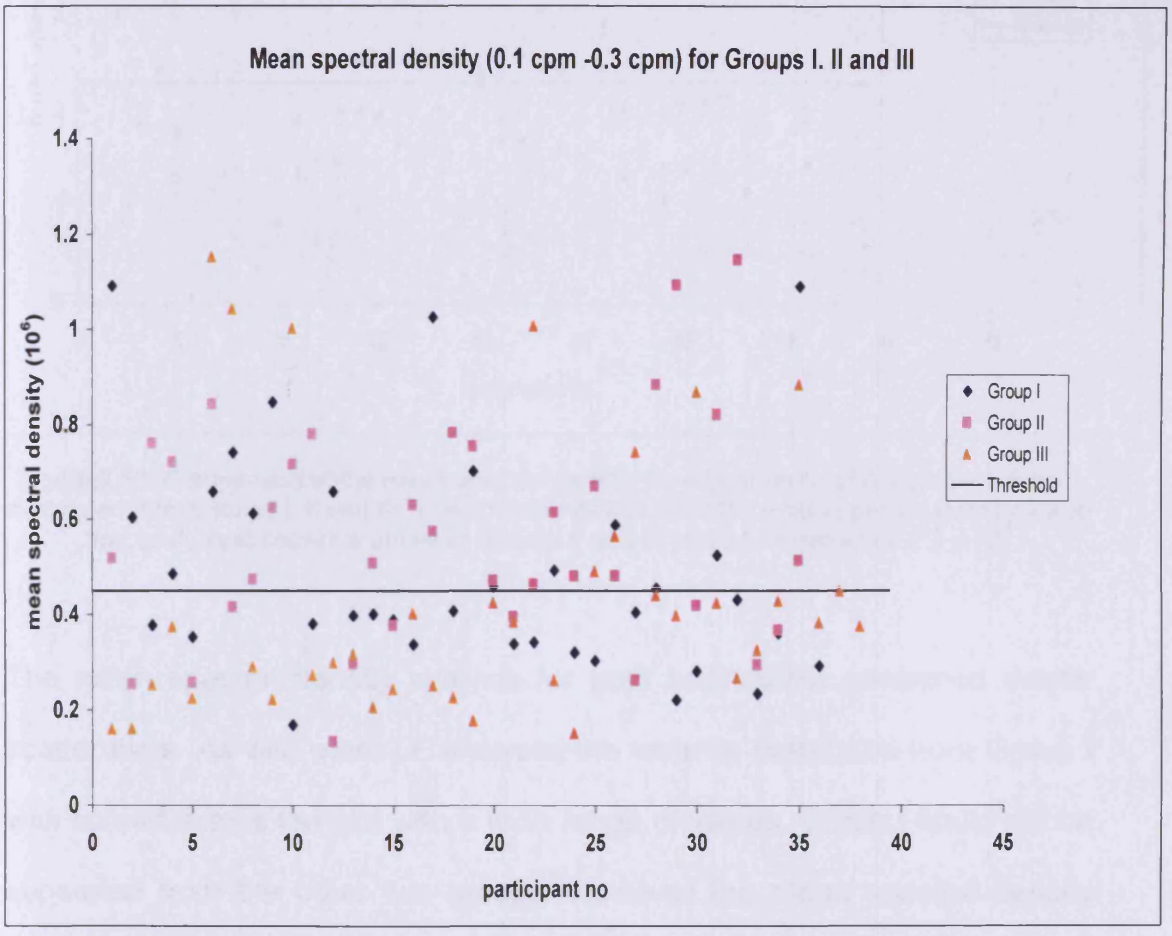

Figure 7.12: Comparison of the mean spectral density for a bandwidth of 0.1 cpm – 0.3 cpm calculated from Groups I, II and III. The optimum threshold of the mean spectral density value that could best separate between Groups II and III was observed to be 0.45 x 10^6

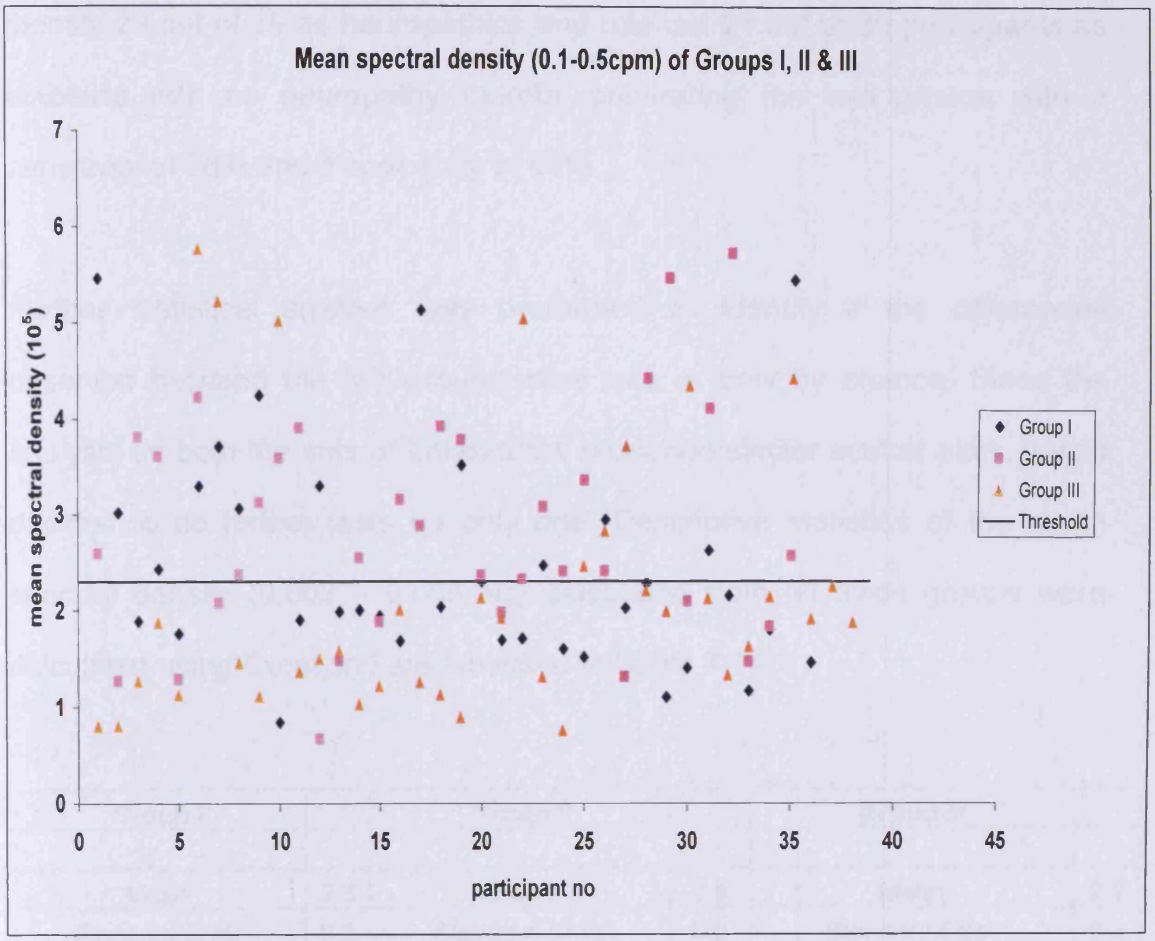

Figure 7.13: Comparison of the mean spectral density for a bandwidth of 0.1 cpm – 0.5 cpm calculated from Groups I, II and III. The optimum threshold of the mean spectral density value that could best separate between Groups II and III was observed to be 2.3 x 10^5

The mean spectral density analysis for both bandwidths generated similar scatter plots. As with other LF analysis, the variable calculated from Group I was spread across the plot with a wide range of values. Group I could not be separated from the other two groups. However the mean spectral density calculated from Group II could be separated from the values generated from Group III with some success. The participants with a mean spectral density value equal to or less than the threshold were considered to be diseased, while those with values greater than the threshold were considered to be non-diseased. Using both bandwidths separately the test was able to rightly

identify 29 out of 38 as neuropathics and rule out 24 out of 35 participants as diabetics with no neuropathy thereby separating the two groups with a sensitivity of 76% and a specificity of 69%.

Further statistical analysis was performed to identify if the differences observed between the two groups were true or only by chance. Since the analysis on both the sets of bandwidths produced similar scatter plots, it was decided to do further tests on only one. Descriptive statistics of the mean spectral density (0.002 – 0.008 Hz) calculated from all three groups were calculated using Excel and are tabulated in figure 7.14.

Group I		***Group II***		***Group III***	
Mean	2.5	Mean	2.8	Mean	2.2
Standard Error	0.2	Standard Error	0.2	Standard Error	0.2
Median	2	Median	2.6	Median	1.9
Standard Deviation	1.2	Standard Deviation	1.2	Standard Deviation	1.4
Sample Variance	1.4	Sample Variance	1.4	Sample Variance	1.9
Kurtosis	1.2	Kurtosis	0.02	Kurtosis	0.8
Skewness	1.3	Skewness	0.5	Skewness	1.4
Range	4.6	Range	5.1	Range	5
Minimum	0.8	Minimum	0.7	Minimum	0.8
Maximum	5.5	Maximum	5.7	Maximum	5.8
Confidence Level (95.0%)	0.4	Confidence Level (95.0%)	0.4	Confidence Level (95.0%)	0.5

Figure 7.14: Descriptive statistics on the mean spectral density for bandwidths of 0.1 – 0.5 cpm calculated from all three groups.

From the above table we can see that Group II had the highest mean spectral density value, while the participants from Group III had the smallest mean spectral density value. Though the scatter plot failed to distinguish between the healthy individuals (Group I) and the neuropathic group (Group III), their

mean spectral density values were different. The participants of Group I were observed to have a higher mean spectral density value compared to the neuropathics and this was more in line with the expected result. The histograms of the variable calculated from the three groups were also analysed. They have been illustrated in figure 7.15.

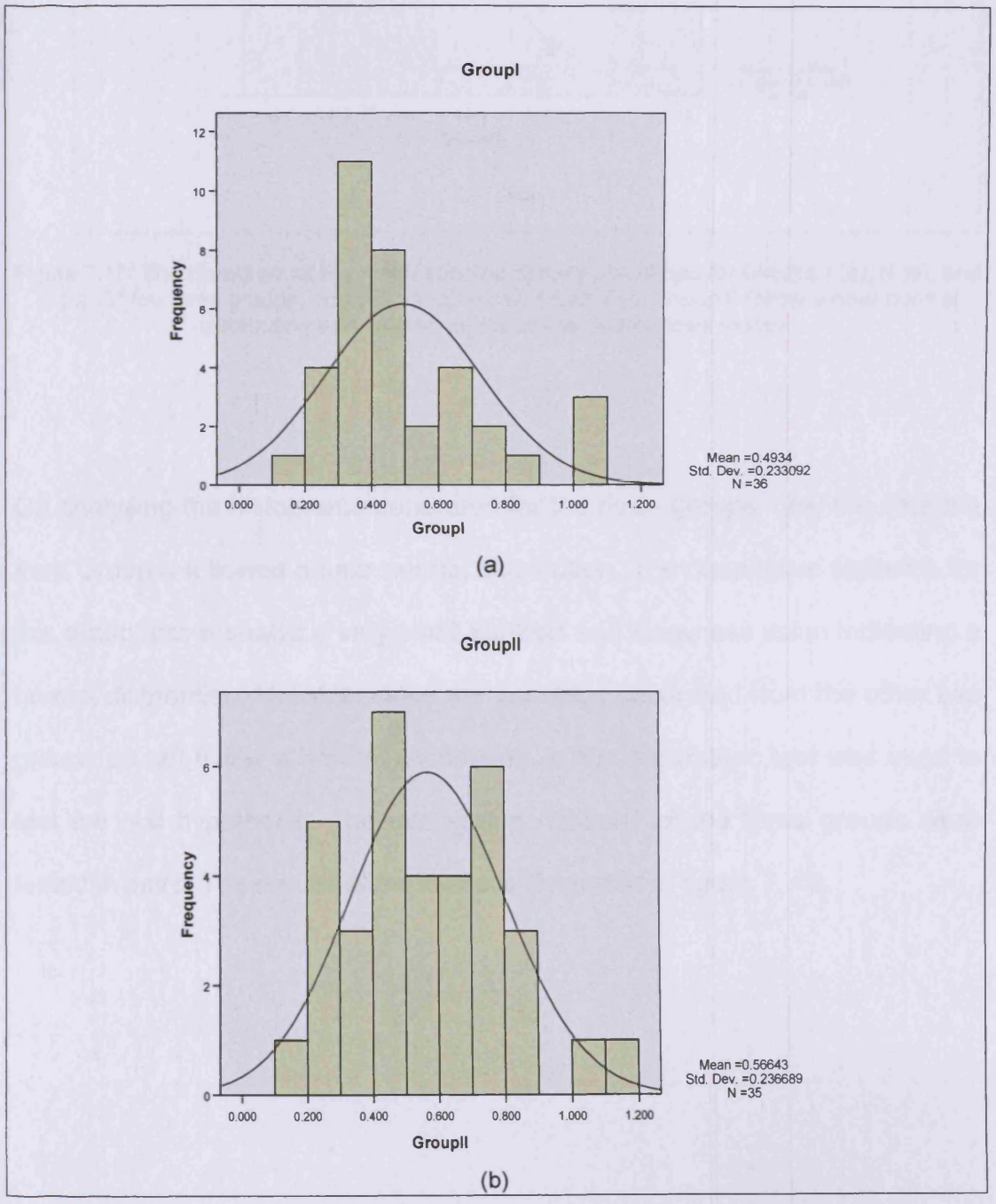

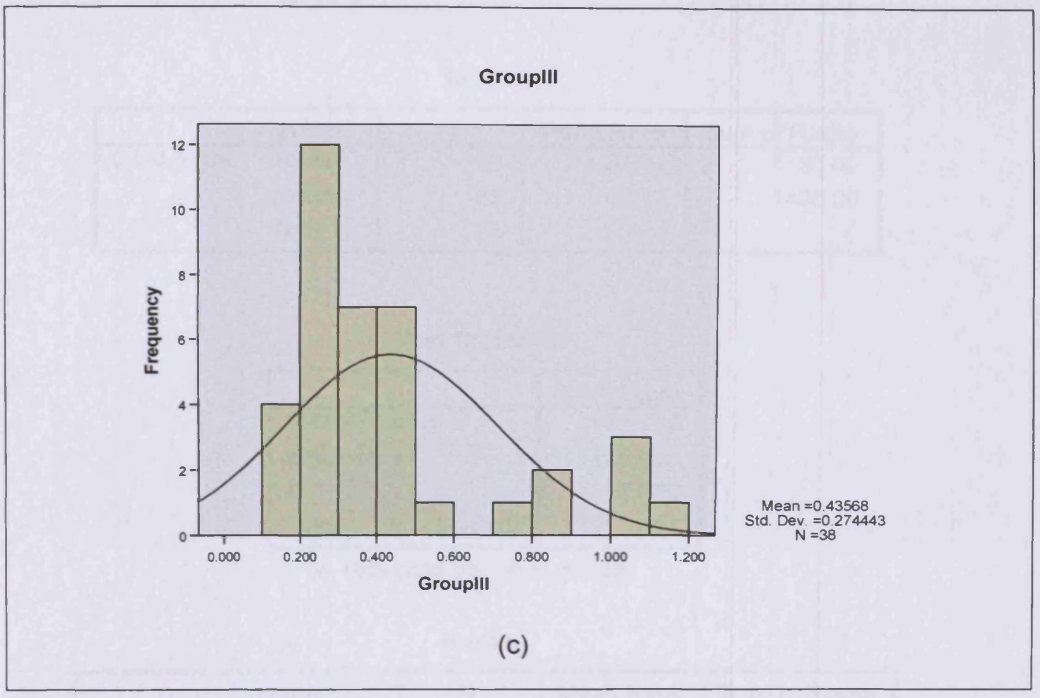

Figure 7.15: The histogram of the mean spectral density calculated for Groups I (a), II (b), and III (c). Of the three groups, only the variable calculated from Group II follow a near normal distribution with very small skewness and kurtosis values

On analysing the histograms generated for the three groups, only the variable from Group II followed a near normal distribution. The descriptive statistics for this group also revealed a very small kurtosis and skewness value indicating a normal distribution. However since the variables generated from the other two groups do not follow a normal distribution, a non-parametric test was used to test the null hypothesis. The inter-group relations of the three groups were tested in pairs. The results of the test are illustrated in figure 7. 16.

Ranks

	groups	N	Mean Rank	Sum of Ranks
0.1-0.5cpm	normal	36	31.94	1150.00
	diabetic	35	40.17	1406.00
	Total	71		

Test Statistics[a]

	0.1-0.5cpm
Mann-Whitney U	484.000
Wilcoxon W	1150.000
Z	-1.679
Asymp. Sig. (2-tailed)	.093

a. Grouping Variable: groups

Ranks

	groups	N	Mean Rank	Sum of Ranks
0.1-0.5cpm	diabetic	35	44.40	1554.00
	neuropathic	38	30.18	1147.00
	Total	73		

Test Statistics[a]

	0.1-0.5cpm
Mann-Whitney U	406.000
Wilcoxon W	1147.000
Z	-2.860
Asymp. Sig. (2-tailed)	.004

a. Grouping Variable: groups

Ranks

	groups	N	Mean Rank	Sum of Ranks
0.1-0.5cpm	normal	36	42.28	1522.00
	neuropathic	38	32.97	1253.00
	Total	74		

Test Statistics[a]

	0.1-0.5cpm
Mann-Whitney U	512.000
Wilcoxon W	1253.000
Z	-1.860
Asymp. Sig. (2-tailed)	.063

a. Grouping Variable: groups

Figure 7.16: Man-Whitney test to compare the mean spectral densities calculated from the three groups; a pair at a time

The null hypothesis that was established for this analysis was that there was no difference in the mean spectral density values between the two groups. The relation between the groups were analysed using a pair at a time. The mean ranks, the sum of mean ranks, the Mann-Whitney variable (U), the Wilcoxon variable (W), the z value and its corresponding p value for the given degree of freedom were all calculated using the statistical package SPSS. On comparing the variable calculated from Groups I and II, the p value (0.093) generated for the test was found to be greater than 0.05 and the null hypothesis could not be rejected. Thus no statistical difference could be established between the mean spectral density calculated for Groups I and II and any difference observed is only by chance.

A high p value of 0.063 was also obtained while comparing the mean spectral densities obtained from Groups I and III. Though no statistical difference could be established between the two groups, the p value was smaller than the previous comparison and was closer to 0.05. As expected from the scatter plot, a statistically significant difference could be established between the mean spectral density values calculated from Groups II and III. The p value generated was very low at 0.004 suggesting a highly significant difference between the two groups. In chapter 4B and so far in this chapter, we have seen that Groups II and III can be separated with some success using both HF and LF information from the Fourier spectrum of the raw PPG signal. In the next part of this chapter, both the HF and LF analysis were combined with an aim to further improve the screening capability of the test.

7.4 Combination of HF and LF analysis of the spectrum

Both the low and the HF analysis individually were able to differentiate between groups II and III at a statistically significant level. It was decided to combine the two analyses by calculating a new variable called the 'hrbylf', which is a ratio of the mean spectral density of the HR bandwidth to the mean spectral density of the selected LF bandwidth. From the discussion of the table in figure 7.11, it was observed that the LF spectral density analysis on the whole signal and the resting phase produced similar results, which were satisfactory while the same analysis on the breathing phase gave better sensitivity and specificity value for the tests. It was also revealed that analysing the LF spectrum over the bandwidths of 0.05-0.11 Hz (3-7cpm) and 0.05-0.33 Hz (3-20cpm) produced the best sensitivity and specificity values for the test.

Although the mean spectral density of the very LF end of the spectrum also produced favourable results, they were not used throughout this analysis. At low frequencies like 0.003 Hz, it takes nearly five minutes to complete one cycle. Thus over a whole ten minute of the raw signal, we can only obtain 2 of these cycles. The new variable 'hrbylf' was calculated for the whole, resting and the breathing phases of the signal. Such low frequencies cannot be obtained within the segments of the raw PPG signal as each of the phases only lasts between 2-3minutes. However, in the calculation of the hrbylf on the whole signal the spectral densities at the very LF end of the spectrum were also used. Thus it was decided to calculate and analyse the variable hrbylf, with the LF spectrum defined by the bandwidths of 0.05- 0.12 Hz (3-7cpm)

and 0.05- 0.33 Hz (3-20cpm) for all three combination of signals with the addition of LF bandwidth of 0.002- 0.008 Hz (0.1-0.5 cpm) for the whole signal.

Through out the LF analysis, data from all participants in Group III were used for the analysis as no difference in the LF spectrum could be established both visually and statistically between Groups III as a whole and the new subset Group IIIa (as explained in section 7.3.2). However the HF information was completely lost in the thirteen individuals excluded from the subset Group IIIa. The new variable 'hrbylf' involves both the HF and the LF end of the spectrum. Thus it was necessary to use the new subset Group IIIa rather than the data from all the participants in Group III for calculating this variable.

The MATLAB program written for the HF and the LF analysis were combined with slight modification to calculate the new variable hrbylf for all three groups. This variable was calculated as a ratio of the mean spectral density of the HR frequencies to the mean spectral density of the selected bandwidth. The flow chart illustrating the different stages of the analysis is shown in figure 7.17. The program was written in two stages.

The first part was used to calculate the ratio called hrbylf for each of the participants within a group and to produce a scatter plot of the distribution of this variable across a group for all the three groups. The mean spectral densities of the HR frequencies and the low frequencies were calculated as two separate sections within the program. The signal was re-sampled to a

suitable sampling frequency in the two sections before any further analysis. An anti-aliasing filter was also used in both cases. The signal was subjected to an anti-aliasing Butterworth 2nd order low pass filter with a cut off frequency of 0.5 Hz (30cpm) in order to attenuate the signal beyond the cut-off limit. The signal was then re-sampled at a lower sampling rate of 2 Hz deemed sufficient to analyse the frequency components between 0.03- 0.45 Hz (2 and 27 cpm). This re-sampled signal was then band-pass filtered using a high-pass 1st order Butterworth filter with a cut-off frequency of 0.02 Hz and a low-pass 3rd order Butterworth filter with a cut-off of 0.45 Hz in combination. This band-pass filtered signal was then spectrally analysed using the FFT function. The area under the curve between 0.05- 0.12 Hz (3-7cpm) and 0.05- 0.33 Hz (3-20cpm) bandwidths were calculated and the mean spectral density was obtained for the two bandwidths.

In order to calculate the spectral density of the HR bandwidth the signal was first re-sampled to 8.7 Hz (520cpm). The re-sampled signal was then band-pass filtered using a high-pass 3rd order Butterworth filter with a cut-off frequency at 1 Hz (60cpm) and a low pass 1st order Butterworth filter with a cut-off frequency of 1.7 Hz (100cpm) to preserve the signal between 1-1.7 Hz while attenuating the rest of the signal beyond these cut-off limits. A Fourier transform was performed on the band-pass filtered signal and the location of the maximum amplitude of the spectrum was determined. The HR in man is a highly variable entity and does not constitute of only a single frequency, instead it is represented by a band of frequencies with a main central frequency. The bandwidth of the HR frequencies was determined by

calculating the lower and upper limit of the bandwidth. These limits were calculated as the upper and lower 70% of the maximum amplitude determined. The next step was to calculate the mean spectral density of the HR bandwidth determined earlier. The ratio of the two mean spectral densities was calculated to obtain the variable hrbylf.

The variable hrbylf calculated for all participants of all three groups was presented as a scatter plot and analysed. Once again the normals and the neuropathic groups produced similar results. On detailed visual analysis of the plot it was observed that the patients with no known neuropathy produced smaller ratios as compared to the neuropathic patients. This was an expected result. In the HF analysis, the spectral activity at the HF end of the spectrum was observed to be around similar values in Groups II and IIIa, while in the LF analysis the spectral density was observed to be much greater in Group II when compared with Group III, thereby generating a higher hrbylf ratio in Group II than in Group IIIa participants. Visual analysis revealed a marked separation between the ratios obtained from Group II (diabetics with no neuropathy) and Group IIIa (neuropathic patients). A range of possible values of the hrbylf index were chosen as thresholds that could best separate the ratios of the two groups.

The second part of the program was used to apply each threshold value from the selected range to calculate the number of positives (neuropaths) and negatives (diabetics with no neuropathy) identified by the program. If the hrbylf index of a participant was equal to or greater than the chosen threshold

value then the participant was considered positively neuropathic or else they were considered as negative or diabetics with no neuropathy. Since no clear demarcation could be obtained between the ratios of the two groups (Group I and Group II), some degree of cross over was expected.

The positives and the negatives calculated for Group IIIa were called the true positives and the false negatives respectively. Similarly the positives and the negatives calculated from patients within group II were called false positive and true negatives of the study respectively. These variables were calculated for each threshold within the range of values selected. These numbers were then exported to Excel spread sheet to calculate the sensitivity, specificity, the positive predictive value, the negative predictive value and the accuracy of the tests for each selected threshold value. The analysis was repeated on the breathing and the intermediate resting segment of the signal as well. For each segment of raw signal analysed, the variable hrbylf was calculated with LF bandwidths of 0.05-0.12 Hz (3-7cpm) and 0.05-0.33 Hz (3-20cpm). The hrbylf variable was calculated for LF bandwidths of 0.05-0.12 Hz, 0.05-0.33 Hz and 0.0002-0.0008 Hz (0.1-0.5 cpm) for the whole signal. The results were tabulated as shown in figure 7.18.

.

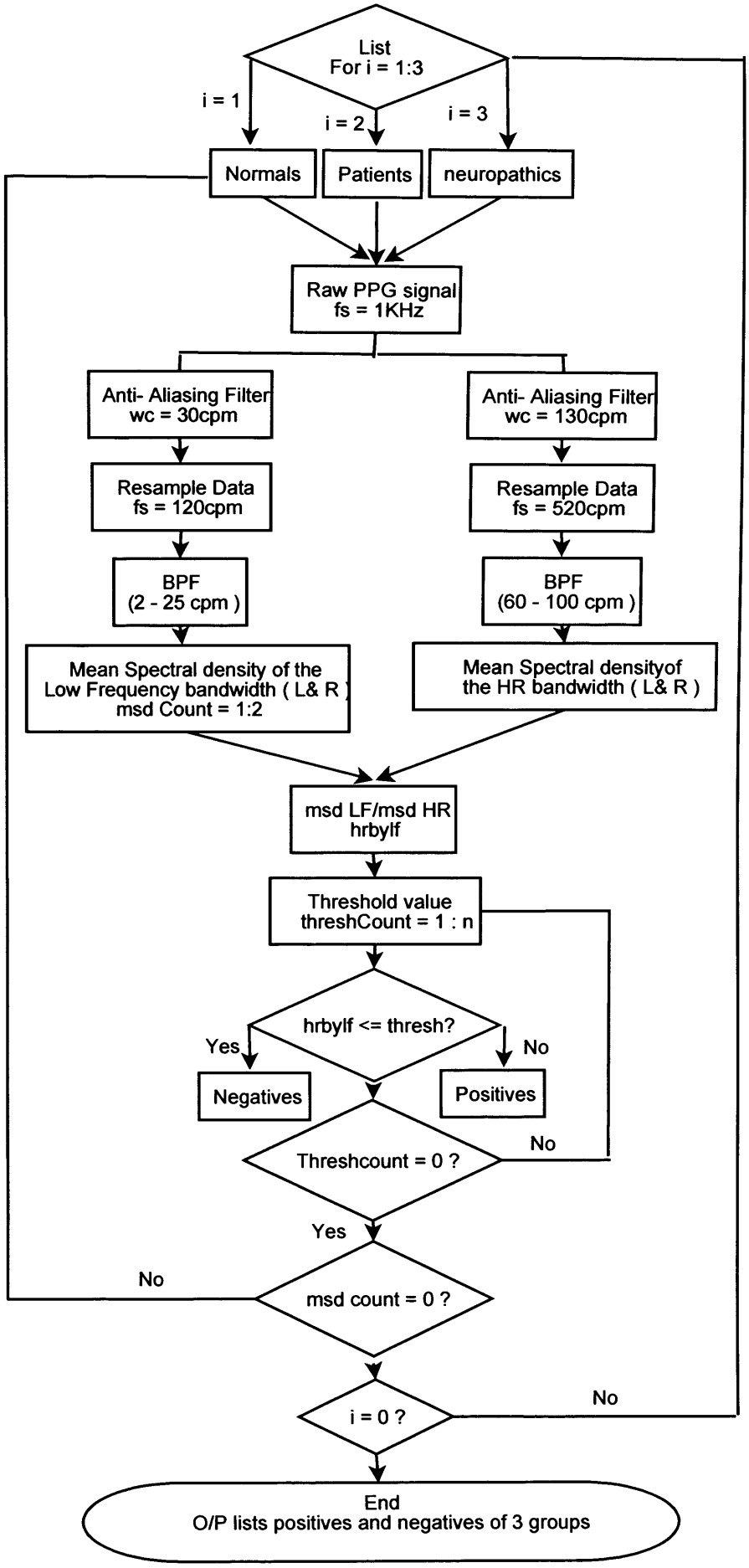

Figure 7.17: Flow chart of the MATLAB program written to calculate the sensitivity and specificity of the analysis using hrbylf index

	Bandwidth (Hz)	Sensitivity (%)	Specificity (%)	PPV (%)	NPV (%)	Accuracy (%)
Whole Signal	0.05-0.12	76	54	54	76	63
	0.05-0.33	76	63	59	79	68
	0.0002-0.0008	76	63	59	79	68
Resting Phase	0.05-0.12	72	63	58	76	67
	0.05-0.33	84	60	60	84	70
Breathing Phase	0.05-0.12	68	63	57	73	65
	0.05-0.33	**80**	**63**	**60**	**81**	**70**

Figure 7.18: The screening capability of the study expressed in the form of sensitivity, specificity, positive predictive value, negative predictive value and accuracy. The variable 'hrbylf' was calculated for the whole, resting and breathing phase with different LF bandwidths

The two main bandwidths of the LF spectrum i.e. 0.05-0.12 Hz (3-7 cpm) and 0.05-0.33 Hz (3-20 cpm) that produced the best separation between groups II and III were used for further analysis in the calculation of the hrbylf index. A combination of the HF analysis and the LF analysis was expected to further

increase the sensitivity of the test. From the conclusions drawn in the LF study it was decided to perform this analysis on the whole signal, the breathing segment of the signal and the intermediate resting segment. Both the HF and the LF analysis were combined with an aim to improve the screening capability of the test, however using hrbylf the sensitivity of the test was observed to slightly drop, while a small increase was observed in its specificity.

The hrbylf index was calculated for 0.05-0.12 Hz (3-7 cpm), 0.05-0.33 Hz (3-20 cpm) and 0.0002-0.0008 Hz (0.1-0.5 cpm) bandwidths on the whole signal. Similar scatter plots were generated when the LF bandwidth of 0.05-0.12 Hz and 0.05-0.33 Hz were used. With a threshold value of hrbylf set at 0.0014 absolute units, the test generated a sensitivity value of 76% and specificity of 54% while using 0.05-0.12 Hz and sensitivity and specificity value of 76% and 63% while using 3-20 cpm. Using the very LF information of 0.0002-0.0008 Hz, the variable hrbylf thus calculated was able to separate Groups II and IIIa with exactly the same sensitivity and specificity values as generated using 0.05- 0.33 Hz LF information.

Similar analysis on the resting phase produced slightly better results as compared to analysis on the whole signal. On comparing the hrbylf calculated for LF bandwidth of 0.05-0.12 Hz between groups II and III, the study was able to distinguish between the two with a sensitivity of 72% and specificity of 63%. Using 0.05-0.33 Hz the study generated a very good sensitivity of 84% with a specificity of 60%.

As expected the analysis on the breathing segment of the whole signal produced the best results as compared to the analysis on the other segments of the signal. Similarly analysis of the hrbylf ratio with LF bandwidth of 0.05-0.33 Hz (3-20cpm) produced better results as compared with LF bandwidth of 0.05- 0.12 Hz (3-7cpm). Using the latter as the LF bandwidth, the hrbylf calculated could only separate the two groups with sensitivity and specificity value of 68% and 63%. However the hrbylf calculated with LF bandwidth of 0.05- 0.33 Hz separated the diseased (Group IIIa) from the non diseased (Group II) with the best sensitivity of 80% and specificity of 63%. The scatter plot with the threshold selected has been illustrated in figure 7.19.

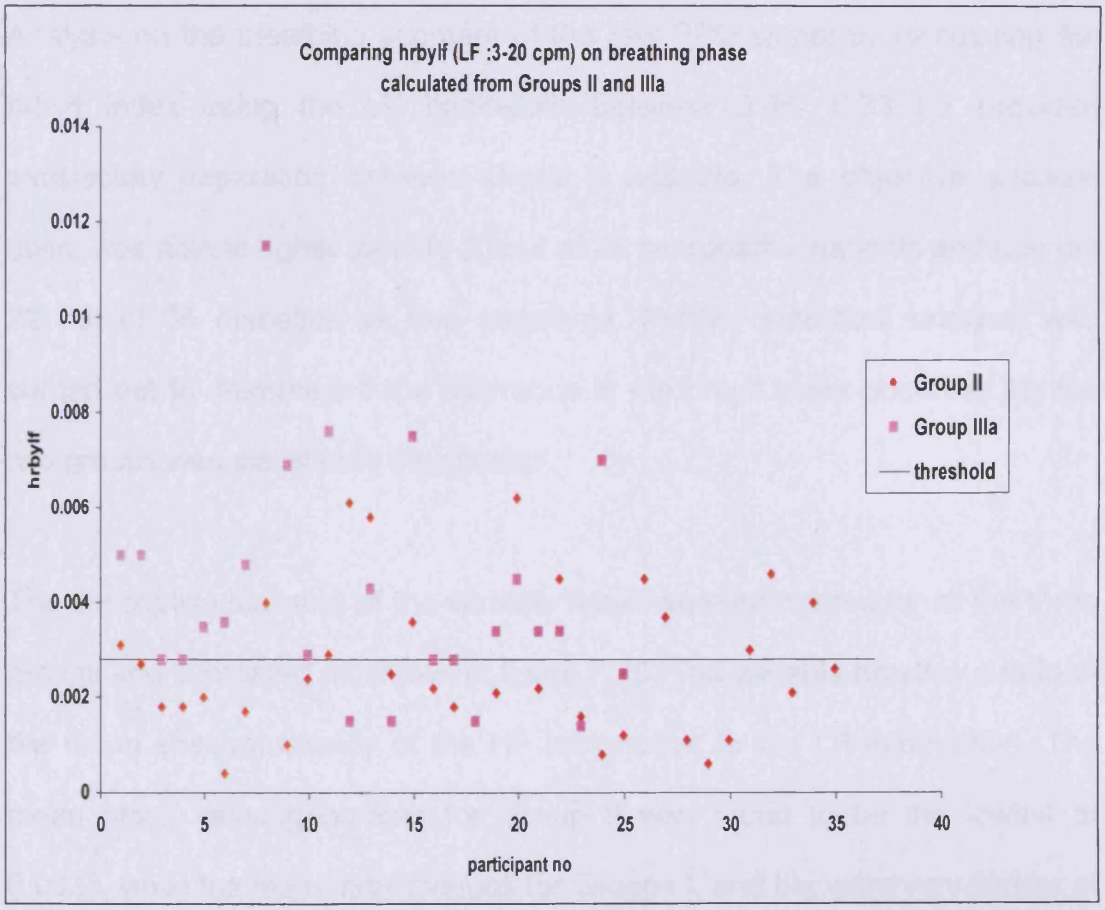

Figure 7.19: 'hrbylf' calculated for groups I, II and IIIa. The best separation between Groups II and IIIa was achieved at the threshold value of hrbylf set at 0.0028 absolute units

As mentioned earlier, the sensitivity and specificity value of any test is a trade off between each other. Hence most of the analysis done so far a higher sensitivity of the test could be achieved only at the cost of very low specificity value. However analysis of the hrbylf index i.e. ratio of the mean spectral density of the HR bandwidth to the mean spectral density of the LF bandwidth between 0.05- 0.33 Hz (including the breathing components) on the breathing segment of the whole signal resulted in a reasonably good sensitivity value of 80% while still maintaining the specificity at 63%.

7.4.1 Statistical Analysis of 'hrbylf'

Analysis on the breathing segment of the raw PPG signal by calculating the hrbylf index using the LF bandwidth between 0.05- 0.33 Hz provided satisfactory separation between Group II and IIIa. The objective analysis used, was able to rightly identify 20 out of 25 neuropathic patients and rule out 22 out of 35 diabetics as true negatives. Further statistical analysis was carried out to determine if the difference in the hrbylf index observed for the two groups was statistically significant.

The descriptive statistics of the variable hrbylf were calculated for all the three groups and compared as shown in figure 7.20. The variable hrbylf is a ratio of the mean spectral density of the HF information to the LF information. The mean hrbylf value generated for Group II was found to be the lowest at 0.0027, while the mean hrbylf values for Groups I, and IIIa were very similar at 0.0041 and 0.0042 respectively. Both the HF and LF analysis could not separate the normals from the neuropathic group successfully as the mean

spectral densities at both ends of the spectrum were found to be around a similar range of values for the two groups. Thus similar values of 'hrbylf' was expected and observed for these two groups.

Group I		*Group II*		*Group IIIa*	
Mean	0.0041	Mean	0.0027	Mean	0.0042
Standard Error	0.0006	Standard Error	0.0003	Standard Error	0.0005
Median	0.0034	Median	0.0022	Median	0.0034
Mode	0.0033	Mode	0.0018	Mode	0.0028
Standard Deviation	0.0034	Standard Deviation	0.0015	Standard Deviation	0.0024
Kurtosis	11.316	Kurtosis	0.0064	Kurtosis	2.3441
Skewness	2.8617	Skewness	0.8024	Skewness	1.4013
Range	0.0187	Range	0.0058	Range	0.0101
Minimum	0.0007	Minimum	0.0004	Minimum	0.0014
Maximum	0.0194	Maximum	0.0062	Maximum	0.0115
Largest(1)	0.0194	Largest(1)	0.0062	Largest(1)	0.0115
Smallest(1)	0.0007	Smallest(1)	0.0004	Smallest(1)	0.0014
Confidence Level (95.0%)	0.0011	Confidence Level (95.0%)	0.0005	Confidence Level (95.0%)	0.001

Figure 7.20: The descriptive statistics of 'hrbylf' calculated for all three groups.

The very high skewness value obtained for Groups I and IIIa indicate a much-skewed distribution of the variable in these groups. The histograms generated for the variable for all three groups corroborate these values. They are illustrated in figure 7.21.

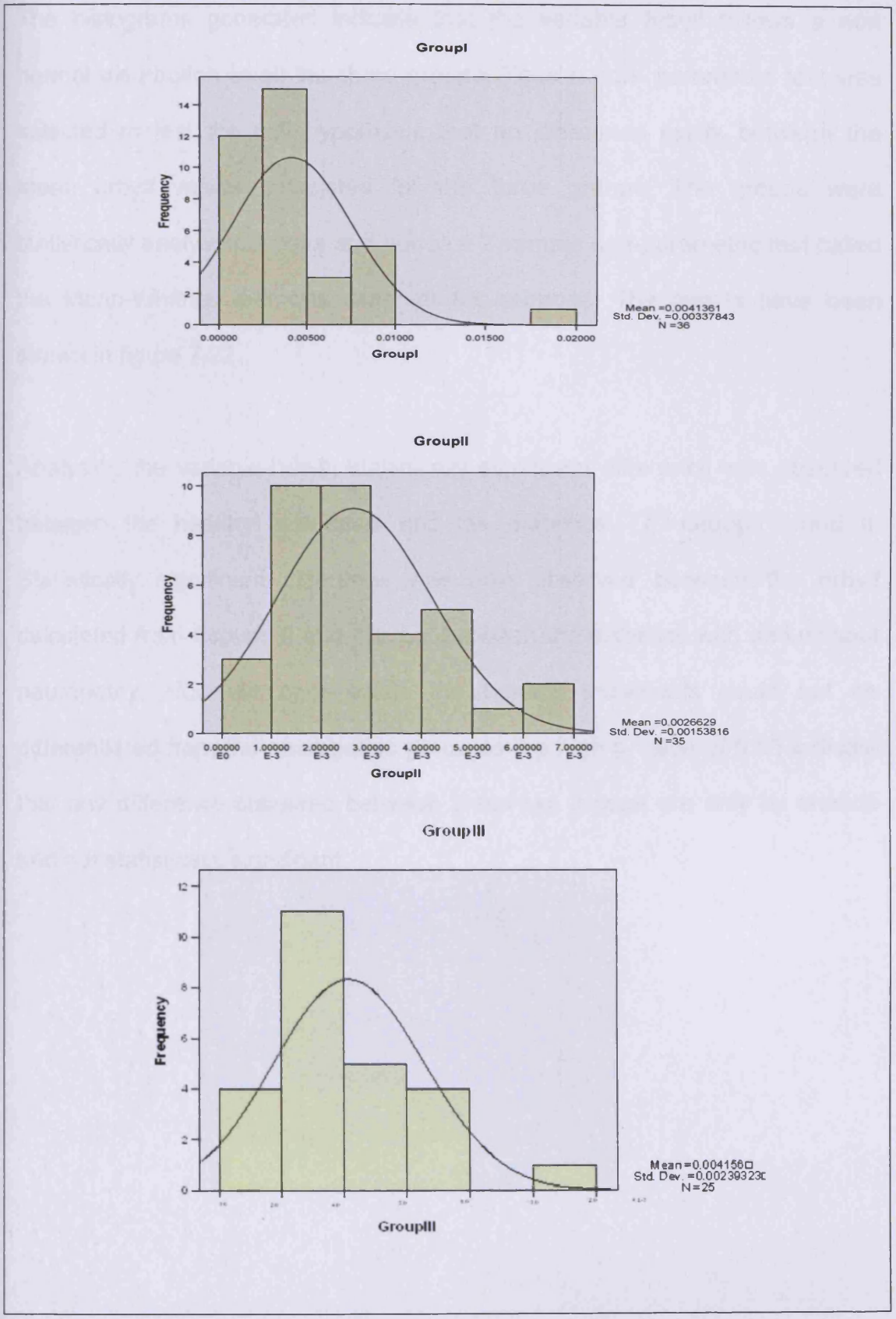

Figure 7.21: Histograms of hrbylf for Groups I, II and IIIa

The histograms generated indicate that the variable hrbylf follows a non normal distribution in all the three groups. Thus a non- parametric test was selected to test the null hypothesis that no difference exists between the mean hrbylf values calculated for the three groups. The groups were statistically analysed in pairs and hence a 2 sample non-parametric test called the Mann-Whitney test was used for the purpose. The results have been shown in figure 7.22.

Analysing the variable hrbylf, statistically significant difference was observed between the healthy individuals and the diabetics, i.e. Groups I and II. Statistically significant difference was also observed between the hrbylf calculated from Groups II and IIIa, i.e. between the diabetics with and without neuropathy. However once again the healthy individuals could not be differentiated from the neuropathic group as the high p value of 0.55 indicate that any difference observed between these two groups are only by chance and not statistically significant.

Ranks

	groups	N	Mean Rank	Sum of Ranks
3-20cpm on breathing phase	normal	36	41.21	1483.50
	diabetic	35	30.64	1072.50
	Total	71		

Test Statistics[a]

	0.1-0.5cpm
Mann-Whitney U	442.500
Wilcoxon W	1072.500
Z	-2.157
Asymp. Sig. (2-tailed)	.031

a. Grouping Variable: groups

Ranks

	groups	N	Mean Rank	Sum of Ranks
3-20cpm on breathing phase	diabetic	35	25.43	890.00
	neuropathic	25	37.60	940.00
	Total	60		

Test Statistics[a]

	0.1-0.5cpm
Mann-Whitney U	260.000
Wilcoxon W	890.000
Z	-2.663
Asymp. Sig. (2-tailed)	.008

a. Grouping Variable: groups

Ranks

	groups	N	Mean Rank	Sum of Ranks
3-20cpm on breathing phase	normal	36	29.88	1075.50
	neuropathic	25	32.62	815.50
	Total	61		

Test Statistics[a]

	0.1-0.5cpm
Mann-Whitney U	409.500
Wilcoxon W	1075.500
Z	-.594
Asymp. Sig. (2-tailed)	.552

a. Grouping Variable: groups

Figure 7.22: Mann- Whitney tests used to statistically compare the hrbylf generated for all three groups using a pair at a time.

7.5 Summary

A detailed explanation of the various signal processing analysis preformed on the raw Photoplethysmographic signal have been provided through out the results chapter. The spectral analysis of the raw PPG signal revealed activities at both the higher and the lower end of the spectrum. While the higher end of the spectrum represented the cardiac activity of the individual, the lower end of the spectrum represented a combination of the breathing, sympathetic and local activity within the skin microcirculation.

The difference observed between the HR traces obtained from groups I and II and the HR traces obtained from groups II and IIIa were statistically significant. Attempts to distinguish groups I and III were not successful even though they were visually distinctively different from each other. The normals and the neuropathic patients represent the two end of the disease spectrum. Thus the results obtained from these two groups were expected to be significantly different both visually and statistically. However for some unexplained reasons the analysis on both end of the spectrum revealed similar results for normals and the neuropathic group. Since the main aim of this study was to identify those diabetic patients who could be at risk of developing foot ulcers, several analysis were performed to identify the best possible method that could separate the neuropathics from the diabetic patients with no known neuropathy.

Reduced LF spectral density was observed in participants from Group II as compared to the spectral density values obtained from the neuropathic group.

Analysis on the LF end of the spectrum alone was able to differentiate between the diabetics with and without neuropathy with reasonable success of 84% sensitivity and 61% specificity. The variable hrbylf used both HF and LF information. The screening ability of the test using this variable remained more or less the same with a slight decrease in the sensitivity at 80% and a relative increase in the specificity at 63%.

The best sensitivity and specificity values were obtained from the analysis on the breathing phase of the raw PPG signal suggesting the importance of the breathing test in the test protocol. The breathing exercise was included in the protocol to obtain an exaggerated response of the autonomic system. The breathing activity altered the instantaneous skin blood volume, which was also reflected in the raw PPG signal. The strength of this response decreased to a considerable extent among the participants of group III as compared to the response from the other two groups.

The grip test was the second stress test used in this study. The participant was asked to grip the dynamometer at 10% of his or her maximum grip strength. The decreased response to this stress test could be due to the inadequate level of stress and better results could perhaps be obtained by increasing the level of grip to 30% of his or her maximum grip strength. However at such high percentage of the grip strength, the test fails to remain patient compliant that is a vital requirement for any good screening tool. The results of the test could also be further improved by using a PPG probe with a higher signal to noise ratio.

Thus results from the visual, LF and the HF analysis of the raw PPG signal can be summarised as follows:

- Visual analysis of the raw PPG signal and its Fourier spectrum revealed characteristic differences between the three groups
- In the HR bandwidth analysis-
    - The bandwidth was found to be largest in Group I participants indicating high HR variability, while similar values were observed in participants from Group II and IIIa
    - Statistical difference could be established only between Groups I and II
- In the analysis of the skewness of HR distribution-
    - Maximum mean skewness value was observed in Group I participants, while similar mean skewness values were obtained from Groups II and IIIa
    - The test was able to distinguish between healthy individuals (Group I) and the diseased (Group IIIa) with a sensitivity of 68% and a specificity of 72%
    - Statistical difference could be established between Groups I and II and between Groups I and IIIa but not between the diabetics with and without neuropathy
- The HF analysis in general was able to statistically and visually separate Groups I and II/IIIa but not between the diabetics with and without neuropathy. This could be because the new subgroup Group IIIa contained data from patients with similar characteristics as Group II participants

- In the LF analysis, reduced spectral activity was observed in participants from Group III and I when compared to Group II
- The mean spectral density of LF bandwidth of 0.05- 0.33 Hz (3- 20 cpm) on the breathing segment of the PPG signal produced the best separation between Groups II and III with a sensitivity and specificity value of 84% and 61% respectively
- Analysis of the mean spectral density of LF bandwidth of 0.0003-0.0008 Hz (0.1 – 0.5 cpm) on the whole PPG signal also helped to separate between the two groups with a sensitivity and specificity of 76% and 69% respectively
- Using the information at the very LF end of the spectrum, statistical difference could only be established between Groups II and III
- Analysis using 'hrbylf'-
    - Decreased ratio observed in Group II as compared with Groups III and I
    - Using hrbylf calculated over the breathing phase, a sensitivity of 80% with a specificity of 63% was achieved in separating Groups II and IIIa
    - Statistical difference was established between Groups I and II and between Groups II and IIIa
    - No statistical difference could be established between Groups I and III

The results obtained indicate that the foot microcirculation in diabetics with and without neuropathy behave differently and can be separated using PPG with moderate success.

Chapter – VIII

Summary and Conclusion

8.1 Aim of the Study

Constant effort has been made towards the early detection of diabetic neuropathy, as it not only helps to prevent the serious complications of the disease but also to improve the prognosis of the patients to a considerable extent. Foot ulcers below the knee are a common but serious complication of diabetes. In most cases the primary aetiology of these ulcers is a combination of microvascular and macrovascular dysfunction and if left untreated can even lead to lower limb amputations. Diabetic neuropathy affecting both the sensory and the autonomic neurons is a major risk factor in developing ulcers. Sensory neuropathy leads to a loss of sensation in the feet that may cause any kind of trauma in the affected limb to go un-noticed. Autonomic sympathetic dysfunction on the other hand can cause a delay in the wound healing process and subsequent alterations in the skin blood flow due to increased shunting of blood flow through the arterio-venous shunts. Autonomic neuropathy can remain asymptomatic for a long period of time despite an early onset.

The main aim of this study was to identify methods to devise a simple, low cost screening tool to detect DAN in the early stages of diabetes and thereby help to identify those diabetic patients who may be at risk of developing

diabetic foot ulcers. The simple electronics and the low manufacturing cost of the photoplethysmographic (PPG) technique makes it a promising tool for the desired purpose. In this study PPG probes were used to obtain vascular signals from the soles of the feet of the test subjects. The signals collected were then post processed using different signal processing methods as explained in the earlier chapters.

8.2 Participant Groups

Signals were collected from three different groups of people. By doing so the study population represented the whole spectrum of the disorder, ranging from healthy individuals to patients with severe diabetic neuropathy. The participants in group II (diabetic patients) and group III (diabetics with known neuropathy) had an age range of 45-76 years and 55-79 years respectively. Participants from group I had an age range of 24-61 years and were not age matched to the other two groups. Participants for this group were specifically recruited with a younger age range so that the signals obtained from this group could be analysed and the general characteristics of what a "normal" signal should be like could be determined. These "normal" signals provided the baseline with which signals from diseased individuals could be compared with.

The analysis of the raw PPG signals were done in stages with a view to achieve the ultimate aim of the study i.e. to identify if PPG could be used to pre- diagnose diabetic neuropathy. Though the signals from all three groups were compared at each stage, the primary aim was to identify if the analysis

methods used in this study could rightly distinguish the signals obtained from neuropathic patients and those obtained from diabetics with no known neuropathy.

8.3 Results Summary

The visual analysis of the raw PPG signals from all three groups revealed certain features individual to its own group. However due to the large inherent variations in the signals within the groups, characteristic models of the PPG signal specific to each group could not be determined. Variations in the instantaneous skin blood volume under the probe were represented by the changes in the signal amplitude. The raw PPG signals from Group I exhibited a strong response to the two stress tests. This response was fairly reduced in signals from Group II and was nearly absent in signals from Group III.

The instantaneous changes in the skin microcirculation regulated by both intrinsic and extrinsic factors were reflected in its frequency spectrum. The Fourier spectrum of a raw PPG signal obtained from participants in Group I showed prominent peaks both at the HF and the LF end of the spectrum. At the HF end of the spectrum, the prominent peak along with side bands observed between 1- 2 Hz (60-120 cpm) represented the microvascular changes due to the cardiac events and the prominent peak represented the individual's fundamental HR (Kamal 1989).

At the LF end of the spectrum, several prominent frequency bands were observed between 0.03- 0.33 Hz (2-20 cpm). Frequency bands of 0.012- 0.05

Hz (1- 3 cpm) representing the thermoregulatory changes, 0.67- 0.13 Hz (4-8 cpm) representing the vasomotor changes and 0.17- 0.33 Hz (10-20 cpm) representing the respiratory changes were observed at the LF end of the spectrum (Kamal et al 1989). These frequency bands represent the autonomic influence on the microcirculation. Thus both visual and objective analyses of the frequency spectrum were performed in this study.

Visual analysis of the whole frequency spectrum obtained from all three groups revealed certain interesting observations. The HF end of the spectrum was preserved to a large extent among the participants from Group II. However decreased activity was observed at the lower end of the spectrum where two or more prominent frequency bands had decreased amplitudes or were totally absent. The spectrums obtained from participants of group III had a distinctively different appearance from the ones obtained from the other two groups. Prominent frequency bands at both ends of the spectrum were either severely reduced in amplitude or were totally absent. The presence of these frequency bands in both the left and the right foot indicated its central origin.

In the HF analysis, the mean bandwidth and the beat-by-beat HR trace were compared between the three groups. However the MATLAB program written to extract the beat-by-beat HR traces failed to extract the beat-by-beat HR from 13 participants in Group III. All of these 13 participants had a very high VPT score suggesting the increased progression of neuropathy in these patients. These patients had severely reduced HF response thereby making it difficult for the program to detect the HR bandwidth accurately. Therefore by

omitting the data from these 13 individuals of Group III a new subgroup called Group IIIa was created for the HF analysis. The HR traces obtained from the new subgroup IIIa, had similar properties to the ones obtained from Group II. The participants in Group III were selected on the basis of their VPT score and they were at varying stages of the progression of the disease. It is therefore possible that the participants in Group IIIa may be at the early neuropathic stage where the microvascular characteristics are similar to the participants of Group II. Thus the HR analysis could not statistically differentiate between the participants of Groups II and IIIa. However statistically significant difference was observed between Groups I and II and between Groups I and IIIa. Using the HF analysis, the participants of Groups I and IIIa could be separated with a sensitivity of 68% and a specificity of 72%.

The LF analysis of the frequency spectrum mostly involved the comparison of the spectral densities of the various frequency bands present at the LF end of the spectrum. The prominent spectral peaks along with the sidebands present in the LF spectrum could be grouped together in different combinations to produce several frequency bandwidths of interest. The bandwidth defined by frequencies of 0.03 Hz to 0.13 Hz (2-8 cpm) was considered a good starting point as these were considered to be representative of the vascular changes due to the sympathetic activities like blood pressure regulation, vasomotion, etc (Kamal 1989). Some of the other frequency bandwidths that were analysed include 0.08 Hz to 0.13 Hz (5-8 cpm), 0.05 Hz to 0.11 Hz (3-7 cpm), 0.06 Hz to 0.11 Hz (4-7 cpm), 0.05 Hz to 0.33 Hz (3-20 cpm) and 0.08 Hz to 0.33 Hz (5-20 cpm).

In this study the effect of the stress tests on the LF spectrum were also analysed individually. Ten minutes of the raw PPG signal was split into three main segments viz; two minutes of breathing phase, two minutes of the grip phase and three minutes of the resting phase, intermediate to the two stress tests. These phases were also individually analysed along with the whole raw PPG signal. Although the visual analysis revealed significant differences in the physical appearances of the LF spectrum obtained from Group I as compared to Group III participants, the spectral densities calculated from the healthy individuals (Group I) were observed to be low and comparable to the values obtained from the neuropathic group (Group III). Thus the LF analysis similar to the HF analysis failed to statistically separate Groups I and III even though they represented the two extremes of the disease spectrum used in this study. However statistical significant differences were observed between the values calculated from Groups II and III.

Meyer, et al in their work compared the amplitude of vasomotion obtained from Type 1 and Type 2 diabetics. The test subjects were also subjected to the standard protocol of CAN tests. In their study they observed higher amplitude of vasomotion amongst diabetics with normal CAN tests as compared to those with one or more abnormal CAN test result (Meyer et al. 2003). The results obtained in this study were also in line with these findings where the spectral densities obtained from Group III (neuropathic group) were significantly lower than the values obtained from Group II (diabetic group).

Of all the different combination of bandwidths analysed, 0.05- 0.33 Hz frequency bandwidth deserved special mention. This bandwidth included the thermoregulatory components, the vasomotor and blood pressure response and the breathing components. This bandwidth contained almost all the prominent spectral peaks that generally occur at the LF end of the spectrum and represented both the sympathetic and the parasympathetic controls. Also on comparing the two stress tests used in this study, the breathing test produced stronger responses in the peripheral circulation when compared to the grip test. The analysis on the breathing phase by calculating the spectral density of 0.05 - 0.33 Hz bandwidth produced the best result of separating Groups II from III with a sensitivity of 84% and a specificity of 61%. A high sensitivity and specificity value is vital for a test to be able to be used, as a successful screening tool i.e. ideally the test must be capable of identifying maximum number of diseased patients while simultaneously ruling out all the non-diseased individuals. Thus with an attempt to further improve the sensitivity and specificity value of this study, both HF and LF information was combined and new variable called the 'hrbylf' was calculated. This variable was the ratio of the spectral density of the HF bandwidth to the LF bandwidth.

The variable 'hrbylf' was calculated on the resting, breathing and the whole signal for various combinations of frequency bandwidths. Of all the different phases, once again the analysis on the breathing phase, the hrbylf calculated for the LF bandwidth of 0.05- 0.33 Hz and the HR bandwidth produced the best separation between the diabetics and the neuropathic group with a sensitivity of 80% and a specificity of 63%. Although the over all sensitivity of

the test fell by 4% by combining both the HF and LF information, the specificity rose by 2%.

8.4 Discussion and Conclusions

Combining both the HF and LF information did not improve the overall sensitivity and specificity of the test. In the HF analysis the participants of Groups II and IIIa exhibited similar characteristics hence using the HR information alone the two groups could not be objectively or statistically separated from each other. However significant differences were observed between the two groups while analysing the LF spectrum. Thus not much improvement was observed in the performance of the test by combing both the HF and LF analysis.

The participants selected for both Groups II and III were at varying stages of both diabetes and its complications. In Group III the 13 participants that were excluded from the analysis had a very high VPT score and 85% of them (11 out of 13) had a VPT score greater than 30 in at least one of their feet. Also 70% of them (9 out of 13) complained of other cardiovascular problems. The very high VPT score suggests a greater sensory loss in these patients. The program failed to detect the HF response in these individuals due to severely reduced amplitude of the HR bandwidth. However in all other participants apart from these 13 patients, the HR information although reduced when compared to the response from the healthy individuals, was found to be intact. The HF analysis used in this study mainly involved comparing the HR bandwidth and the skewness of the beat-by-beat HR distribution. Both these

variables were a measure of the degree of HR variability in an individual. The HR variability tests used commonly in the CAN assessment are primarily indicative of the cardiac parasympathetic integrity, although both sympathetic and parasympathetic innervations play some role in all these tests (Meyer et al. 2003).

The LF analysis in this study mainly involved comparing of the spectral densities of 3-20 cpm frequency bandwidth. This bandwidth as mentioned earlier represents both sympathetic and parasympathetic controls and contains several physiologically important spectral peaks. The mean spectral density of the LF bandwidth for Group III was significantly lower than the value obtained from Group II. As mentioned in section 7.3.2 no statistical difference was observed between Groups III and IIIa. Therefore reduced spectral densities were obtained not only from those 13 participants with reduced HF information, but also from the remaining 25 participants with intact HR response. This observation was in line with some of the previous studies, where the 6 cpm vasomotor response was found to be reduced not only in patients with one or more altered CAN tests, but also in some of those with intact CAN assessment test (Bernardi et al. 1997) (Meyer et al. 2003)

These findings suggest the possibility of the sympathetic dysfunction preceding parasympathetic dysfunction as assessed by the HR variability tests. No significant differences could however be established between the healthy individuals of group I and the neuropathic patients of Group III using both the HF and LF analysis. Although the HF analysis in this study failed to

separate Groups II and III, the LF analysis was able to achieve the same with moderate success.

The failure to achieve a 100% sensitivity and specificity using the LF analysis could be due to few shortcomings identified in the study. The participants for group III were recruited on the basis of their VPT (vibration perception threshold) score recorded three years prior to this study as part of another trial. Those individuals with a VPT score of 25 or over and with no peripheral vascular disease were selected for this study. However due to limitation in the resources, these individuals could not be assessed by a doctor to review their medical condition at the time of the recruitment. They were selected for the study on the assumption that with time the disease would progress further as it was an irreversible condition. Current diagnosis of autonomic dysfunction is very elaborate and consists of a battery of tests.

Studies have revealed that autonomic dysfunction could set in at the early stages of diabetes. Previous studies have also found that often damage to the sensory neurons is also accompanied by damage to the autonomic neurones. The detailed medical history of the participants recorded prior to the recruitment revealed that almost all of them suffered from symptoms relating to sensory neuropathy. Though being symptomatic to sensory neuropathy, there is a strong possibility that some of them may not have autonomic dysfunction. The group III participants therefore could be at various stages of neuropathic dysfunction (either autonomic or sensory) ranging from early to the advance stage of the disease. This could possibly explain the spread in

the variables calculated from this group across the spectrum making it difficult to separate Group II and III with higher sensitivity and specificity values.

The two stress tests were used to produce an exaggerated vascular response. However with the aim to make it patient compliant the level of stress had to be kept at minimum. Though some positive response was recorded for the breathing test, the grip test proved to be clearly inadequate as it failed to provide any satisfactory response from any of the three groups. Better PPG probes have been developed since the study by Huntleigh Diagnostics with better signal to noise ratio. Finally the limitation in the MATLAB program to detect very low amplitude of the HF response in neuropathic participants accurately may have also contributed to the inability to further improve the sensitivity and specificity of the test

8.5 Future Work

Though the various analysis methods used in this study could only differentiate the neuropathic patients from the diabetic group with a sensitivity of 84%, the results have shown that some microvascular changes does occur in participants of Group III. Better results could be expected if the study were to be carried out only on formally diagnosed neuropathic patients with autonomic dysfunction. However the participants in Group II and III represent the true patient population that are screened for high-risk patients for developing diabetic foot disease. It is a well-established fact that the very LF end of the PPG spectrum represents the autonomic activity. The participants

of Group III were suffering from severe sensory neuropathy. Signal analysis indicated severely altered LF information in this group as compared to participants of Group II. This change could be mainly attributed to the sympathetic dysfunction in these patients.

The primary aim of this study was to identify if PPG technique could be used to detect changes in skin microcirculation and results from this study indicate that PPG could be used to detect these vascular changes with moderate success. A more robust and improved MATLAB program for extracting the HF information from raw PPG signal along with new PPG probes with better signal to noise ratio could be used to develop a successful screening tool for identifying diabetic patients who may be at risk of developing diabetic foot disease. Further research work needs to be carried out on a larger sample size and the participants should also be tested with the gold standard tests used in the diagnosis of DAN. This way it becomes possible to compare the study with a standard method and also help to identify the true diagnostic capability of the method. The study also demonstrated the importance of the breathing test in the study protocol as compared with the grip test. An improved version of the protocol could be used in future with greater preference to the breathing exercise. Increasing the level of difficulty of the grip test would reduce the patient compliance of the study significantly and hence is better omitted from the protocol.

Although the general review of the diabetic patients include tests to detect sensory neuropathy, the tests for detecting autonomic dysfunction are not

very common. This is because these tests are elaborate and require highly skilled professionals to perform and report them. Diagnosis of DAN has always drawn less interest as they remain asymptomatic for most part of the disease. Often intervention at the later symptomatic stages of DAN results in poor prognosis of the disease. A report presented at a conference on management of diabetes indicated a trend prevalent amongst the physicians of not giving due importance to the early diagnosis of DAN. This could be due to the limited treatment options and poor prognosis of the disease (Vinik et al 2003).

There is however a strong potential for developing a screening tool that could be used in primary care as part of their routine review of the diabetic patients. Previous studies have found that DAN could set in during the early stages of diabetes (Braune 1997). Changes in the skin microcirculation may be one of the earliest manifestations of DAN and is also one of the primary causes for developing diabetic foot disease (Vinik et al 2003). The single most important benefit of the early diagnosis of DAN is the possibility of early tight glycaemic control. Studies have found that near normal glycaemic control is the most effective was to delay the progression of DAN (Vinik et al 2003).

Early diagnosis of DAN can aid in providing necessary help to those individuals who may be at risk, in the form of counselling and spreading awareness regarding the benefits of healthy lifestyle, tight glycaemic control etc. Three types of tests viz; HRV with deep breathing, Valsalva manoeuvre and the sustained grip test were recommended by the expert panel at the

1988 San Antonio for routine clinical use in the diagnosis of CAN (Vinik et al 2003). However no tests were recommended for diagnosis of other types of autonomic dysfunction. Thus even though there is a strong evidence of early changes in skin microcirculation, currently no tests are being clinically used that looks into these changes.

Several studies however have been reported that have analysed the changes in skin microcirculation using LASER Doppler technique. Once again the design complexity and the expensive nature of LASER Doppler do not make it a suitable screening tool. With increasing awareness regarding diabetes and its microvascular complications, several research projects are being carried to try and develop new methods to stop or even reverse the effects of neuropathy. Any significant break through in this area would increase the need for pre diagnosis of DAN significantly thereby increasing the demand for cheap, simple screening device. Even in the absence of any such pharmacological breakthrough, the early detection of DAN can at least help to delay the progression of the dysfunction. Results from this study have demonstrated the use of PPG technique in analysing the microvascular changes in the skin. Efforts have also been made to study both the advantages and the disadvantages of this technique and in recognising its future as an efficient screening device in the pre diagnosis of autonomic dysfunction among diabetic patients.

Appendix

MATLAB programs used to analyse the DPPG signal in this study

---

MATLAB codes used in this study are included in this section. They are as follows:

Appendix A: MATLAB code generated to extract the heart rate information from raw PPG signal as shown in figure 6.8

Appendix B: MATLAB code generated to measure the sensitivity and specificity of the test by generating the mean spectral densities of six different low frequency bandwidth combinations as shown in figure 7.10

Appendix C: MATLAB code generated to measure the sensitivity and specificity of the test by calculating the hrbylf index as shown in figure 7.17

Appendix D: MATLAB code generated as functions that were called in the main program written to extract the heart rate trace from raw PPG signals

Appendix A: Heart rate extraction

```
%This program extracts the HR trace from the raw PPG signals obained from
%each of the participants of the three groups.

close all
clear all
clc
%
%=========================================================================
%=========================================================================
%   Constants
fs = 1000 * 60;  % samples per minute
fN = fs / 2;

fsNEW = 520 %240,360;        %   new sampling rate
fNNEW = fsNEW / 2;  %   new Nyquist point
N = round (fs / fsNEW);     %   downsample parameter ie every Nth sample


LF = 1; RF = 2;
%
%=========================================================================
%=========================================================================
%   READ RAW PPG SIGNALS AND CALCULATE THE TIME AXIS!!!!
%
N4 =   ('../data_file/trial3/r1gr10/patients/P35.csv');
% N4 = ('../data_file/trial3/r1gr10/normals/N36.csv') ;
```

```
% N4 = ('../data_file/trial3/r1gr10/neuropaths/PB38.csv');
%
Name = N4(1,39:42)

N4 = csvread (N4,4,0);
VMLF = N4( :, LF  );
VMRF = N4( :, RF );

VMLF = VMLF - mean(VMLF);%removing the mean and hence the large DC offset
VMRF = VMRF - mean(VMRF);


%%=========================================================================
%%=========================================================================

%%=========================================================================
%%Step 1: BPF the raw signal for the high freq components

tNEW = downsample( t1, N );

[ Bhi Ahi ] = butter( 3, 60/fN, 'high' );
[ Blo Alo ] = butter( 1,100/fN, 'low' );

CPLF = filtfilt( Bhi, Ahi, VMLF );
CPRF = filtfilt( Bhi, Ahi, VMRF );

CPLF = filtfilt( Blo, Alo, CPLF );
CPRF = filtfilt( Blo, Alo, CPRF );



%%=========================================================================
%%=========================================================================

cplf = downsample( CPLF, N );
cprf = downsample( CPRF, N );
```

```
siglen = length( cplf );
win = hanning( 1, siglen );

cplf = cplf .* win;
cprf = cprf .* win;

fftlen = siglen;
fftlendiv2 = floor( fftlen / 2 );

FFTCPLF = abs( fft( cplf, fftlen ) );
FFTCPRF = abs( fft( cprf, fftlen ) );
%
%=========================================================================
%   FFT envelope

[ Bfftlo Afftlo ] = butter( 2, 0.005 );
fftcplf = filtfilt( Bfftlo, Afftlo, FFTCPLF );
fftcplf = fftcplf ./  max( fftcplf( 1:fftlendiv2 ) );
fftcprf = filtfilt( Bfftlo, Afftlo, FFTCPRF );
fftcprf = fftcprf ./  max( fftcprf( 1:fftlendiv2 ) );

%=========================================================================
%=========================================================================
%   Find the N% thresholds of the FFT
%
    iq = find( round( faxis ) == 60 )
    iq = iq( 1 )
    faxis( iq )

    thresh = 0.7;
    [ MAXFFTLF ILF ] = max( fftcplf( iq:fftlendiv2 ) );
    MAXFFTLF
    ILF
    ILF = ILF + iq
    THRESH = thresh * MAXFFTLF
```

```
    lfindexLF = 0; hfindexLF = 0; i = ILF;
    while ( fftcplf( i ) > THRESH ) && ( i > 10 )
        i = i - 1;
    end
    lfindexLF = i;
    i = ILF;
    while ( fftcplf( i ) > THRESH ) && ( i < fftlendiv2 - 10 )
        i = i + 1;
    end
    hfindexLF = i;

    [ MAXFFTRF IRF ] = max( fftcprf( iq:fftlendiv2 ) )
    IRF = IRF + iq

    THRESH = thresh * MAXFFTRF;
    lfindexRF = 0; hfindexRF = 0; i = IRF;
    while ( fftcprf( i ) > THRESH ) && ( i > 10 )
        i = i - 1;
    end
    lfindexRF = i;
    i = IRF;
    while ( fftcprf( i ) > THRESH ) && ( i < fftlendiv2 - 10 )
        i = i + 1;
    end
    hfindexRF = i;

%=========================================================================
%=========================================================================
%   Plot the FFTs

faxis = ( fNNEW/fftlendiv2:fNNEW/fftlendiv2:fNNEW );

figure( 1 )
subplot( 2, 1, 1 )
hold on
```

```
for i = 1:fftlendiv2
    plot( [ faxis( i ) faxis( i ) ], [ 0 fftcplf( i ) ], 'r' )
end

plot( faxis, fftcplf( 1:fftlendiv2 ), 'r-' )
plot( [ faxis( lfindexLF ) faxis( lfindexLF ) ], [ 0 MAXFFTLF + 0 ], 'k' )
plot( [ faxis( hfindexLF ) faxis( hfindexLF ) ], [ 0  MAXFFTLF + 0 ], 'k' )
grid on
title( 'Heart Rate bandwidth from the left foot' )
xlabel( 'cycles per minute' )
ylabel ( ' amplitude ' )
subplot( 2, 1, 2 )
hold on

for i = 1:fftlendiv2
    plot( [ faxis( i ) faxis( i ) ], [ 0 fftcprf( i ) ], 'r' )
end
plot( faxis, fftcprf( 1:fftlendiv2 ), 'r' )
plot( [ faxis( lfindexRF ) faxis( lfindexRF ) ], [ 0 MAXFFTRF + 0 ], 'k' )
plot( [ faxis( hfindexRF ) faxis( hfindexRF ) ], [ 0  MAXFFTRF + 0 ], 'k' )
grid on
title( 'Heart Rate bandwidth from the right foot ' )
xlabel( 'cycles per minute' )
ylabel ( ' amplitude ' )

%%=============================================================================
%%=============================================================================
%   Band pass CPLF and CPRF using LP filter with fc equal to the N%
%   thershold level at the high frequency side of the FFT main lobe and a
%   HP filter with fc equal to the N% threshold level at the low frequency
%   side of the FFT main lobe
%
[ Bhi Ahi ] = butter( 4, faxis( lfindexLF )/fN, 'high' );
[ Blo Alo ] = butter( 2, faxis( hfindexLF )/fN, 'low' );

CPLF = filtfilt( Bhi, Ahi, CPLF );
```

```
CPLF = filtfilt( Blo, Alo, CPLF );

[ Bhi Ahi ] = butter( 4, faxis( lfindexRF )/fN, 'high' );
[ Blo Alo ] = butter( 2, faxis( hfindexRF )/fN, 'low' );

CPRF = filtfilt( Bhi, Ahi, CPRF );
CPRF = filtfilt( Blo, Alo, CPRF );

%=========================================================================
%=========================================================================
% Complex demodulation of the high pass filtered raw signal at a frequency
% eaqual to the mean of the freq at which the peak occurs at both left and
% right foot. This is achieved by calling a separate function - complex_demod1.
% This program calculates the CDM of the input signal


CDLF = complex_demod1( CPLF, mean( [ faxis( ILF ), faxis( IRF ) ] ), 20, fs );%20
CDRF = complex_demod1( CPRF, mean( [ faxis( ILF ), faxis( IRF ) ] ), 20, fs );


%%=========================================================================
%%=========================================================================
% Peak detection program. This section generates the HR trace from the complex
% demodulated signal by calling another separate function called DNAVPPGPEAKDETECT5

ctLF = DNAVPPGFHRPEAKDETECT5( CDLF( :, 1 ), t1 );
ctRF = DNAVPPGFHRPEAKDETECT5( CDRF( :, 1 ), t1 );

CILF = ( diff( ctLF ) );
CIRF = ( diff( ctRF ) );

HRLF = 1 ./ CILF;
HRRF = 1 ./ CIRF;

a1 = length( HRRF )
a2 = length( HRLF )
```

```
if a1 > a2
   HRRF = HRRF( 1:a2 );
   tHR = ctLF( 1:length( ctLF ) - 1 );
elseif a2 > a1
   HRLF = HRLF( 1:a1 );
   tHR = ctRF( 1:length( ctRF ) - 1 );
else
    tHR = ctRF( 1:length( ctRF ) - 1 );
end

%%=========================================================================
%%=========================================================================
%% Once again a separate function called spikefilt1 was used to remove the
%% spikes from the generated heart rate trace and plot the HR traces calculated
%% from the PPG signals from both the left and the right foot.

HRLF = spikefilt1( HRLF );
HRRF = spikefilt1( HRRF );

MEANHR = mean( [ HRLF'; HRRF' ] );
MEANHR=MEANHR(MEANHR<110);

HRmeans = zeros( 1, 10 );
HRvar = zeros( 1, 10 );
p = floor( length( tHR ) / 10 );
M = 1:p;
for m = 1:10
    HRmeans( 1, m ) = mean( HRLF( M ) );
    HRvar( 1, m ) = var( HRLF( M ) );
    M = M + p;
end
M = 1:p;

    figure(2 )

    subplot( 2, 1, 1 )
```

```
    hold on
    plot( tHR, HRLF )
    for m = 1:10
        plot( [ tHR( M( 1 ) ) tHR( M( p ) ) ], [ HRmeans( m ) HRmeans( m ) ], 'r' )
%         plot( [ tHR( M( 1 ) ) tHR( M( p ) ) ], [ HRmeans( m ) + HRvar( m ) HRmeans( m ) + HRvar( m ) ], 'g' )
        M = M + p;
        M(p)
    end
    grid on
    xlabel('time in mins');
    ylabel('beats per min');
    title( 'HR trace from left leg' );
%     legend(Name,1);
    axis( [ 0 10 60 140 ] )

HRmeans = zeros( 1, 10 );
HRvar = zeros( 1, 10 );
p = floor( length( tHR ) / 10 );
M = 1:p;
    for m = 1:10
    HRmeans( 1, m ) = mean( HRRF( M ) );
    HRvar( 1, m ) = var( HRRF( M ) );
    M = M + p;
end
   M = 1:p;

    subplot( 2, 1, 2 )
    hold on
    plot( tHR, HRRF )
    for m = 1:10
        plot( [ tHR( M( 1 ) ) tHR( M( p ) ) ], [ HRmeans( m ) HRmeans( m ) ], 'r' )
%         plot( [ tHR( M( 1 ) ) tHR( M( p ) ) ], [ HRmeans( m ) + HRvar( m ) HRmeans( m ) + HRvar( m ) ], 'g' )
        M = M + p;
        M(p)
    end
    grid on
```

```
    xlabel('time in mins');
    ylabel('beats per min');
    title( 'HR trace from Right Leg');
%     legend(Name,1);
    axis( [ 0 10 60 140 ] )
    figure (9)
    subplot( 2, 1, 1 )
    plot( t1, VMLF )
    grid on
    axis( [ 0 10 -300 300 ] )
    xlabel('time in mins');
    ylabel('amplitude');
    title( 'VASOMOTION LF' );
%     legend(Name,1);

    subplot( 2, 1, 2 )
    plot( t1, VMRF )
    grid on
    axis( [ 0 10 -300 300 ] )
    xlabel('time in mins');
    ylabel('amplitude');
    title( 'VASOMOTION RF' );
%     legend(Name,1)

%%=========================================================================
%%=========================================================================
% The HR trace obtained from the left and the right foot were tested for
%% their synchronicity by generating a BlandAltman plot of the left and the right
%% HR trace using another function called BlandAlman.

BlandAltman( HRLF, HRRF, 'HR agreement' );
% legend(Name,1);
xlabel ( ' mean difference in the HR in bpm ' )
ylabel ( ' absolute  ifference in the HR in bpm ' )
title ( ' The Bland-Altman plot for the HR agreement ' )
```

Appendix B: Mean spectral density

```
close all
clear all
clc
%
%================================================================================
%================================================================================
%   Constants used in this program
FIXEDfs = 1000 * 60;% sampling frequency of the device was 1 kHz
FIXEDfN = FIXEDfs / 2;
fs = 120; % cpm the new smapling rate
resamplecoefficient = FIXEDfs / fs; % co-efficent to downsample the original signal
fN = fs / 2;
LF = 1; RF = 2;

[ Baa, Aaa ] = butter( 2, 30 / FIXEDfN );

lists = [ 'Nor.mat';...
          'Pat.mat';...
          'Neu.mat';...
                      ];

col = [ 'b';...
        'g';...
        'r';...
              ];
```

```
%%=============================================================================
%%=============================================================================

%  Three lists were generated for the three groups containing the raw PPG signals
%% from each of the participants. This section loads each list at a time
%% and analyses the raw PPG signals colected from that group
%
figure
hold on

for K = 1:3

eval ( [ 'load ' lists( K, : ) ';' ] );
[r c] = size (LIST);
% s = 3
for i = 1:r

N4 = csvread(LIST(i,:),4,0);
Name = LIST(i,36:42)

VMLF = N4( :, LF );% raw PPG signal
VMRF = N4( :, RF );
VMLF = VMLF - mean ( VMLF ); % removing the effect of the large DC offset
VMRF = VMRF - mean ( VMRF );

%% filtering the raw PPG signal to prevent aliasing while downsampling the
%% signal later in the program

VMLF = filtfilt( Baa, Aaa, VMLF );
VMRF = filtfilt( Baa, Aaa, VMRF );

VMLF = VMLF ( 1 : resamplecoefficient : end ); %% resampling the original signal
VMRF = VMRF ( 1 : resamplecoefficient : end );
```

```
%%=========================================================================
%% low pass filter the original signal to obtain very low frequency

[ Bhi Ahi ] = butter( 1, 1 / fN, 'high' );
[ Blo Alo ] = butter( 3, 25 / fN, 'low' );

VMLF = filtfilt( Bhi, Ahi, VMLF );
VMRF = filtfilt( Bhi, Ahi, VMRF );

VMLF = filtfilt( Blo, Alo, VMLF );
VMRF = filtfilt( Blo, Alo, VMRF );

%%=========================================================================
%%=========================================================================

%% FFT of the low frequency signal

len = length ( VMLF );
win = hanning ( 1, len );

VMLF = VMLF .* win;

VMRF = VMRF .* win;

vmlffft = abs ( fft ( VMLF ) );
vmrffft = abs ( fft ( VMRF ) );

l = round ( ( length ( vmlffft ) ) / 2 ) ;

vmlf = vmlffft ( 1 : l );
vmrf = vmrffft ( 1 : l );

vmlfnew = vmlf;
vmrfnew = vmrf;
```

```
%============================================================
% calculate the area under the curve

faxis = fN / 1 : fN / 1 : fN;

x = 1.0 ; % lower limit of bandwidth to be analysed
y = 20.0 ; % upper limit of bandwidth to be analysed
z = y - x ; % bandwidth
a = find ( round ( faxis ) == x );
a = a ( 2 );

b = find ( round ( faxis ) == y );
b = b ( 2 );

specarea ( i, 1 )  = ( sum ( vmlfnew ( a : b ) ) ) / z ; % calculating the spectral density of the bandwidth
specarea ( i, 2 )  = ( sum ( vmrfnew ( a : b ) ) ) / z ;

end

specarea ;

meanarea = mean ( specarea, 2 )
plot ( meanarea, [ ' + ' col( K ) ]  )
xlabel ( ' ID ' )
ylabel ( ' mean spectral density ' )
legend ( ' normal ', ' patients ', ' neuropaths ' )
grid on

%%------------------------------------------------------------------------
%%------------------------------------------------------------------------
%% this section of the program calculates the sensitivity and specificity
%% values generated for a range of thresholds

b = length ( meanarea );
range = [ 0.5 : 0.05 : 1.2 ]; % the range of mean spectral density to be used as threshold
```

```
a = length ( range );
scorematrix = zeros ( b, a );
for p = 1 : a

    thresh = 1.0e+004 * range ( p ) ;

    for q = 1 : b

        if meanarea ( q ) <= thresh
            score ( q ) = 1;
            scorematrix ( q, p ) = 1;
        else
            score ( q ) = 0;
            scorematrix ( q, p ) = 0;
        end

    end
    score;
    scorematrix;

end
scorematrix;

[ m, n ] = size (scorematrix);


for r = 1 : n
    positive = 0;
    negative = 0;

   for s = 1 : m

       if scorematrix ( s, r ) == 1

           positive = positive + 1; % number of participant with mean spectral area below the threshhold
```

```
        else
            negative = negative + 1; % people above the threshold

        end

    end
    pos ( r ) = positive;

    neg ( r ) = negative;

end

pos
neg

clear neg
clear pos
clear scorematrix
end
```

Appendix C: Code used to generate the hrbylf index

```
%%12/-9/07 % calcualte the ratio of the mean spectral density of bandwidth
%%with the mean spectral density of the hr frequencies
close all
clear all
clc
%
%=========================================================================
%=========================================================================
%   Constants
FIXEDfs = 1000 * 60;
FIXEDfN = FIXEDfs / 2;
fsLF = 120; % cpm the new smapling rate
fsHF = 520;

resamplecoefficientLF = FIXEDfs / fsLF;
resamplecoefficientHF = FIXEDfs / fsHF;

fNLF = fsLF / 2;
fNHF = fsHF / 2;

LF = 1; RF = 2;

[ BaaLF, AaaLF ] = butter( 2, 30 / FIXEDfN );
```

```
[ BaaHF, AaaHF ] = butter( 2, 130 / FIXEDfN );


lists = [ 'Nor.mat';...
          'Pat.mat';...
          'Neu.mat';...
                      ];

col = [ 'b';...
        'g';...
        'r';...
              ];

%%=============================================================================
%%=============================================================================

%   READ SIGNALS AND CALCULATE THE TIME AXIS
%
figure
hold on

for K = 1:3

eval ( [ 'load ' lists( K, : ) ';' ] );
[r c] = size (LIST);
% s = 3
for i = 1:r

N4 = csvread(LIST(i,:),4,0);
Name = LIST(i,36:42);

% VMLF = N4( :, LF );
% VMRF = N4( :, RF );

%%=============================================================================
```

```
%%%% LF ANALYSIS
%%=========================================================================
%% low pass filter the original signal to obtain very low frequency

LFLF = filtfilt( BaaLF, AaaLF, VMLF );
LFRF = filtfilt( BaaLF, AaaLF, VMRF );

LFLF = LFLF ( 1 : resamplecoefficientLF : end );
LFRF = LFRF ( 1 : resamplecoefficientLF : end );

[ Bhi Ahi ] = butter( 1, 1 / fNLF, 'high' );
[ Blo Alo ] = butter( 3, 25 / fNLF, 'low' );

vmlf = filtfilt( Bhi, Ahi, LFLF );
vmrf = filtfilt( Bhi, Ahi, LFRF );

vmlf = filtfilt( Blo, Alo, vmlf );
vmrf = filtfilt( Blo, Alo, vmrf );

%%=========================================================================
%%=========================================================================

%% FFT of the low frequency signal

len = length ( vmlf );
win = hanning ( 1, len );

vmlf = vmlf .* win;

vmrf = vmrf .* win;

vmlffft = abs ( fft ( vmlf ) );
vmrffft = abs ( fft ( vmrf ) );

l = round ( ( length ( vmlffft ) ) / 2 ) ;
```

```
vmlf = vmlffft ( 1 : l );
vmrf = vmrffft ( 1 : l );

vmlfnew = vmlf;
vmrfnew = vmrf;
%%=============================================================================
%%=============================================================================
%%HF analysis
%%=============================================================================

HFLF = filtfilt( BaaHF, AaaHF, VMLF );
HFRF = filtfilt( BaaHF, AaaHF, VMRF );

HFLF = HFLF ( 1 : resamplecoefficientHF : end );
HFRF = HFRF ( 1 : resamplecoefficientHF : end );

[ Bhi Ahi ] = butter( 3, 60/fNHF, 'high' );
[ Blo Alo ] = butter( 1,100/fNHF, 'low' );

cplf = filtfilt( Bhi, Ahi, HFLF );
cprf = filtfilt( Bhi, Ahi, HFRF );

cplf = filtfilt( Blo, Alo, cplf );
cprf = filtfilt( Blo, Alo, cprf );

%=============================================================================
%=============================================================================

siglen = length( cplf );
win = hanning( 1, siglen );

cplf = cplf .* win;
cprf = cprf .* win;

fftlen = siglen;
fftlendiv2 = floor( fftlen / 2 );
```

```
FFTCPLF = abs( fft( cplf, fftlen ) );
FFTCPRF = abs( fft( cprf, fftlen ) );
%
%=========================================================================
%   FFT envelope

[ Bfftlo Afftlo ] = butter( 2, 0.005 );
fftcplf = filtfilt( Bfftlo, Afftlo, FFTCPLF );
fftcplf = fftcplf ( 1:fftlendiv2 ) ./  max( fftcplf( 1:fftlendiv2 ) );
fftcprf = filtfilt( Bfftlo, Afftlo, FFTCPRF );
fftcprf = fftcprf ( 1:fftlendiv2 ) ./  max( fftcprf( 1:fftlendiv2 ) );
%=========================================================================
%=========================================================================
%   Find the N% thresholds of the FFT

    faxisHF = ( fNHF / fftlendiv2 : fNHF / fftlendiv2 : fNHF );

    iq = find( round( faxisHF ) == 60 );
    iq = iq( 1 );
    faxisHF( iq );

    thresh = 0.7;
    [ MAXFFTLF ILF ] = max( fftcplf( iq:fftlendiv2 ) );
    MAXFFTLF;
    ILF;
    ILF = ILF + iq;
    THRESH = thresh * MAXFFTLF;
    lfindexLF = 0; hfindexLF = 0; k = ILF;
    while ( fftcplf( k ) > THRESH ) && ( k > 10 )
        k = k - 1;
    end
    lfindexLF = k;
    k = ILF;
    while ( fftcplf( k ) > THRESH ) && ( k < fftlendiv2 - 10 )
        k = k + 1;
```

```
    end
    hfindexLF = k;

    [ MAXFFTRF IRF ] = max( fftcprf( iq:fftlendiv2 ) );
    IRF = IRF + iq;

    THRESH = thresh * MAXFFTRF;
    lfindexRF = 0; hfindexRF = 0; k = IRF;
    while ( fftcprf( k ) > THRESH ) && ( k > 10 )
        k = k - 1;
    end
    lfindexRF = k;
    k = IRF;
    while ( fftcprf( k ) > THRESH ) && ( k < fftlendiv2 - 10 )
        k = k + 1;
    end
    hfindexRF = k;
%=========================================================================
%=========================================================================

% calculate the area under the curve

faxisLF = fNLF / l : fNLF / l : fNLF;

x = 3.0 ; % lower limit of bandwidth to be analysed
y = 20.0 ; % upper limit of bandwidth to be analysed
z = y - x ; % bandwidth
a = find ( round ( faxisLF ) == x );
faxisLF( a ( 1 ) : a ( end ) )
a = a (2 );


b = find ( round ( faxisLF ) == y );
faxisLF( b ( 1 ) : b ( end ) )
b = b ( 2 );
```

```
specareaLF ( i, 1 )  = ( sum ( vmlfnew ( a : b ) ) ) / z ; % 6 being the bandwidth
specareaLF ( i, 2 )  = ( sum ( vmrfnew ( a : b ) ) ) / z ;


%=========================================================================
%=========================================================================

% calculate the area under the curve

xl = lfindexLF ; % lower limit of bandwidth to be analysed
yl = hfindexLF ;  % upper limit of bandwidth to be analysed
xr = lfindexRF ;  % lower limit of bandwidth to be analysed
yr = hfindexRF ;  % upper limit of bandwidth to be analysed

meanx = round ( mean ( [ xl , xr ] ) );  % mean lower index of left and right
s =  round ( faxisHF ( meanx ) );

meany = round ( mean ( [ yl , yr ] ) ); % mean upper index of left and right
t =  round ( faxisHF ( meany ) );

z = t - s ;  %bandwidth of interest

% FFTCPLF = FFTCPLF ( 1:fftlendiv2 ) ;
% FFTCPRF = FFTCPRF ( 1:fftlendiv2 ) ;

specareaHF ( i, 1 )   = ( sum ( fftcplf ( meanx : meany ) ) ) / z ;
specareaHF ( i, 2 )  =  ( sum ( fftcprf ( meanx : meany ) ) ) / z ;

end

specareaLF;
specareaHF;
meanareaLF = mean ( specareaLF, 2 );
meanareaHF = mean ( specareaHF, 2 );
```

```
w = length ( meanareaLF );

for ii = 1 : w

    hrbylf ( ii ) = meanareaHF ( ii ) / meanareaLF (ii );
end

hrbylf = hrbylf'

plot ( hrbylf, [ ' + ' col( K ) ]  )
xlabel ( ' ID ' )
ylabel ( ' meanHRspecden/ meanLFspecden ' )
legend ( ' normal ', ' patients ', ' neuropaths ' )
title ( ' The ratio of the spedenof HR to speden of LF ' )
grid on

b = length ( hrbylf );
range = [ 2.0 : 0.2 : 4.0 ]; % the range of mean spectral density to be used as threshold
a = length ( range );
scorematrix = zeros ( b, a );

for p = 1 : a

    thresh = 1.0e-003 * range ( p ) ;

    for q = 1 : b

        if hrbylf ( q ) <= thresh
%             score ( q ) = 1;
            scorematrix ( q, p ) = 0;
        else
%             score ( q ) = 0;
            scorematrix ( q, p ) = 1;
        end

    end
```

```
%     score;
    scorematrix;

end
scorematrix;

[ m, n ] = size (scorematrix);


for r = 1 : n
    positive = 0;
    negative = 0;

   for s = 1 : m

       if scorematrix ( s, r ) == 1

           positive = positive + 1; % number of participant with mean spectral area below the threshhold

       else
           negative = negative + 1; % people above the threshold

       end

   end
   pos ( r ) = positive;

   neg ( r ) = negative;

end

pos
neg


clear neg
```

```
clear pos
clear scorematrix
clear hrbylf
clear specareaLF
clear specareaHF;
clear meanareaLF
clear meanareaHF

end
```

Appendix D: Functions used in the main programs

```
 %%Function Bland Altmen agreement plot: this program generates the Bland Altman plot to compare L and R HR trace
function OUT =  BlandAltman( vec1, vec2, TITLE )

    [ a b ] = size( vec1 );
    if a > 1
        vec1 = vec1';
    end
    [ a b ] = size( vec2 );
    if a > 1
        vec2 = vec2';
    end
    MEAN = mean( [ vec1; vec2 ] );
    DIFF =  ( vec1 - vec2 );
    DIFFSTD =  std( DIFF );
    DIFFMEAN = mean( DIFF );
    Uplimit = DIFFMEAN + DIFFSTD;
    Lolimit = DIFFMEAN - DIFFSTD;
figure
    hold on
    plot( MEAN, DIFF, '*' )
    plot( [ min( MEAN ) - 0.1*min( MEAN )  max( MEAN ) + 0.1*max( MEAN ) ], [ DIFFMEAN + DIFFSTD DIFFMEAN + DIFFSTD
], 'm' )
    plot( [ min( MEAN ) - 0.1*min( MEAN )  max( MEAN ) + 0.1*max( MEAN ) ], [ DIFFMEAN - DIFFSTD DIFFMEAN - DIFFSTD
], 'm' )
    plot( [ min( MEAN ) - 0.1*min( MEAN )  max( MEAN ) + 0.1*max( MEAN ) ], [ DIFFMEAN DIFFMEAN ], 'm' )
    axis( [ min( MEAN ) - 0.1*min( MEAN )  max( MEAN ) + 0.1*max( MEAN ) ( min( DIFF ) - 0.7*min( DIFF ) ) ( max(
DIFF ) + 0.7* max( DIFF ) ) ] )
    grid on
    title( TITLE )

    OUT = [ Uplimit, Lolimit,DIFFMEAN ] ;
%% This program complex demodulates the I/P signal using the specified  cut off
```

```
%% frequency and the sampling frequency
%%=========================================================================
function OUT = complex_demod( Data, w_demod, LP_cutoff, fs )

NyquistPoint = (fs / 2);

    LP_cutoff = ( LP_cutoff / NyquistPoint );
    LP_order = 4;
    [ B, A ] = butter( LP_order, LP_cutoff );

    t = ( 1/fs:1/fs:length( Data ) * (1/fs) )' * 60;

    w_demod = w_demod / 60;
    w_demod = 2 * pi * w_demod;

    signal_1 = Data .* ( 2 * exp( -i * ( w_demod ) .* t ) );

    %   Low pass filter the resulting signal

    signal_2 = filtfilt( B, A, signal_1 );

%   Turn the signal back into its real equivalent
    M = sqrt( real( signal_2 ).^2 + imag( signal_2).^2 );

    PHI_ATAN = atan( imag( signal_2 ) ./ real( signal_2 ) );

    PHI_ANGLE = angle( signal_2 );

%=========================================================================
%=========================================================================
    signal_3 = 1 .* sin( w_demod .* t + PHI_ANGLE );


     OUT = [ signal_3, M, PHI_ANGLE, PHI_ATAN ];
%=========================================================================
```

```
%This program removes the spikes from the HR trace extracted from the raw
%PPG signal
function OUT = spikefilt( IN )

    SDthresh = 2.0
    In = IN;
    l = length(IN);
    ps = length( IN )/10; % the pseudo sampling rate is the number of HR detected over one min
    pn = ps / 2 % This is the pseudo Nyqyst freq
    L_cutoff1 = 25 %25,30 cpm
    L_cutoff2 = 10;%15

    [ Bhi1 Ahi1 ] = butter( 2, L_cutoff1 / pn , 'high' );

    [ Blo Alo ] = butter( 2, L_cutoff2 / pn );


    in = filtfilt( Bhi1, Ahi1, IN ); % filtering to remove all the high frequency noise

    SD = std( in );

    for i = 2:l
        if ( in( i ) >= SDthresh*SD ) || ( in( i ) <= -SDthresh*SD )
            IN( i ) = IN( i - 1 );
        end
    end
%
    OUT = filtfilt( Blo, Alo, IN ); % low pass filtering the HRV signal which has had
    %its spikes removed to obtain the very low frequency trend of the HR




%%=============================================================================================
```

Bibliography

Allen, J. (2007). "Photoplethysmography and its application in clinical physiological measurement." Physiological Measurement **28**(3): R1 - R39.

Altman, D. G. (1992). Practical Statistics for Medical Research. London, Chapman & Hall.

Barron, S. A., Rogowski, Z., Kanter, Y., Hemli, J. (1993). "DC photoplethysmography in the evaluation of sympathetic vasomotor responses." Clinical Physiology **13**(6): 561-72.

Bernardi, L., Radaelli, A., Solda, P. L., Coats, A. J. S., Reeder, M., Calciate, A., Garrard, C. S., Sleight, P. (1996). "Autonomic control of skin microvessels: assessment by power spectrum of photoplethysmographic waves." Clinical Science **90**(5): 345-55.

Bernardi, L., Rossi, M., Leuzzi, S., Meno, E., Fornasri, G., Calciate, A., Orlandi, C. (1997). "Reduction of 0.1 Hz microcirculatory fluctuations as evidence of sympathetic dysfunction in insulin-dependent diabetes." Cardiovascular Research **34**(1): 185-91.

Bhadada, S. K, Jyotsna, V. P., Agarwal, J. K (2001). "Diabetic neuropathy : current concepts." Journal, Indian Academy of Clinical Medicine **2**(4): 305-318.

Bland, J. M., Altman, D. G. (2003). "Applying the right statistics : Analyses of measurement studies." Ultrasound Obstet Gynecology **22**: 85 - 93.

Blazek, V., Ehrenburg, U. S. (1996). Quantitative photoplethysmography: Basic fact and examination for evaluating periheral vascular funktions. Dusseldorf, VDI Verilag

Boulton, J. M. A., Connor,H., Cavanagh,R.P., Ed. (2000). The foot in diabetes. Chichester, John Wiley & Sons Ltd.

Braune, H. J. (1997). "Early detection of diabetic neuropathy: A neurophysiological study on 100 patients." Electromyography and clinical neurophysiology **37**: 399-407.

Buchs, A., Slovik,Y., Rapport,M., Rosenfeld,C., Khanokh,B., Nitzan,M. (2005). "Right-Left correlation of the sympathetically induced fluctualtions of photoplethysmographic signal in diabetic and non diabetic subjects." Medical & Biological Engineering and Computing **43**(2): 252-257.

Chittenden J.S., S., S.K. (1993). "Microvascular investigation in diabetes." Postrgraduate Medical Journal **69**: 419-428.

Creager, M., Dzau, V.J., and Loscalzo, J., Ed. (1992). Vascular medicine : a textbook of vascular biology and diseases Boston, Little Brown

DeFronzo, R. A., Ferrannini,E., Keen,H., Zimmet,P., Ed. (2004). International Textbook of Diabetes Mellitus : Third Edition, John Wiley & Sons.

Duby JJ, C. R., Setter SM, White JR, Rasmussen KA (2004). "Diabetic nuropathy : intensive review." American Society of Health-system Pharmacists **61**(2): 160-176.

Eicke, B. M., Hlawatsch,A., Bauer,J., Kustner,E., Mink,S., Victor,A., Kuhl,V. (2003). "Sympathetic vasomotor responses of the radial artery in patients with diabetic foot syndrome." Diabetes Care **26**(9): 2616-21.

Fagrell, B. and Intaglietta, M. (1997). "Microcirculation: Its significance in clinical and molecular medicine." Journal of Internal Medicine **241**(5): 349-362.

Frewin, D. B. (1969). "The Physiology of the cutaneous circulation in man." Australasian Journal of Dermatology **10**(2): 61-74.

Hayano, J., Taylor, A. .J., Mukai, S., Okada, A., Watanabe, Y., Takata, K., Fujinami, T. (1994). "Assessment of frequency shifts in R-R interval variability and respiration with complex demodulation." Journal of Applied Physiology **77**(6): 2879-2888.

Hayano, J., Taylor,A.J., Mukai,S., Okada,A., Watanabe,Y., Takata,K., Fujinami,T., Yamada, A., Hori, R., Asakawa, T., Yokoyama, K. (1993). "Continuous assessment of hemodynamic control by complex demodulation of cardiovascular variability." American Journal of Physiology **264**(Heart Circulation Physiology,33): H1229 -H1238.

Hittel, N., Donelly, R. (2002). "Treating peripheral arterial disease in patients with diabetes." Diabetes, Obesity and Metabolism **4** (2): S26-S31.

Intaglietta, M. (1990). "Vasomotion and flowmotion:physiological mechanisms and clinical evidence." Vascular Medical Reviews **1**: 101-112.

Kalbfleisch, J. H. S. D., Smith, J. J. (1978). "Evaluation of the heart rate response to the valsalva maneuver." American Heart Journal **95**(6): 707-15.

Kamal, A. A. R., Harness, J. B., Irving, G., Mearnes, A .J. (1989). "Skin Plethysmography- A review." Computer Methods and Programs in Biomedicine **28**: 257-269.

Kenneth, M. S., Cummings, H. M., Ed. (2005). Diabetes: Chronic complications. Chichester, John Wiley & Sons Ltd.

Kilo, S., Berghof, M, Aliz, M., Freeman, R. (2000). "Neural and endothelial control of the microcirculation in diabetic peripheral neuropathy." Neurology **54**(6): 1246-1252.

Kim, S. Y., Euler, D. E. (1997). "Baroreflex Sensitivity Assessed by Complex Demodulation of Cardiovascular Variability." Hypertension **29**(5): 1119-1125.

Lavery, L. A., Armstrong, D. G., Vela, S. A., Quebedeaux, T. L., Fleischli, J. G. (1998). "Practical criteria for screening patients at high risk for diabetic foot ulceration". Archives of Internal Medicine **158**: 157-162

Lefrandt, J. D., Bosma, E., Oomen, P. H. N., Roon, A. M., Smit, A. J., Hoogenberg, K. (2003). "Sympathetic mediated vasomotion and skin capillary permeability in diabetic patients with peripheral neuropathy." Diabetologia **46**: 40-47.

LeRoith, D., Taylor, I. S., Olefsky, M. J., Ed. (2004). Diabetes Mellitus : A Fundamental and Clinical Text. Philadelphia, USA, Lippincott Williams & Wilkins.

Levick, J. R. (2000). An Introduction to Cardiovascular Physiology. London, Arnold Publishers.

Lynn, A. P. (1993). An Introduction to the Analysis and Processing of Signals. London, MacMillan.

Mackay, J. D., Cambridge, J., Watkins, P. J. (1980). "Diabetic autonomic neuropathy :the diagnostic value of heart rate monitoring." Diabetologia. **18**: 471-478.

Marieb, E., N. (2001). Human Anatomy and Physiology, Addison Wesley Longman

Marvin, E. Levin, L. W. O. N., John, H. Bowker, Ed. (1993). The Diabetic foot St. Louis : Mosby Year Book,.

Maser, R. E. (1998). "Autonomic Neuropathy: Patient Care." Diabetes Spectrum **11**(4): 224 - 227.

Meyer, M. F., Rose, C. J., (2003). "Impaired 0.1-Hz vasomotion assessed by laser Doppler anemometry as an early index of peripheral sympathetic neuropathy in diabetes." Microvascular Research **65**(2): 88-95.

Neumann, H. A., Maessen-Visch, M. B. (1999). "Plethysmography." Current Problems in Dermatology **27**: 114-23.

Nilsson, H., Aalkjaer, C. (2003). "Vasomotion: Mechanisms and physiological importance." Molecular Interventions **3**: 79-89.

Nitzan, M., Babchenko, A. Khanokh, B., Landau, D. (1998). "The variability of the photoplethysmographic signal - a potential method for the evaluation of the autonomic nervous system." Physiological Measurement **19**(1): 93-102.

Oberg, P. A., Lindberg, L. G. (1991). "Photoplethysmography - Part 2 Influence of light source wavelength." Medical & Biological Engineering and Computing **29**: 48-54.

Peter, S., Ed. (1978). The Control of the Cardiovascular System. London, Medi-Cine Limited.

Prof Vladimir Blazek, P. U. S.-E. (1996). Quantitative Photoplethysmography: Basic facts and examintation tests for evaluating peripheral vascular funktions. Dusseeldorf, VDI Verilag.

Rendell, M., Bergman, T., O'Donnell, G., Drobny, E., Borgos, J. &Bonner, R.F. (1989). "Microvascular blood flow , volume and velocity measured by LASER Doppler techniques in IDDM." Diabetes **38**: 819-824.

Riffenburgh, R. H. (2006). Statistics in Medicine. Oxford, UK, Elsevier Academic Press.

Rushmer.F.R., M. (1976). Organ Physiology - Structure and Function of the Cardiovascular System. Philadelphia, London, Toronto, W.B. Saunders Company.

Shapiro, S. A., Stansberry, K. B., Hill, M. A., Meyer, M. D., McNitt, P. M., Bhatt, B. A., Vinik, A. I. (1998). "Normal blood flow response and vasomotion in the diabetic Charcot foot." Journal of Diabetes and Its Complications **12**(3): 147-153.

Smith, S. W. (1997). The Scientist and Engineer's Guide to Digital Signal Processing, California Technical Publishing.

Spijkerman, A., Dekker, J.M., Nijpels, G., Adriaanse, M. C., Kostense, P.J., Ruwaard, D., Stehuwer, C .D. A., Bouter, L. .M., Heine, R. .J. (2003). "Microvascular complications at time of diagnosis of Type 2 diabetes are similar among diabetic patients detected by targeted screening and patients newly diagnosed in general parctice. The Hoorn Screening Study." Diabetes Care **26**: 2604-2608.

Stansberry, K. B., Shapiro, S. A., Hill, M. A., Mc Nitt, P. M., Meyer, M. D., Vinik, A.. I. (1996). "Impaired peripheral vasomotion in diabetes." Diabetes Care **19**: 715-721.

Tooke, J. E. (1995). "Perspective in Diabetics Microvascular Function in Human Diabetes A physiological perspective." Diabetes **44**: 721-726.

Vinik, A. I. (2002). "Neuropathy: new concepts in evaluation and treatment." Southern medical association **95**(1): 21-23.

Vinik, A. I., Erbas, T. (2001). "Recognizing and treating diabetic autonomic neuropathy." Cleveland Clinic Journal of Medicine **68**(11): 928-944.

Vinik, B. D., Raelene E. M, Freeman, R. (2003). "Diabetic autonomic neuropathy." Diabetes Care **26**(5): 1553-1579

Wiernsperger, N. F. (2001). "In Defense of Microvascular Constriction in Diabetes." Clinical Hemorheology & Microcirculation **25**(2): 55-62.

Young, M. J., Breddy, J.L., Veves, A., Boulton, A.J. (1994). "The prediction of diabetic neuropathic foot ulceration using Vibration perception thresholds: a prospctive study." Diabetes Care 176(6): 557-560.

Yuan, S., Liu, Y., Zhu, L. (1999). "Vascular complications of diabetes mellitus." Clinical and Experimental Pharmacology and Physiology **26**: 977-978.